AD-A282 026

UMENTATION PAGE

Form Approved
OMB No. 0704-0188

2. REPORT DATE	3. REPORT TYPE AND DATES COVERED
	THESIS/~~DISSERTATION~~

4. TITLE AND SUBTITLE
The Oxidative Stabilization And Carbonization of Mesophase Pitch

5. FUNDING NUMBERS

6. AUTHOR(S)
Joseph Drbohlav III

7. PERFORMING ORGANIZATION NAME(S) AND ADDRESS(ES)
AFIT Student Attending:
Wichita State Univ.

8. PERFORMING ORGANIZATION REPORT NUMBER
AFIT/CI/CIA-
94-055

9. SPONSORING/MONITORING AGENCY NAME(S) AND ADDRESS(ES)
DEPARTMENT OF THE AIR FORCE
AFIT/CI
2950 P STREET
WRIGHT-PATTERSON AFB OH 45433-7765

10. SPONSORING/MONITORING AGENCY REPORT NUMBER

11. SUPPLEMENTARY NOTES

12a. DISTRIBUTION/AVAILABILITY STATEMENT
Approved for Public Release IAW 190-1
Distribution Unlimited
MICHAEL M. BRICKER, SMSgt, USAF
Chief Administration

12b. DISTRIBUTION CODE

13. ABSTRACT (Maximum 200 words)

2286 94-22540

94 7 19 021

14. SUBJECT TERMS	15. NUMBER OF PAGES 204
	16. PRICE CODE

17. SECURITY CLASSIFICATION OF REPORT	18. SECURITY CLASSIFICATION OF THIS PAGE	19. SECURITY CLASSIFICATION OF ABSTRACT	20. LIMITATION OF ABSTRACT

ABSTRACT

THE OXIDATIVE STABILIZATION AND CARBONIZATION OF MESOPHASE PITCH

By

Joseph Drbohlav III
Captain, USAF

1994
204 pages

Master of Science in Chemistry
The Wichita State University

The transformation of mesophase pitch to an ordered carbon by high temperature heat treatment or pyrolysis in an inert atmosphere must be preceeded by a suitable period of thermosetting or oxidative stabilization. The chemical process of oxidative stabilization is not well characterized, although research has clearly indicated that the oxidation history of the mesophase has a profound impact on the mechanical qualities of the resultant carbon product. In this study, we oxidized samples of a commercially available, synthetic mesophase pitch to determine what effect different time and temperature profiles of oxidation had on the quantity and type of introduced oxygen functionality. Samples of pitch were then carbonized to investigate the effect of introduced oxygen functionality on that process. Fourier Transform Infrared Spectroscopy (FT-IR) was used to characterize and quantify oxygen functionality present in oxidized pitch. Thermal Gravimetric Analysis (TGA) and Thermal Volatilization Analysis

(TVA) were then used to characterize the carbonization process. It was concluded that changing the time/temperature profile of oxidation affects primarily the quantity of introduced oxygen functionality as opposed to the type of functionality. Samples of insufficiently oxidized pitch melted during carbonization and were thermally "cracked" to produce short alkanes and a large oligomeric fraction. Sufficiently oxidized pitch maintained its powdered nature, releasing primarily CO_2, CO, H_2O, and a small oligomeric fraction.

BIBLIOGRAPHY

[1] Fujiura, R., Kojima, T., Kanno, K., Mochida, I., and Korai, Y., Carbon, 31 (1), 97 (1993).

[2] Kochi, Jay K., Free Radicals, New York: John Wiley & Sons, 1973.

[3] Korai, Y., Nakamura, M., Mochida, I., Sakai, Y, and Fujiyama, S., Carbon, 29 (4/5), 561 (1991).

[4] Lavin, J. G., Carbon, 30 (3), 351 (1992).

[5] Marsh, Harry, Introduction to Carbon Science, London: Butterworths, 1989.

[6] Matsumoto, T., and Mochida, I., Carbon, 30, 1041 (1992).

[7] McNeill, I.C., European Polymer Journal, 3, 409 (1967).

[8] McNeill, I.C., Polymer Engineering and Science, 20 (10), 668 (1980).

[9] McNeill, I.C., Developments in polymer Degradation I, N. Grassie (Ed.), London: Applied Science Publishers, 1977.

[10] Mochida, I., Toshima, H., Korai, Y., and Matsumoto, T., Journal of Materials Science, 25, 76 (1990).

[11] Mochida, I., Toshima, H., Korai, Y., and Matsumoto, T., Journal of Materials Science, 24, 2191 (1989).

[12] Mochida, I., Shimizu, K., Korai, Y., Otsuka, H., Sakai, Y., and Fujiyama, S., Carbon, 28 (2/3), 311 (1990).

[13] Pierson, R. H., Fletcher, A.N., and St. Clair Gantz, E., Analytical Chemistry, 28 (8), 1218 (1956).

[14] Silverstein, R.M., Bassler, G.C., and Morrill, T.C., Spectrometric Identification of Organic Compounds, New York: John Wiley & Sons, 1981.

[15] White, J.L., and Sheaffer, P.M., Carbon, 27 (5), 697 (1989).

[16] Yang, C.Q., and Simms, J.R., Carbon 31 (3), 451 (1993).

THE OXIDATIVE STABILIZATION AND CARBONIZATION OF MESOPHASE PITCH

By

JOSEPH DRBOHLAV III

B.S., United States Air Force Academy, 1988

Submitted to the Department of Chemistry
and the faculty of the Graduate School of
The Wichita State University in Partial Fulfillment of
the requirements for the Degree of
Master of Science

May 1994

THE OXIDATIVE STABILIZATION AND CARBONIZATION OF MESOPHASE PITCH

I have examined the final copy of this thesis for form and content and recommend that it be accepted in partial fulfillment of the requirements for the degree of Master of Science, with a major in Chemistry.

_____

Dr. W.T.K. Stevenson, Major Professor

We have read this thesis and recommend its acceptance:

_____

Dr. McCormick, Committee Member

_____

Dr. Wimalasena, Committee Member

_____

Dr. Burns, Committee Member

_____

Dr. Loper, Committee Member

DEDICATION

This thesis is dedicated to my wife, Carol,
who never receives all the credit she deserves.

Proverbs 31:10-31

ACKNOWLEDGMENTS

I would like to thank my research advisor, Dr. W.T.K. Stevenson, for his leadership and advice, and for introducing me to the interesting field of carbon science. I am grateful that he led me to select a research topic that was relevant to my education as both a chemist and an Air Force Officer. I enjoyed this project tremendously and benefited from his "hands-off" approach that forced me to learn from my own mistakes. I am grateful also to the members of my thesis committee for their advice and guidance in the completion of this work. I would like to recognize Koch Industries in Wichita, Kansas for allowing me generous use of their Thermal Gravimetric Analysis (TGA) system. I thank my wife, Carol, for her tremendous support and dedication during this stressful time. I know all the extra evenings and weekends spent alone with the kids weren't easy, and I admire her patience and understanding. Finally, I am sincerely grateful to the U.S. Air Force and, specifically, the Chemistry Department of the United States Air Force Academy for granting me this opportunity to return to the halls of academia. This project would not have been possible otherwise.

ABSTRACT

The transformation of mesophase pitch to an ordered carbon by high temperature heat treatment or pyrolysis in an inert atmosphere must be preceeded by a suitable period of thermosetting or oxidative stabilization. The chemical process of oxidative stabilization is not well characterized, although research has clearly indicated that the oxidation history of the mesophase has a profound impact on the mechanical qualities of the resultant carbon product. In this study, we oxidized samples of a commercially available, synthetic mesophase pitch to determine what effect different time and temperature profiles of oxidation had on the quantity and type of introduced oxygen functionality. Samples of pitch were then carbonized to investigate the effect of introduced oxygen functionality on that process. Fourier Transform Infrared Spectroscopy (FT-IR) was used to characterize and quantify oxygen functionality present in oxidized pitch. Thermal Gravimetric Analysis (TGA) and Thermal Volatilization Analysis (TVA) were then used to characterize the carbonization process. It was concluded that changing the time/temperature profile of oxidation affects primarily the quantity of introduced oxygen functionality as opposed to the type of functionality. Samples

of insufficiently oxidized pitch melted during carbonization and were thermally "cracked" to produce short alkanes and a large oligomeric fraction. Sufficiently oxidized pitch maintained its powdered nature, releasing primarily CO_2, CO, H_2O, and a small oligomeric fraction.

TABLE OF CONTENTS

LIST OF TABLES

TABLE PAGE

LIST OF FIGURES

FIGURE PAGE

FIGURE PAGE

FIGURE PAGE

FIGURE PAGE

FIGURE PAGE

FIGURE PAGE

FIGURE PAGE

FIGURE PAGE

FIGURE PAGE

94-055

THE OXIDATIVE STABILIZATION AND CARBONIZATION OF MESOPHASE PITCH

by

JOSEPH DRBOHLAV III

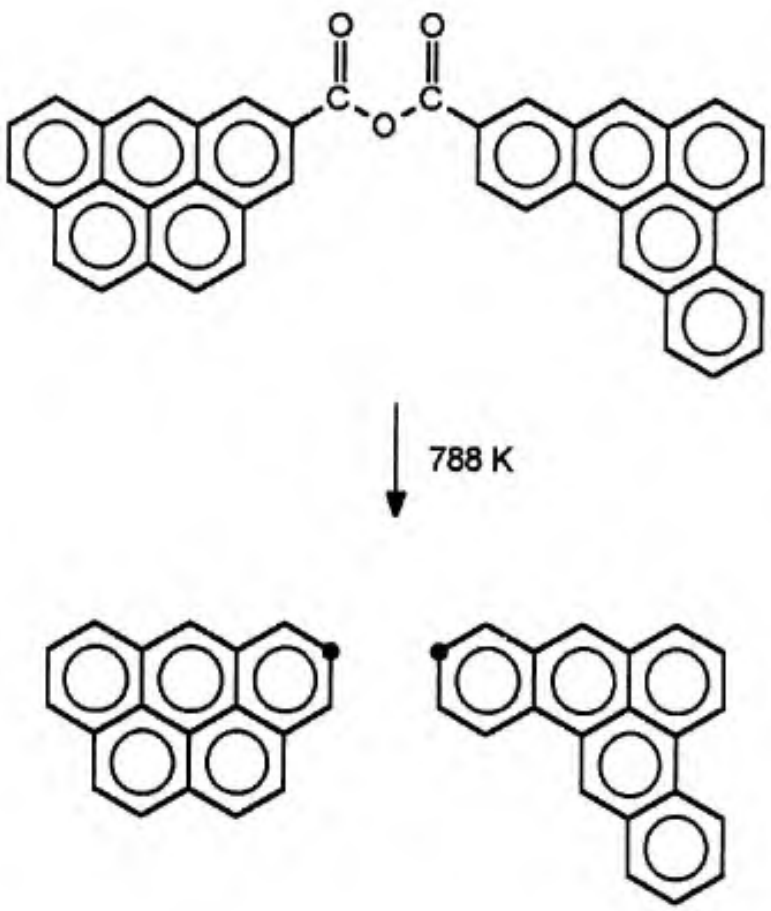

+ carbon monoxide, carbon dioxide

1. INTRODUCTION

1.1 MESOPHASE PITCH

Mesophase pitch is an anisotropic material formed by the liquid crystalline growth of large, polynuclear aromatic molecules found in coal tars and petroleum oils. The great interest in mesophase pitch stems from its ability to be pyrolyzed into an ordered carbon for use in carbon fibers and carbon-carbon composites [1]. In order to fully comprehend the significance of mesophase pitch, it is necessary to understand the difference between a graphitizable and a nongraphitizable carbon. Graphite is an allotropic form of carbon consisting of sheets of hexagonally arranged carbon atoms in a planar ring system [1]. The layers of condensed rings are stacked parallel to each other with covalent, sp^2 hybridized bonds within the layers, and van der Waals bonding between the layers [1]. The process of converting an unordered organic carbon material into such a graphite structure by way of heat treatment or other energy input is a major concern of the carbon industry [1]. Subsequently, nongraphitizable carbons are carbons which cannot be transformed into graphitic carbon by heat treatment (pyrolysis) alone; graphitizable carbons may be converted to the desired graphite structure via

pyrolysis alone [1]. Examples of nongraphitizable carbons include wood, nut-shells, and certain coals which produce chars upon pyrolysis [1]. Simple pitch, comprised largely of aromatic and heterocyclic molecules found in coal tars and petroleum oils, is an isotropic, organic carbon. Were it to be pyrolyzed in this form, the pitch would not form the desired graphite structure. Thus, the key to using pitch is to transform it first into a graphitizable form that can then be pyrolyzed into the desired graphite structure. If an appropriate pitch precursor, whether it be from coal tar or petroleum, is heated to a temperature above 400°C, condensations occur and alignment of the lamellar products leads to the formation of liquid crystal-like domains [2]. The liquid crystal-like domains are a consequence of the formation of large "sheets" of aromatic molecules that form via a homogeneous nucleation mechanism and then stack themselves in a parallel fashion [2]. This liquid crystal phase of pitch has been termed "mesophase" because it is a necessary middle step in the transformation of nongraphitizable, isotropic pitch (with no ordering of molecules in any particular direction) into a graphite structure [2]. Mesophase pitch is significant because it is the "missing link" between the cheap and relatively abundant isotropic pitch and the desired graphite; it is an anisotropic material (has ordering of molecules along a certain

axis) capable of being pyrolyzed into a graphite structure.

Mesophase pitch, once formed from the heat treatment of isotropic pitch, can be melt spun into pitch fibers. Prior to their pyrolysis to ordered carbon at temperatures as high as 2500°C, the fibers must be oxidatively stabilized [3]. The oxidative stabilization or thermosetting of the pitch is believed to involve the formation of oxygen crosslinks between molecules, "locking" in the parallel arrangement of mesophase molecules and ensuring the preservation of this morphology during high temperature pyrolysis [3]. Currently, the greatest hurdle to the development of low cost, hiqh quality pitch-based fibers is the poorly defined process of oxidative stabilization [4]. The actual chemical processes involved in the oxidative stabilization of mesophase pitch have not been adequately characterized, although much work has been done to gain insight into the types of reactions that take place, and the quantity and types of functionality introduced during stabilization [5-7].

In summary, the production of high quality graphitic carbon from pitch involves three major events. First, the transformation of isotropic pitch to anisotropic, mesophase pitch by heat treatment in an inert atmosphere. This is followed by the oxidative stabilization of the mesophase pitch to preserve or

"lock-in" orientation, and finally, the pyrolysis or carbonization of the pitch into its graphite structure. The mechanisms of formation of mesophase pitch and the variables affecting its growth from isotropic pitch have already been well characterized and reported [2]. The proper oxidative stabilization of mesophase pitch and its affect on the pyrolysis process remains the least understood area. A better understanding of the reactions taking place in the oxidative stabilization of mesophase pitch would allow for appropriate changes to be made in the manufacturing process, with the realization of higher quality pitch-based carbon materials at a lower cost.

1.2 PUBLISHED WORK OF SPECIFIC RELEVANCE TO OUR WORK

Most of the published works of direct relevance to our study are those that speculate on the chemical reactions taking place during the stabilization of mesophase pitch. From a review of recent publications, it is clear that the chemical process of oxidative stabilization is affected by such variables as the time and temperature of oxidation [5-7], the blending of other compounds with the mesophase pitch [8], and the aromatic content of the unoxidized mesophase pitch [9]. Japanese researchers have recently reported on the development of mesophase pitches derived by synthetic routes. Of particular interest to us is a series

of reports describing the synthesis and characterization of mesophase pitch prepared from napthalene using HF/BF_3 [10-11]. These napthalene derived pitches display superior viscosity characteristics compared to coal tar and petroleum pitches and appear to be well suited for spinning into fibers and as a binder material for carbon-carbon composites [12]. Another major advantage of synthetic pitches is the ability to define optimum stabilization conditions, which should not change significantly if the same synthetic route is used.

Lavin's study [5] is particularly interesting because he analyzed gases evolved by model mesophase pitches during oxidative stabilization at different time/temperature profiles. His studies indicate that water vapor is evolved from the pitch during stabilization at lower temperatures and shorter time periods, coincident with an increase in weight. At higher temperatures of oxidation, Lavin reported that the model pitch compounds released carbon dioxide and carbon monoxide with an associated loss of weight. Lavin concludes that H_2O production is independent of CO_2 and CO production, contrasting with combustion reactions, where the gases are byproducts of the same reactions. This finding is significant because it suggests that weight gain and weight loss during oxidation are the results of different chemical processes, evidence that the time/temperature profile

is a critical variable in the proper oxidative stabilization of pitch.

Isao Mochida and co-workers have produced a wealth of important publications concerning the chemistry involved in oxidative stabilization of mesophase pitch-based carbon fibers [6-8]. Matsumoto and Mochida [7] summarized the oxidation of mesophase pitch as involving three major reactions. The first reaction occurs at lower temperatures and predominately involves the alkyl functionality of the mesophase pitch, forming alcohols, alkyl ethers, aldehydes, ketones, and carboxylic acids. At higher temperatures, crosslinkage or condensation reactions occur, involving the formation of aryl esters and ethers. Matsumoto and Mochida claim that these reactions contribute to the tensile properties of the final carbon fibers by maintaining molecular structure during pyrolysis. At yet higher temperatures, oxidation results in the decomposition of aromatic rings, producing carbon monoxide and carbon dioxide, as well as phenols, carboxylic acids, and aldehydes. These high temperature reactions seem to adversely affect the tensile properties of the resultant carbon fibers. These investigations made extensive use of elemental analysis, solid state FT-IR, solid state NMR, and Secondary Ion Mass Spectrometry (SIMS) to characterize functionality present in samples of stabilized pitch oxidized under different time

and temperature profiles, clearly indicating that oxygen functionality and content are directly dependent on the time/temperature profile of oxidation. Perhaps more importantly, Matsumoto and Mochida [7] have shown there is a distinct relationship between the oxidation history of pitch-based carbon fibers, and the ultimate mechanical qualities of the fibers following carbonization. Some of these qualities affected include tensile strength, modulus, and carbon yield. Clearly, knowledge of the chemistry of oxidative stabilization is a key to understanding and perfecting the overall process of carbonization.

1.3 A RATIONAL FOR OUR RESEARCH

Our goals in the current study can be largely summarized by two major objectives. First, we wished to study the effect that different time/temperature profiles of oxidation had on the type and quantity of functionality introduced into the pitch. We felt this could be best realized by selecting three representative oxidation temperatures; one temperature would be relatively low, just above the softening point of the pitch. The second temperature would be close to that reported in the literature as the most beneficial oxidation temperature. The final temperature would be one which was considered excessive for proper oxidative stabilization. Pitch samples would then be oxidized at these selected

temperatures, following a suitable heating ramp from room temperature, for periods of time ranging from a few minutes to several hours. Weight gain due to oxidation would be measured simply by calculating the difference in weight prior to and following oxidation. Types and relative quantities of functionality would then be determined by solid state FT-IR.

As our second objective, we wished to determine the effect that different time/ temperature oxidation profiles and differing types and quantities of introduced oxygen functionality had on the carbonization process. We chose to attack this problem by applying two popular and effective methods of thermal analysis-- Thermal Gravimetric Analysis (TGA) and Thermal Volatilization Analysis (TVA). TGA and TVA are powerful and complimentary methods for studying thermal degradation processes.

TGA is a very popular method which has been used extensively to study the kinetics of weight loss processes and to determine relative thermal stabilities of materials. TGA can be used to determine the activation energy of a weight loss process by applying one of the previously published methods of Flynn-Wall [13] or other authors [14]. Both methods allow for the determination of the activation energy of a weight loss process by studying the profile of a weight loss process as

it changes with different heating rates. It was our intent to apply the method published by Kissinger [14] to our TGA studies to analyze how different time/ temperature profiles of oxidation affected the activation energy of the carbonization process. In addition, TGA offered an easy means of measuring the percent carbon yield by simply recording the weight of the residue remaining after the carbonization process was complete.

Thermal Volatilization Analysis (TVA), a technique developed by I.C. McNeill at the University of Glasgow [15], was particularly suited to this study because it allows for the separation and characterization of the complete product spectrum resulting from the carbonization process. Although TVA is not as well known as TGA, the two techniques complement each other well; TGA allowing for the study of the kinetics of a weight loss process, and TVA making possible the determination of products resulting from that process. As its name implies, TVA is especially suited for studying volatile emissions associated with a weight loss process. It can accurately record the release of volatiles as a function of temperature, and then allow for the separation of different gases based on differences in volatility. This separation technique has been termed Sub-Ambient Thermal Volatilization Analysis (SATVA) and is described in a number of excellent

reviews [16-17]. TVA and SATVA were found to be excellent methods for separating and identifying the major volatile products of the carbonization process. In addition, they allowed us to determine the influence of different time/temperature profiles of oxidation on the nature of volatile emissions during the carbonization process. With kinetic information provided by the TGA studies and product information from TVA and SATVA studies, our ultimate objective was to develop mechanisms for the carbonization of oxidatively stabilized mesophase pitch. Unfortunately, the pitch did not behave as expected during the TGA studies. It was discovered that the carbonization behavior of the pitch was strongly affected by changes in the heating rate and sample size, resulting in much instrument noise and nonreproducible curve shapes that prevented us from determining activation energies for the carbonization process. Fortunately, the results from TVA and SATVA experiments were especially informative, giving extensive information on the products resulting from the carbonization of pitch. These results are covered in greater detail in chapter 4.

2. MATERIALS

2.1 MESOPHASE PITCH

The mesophase pitch used in this study was a synthetic, napthalene derived mesophase pitch developed by Isao Mochida at Kyushu University in Japan, marketed by Mitsubishi Gas Chemical Company, Inc., and supplied to us by the U.S. Air Force. We felt it would be advantageous to study this mesophase pitch for two reasons. First, this pitch was already being investigated by the Air Force [18] and any information we might learn about its oxidation and carbonization behavior would be mutually beneficial. Second, because it is a synthetic pitch, its aromatic content, hydrogen/carbon ratio, softening point, and aliphatic carbon content would be relatively consistent from batch to batch, unlike most petroleum or coal tar pitches whose characteristics can vary drastically depending on the precursor isotropic pitch. In short, we felt that our study of the stabilization and carbonization behavior of this synthetic pitch would give results that would be valid for future pitches derived from the same synthetic route. The pitch was designated by the Air Force as AR-00716, AR being the acronym for Aromatic Resin. It has a softening point of 224°C and a hydrogen/carbon ratio ranging

from 0.61 to 0.69. The anisotropic content is 100% by volume. Figure 1 contains some representative molecular structures present in the pitch. A complete description of the pitch and its synthetic route is contained in the literature [10].

2.2 THE OXIDATIVE STABILIZATION PROCESS

Mesophase pitch samples were oxidized in a dynamic oxygen atmosphere inside 45mm diameter pyrex tubing. The pyrex tubing was placed horizontally within a Lindberg Model 55122 rectangular muffle furnace with heating power controlled by an Omega CN 2011K microprocessor driven temperature controller and solid-state relay. Sample temperature was measured by a thermocouple placed inside the pyrex tubing adjacent to the sample location. Oxygen flow was controlled at 450 ml/min as measured by a bubble flowmeter. The micro-processor temperature controller provided a reproducible heating ramp to the selected isothermal oxidation temperature at a rate of 10°C/min from room temperature to 200°C, and 5°C/min from 200°C to the soak temperature. It was necessary to perform a temperature calibration to ensure that the temperature measured by the thermocouple was identical to the temperature at the actual sample location over the entire temperature range. The reference thermocouple used in all experiments was placed exactly eight inches inside of the oven as

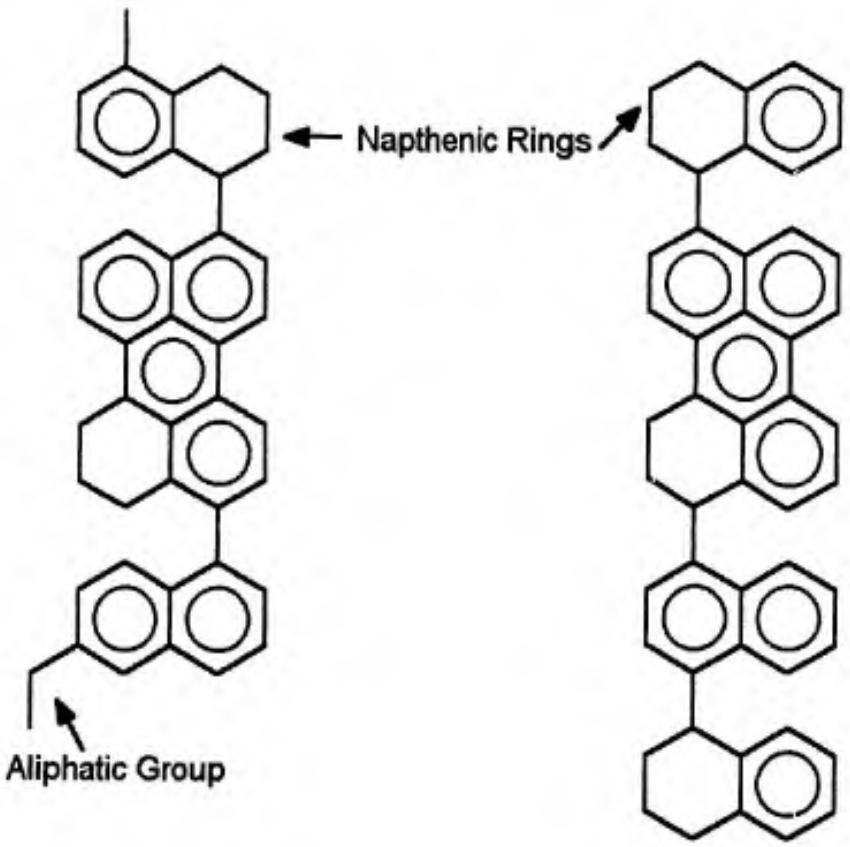

Figure 1. Representative molecules present in napthalene-derived mesophase pitch

Source: Isao Mochida, Kiyoyuki Shimizu, Yozo Korai, Hiroyuki Otsuka, Yukio Sakai, and Susumu Fujiyama, Carbon, 28 (2/3), 311 (1990)

measured from the left wall of the oven. The sample boat was centered at exactly nine inches inside of the oven, measured from the same reference point. In the calibration experiment, two thermocouples were used; one placed at eight inches and one at nine inches. The resulting calibration curve showed the temperatures were identical up to approximately 200°C, at which point the temperature at nine inches maintained a consistent 10°C advantage over the temperature at eight inches into the oven. This result is not surprising since the location of the sample at nine inches into the oven is closer to the center of the muffle furnace's array of heating elements. The temperature controller provided excellent control at the soak temperatures of 240°C, 270°C, 290°C, and 340°C. Thermocouple output was monitored by an Omega strip chart recorder to give a record of all heating ramps and soaks. The exhaust end of the furnace was elevated at an incline of about 5° above horizontal to aid in the oxygen flow by convection through the furnace. An illustration of the mesophase pitch oxidation apparatus is shown in figure 2.

Mesophase pitch samples were pulverized into a powder prior to oxidation. Particle size was determined by optical microscopy under a magnification of 100X. Pitch prepared in a mortar and pestle gave particle sizes in the range of

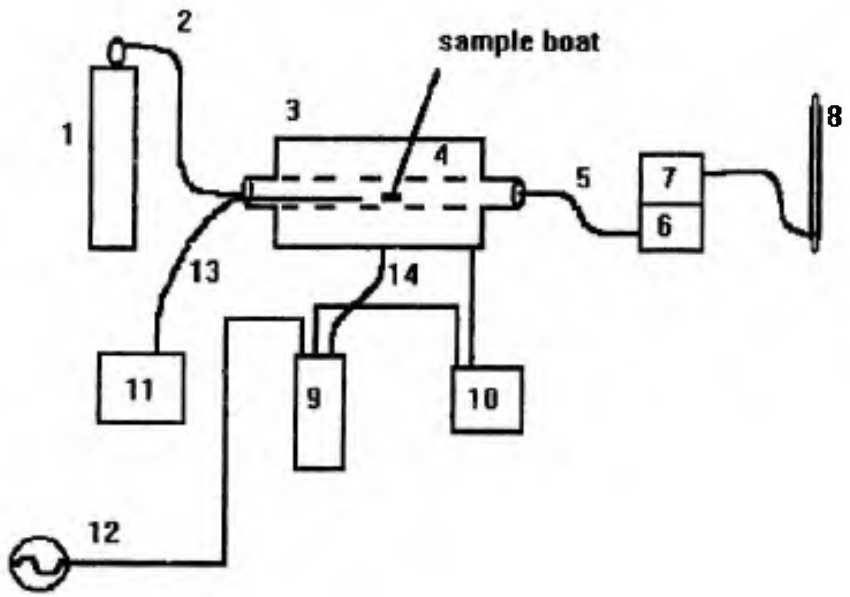

1. Oxygen Supply
2. Oxygen Stream
3. Muffle Furnace
4. Pyrex Tubing
5. Exhaust Stream
6. Molecular Sieve
7. Activated Charcoal
8. Bubble Flowmeter
9. Microprocessor Temperature Controller
10. Solid State Relay
11. Recorder
12. 110 Volt AC Power Supply
13. Sample Temperature Thermocouple
14. Oven Temperature Thermocouple

Figure 2. Mesophase pitch oxidation apparatus

100-200 micrometers. Grinding the pitch in a Tekmar A-10 cryogenic analytical mill gave a smaller particle size, ranging from 10-100 micrometers, however there was a significant aggregation of pitch particles, probably a result of static electrical effects. The preparation of pitch powder in the analytical mill was abandoned in favor of the mortar and pestle due to excessive waste of material in the former.

Sample boats were molded from the bottom of a wooden block with aluminum foil, giving a consistent surface area of 6 cm^2. A tare weight of each sample boat was recorded prior to the addition of approximately 200mg of pitch powder. The pitch was sifted within the boat to give an even distribution over the entire bottom surface area. Volatiles released by the pitch during oxidation were routed through molecular sieve and activated charcoal prior to the bubble flowmeter as a health precaution.

3. METHODS

3.1 FOURIER TRANSFORM INFRARED SPECTROSCOPY (FT-IR)

A Mattson Research Series FT-IR was used to collect the infrared spectra. Each sample was scanned 128 times at a resolution of 4 cm^{-1}. All spectra were collected in the absorbance mode. No base-line correction was used. Both the sample compartment and the interferometer chamber were continuously purged with dry nitrogen gas.

3.1.1 SOLID-STATE FT-IR

All oxidized mesophase pitch samples and carbonization residues were analyzed by FT-IR using the KBr pellet technique. Pellets were formed of approximately 400 mg of dried, spectrometric grade KBr salt and approximately 2.5 mg of sample. The sample and salt mixture was finely pulverized and thoroughly mixed in a ball and mill pestle that was placed in a "wig-l-bug" amalgamator for one minute. The mixture was placed in a 13 mm KBr die and "triple" pressed under vacuum in a hydraulic laboratory press. A load of 12,000 pounds was applied each time. The 2 mm thick pellets were placed in a 13 mm diameter magnetic holder for subsequent IR analysis.

3.1.2 THIN FILM FT-IR

The oligomeric or "coldring" product fraction resulting from the carbonization of pitch was studied by FT-IR on 25 mm diameter NaCl salt plates. The coldring fraction was dissolved in HPLC grade chloroform and cast on to the salt plates. The chloroform was allowed to evaporate and additional coldring fraction was cast onto the plates. This procedure was repeated until a uniform, thin film of coldring fraction residue covered the surface of both salt plates and the chloroform was completely evaporated. The plates were placed in a 25 mm diameter cell holder for IR analysis.

3.1.3 GAS PHASE FT-IR

Gaseous products resulting from the carbonization of mesophase pitch were analyzed by FT-IR by distilling them under vacuum into a gas IR cell cooled to -196°C with liquid nitrogen. Condensible volatiles were distilled into a cold finger under a 32 mm diameter window gas IR cell with NaCl windows. Noncondensible volatiles were distilled into a second gas IR cell containing 5 angstrom molecular sieve in a cold finger and possessing 25 mm diameter NaCl windows. The cells were heated with a hot air gun following their removal from the vacuum line to ensure rapid evolution of gasses from the cold finger into the

body of the cell. The gas IR cells were placed directly in the FT-IR sample compartment and held in place by a specially designed and constructed cell holder. Three separate scans approximately 10 minutes apart were accomplished in order to ensure complete equilibration of the noncondensible gases over the molecular sieve.

3.2 THERMAL GRAVIMETRIC ANALYSIS

Thermal Gravimetric Analysis (TGA) of unoxidized and oxidized pitch samples were performed on a Perkin Elmer TGA-7 thermogravimetric analyzer under a nitrogen atmosphere (flow rate controlled at 30-40 ml/min). Sample size was in the range of 5 to 10 mg. Pitch samples were heated from room temperature to 1000°C at a rate of 10°C per minute.

3.3 THERMAL VOLATILIZATION ANALYSIS

Samples of unoxidized and oxidized pitch (100mg) were studied by Thermal Volatilization Analysis (TVA) in a continuously evacuated system. A vacuum on the order of 10^{-4} Torr was achieved through the combination of a rotary oil vacuum pump and a silicon oil diffusion pump with cold traps. Samples of pitch were placed in a quartz crucible and heated in a Vicor™ glass tube which was surrounded by a muffle furnace and attached to the vacuum line by an adapter with

an internal cold finger. A reproducible heating ramp of approximately 9°C/min from room temperature to 900°C was achieved by use of an Omega CN 2011K microprocessor temperature controller. A calibration experiment was performed to determine the true sample temperature based on oven temperature data as measured by the thermocouple output over the course of the experiment. A description of this calibration experiment is contained in the literature [19]. The internal cold finger was kept cool by a continuous flow of water. Volatiles emitted during the carbonization process were recorded by a series of 4 Edwards PRE 10K pirani gauges attached to the vacuum line at different points. Pirani gauge 1 was situated adjacent to the sample tube and measured total volatile production. Pirani gauge 2 was located immediately following a trap cooled to -75°C with an acetone/dry ice slurry. The difference between the two gauges represents a nonlinear measure of the production of room-temperature liquids such as water and benzene. Pirani gauge 3 was located following a trap cooled to -196°C with liquid nitrogen. The difference in readings between gauges # 2 and 3 measured the content of condensible gasses, mainly carbon dioxide. The final guage, pirani number 4, was situated following a molecular sieve trap cooled to -196°C with liquid nitrogen, and measured the production of hydrogen gas. The

difference between gauges # 3 and 4 represents a measure of other noncondensible gases (CO, CH_4, N_2, etc.) produced during degradation. Pirani gauge output was routed through an Omega Dataplex 10™ signal switcher to a two pen stripchart recorder, along with the output from the oven temperature thermocouple. This arrangement allowed for the recording of volatile production as a function of oven temperature. Referencing the calibration curve obtained from the calibration experiment then yielded true sample temperature at any stage of the ramp.

Upon completion of the temperature ramp, the residue (coke) of carbonization was then collected and weighed. The internal cold finger was washed with chloroform to collect the oligomeric "coldring" fraction for subsequent gravimetric and IR analysis.

3.4 SUB-AMBIENT THERMAL VOLATILIZATION ANALYSIS

Sub-Ambient Thermal Volatilization Analysis (SATVA) was performed on all condensible and noncondensible volatiles collected during the TVA experiments.

Condensible volatiles collected in the traps at -75°C and -196°C were distilled under vacuum to a third trap cooled to -196°C with liquid nitrogen and surrounded by parrafin wax. The parrafin wax contained a chromel alumel thermocouple which was connected to an Omega cold junction compensator. The compensator

produced a voltage output corresponding to an ice/water trap, thus standardizing the thermocouple output. The mV output from the thermocouple circuit was recorded on a stripchart recorder, giving a record of the trap temperature as a function of time. The liquid nitrogen was removed from the trap, and the parrafin wax was allowed to warm up slowly to room temperature, achieving a temperature of 0°C after approximately 90 minutes. Gases evolved from the trap as it warmed up were detected by pirani gauge 3 and recorded on the strip-chart recorder along with trap temperature. Evolving gases were condensed into a "collection" trap cooled to -196°C and then distilled directly into a gas IR cell for subsequent IR analysis.

Noncondensible volatiles were released from the molecular sieve trap by surrounding the trap with a hot water bath. The gas was then condensed directly into a gas IR cell which contained molecular sieve cooled to -196°C with liquid nitrogen in a cold finger. The efficiency of the transfer was recorded using a pirani gauge within the distillation chamber and was routinely estimated as greater than 99%.

4. RESULTS AND DISCUSSION

4.1 OXIDATIVE STABILIZATION

4.1.1 WEIGHT CHANGE CURVES AND THE OXIDATION PROCESS

A common means of characterizing the oxidation of mesophase pitch is to record weight change as a function of time at a given oxidation temperature [20]. The resulting curve(s) are designated as "weight change curves" and offer some degree of insight into the chemical processes occurring during oxidation. The weight change curves for the oxidation of napthalene-derived mesophase pitch at temperatures of 240, 270, 290, 320, and 340°C are given in figure 3. The most fundamental feature of these curves is that they indicate a competition between the weight gain and weight loss processes. In addition, the shape of the curve is clearly related to the oxidation temperature. At a relatively low oxidation temperature of 240°C, we see an extended period of weight gain out to approximately 4 hours, at which point the weight gain reaches a maximum value of about 10%, and then begins to decrease. As the oxidation temperature is increased, we see a shorter period of weight gain, a lower value for the maximum % weight gain, and a more rapid rate of weight loss thereafter. At the relatively high

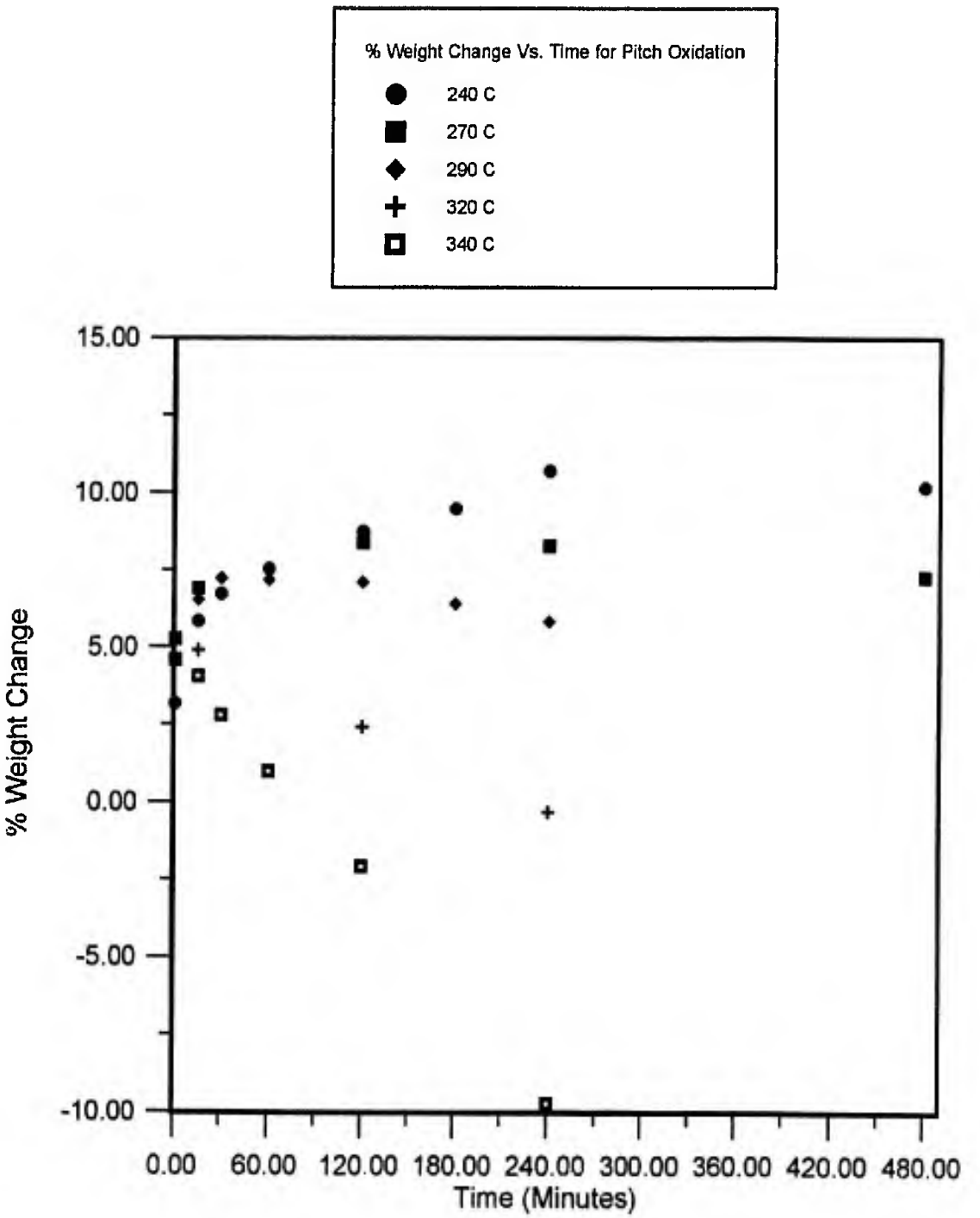

Figure 3. Weight change curves for mesophase pitch oxidation

oxidation temperature of 340°C , the weight change curve indicates that the weight gain has reached a maximum recorded value, about 5%, at the end of the heating ramp from room temperature to 340°C, corresponding to zero minutes on the isothermal time scale. During the remainder of the isothermal oxidation profile at 340°C, the pitch shows only weight loss. At an oxidation temperature of 290°C, between the two extremes, we see a maximum weight gain of approximately 7% at 30 minutes oxidation time, and then a weight loss rate that appears to be intermediate between that observed at 240 and at 340°C.

It is important at this point to note that we cannot describe or characterize the full chemical process associated with mesophase pitch oxidation from an analysis of the weight change curves alone. This has been attempted by other researchers; some of whom have tried to relate the complete oxidative stabilization of a pitch sample to the point on the weight change curve where the weight gain has reached a maximum value [7, 9]. From an analysis of the weight change curves alone we can state only that there is a competition between chemical processes involving both weight gain and weight loss. Furthermore, it appears that the chemical process resulting in weight gain predominates at lower oxidation temperatures and time periods, while that corresponding to weight loss predominates at higher

oxidation temperatures and longer periods of oxidation. To try to ascribe the weight gain or weight loss to a specific chemical reaction or to the involvement of any single molecular structure in the pitch is not possible at this point.

4.1.2 KINETIC ANALYSIS OF PITCH OXIDATION

It is possible to construct a plot from the data contained in the weight change curves that gives relative information on the kinetics involved in the oxidation of mesophase pitch. Knowing the weight of the pre-oxidized pitch sample, along with the % weight change and time information used to construct the weight change curves, we can obtain the curves shown in figure 4. These curves are Arrhenius-type plots in that they relate the natural log of a reaction rate to the inverse of the reaction temperature in Kelvin. For the oxidation of mesophase pitch, we have defined the rate of reaction as:

$$\text{Rate} = 1/w \, (dw/dt)$$

where w is the weight of the pitch sample and dw/dt is the change in weight for a given change in time. The absolute value of dw/dt is used because we have both weight gain and weight loss processes to account for. Because the shape of the weight change curves indicate a competition between weight gain and weight loss processes, it was necessary to first separate the two processes on the time scale

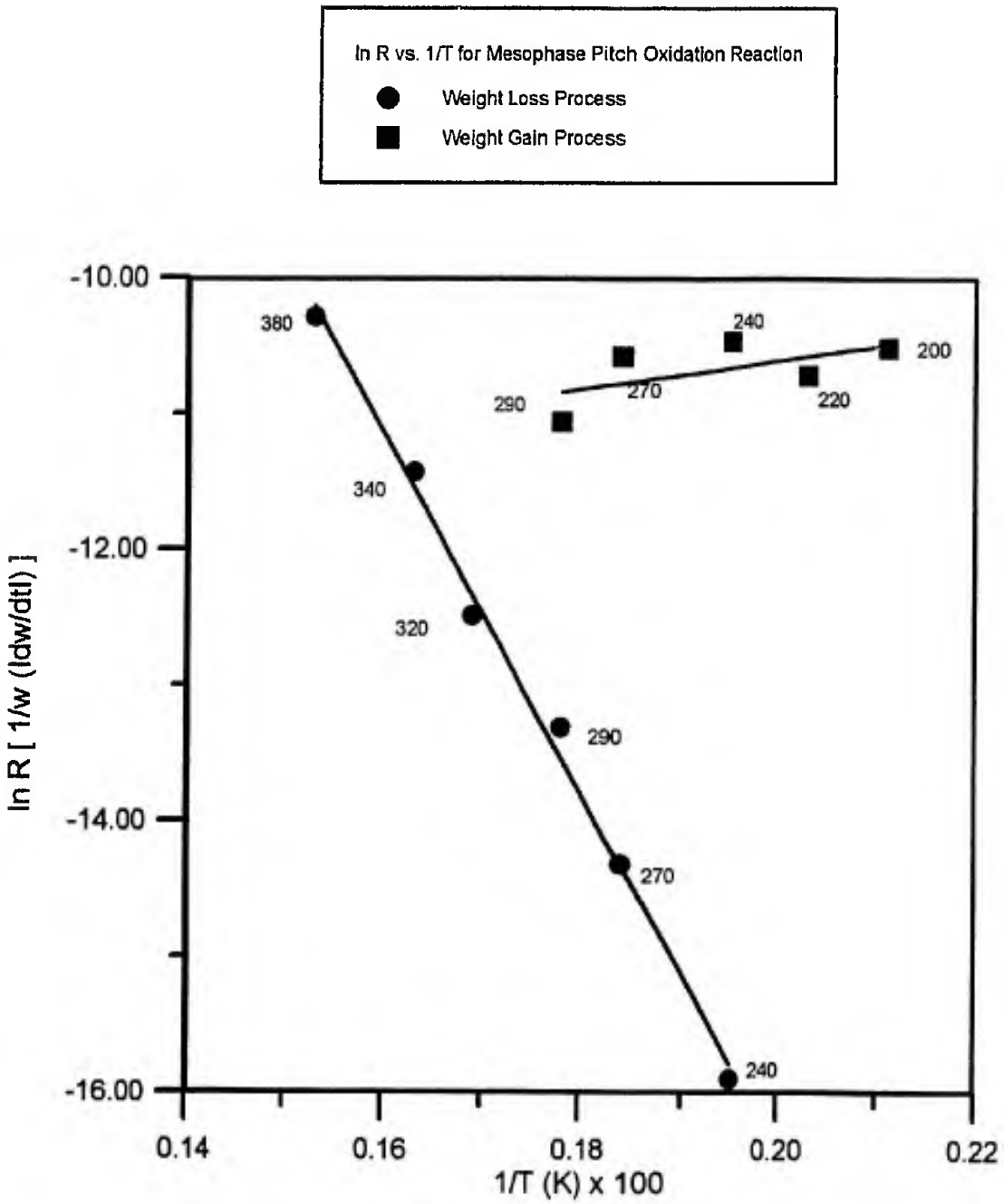

Figure 4. Arrhenius-type plot of mesophase pitch oxidation data

as completely as possible and perform calculations within time periods at which sample weight changed in an approximate linear fashion with time. To accomplish this, the rate of the weight gain process was computed as an average of that observed between 0 and 15 minutes oxidation time at lower isothermal oxidation temperatures (i.e., dt = 15 min and dw = weight change within that time interval). The weight loss reaction rate was taken as that observed between 2 and 4 hours (120 and 240 minutes) oxidation time for all temperatures with the exception of 240°C where it was calculated between 8 to 12 hours oxidation time.

A comparison of the resultant curves in figure 4 for the weight gain and weight loss processes indicates that the weight loss process has a much steeper slope and thus a greater temperature dependency and therefore overall activation energy than the weight gain process. At lower temperatures (240°C and below) it is quite evident that the weight gain process proceeds much more rapidly than the weight loss process, on the order of 250 times faster. This fact would lead us to believe that at 240°C we would see only weight gain during the entire course of the oxidation profile. However, this is not the case, as observed in the weight change curve at 240°C in figure 3. We know that the weight gain has reached a maximum at approximately 240 minutes oxidation time, after which weight begins to be lost.

The simple consequence of this is that the weight gain process (for whatever reason) is eventually exhausted; that is, the reaction pathway resulting in weight gain produces a limited yield of product, and once exhausted allows us to detect the reaction pathway resulting in weight loss (which we believe to be operative from the onset of the oxidation process). As the oxidation temperature is increased, we see a narrowing of the gap in the relative reaction rates of the weight gain and weight loss processes. Consequently, we see in the weight change curves an apparent shorter period of weight gain, a lower value for the maximum % weight gain, and a steeper slope associated with the weight loss process. The reason for the apparent decrease in the rate of the weight gain process as the temperature is increased is easily explained. At temperatures above approximately 270°C, a significant fraction of the weight gain is occurring during the actual heating ramp. By the time the isothermal oxidation temperature is reached, a significant fraction of the reaction pathway resulting in weight gain has been exhausted. Thus, when the rate of the weight gain process is measured between 0 and 15 minutes, we see an apparent decrease in the rate. We know, of course, that the process resulting in weight gain is actually faster at higher temperatures, but this is a difficult process to depict quantitatively throughout a heating ramp.

Furthermore, at oxidation temperatures above 320°C, the weight gain process is exhausted during the heating ramp so that we "see" a maximum % weight gain at time zero on the weight change curve and a steady weight loss thereafter, with a slope corresponding to the absolute rate of the weight loss "reaction" as shown in figure 4.

We now have a better qualitative understanding of the kinetics of the chemical processes involved in the oxidation of mesophase pitch. We know there exists a reaction pathway for weight gain that is limited. There is also a reaction pathway for weight loss that proceeds much more slowly than the weight gain process at oxidation temperatures below 320°C. The weight gain process thus "masks" the weight loss process until it is exhausted. Thereafter we observe only the weight loss process. It is important to realize that even though the weight loss process is effectively "masked" by the weight gain process at lower oxidation temperatures and shorter times, it is still occurring and must be taken into account in any rationalization of the "overall" reaction. For this reason, the following relationship was used when constructing the plot of reaction rate vs. 1/T in figure 4 for the weight gain process:

$$\text{Measured Weight Change}_{(0\text{-}15\ \text{min})} = \text{Weight Gain}_{(0\text{-}15\ \text{min})} - \text{Weight Loss}_{(0\text{-}15\ \text{min})}$$

The value corresponding to "Measured Weight Change $_{(0\text{-}15\ min)}$" in the equation above is the actual recorded value of weight change measured between 0 and 15 minutes oxidation time. This measured value, however, does not reflect purely weight gain because the process resulting in weight loss is also occurring between 0 and 15 minutes oxidation time but is "masked" by the weight gain. Therefore, to find the true weight gain occurring between 0 and 15 minutes, we must re-arrange the above equation:

$$\text{True Weight Gain}_{(0\text{-}15\ min)} = \text{Measured Weight Change}_{(0\text{-}15\ min)} + \text{Weight Loss}_{(0\text{-}15\ min)}$$

The value used for true weight gain is then equal to the measured weight change occurring between 0 and 15 minutes, plus a value for the calculated weight loss occurring between 0 and 15 minutes. This calculated weight loss value is determined simply by multiplying the measured value for dw/dt occurring between 120 and 240 minutes oxidation time at the particular oxidation temperature by 15 minutes.

The same process above for finding true weight gain is not necessary for finding the true weight loss used in constructing the plot in figure 4. This is because the actual measured weight change occurring between 120 and 240 minutes is equal to true weight loss; the weight gain reaction is not occurring at

this point in the oxidation profile. The equation is thus:

$$\text{Measured Weight Change}_{(120\text{-}240\ min)} = \text{True Weight Loss}_{(120\text{-}240\ min)}$$

As it turned out, the amount of weight loss occurring between 0 and 15 minutes oxidation time was so small in comparison to the weight gain at these lower temperatures, that adding the calculated value for weight loss changed the measured value for the weight change by less than 1%.

The other major piece of information we get from the kinetic analysis of the pitch oxidation data is that the weight loss process has a greater temperature dependency than the weight gain process. This is equivalent to stating that the weight loss process has a greater activation energy than the weight gain process. The slope of the line corresponding to the weight loss process in figure 4 yields an activation energy of about 111 KJ/mole. An activation energy for the weight gain process has not been calculated because the slope of the line in figure 4 for the weight gain process would yield a negative value for the activation energy. Once again, this is due to the fact that at higher oxidation temperatures, the weight gain reaction is occurring predominately during the temperature ramp. This results in a decrease in the measured rate of the weight gain reaction when measured between 0 and 15 minutes oxidation time. In addition to the negative slope, the

calculated best fit line for the weight gain process in figure 4 has a coefficient of determination value (R) of 0.597. This value reflects the significant scatter in the points and is a consequence of the weight gain process occurring partly during the heating ramp. In contrast, the weight loss process yields a calculated best fit line with an R of 0.998. We believe, however, based on the magnitude of the weight gain experienced and the fact that it occurs rapidly during the temperature ramp, that the weight gain is the result of a very low activation energy process. At this point we still do not know the chemical species or molecular structures involved in these competing processes.

4.1.3 FT-IR SPECTRA OF OXIDIZED PITCH

Figure 5 compares the IR spectra of unoxidized pitch with that of pitch oxidized at 200°C for 48 hours from 700 to 2000 wavenumbers. In this region of the IR spectrum we can see some remarkable differences between oxidized and unoxidized pitch. Unoxidized pitch shows two absorbance bands of similar intensity at approximately 1440 and 1600 cm^{-1}. These bands are ascribed to the methylene hydrogen in-plane bending or "scissoring" mode of saturated hydrocarbons, and the aromatic carbon-carbon ring stretching mode, respectively [21]. The relatively strong intensity of the methylene hydrogen bending mode centered

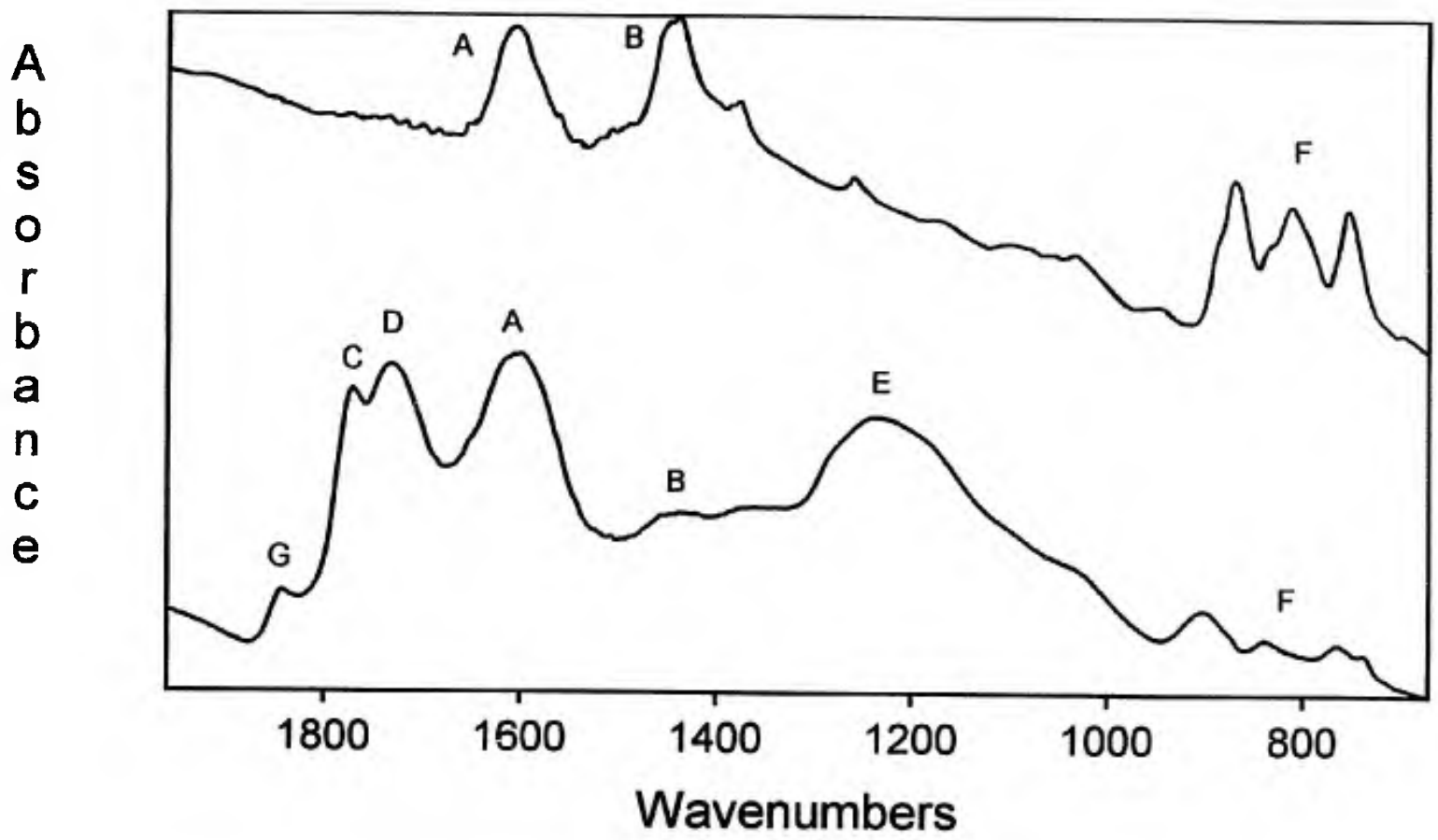

Figure 5. IR spectra of unoxidized pitch (top) and pitch oxidized at 200°C for 48 hours (bottom); A = 1600 cm^{-1}, B = 1440 cm^{-1}, C = 1772 cm^{-1}, D = 1734 cm^{-1}, E = 1250 cm^{-1}, F = 700-900 cm^{-1}, G = 1845 cm^{-1}

at 1440 cm^{-1} is due to the presence of significant quantities of saturated or napthenic rings in the unoxidized pitch (see figure 1). It is possible to compare the relative intensities of this absorbance at 1440 cm^{-1} to that at 1600 cm^{-1} resulting from aromatic carbon-carbon stretching to gauge the relative quantities of saturated (aliphatic) and unsaturated (aromatic) carbons in the pitch. Notice in figure 5 that the intensity of the peak due to the methylene hydrogen bending mode is absent from the IR spectrum of oxidized pitch, while the intensity of the carbon-carbon stretching mode at 1600 cm^{-1} remains at a similar strength. This suggests that aliphatic material is quantitatively consumed during the oxidation process.

Another major difference in the two spectra is the appearance of a carbonyl stretching band centered at about 1700 cm^{-1} in the oxidized pitch. Upon closer examination it appears that the band is comprised of at least two bands, one at approximately 1734 wavenumbers, and the other at 1772 wavenumbers. These bands are ascribed to ester and anhydride functionality, respectively. The relatively weak band appearing at 1845 wavenumbers is assigned to the asymmetric carbonyl stretching mode of phthalic anhydride [22]. A broad band centered at approximately 1250 cm^{-1} also appears in the IR spectra of oxidized

pitch. This band is ascribed to the carbon-oxygen-carbon asymmetric stretching mode which is common to esters, anhydrides, and ethers [21]. Figures 6, 7, and 8 illustrate oxygen functionalities and their characteristic IR absorbance bands as measured in reference compounds. They are included here as a resource to help analyze the many different IR absorbance bands appearing in the IR spectra of oxidized pitch.

Finally, in figure 5, we see a series of 3 distinct peaks for unoxidized pitch in the region of 700-900 wavenumbers. These peaks arise from the out-of-plane bending mode of isolated, 2-adjacent, and 4-adjacent aromatic hydrogens [21]. This triplet of peaks is helpful in gauging the relative concentration of aromatic hydrogens in different pitch samples; notice the significant decrease in the intensity of this triplet upon oxidation.

Figure 9 shows the IR spectra of unoxidized and oxidized pitch in the region of 3200-2800 wavenumbers. In this region of the IR spectrum we can see absorbances due to aromatic carbon-hydrogen stretching at approximately 3050 cm^{-1}, and aliphatic carbon-hydrogen stretching at 2920 cm^{-1} [21]. Notice that the intensity of the aliphatic carbon-hydrogen stretching band in unoxidized pitch is much greater than that of the aromatic carbon-hydrogen stretching mode. This is

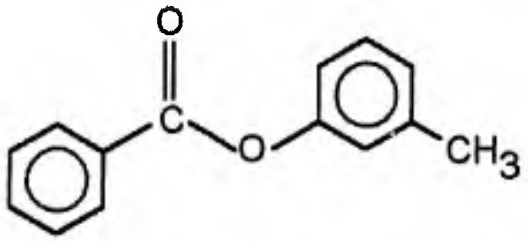

Benzoic acid p-tolyl ester [1735]

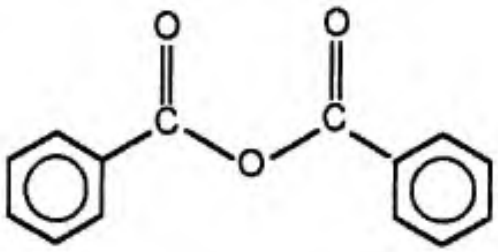

Benzoic anhydride [1770, 1219, 1169]

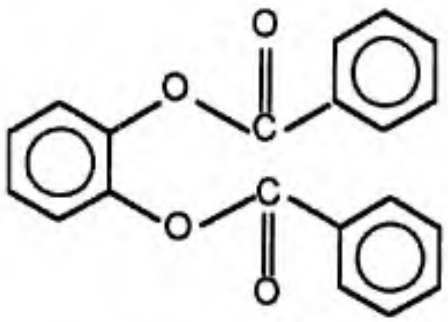

Pyrocatechol dibenzoate [1750, 1250, 1169]

Figure 6. Sample compounds containing ester and anhydride functionality; characteristic absorbance bands shown in brackets as wavenumbers

Source: The Sadtler Handbook of Infrared Spectra, William W. Simons, Ed., Philadelphia: Sadtler Research Laboratories, Inc., 1978

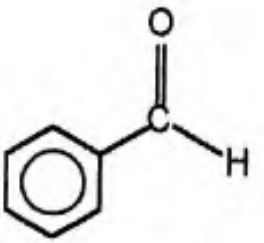

Benzaldehyde [1700]

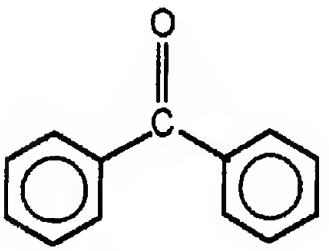

Benzophenone [1660]

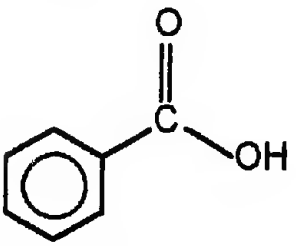

Benzoic Acid [1698, 1294]

Figure 7. Sample compounds containing other carbonyl functionality; characteristic absorbance bands shown in brackets as wavenumbers

Source: The Sadtler Handbook of Infrared Spectra, William W. Simons, Ed., Philadelphia: Sadtler Research Laboratories, Inc., 1978

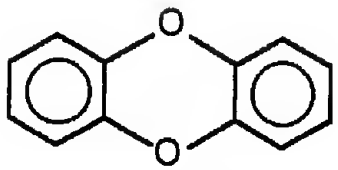

Dibenzo-p-dioxin [1290, 1190]

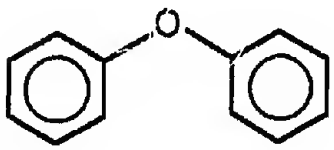

Diphenyl Ether [1250, 1171]

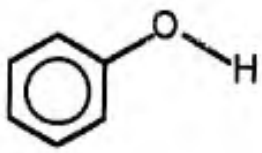

Phenol [1285, 1162]

Figure 8. Sample compounds containing ether/phenol structures; Characteristic absorbance bands shown in brackets as wavenumbers

Source: The Sadtler Handbook of Infrared Spectra, William W. Simons, Ed., Philadelphia: Sadtler Research Laboratories Inc., 1978

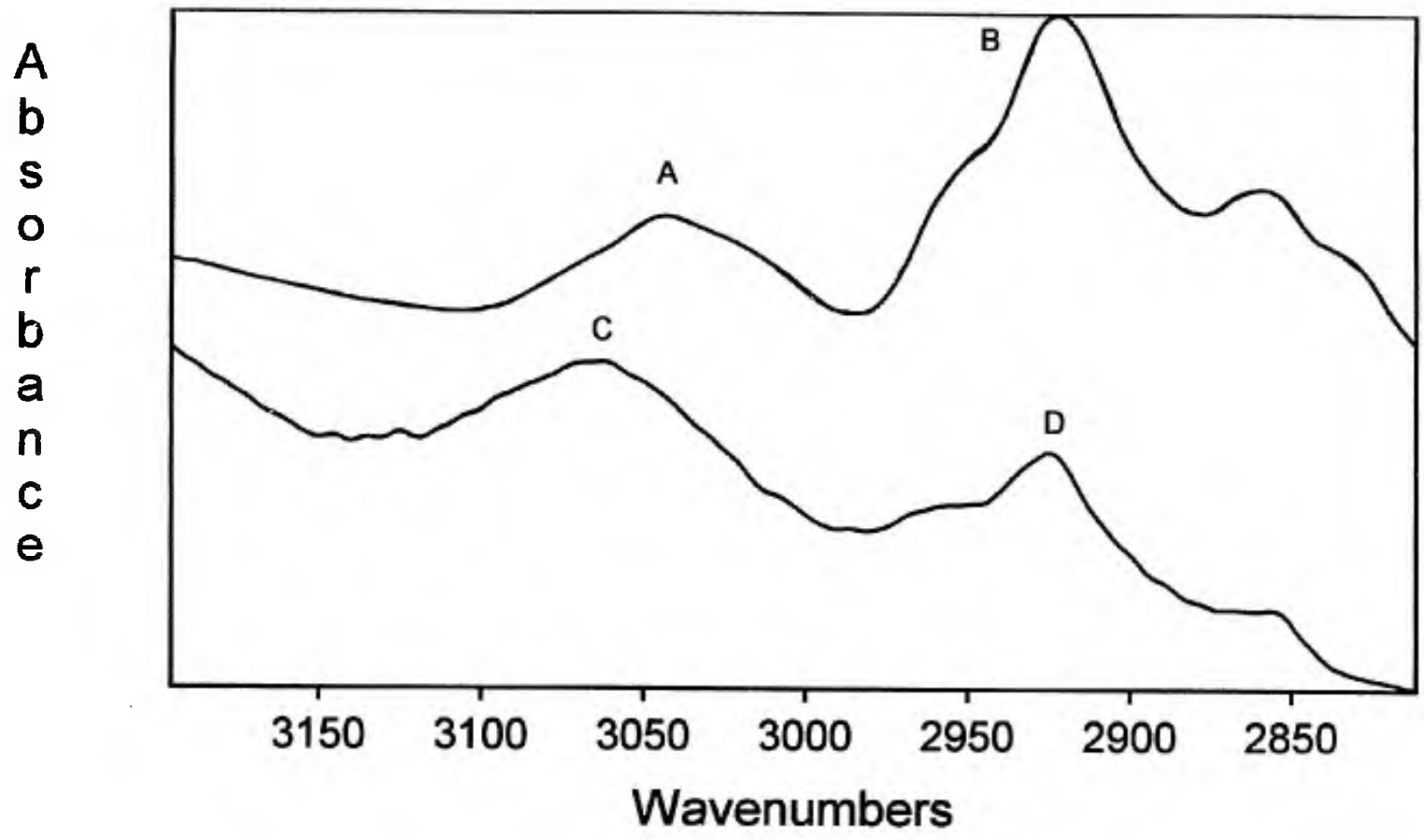

Figure 8. IR spectra of unoxidized pitch (top) and pitch oxidized at 200°C for 48 hours (bottom), 2800-3200 wavenumbers; A = 3050 cm^{-1}, B = 2920 cm^{-1}, C = 3060 cm^{-1}, D = 2920 cm^{-1}

in part due to the much greater extinction coefficient of the aliphatic mode. For oxidized pitch, the stretching modes are of approximately equal intensity, indicating a loss of aliphatic content upon oxidation, thus confirming our conclusions with regards the loss of absorbance at 1440 cm^{-1}.

Figure 10 compares the IR spectra of a pitch oxidized at 240°C for 4 hours to the same spectra following a computer-enhanced self deconvolution of the peaks. The deconvolution program can provide some isolation of the individual, overlapping absorbance modes which contribute to a broad absorbance band. For this particular spectra, the deconvolution showed clearly that the IR absorbance mode centered at about 1700 cm^{-1} is made up of 5 distinct peaks: 1686, 1700, 1717, 1734, and 1772 cm^{-1}. Referencing figures 6 and 7 indicates that our oxidized pitch contains ketone, acid, and aldehyde functionality in addition to esters and anhydrides.

Figure 11 compares the IR spectra of pitch oxidized at 240°C at t_0 (corresponding to the end of the heating ramp to 240°C) to pitch oxidized at 240°C for 4 hours. We see a decay in the intensity of the methylene hydrogen bending mode at 1440 wavenumbers between time zero and 4 hours, indicating a loss of napthenic ring structures in the pitch. If we compare the spectra of pitch oxidized

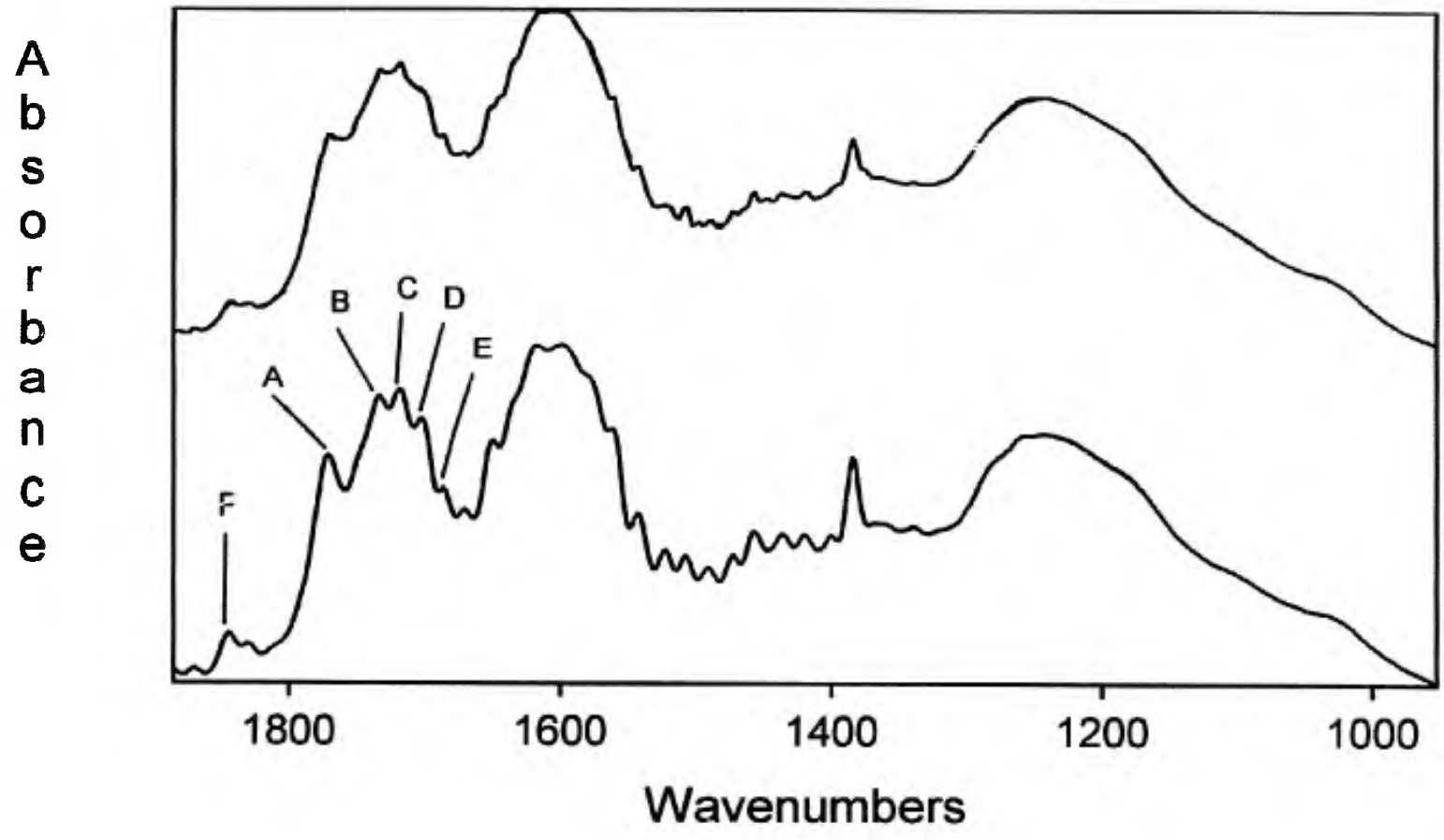

Figure 10. IR spectra of pitch oxidized at 240°C for 4 hours (top) and same spectra after computer enhanced deconvolution of peaks (bottom); A = 1772 cm^{-1}, B = 1734 cm^{-1}, C = 1717 cm^{-1}, D = 1700 cm^{-1}, E = 1686 cm^{-1}, F = 1845 cm^{-1}

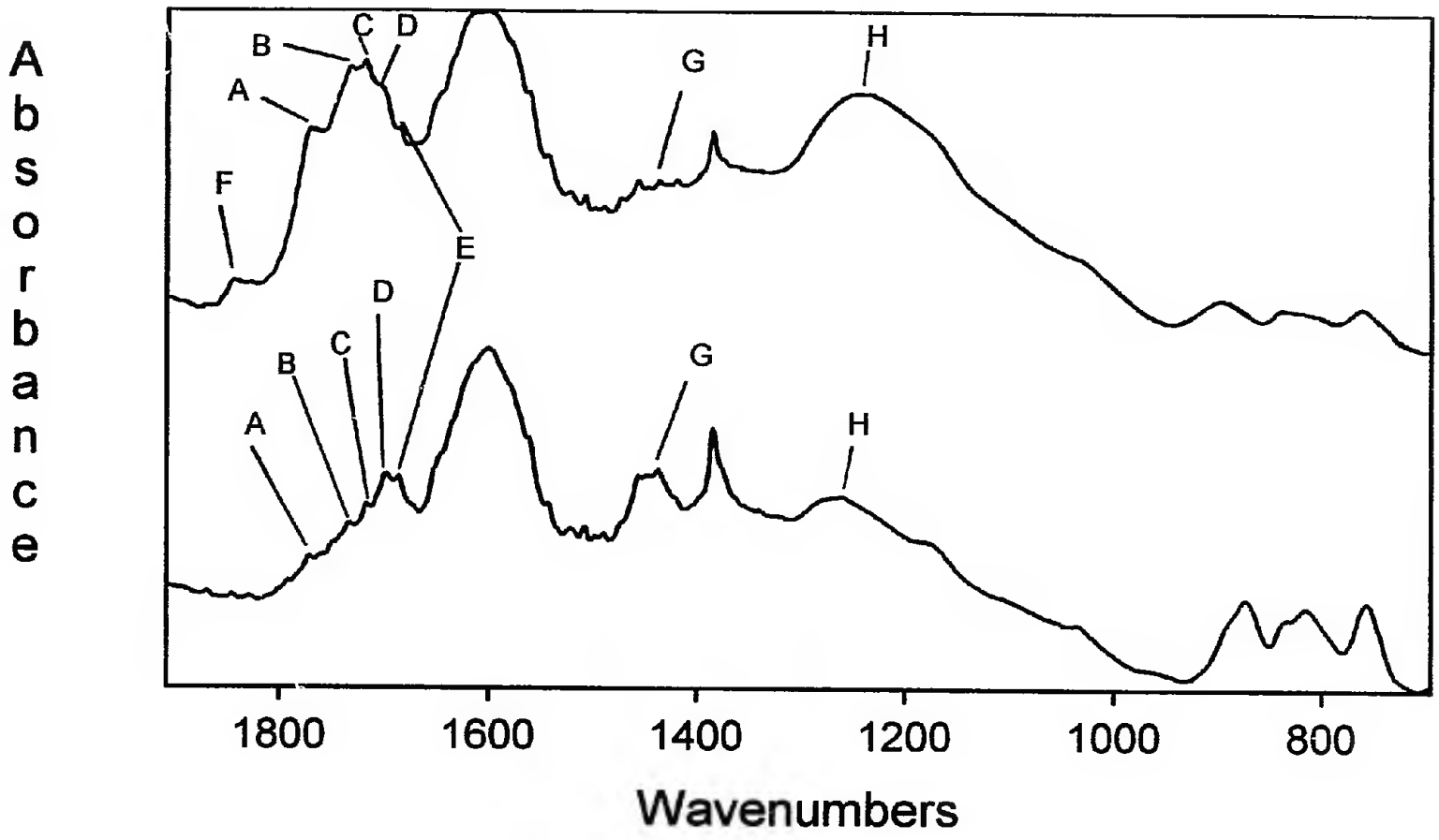

Figure 11. IR spectra of pitch oxidized at 240°C for 4 hours (top) and to end of heating ramp to 240°C (bottom); A = 1772 cm^{-1}, B = 1734 cm^{-1}, C = 1717 cm^{-1}, D = 1700 cm^{-1}, E = 1686 cm^{-1}, F = 1845 cm^{-1} G = 1440 cm^{-1}, H = 1250 cm^{-1}

at 240°C at t_0 to the spectra of unoxidized pitch in figure 5, we see an already significant loss of peak intensity at 1440 cm^{-1} upon completion of the heating ramp to 240°C. The 1440 cm^{-1} peak in unoxidized pitch is approximately equal in intensity to the aromatic carbon-carbon stretching mode at 1600 cm^{-1}. The 1440 cm^{-1} peak is severely attenuated in the spectrum of pitch at t_0 (240°C). It is almost completely removed after oxidation at 240°C for 4 hours. There is also a significant decay in the intensity of the triplet of peaks between 700 and 900 cm^{-1} (due to aromatic hydrogen bending) upon oxidation to 4 hours at 240°C. This indicates a loss of both napthenic ring structures and aromatic hydrogens during the oxidation process.

The other major change resulting from the oxidation to 4 hours at 240°C is the growth of the carbonyl stretching band around 1700 wavenumbers. Notice that for oxidation at time zero (t_0, 240°C) the envelope is dominated by lower wave-number absorbances, with the bands at 1686 and 1700 cm^{-1} much stronger in intensity than those at 1717, 1734, and 1772 cm^{-1} which appear as a high wavelength "shoulder" on the carbonyl absorbance. Upon oxidation to 4 hours (figure 11), not only has the entire carbonyl band grown in intensity, but now the band at 1717 cm^{-1} gives the most intense absorbance, with the band at 1734 cm^{-1}

almost equal in intensity. The bands at 1686 and 1700 cm^{-1} are now "shoulder" peaks. Ketone/aldehyde/acid functionality thus seems to predominate at the very shallow oxidation profile of a ramp to 240°C, while ester and anhydride functionality become more predominate after a longer isothermal oxidation at 240°C. The growth of the band centered at 1250 cm^{-1} is also noted, consistent with the expected increase of ester and anhydride functionality in the oxidized pitch.

Figure 12, comparing oxidation of pitch at 340°C at t_0 and after 4 hours, shows a strikingly different result from that corresponding to oxidation at 240°C in figure 11. The methylene hydrogen bending mode has been quantitatively removed during the temperature ramp. Notice there is little further change in the intensity of the bulk of this mode between t_0 and 4 hours, reinforcing our claim that napthenic rings were removed during the heating ramp to 340°C. In addition, the ratio of intensities of the carbonyl stretching band around 1700 cm^{-1} to the aromatic carbon stretching band centered at 1600 wavenumbers remains relatively constant during oxidation at 340°C. There is also very little change in the intensity of the 3 aromatic hydrogen bending modes in the "fingerprint" region of the spectrum between t_0 and 4 hours at 340°C. These results suggest

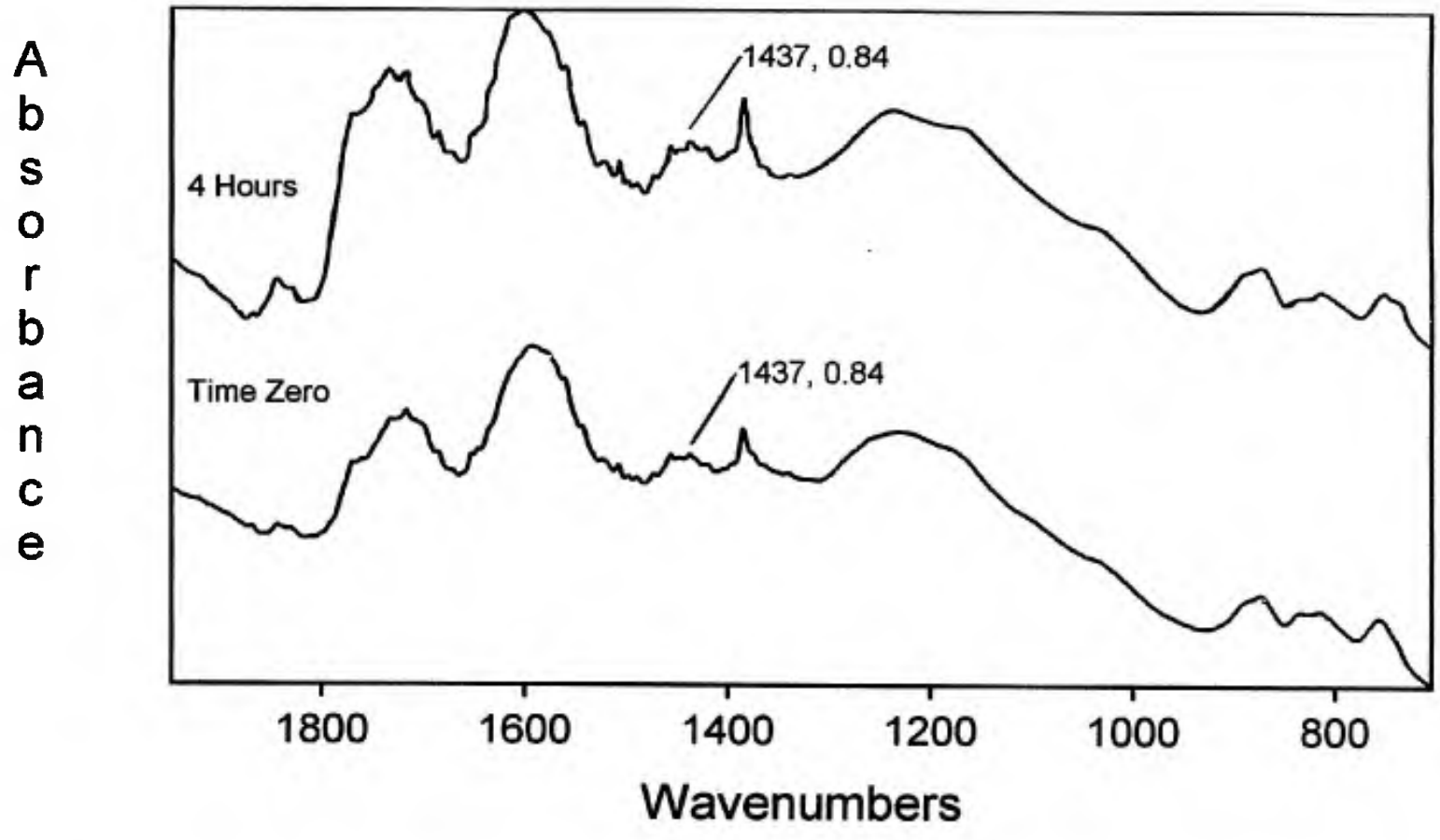

Figure 12. IR spectra of pitch oxidized at 340°C for 4 hours (top) and to end of heating ramp to 340°C (bottom)

that the oxidation reaction is significantly exhausted during the heating ramp to 340°C. This correlates well with the weight change curve for oxidation at 340°C as shown in figure 3. Recall that the pitch had reached its maximum weight at the end of the heating ramp (time zero). In figure 11, we saw that upon completion of the heating ramp to 240°C there was still a relatively intense band at 1440 wavenumbers indicating the presence of residual napthenic ring structures. The peak then disappeared upon oxidation to 4 hours at 240°C. This correlates well with an oxidation process which begins during the heating ramp and is completed during the isothermal "soak" at 240°C. Furthermore, the carbonyl band has clearly grown in intensity between time zero and 4 hours at 240°C when compared to the aromatic band at 1600 cm^{-1}. This observation again is consistent with the shape of the weight change curve for oxidation at 240°C in figure 3 which indicates that the pitch is clearly gaining weight between t_o and 4 hours oxidation time.

Based on the information contained in these IR spectra and in the weight change curves, the qualitative statement can be made that the weight gain process associated with pitch oxidation involves the loss of napthenic ring structures and the introduction of oxygen as carbonyls, specifically as ester and anhydride

functionality; that the weight gain process possessed a lower activation energy than the weight loss process, and that the napthenic ring content is the limiting factor in the conversion to oxidized structures.

4.1.4 SEMI-QUANTITATIVE ANALYSIS OF PITCH OXIDATION

FT-IR spectra of oxidized pitches indicate an uptake of oxygen as carbonyl functionality and a loss of methylene hydrogens as a result of that oxidation. In figure 11 we saw these effects for the oxidation of pitch at 240°C. It would be beneficial if we could define more quantitatively the effect of time and the temperature of oxidation on both the introduction of oxygen into the pitch, and the loss of saturated, napthenic ring structures. It is possible, in the absorbance mode, to track semi-quantitatively both the oxygen content and the saturated ring content of the pitch by integrating the areas under the peaks in the IR spectra corresponding to these functionalities. In order to normalize these integrations with respect to differences in sample concentration, we can use as an internal standard the area of the peak due to aromatic carbon-carbon stretching centered at 1600 cm^{-1}. Recall from figures 5, 11, and 12 that the relative intensity of this band did not appear to change during oxidation. Our strategy, then, was to base our semi-quantitative analysis on a ratio of peak areas with the area of the peak of

interest as the numerator, and the area of the peak at 1600 cm^{-1} as the denominator. Differences in sample concentration resulting from variations in the preparation of the KBr pellets are taken into account by this ratio.

Figure 13 shows a plot of the ratio of the normalized peak areas for the 1700 wavenumber and 1250 wavenumber bands vs. time at an oxidation temperature of 240°C. There is a steady monotonic increase in the magnitude of the peak area ratios for both the 1700 cm^{-1} (carbonyl functionality) and the 1250 cm^{-1} (carbon-oxygen-carbon single bond asymmetric stretching) bands out to approximately 240 minutes (4 hours) oxidation time. At later times the oxygen content continues to rise but at a much reduced rate. Reference to the weight change curve for oxidation at 240°C in figure 3 shows that the reduction in gradient at 240 minutes of the curves in figure 13 is coincident with the point at which the weight change curve reaches its maximum value. This direct correlation between weight gain and oxygen uptake is further substantiated by the plot in figure 14. Here we show a plot of the same ratios of peak area for the normalized 1700 and 1250 wavenumber bands plotted against the percent weight gain. The resulting curves indicate a clear relationship between oxygen content and weight gain during oxidation. Note that the normalized oxygen content continues to rise after the

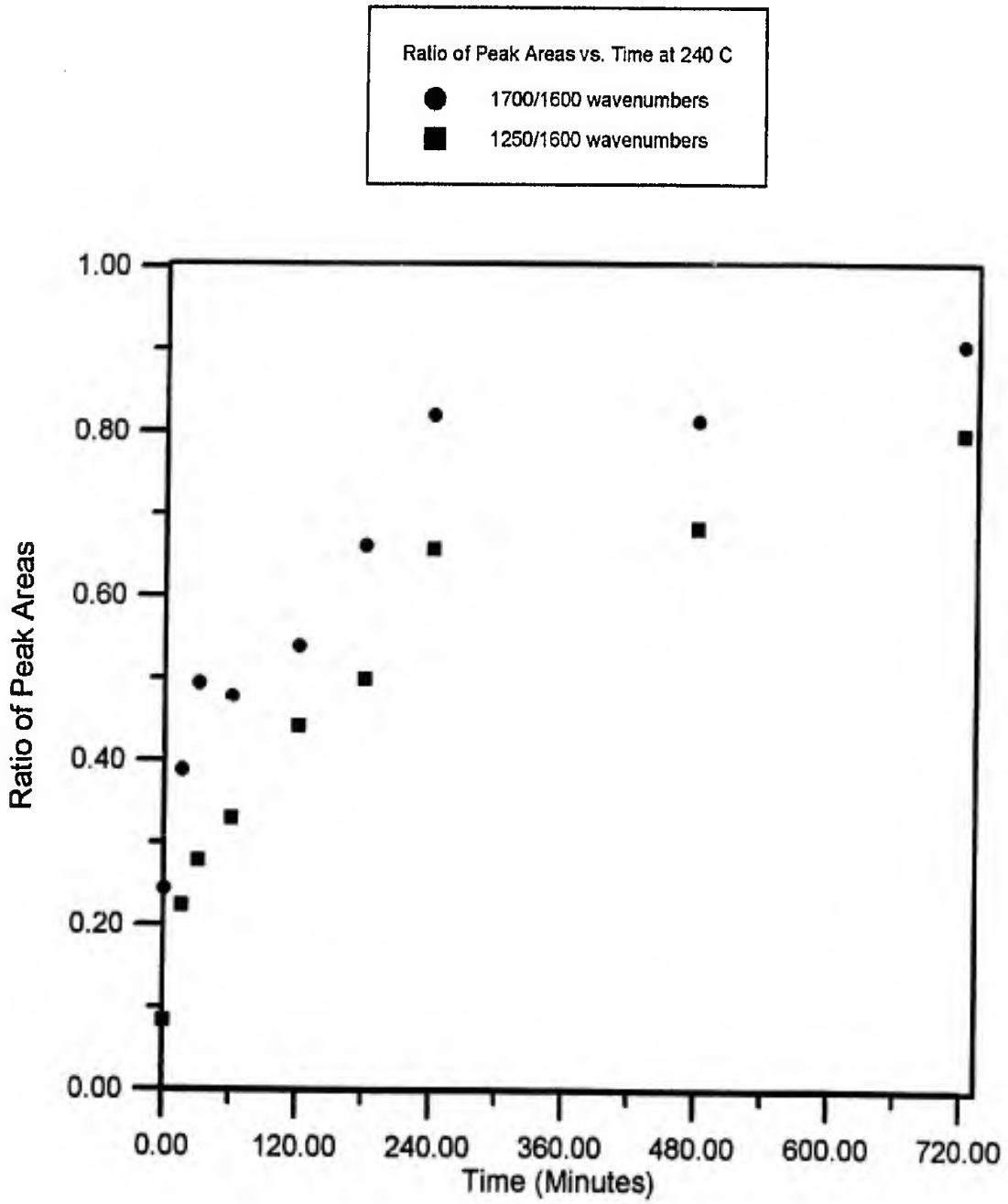

Figure 13. Plot of ratio of peak areas for 1700 and 1250 wavenumbers vs. oxidation time at 240°C

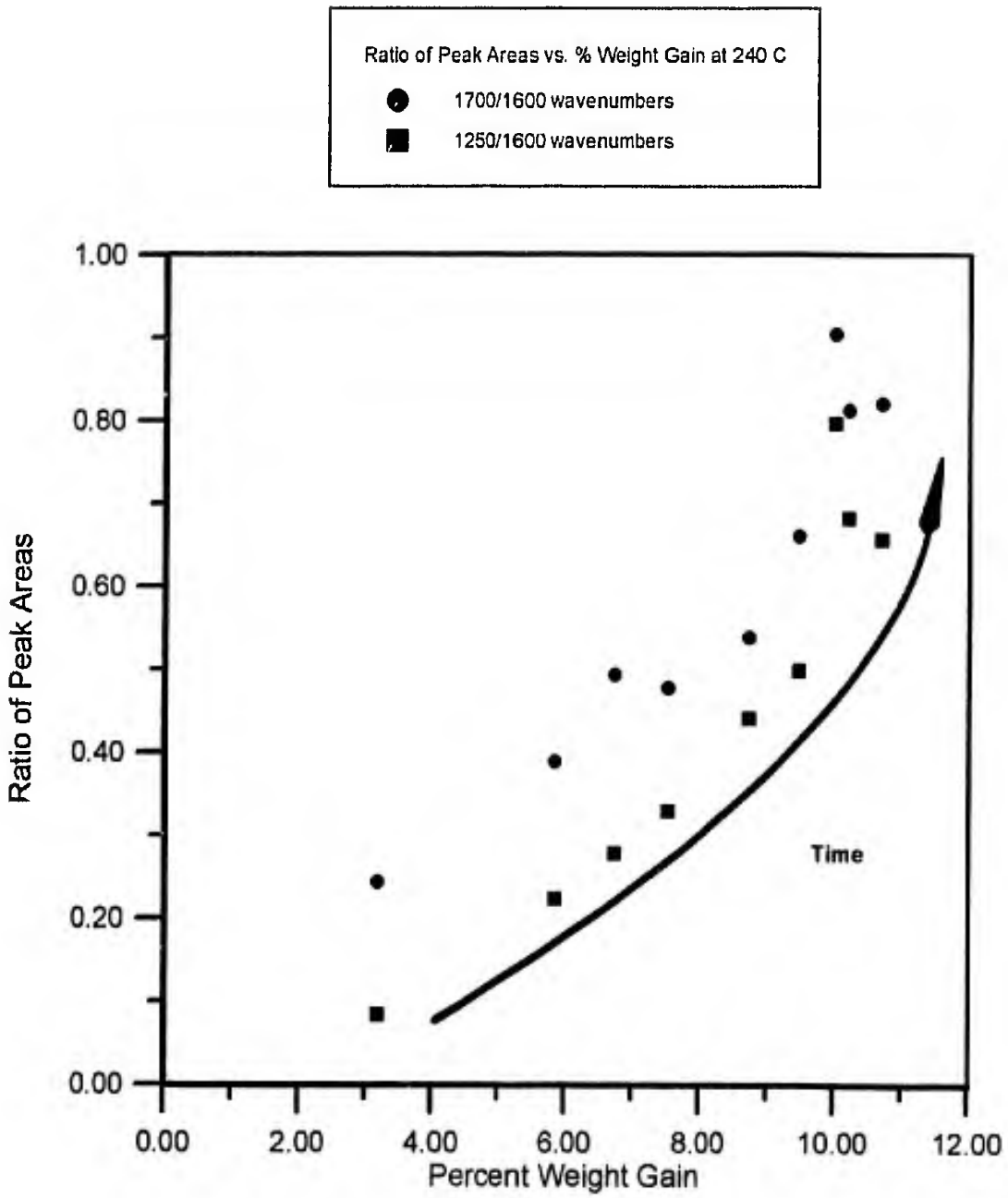

Figure 14. Plot of ratio of peak areas for 1700 and 1250 wavenumbers vs. percent weight gain at 240°C

weight gain has maximized and the material begins to lose weight.

The other functionality of interest is the napthenic ring structures which give rise to an IR absorbance band centered at 1440 cm^{-1} resulting from the bending motion of methylene hydrogens. This functionality is tracked semi-quantitatively by integrating the area of the peak centered at 1440 wavenumbers and ratioing it to the peak area at 1600 wavenumbers. A plot of this peak area ratio, along with that at 880 wavenumbers resulting from the bending mode of isolated aromatic hydrogens, is shown in figure 15 for oxidation at 240°C. There is clearly a decrease in the value of both ratios as oxidation proceeds, indicating a loss of both napthenic rings and isolated aromatic hydrogen during oxidation. The curve levels off at 4 hours oxidation time, once again corresponding to the point in the weight change curve where weight gain is maximized. Apparently, the weight gain process associated with pitch oxidation proceeds with a subsequent loss of napthenic ring structures. This conclusion is supported by the plot in figure 16 which shows the ratios of peak area at 1440 and 880 wavenumbers both vs. that at 1600 cm^{-1} plotted against weight. The resulting curve shapes indicate clearly that weight gain is proceeding with a concurrent loss of normalized methylene hydrogen bending mode intensity. Close examination of the curve for

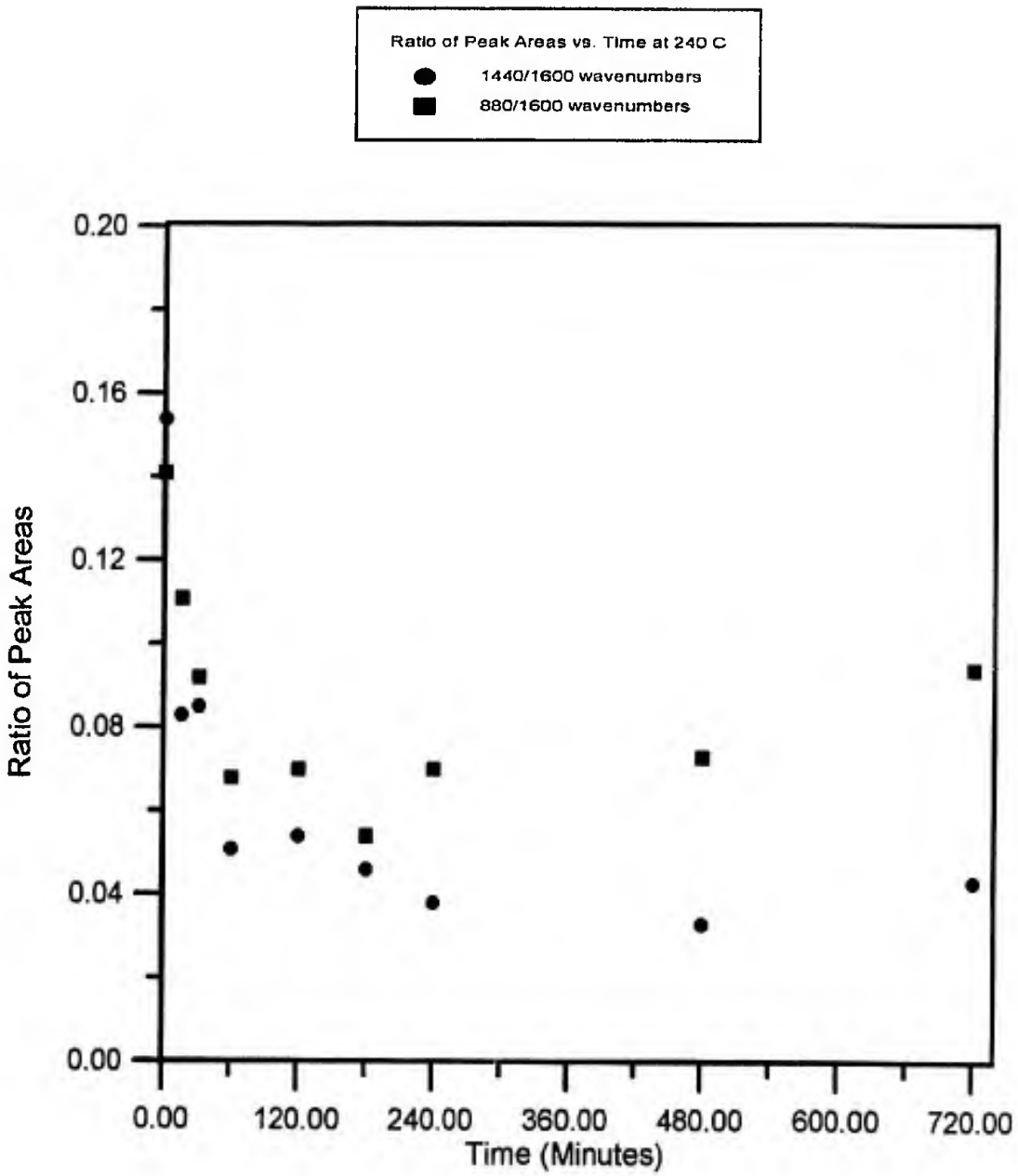

Figure 15. Plot of ratio of peak areas for 1440 and 880 wavenumbers vs. oxidation time at 240°C

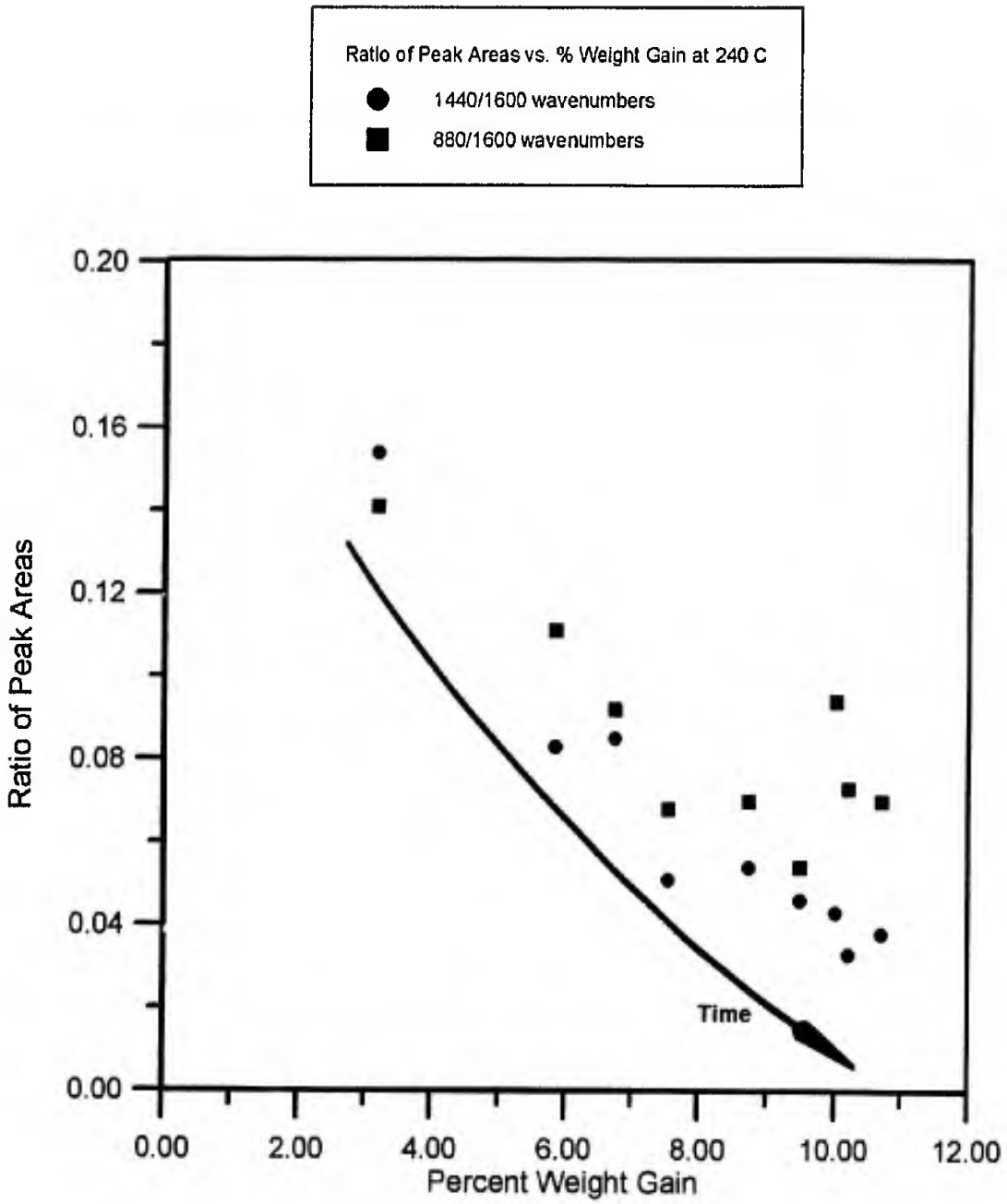

Figure 16. Plot of ratio of peak areas for 1440 and 880 wavenumbers vs. percent weight gain at 240°C

the normalized peak area at 880 cm^{-1} in figure 15 shows an increase in the peak area ratio from oxidation between 480 and 720 minutes. This is a result of the production of phthalic anhydride-like structures in the pitch. The phthalic anhydride ring structure gives rise to an out-of-plane bending mode at approximately 896 cm^{-1} [22]. This peak, when integrated along with the peak due to isolated aromatic hydrogen bending at 880 cm^{-1}, gives an apparent increase in the magnitude of the peak area ratio. It is of interest to note that phthalic anhydride also gives rise to a carbonyl stretching mode in the IR at approximately 1845 cm^{-1} [22] which is seen in figure 11 for the oxidation of pitch at 240°C for 4 hours. The production of phthalates at long times is entirely consistent with the production of a derivative functionality which requires for its formation the condensation of other oxygenated groups.

These ratios of peak areas with respect to the 1600 cm^{-1} band can be used to track, semi-quantitatively, changes in pitch functionality resulting from oxidation at other temperatures. The same calculations for oxidation at 270°C are shown in figures 17 through 20. Figure 17 shows that the ratios of the normalized peak areas at 1700 and 1250 wavenumbers increase with oxidation time. In particular, the ratio of peak areas increases monotonically out to 480 minutes. With

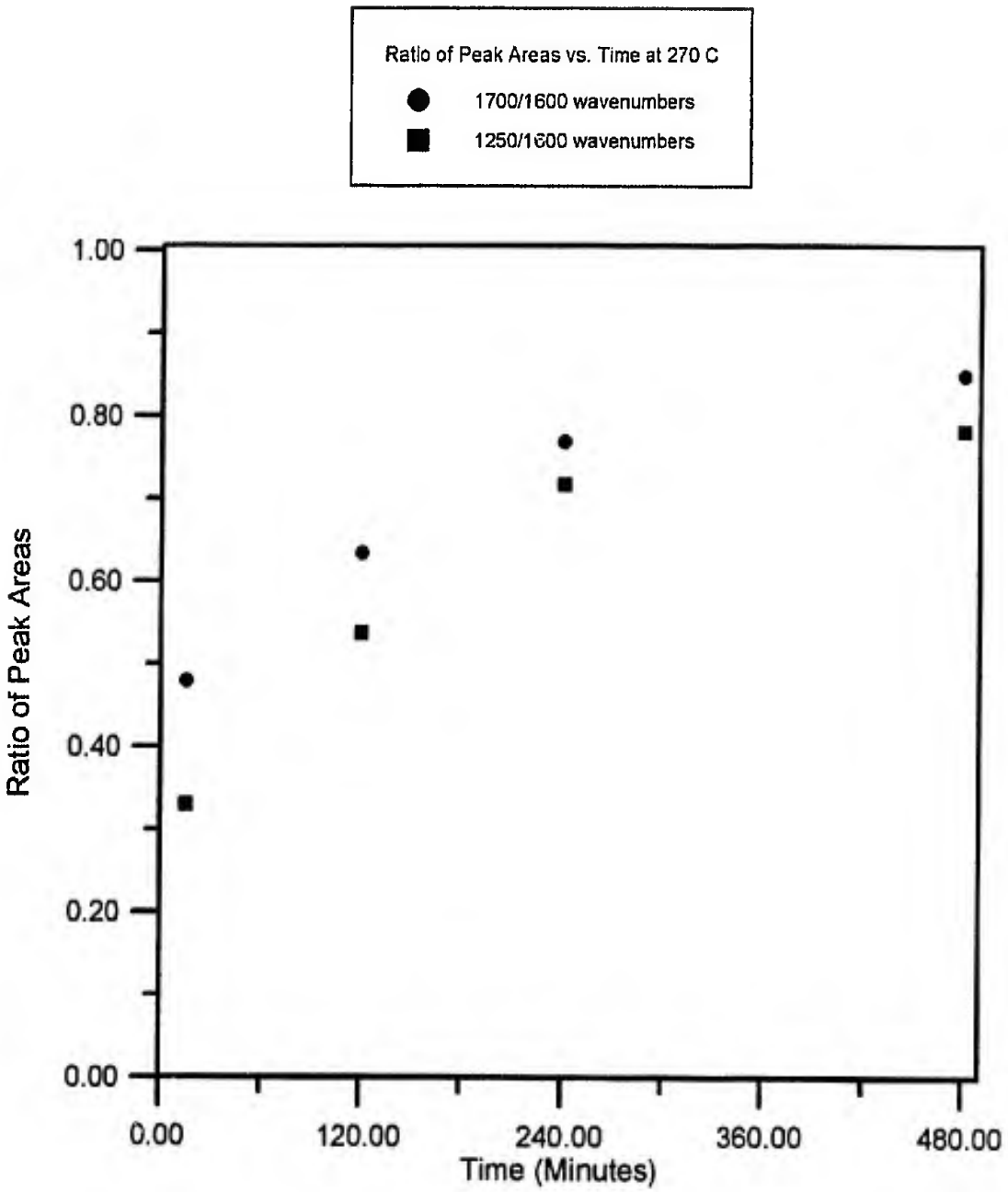

Figure 17. Plot of ratio of peak areas for 1700 and 1250 wavenumbers vs. oxidation time at 270°C

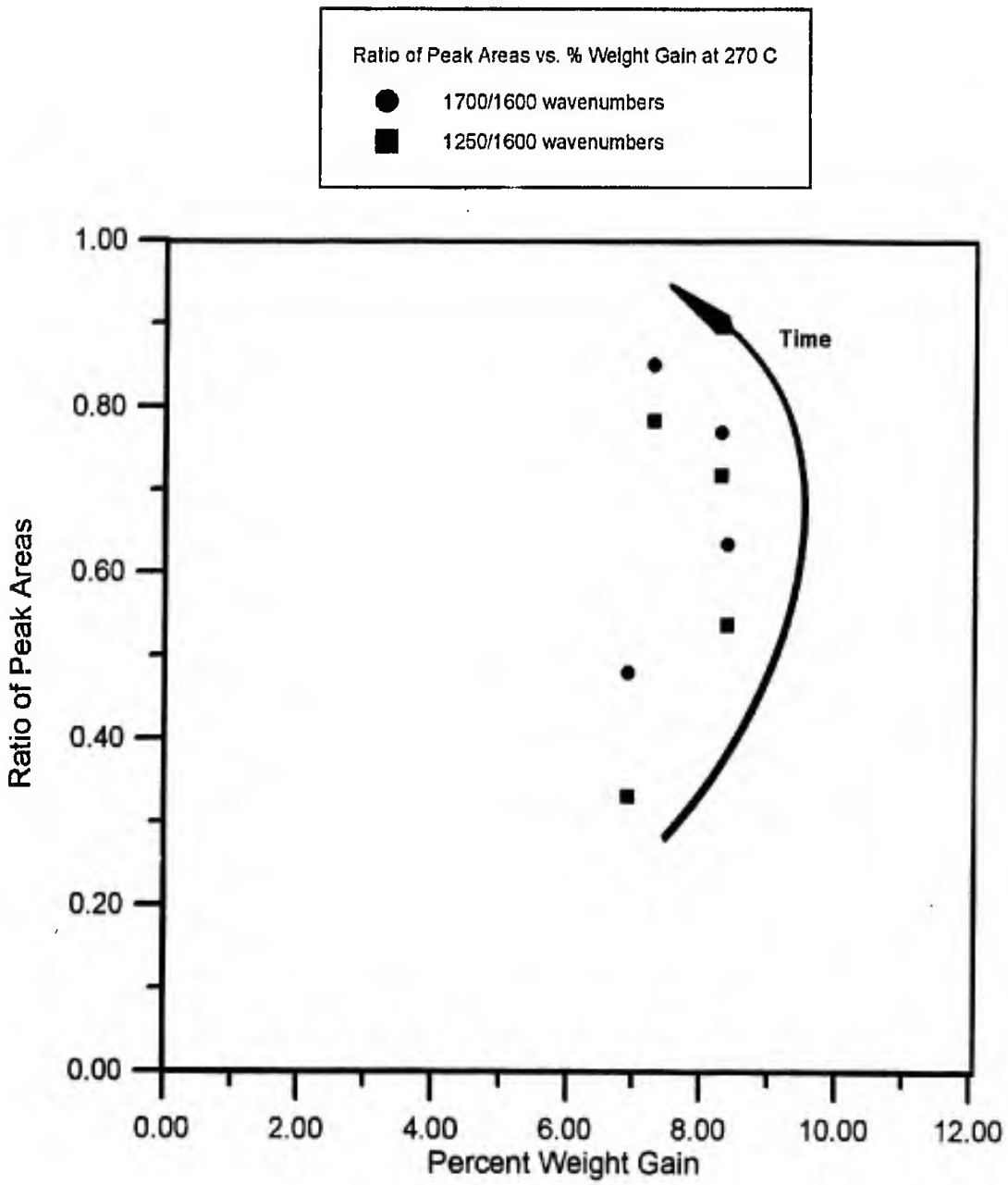

Figure 18. Plot of ratio of peak areas for 1700 and 1250 wavenumbers vs. percent weight gain at 270°C

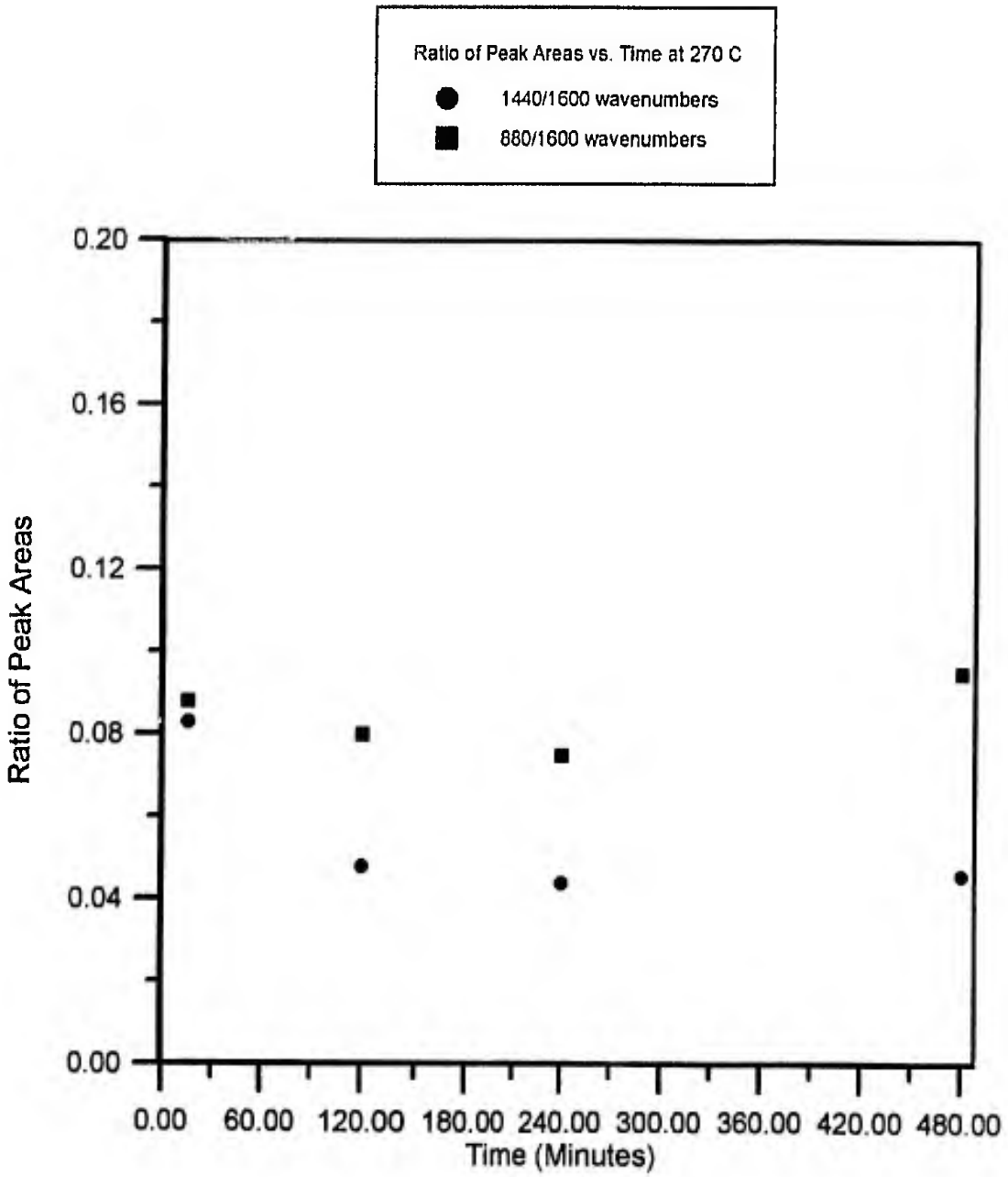

Figure 19. Plot of ratio of peak areas for 1440 and 880 wavenumbers vs. oxidation time at 270°C

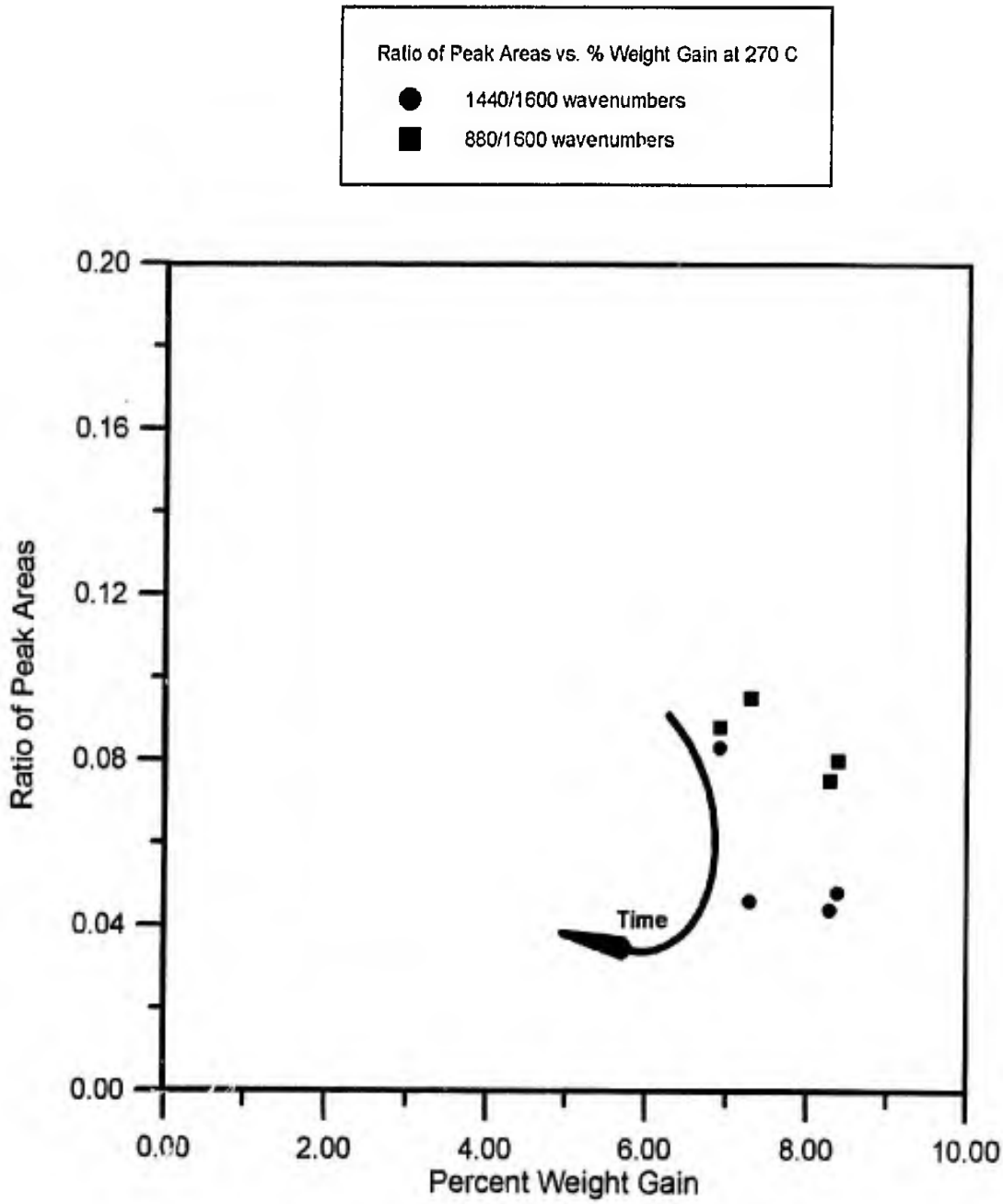

Figure 20. Plot of ratio of peak areas for 1440 and 880 wavenumbers vs. percent weight gain at 270°C

reference to the weight change curve at 270°C (figure 3) we see that weight gain is maximized at approximately 120 minutes oxidation time. The mass of the pitch then decreases upon further oxidation out to 480 minutes. As with the pitch oxidized at 240°C, the indication is that oxygen content in the pitch continues to increase, relative to aromatic carbon content, even after weight begins to be lost. This is shown more clearly in figure 18 where the ratio of normalized peak areas at 1700 cm^{-1} and 1250 cm^{-1} is plotted against percent weight gain. Notice that the weight gain is maximized at approximately 8% at 120 minutes oxidation time, and is reduced to about 7% after 480 minutes. Even so, the ratios of peak areas for both 1700 and 1250 wavenumber bands continue to increase after the onset of weight loss. It must be made clear that an increase of normalized peak area ratios as weight is lost can be the result of two distinctly different phenomena. The first is an actual increase in the concentration of oxygen functionality, resulting from a further uptake of oxygen by the pitch even as weight is lost. The second (because the ratio is based on the integration of the IR band due to aromatic carbon-carbon stretching) is a loss of aromatic carbon content able to absorb in the mid IR region, either because of a loss of aromatic material or its conversion to more symmetric condensed rings possessing lower extinction

coefficients in the mid IR region. Either of the two phenomena would cause the peak area ratios to increase. We can state with confidence at this point, however, that despite any weight loss, the concentration of oxygen in the pitch is increasing relative to simple aromatic carbon content.

Figure 19 illustrates the peak area ratios corresponding to the methylene hydrogen bending mode at 1440 cm^{-1} plotted vs. oxidation time at 270°C. The result is similar to that obtained during oxidation at 240°C in that the peak area ratio decreases with oxidation time out to about 120 minutes, at which point weight gain is maximized. The peak area ratios remain relatively unchanged thereafter, once again indicating that the weight gain process during oxidation proceeds with a subsequent loss of napthenic rings. In addition, the loss of napthenic rings occurs more rapidly at this higher oxidation temperature, with the peak area ratio at 1440 cm^{-1} reaching a minimum value at 120 minutes for 270°C (compared with 240 minutes at 240°C). The plot in figure 20 relating peak area ratios to weight change at 270°C reinforces this hypothesis. The peak area ratio for the 1440 wavenumber band is first measured at 15 minutes oxidation time after which it decreases upon further oxidation to 120 minutes, thereafter remaining relatively constant. Further study of figures 19 and 20 reveals also that

only a very little loss of normalized peak area related to the isolated aromatic hydrogen bending mode at 880 wavenumbers is observed as oxidation time is increased at this temperature.

The four peak area ratio curves for oxidation at 290°C are shown in figures 21 through 24. The plot of normalized peak areas for the bands at 1700 cm^{-1} and 1250 cm^{-1} vs. oxidation time in figure 21 reveals an interesting curve shape. Notice that the ratios increase out to approximately 30 minutes oxidation time, level off, and then begin to increase again beyond 180 minutes oxidation time. Reference to the weight change curve for 290°C (figure 3) reveals that the initial increase in the peak area ratio value corresponds to weight gain, and the leveling off of the ratio value between 30 and 180 minutes corresponds to the area in the weight change curve where weight gain is peaking and then begins to decrease. Finally, the increase in the ratio of peak area value beyond 180 minutes oxidation time occurs in the region of weight loss in the weight change curve as depicted in figure 3. This curve shape supports the conclusion that initial weight gain during oxidation corresponds to an increase in absolute oxygen content. As the oxygen content begins to level off, the weight gain experienced by the pitch is also reaching a maximum and beginning to level off. Then, as the pitch begins

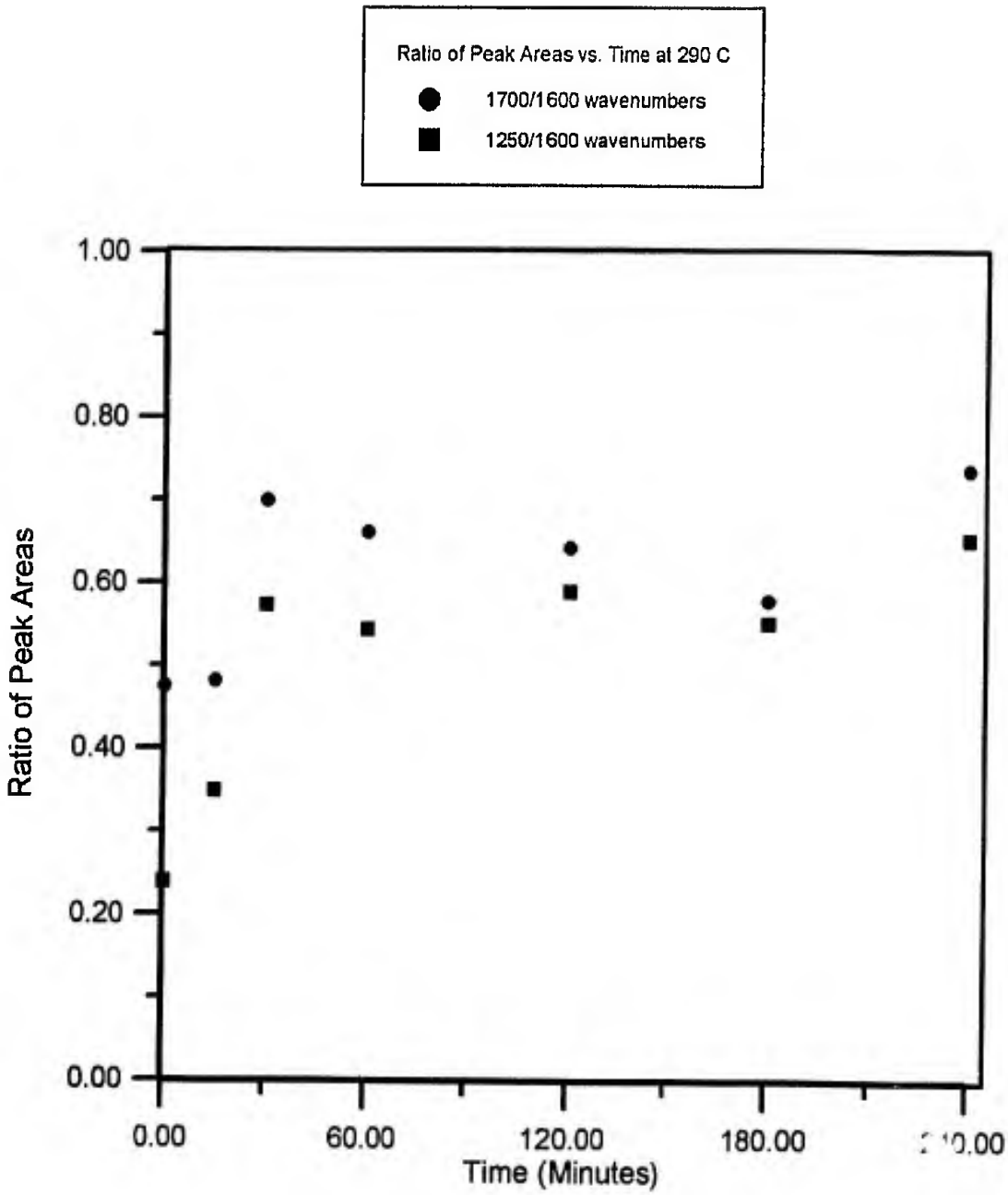

Figure 21. Plot of ratio of peak areas for 1700 and 1250 wavenumbers vs. oxidation time at 290°C

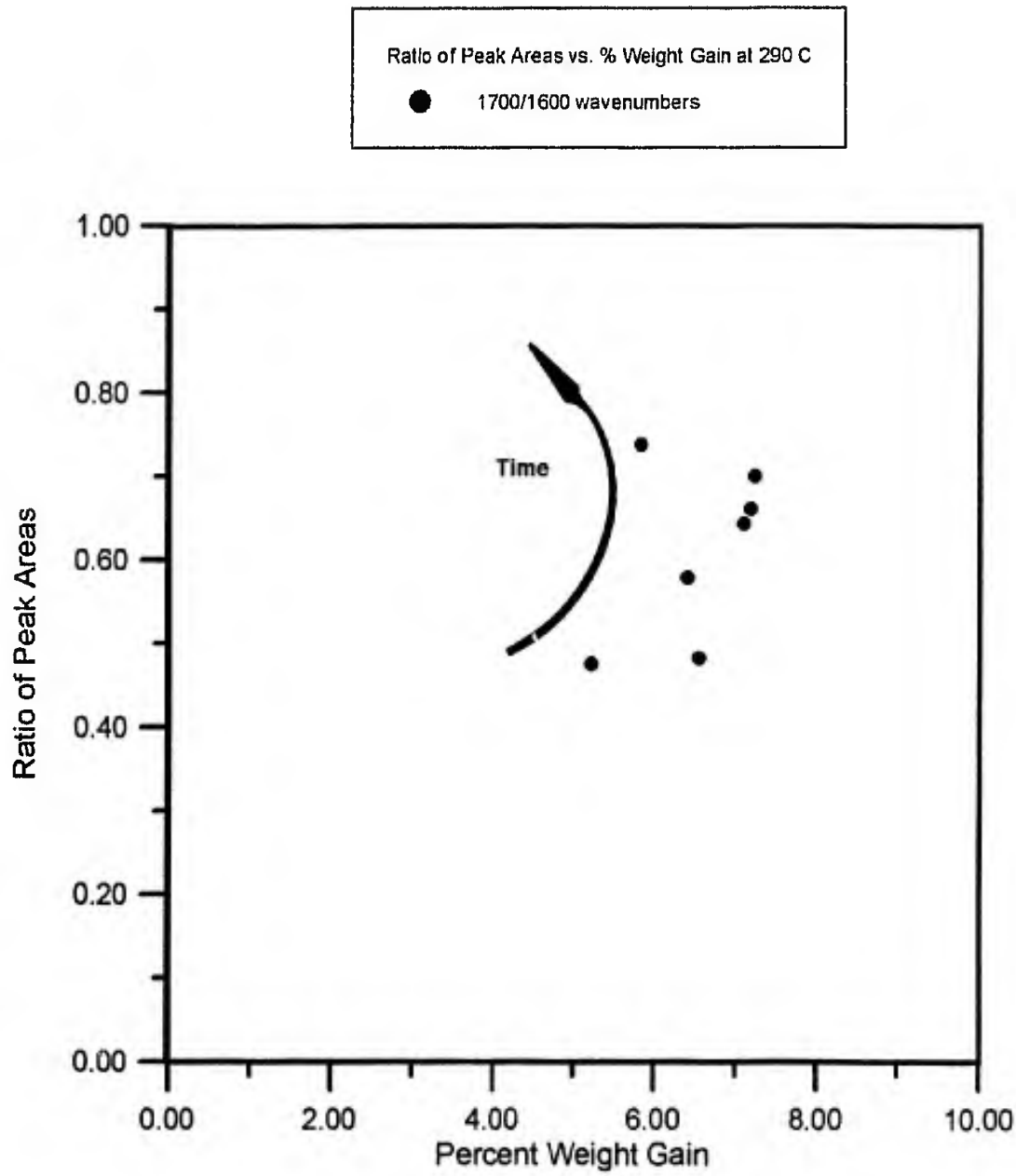

Figure 22. Plot of ratio of peak areas for 1700 wavenumbers vs. percent weight gain at 290°C

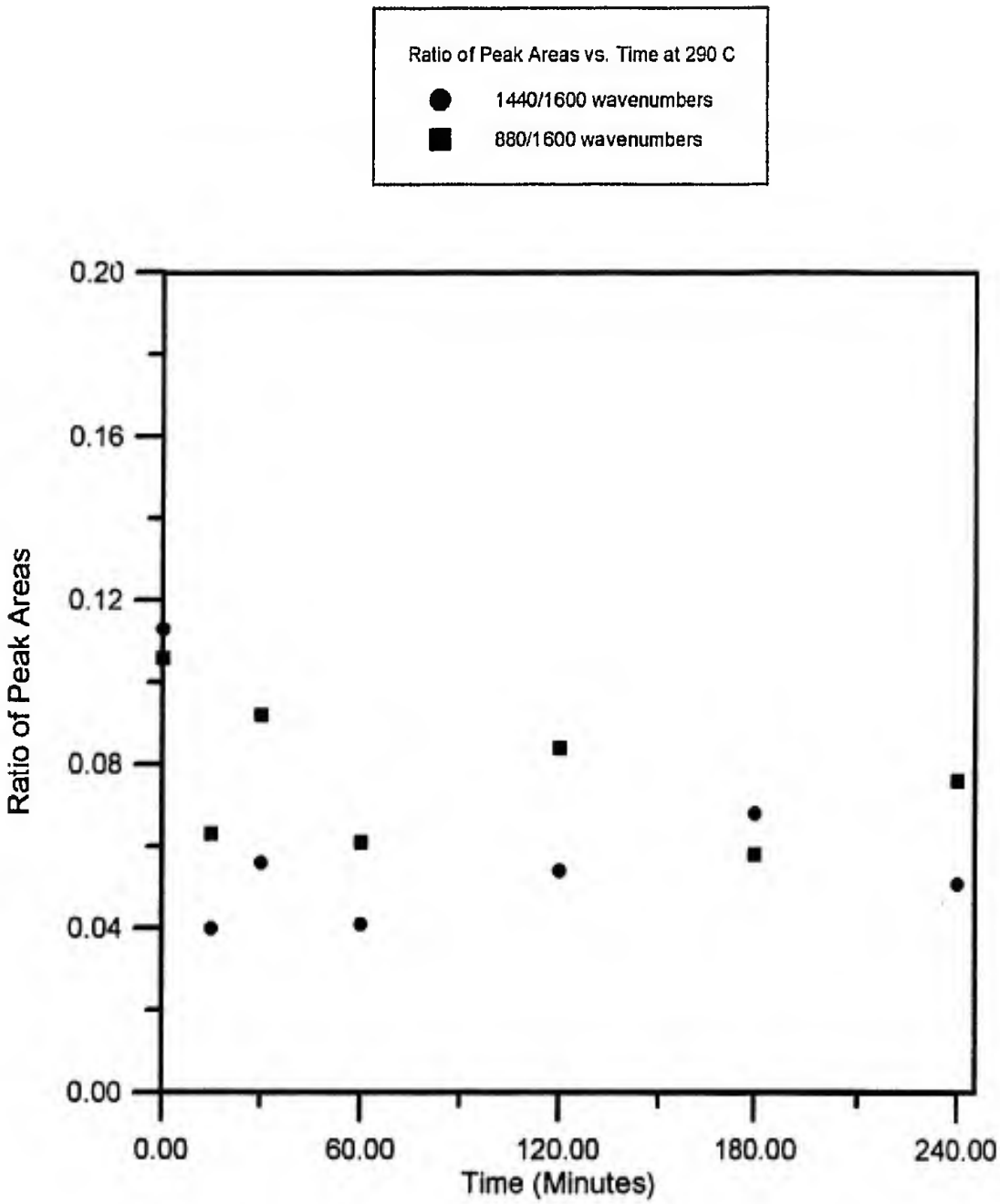

Figure 23. Plot of ratio of peak areas for 1440 and 880 wavenumbers vs. oxidation time at 290°C

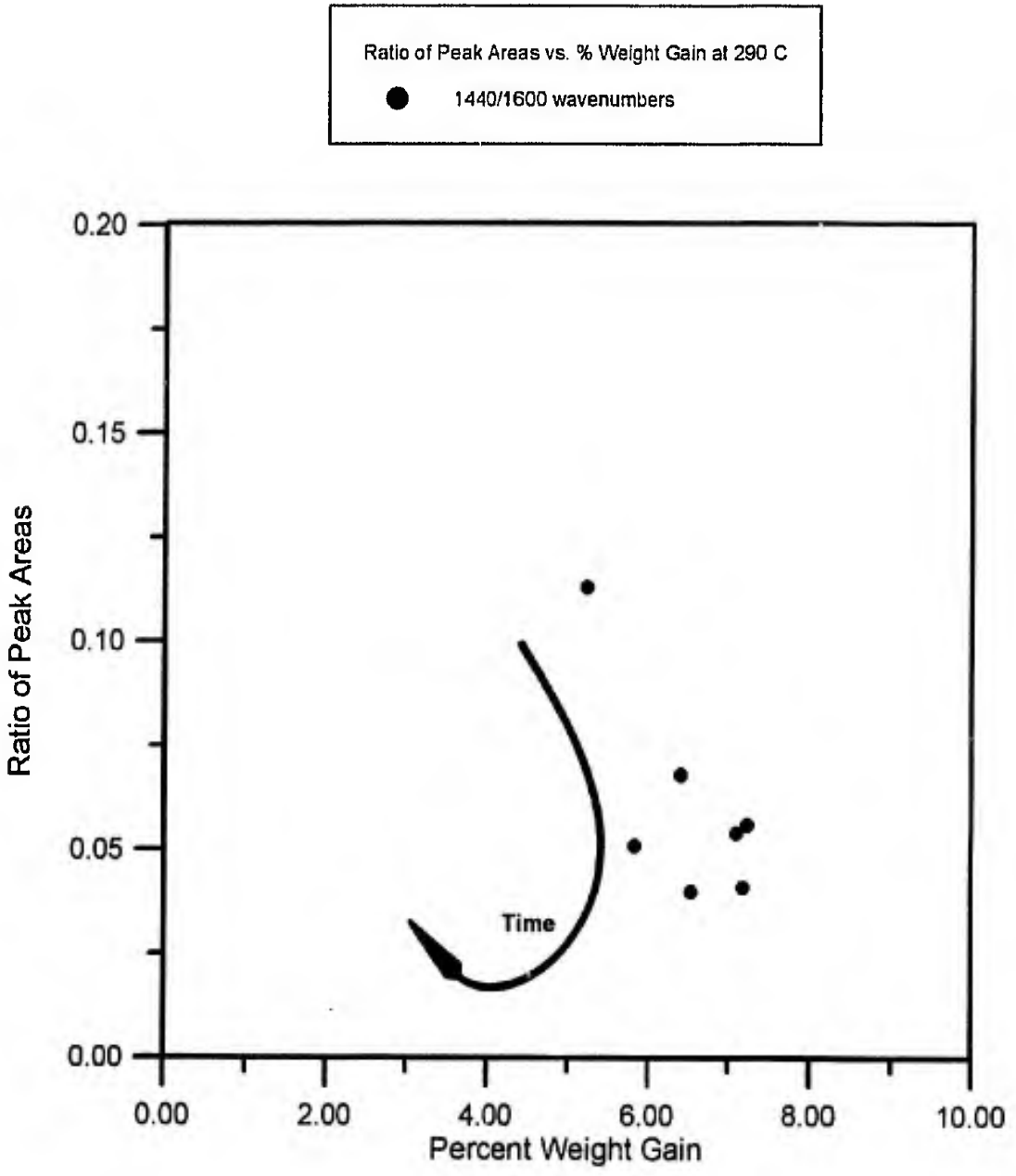

Figure 24. Plot of ratio of peak areas for 1440 wavenumbers vs. percent weight gain at 290°C

to lose weight, the relative oxygen content as indicated by the ratio value appears to climb again. This curve shape is very similar to that observed during oxidation at 240°C (figure 13), but is less pronounced at that temperature because only one point at 720 minutes oxidation time corresponds to weight loss. Reference to figure 13 shows, indeed, that the peak area ratio value at 1700 cm^{-1} corresponding to 720 minutes has increased compared to 480 minutes. The curve shape for oxidation at 270°C in figure 17 is not well developed because experiments were carried out at only four different oxidation time periods, preventing us from collecting enough points around the area in the weight change curve where weight gain is maximized and beginning to change direction. Even so, what was at first perceived as a monotonic increase in carbonyl content between 120 minutes and 480 minutes could conceivably correspond to a plateau followed by a later increase in the carbonyl level.

The remaining graphs showing relationships between peak area ratios and oxidation time at 290°C in figures 22 through 24 are similar to those for oxidation at 270°C. In figure 22 we cannot see a defined relationship between peak area ratio at 1700 cm^{-1} and percent weight gain. In figure 23 we can, however, see that the normalized peak area corresponding to methylene hydrogen bending at

1440 cm^{-1} decreases rapidly during the first 30 minutes of oxidation and then levels off. This suggests that the napthenic ring content in the pitch is quantitatively removed during the first 30 minutes of oxidation at 290°C, compared to 120 minutes at 270°C and 240 minutes at 240°C. Figure 24 shows the same ratio values, but instead plotted against percent weight gain. The significant scatter in the points is noted.

For oxidation at 340°C, normalized peak area relationships are shown in figures 25 through 28. We are now dealing with a situation where the pitch has lost weight throughout the entire isothermal oxidation profile (see figure 3). Consequently, in figure 25 which illustrates the peak area ratios due to bands at 1700 and 1250 wavenumbers plotted vs. oxidation time, we immediately recognize that the relative oxygen concentration in the pitch must be increasing during the entire oxidation profile at this very high temperature, even after loss of all the napthenic units. Clearly, the weight loss process at long times and/or at high temperatures involves the conversion of aromatic material to oxygenated products. Figure 26 shows a clear relationship between peak area ratios and percent weight gain (actually, weight loss) during oxidation at 340°. The slope of the resultant curve is negative, indicating an inverse relationship between weight

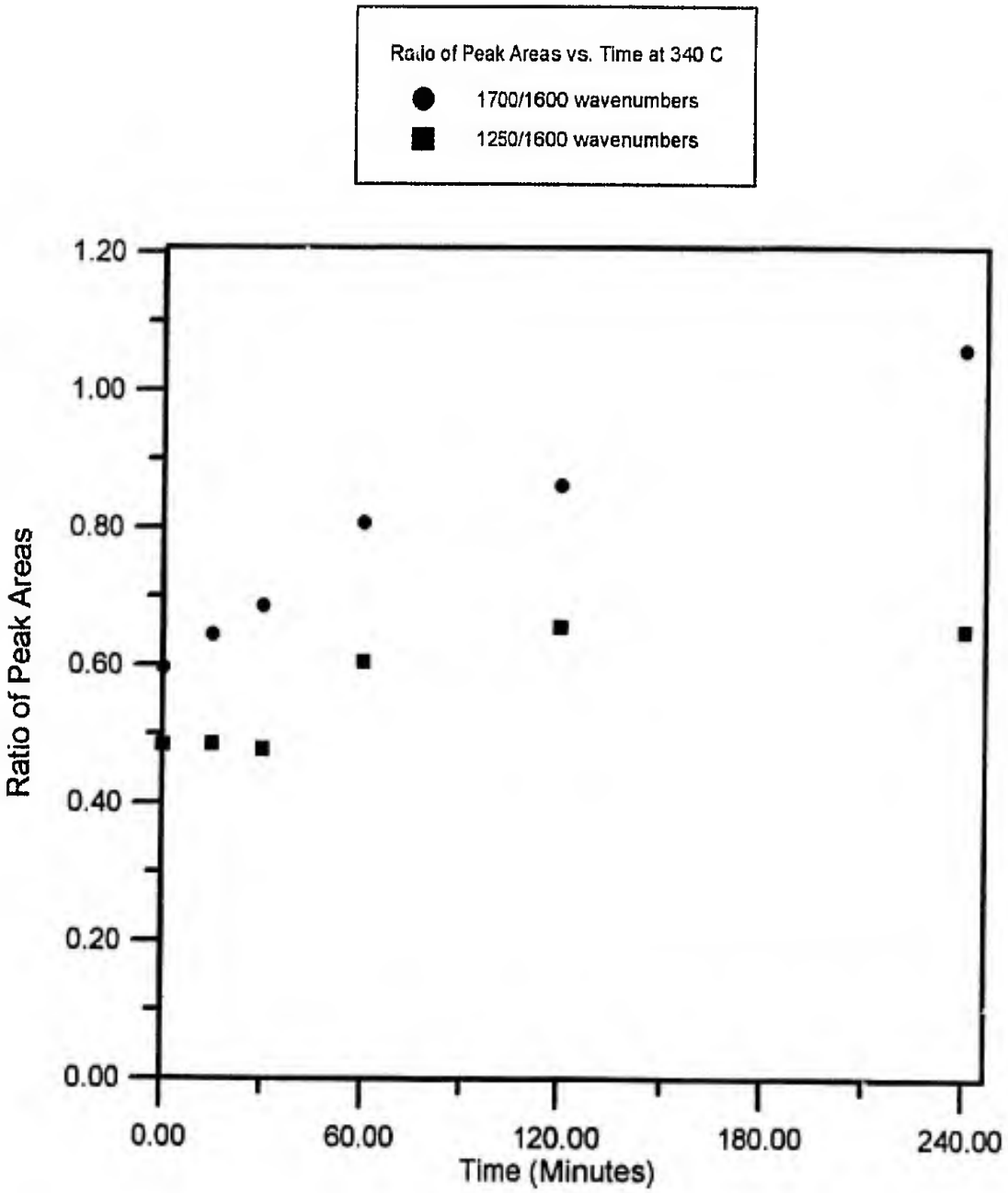

Figure 25. Plot of ratio of peak areas for 1700 and 1250 wavenumbers vs. oxidation time at 340°C

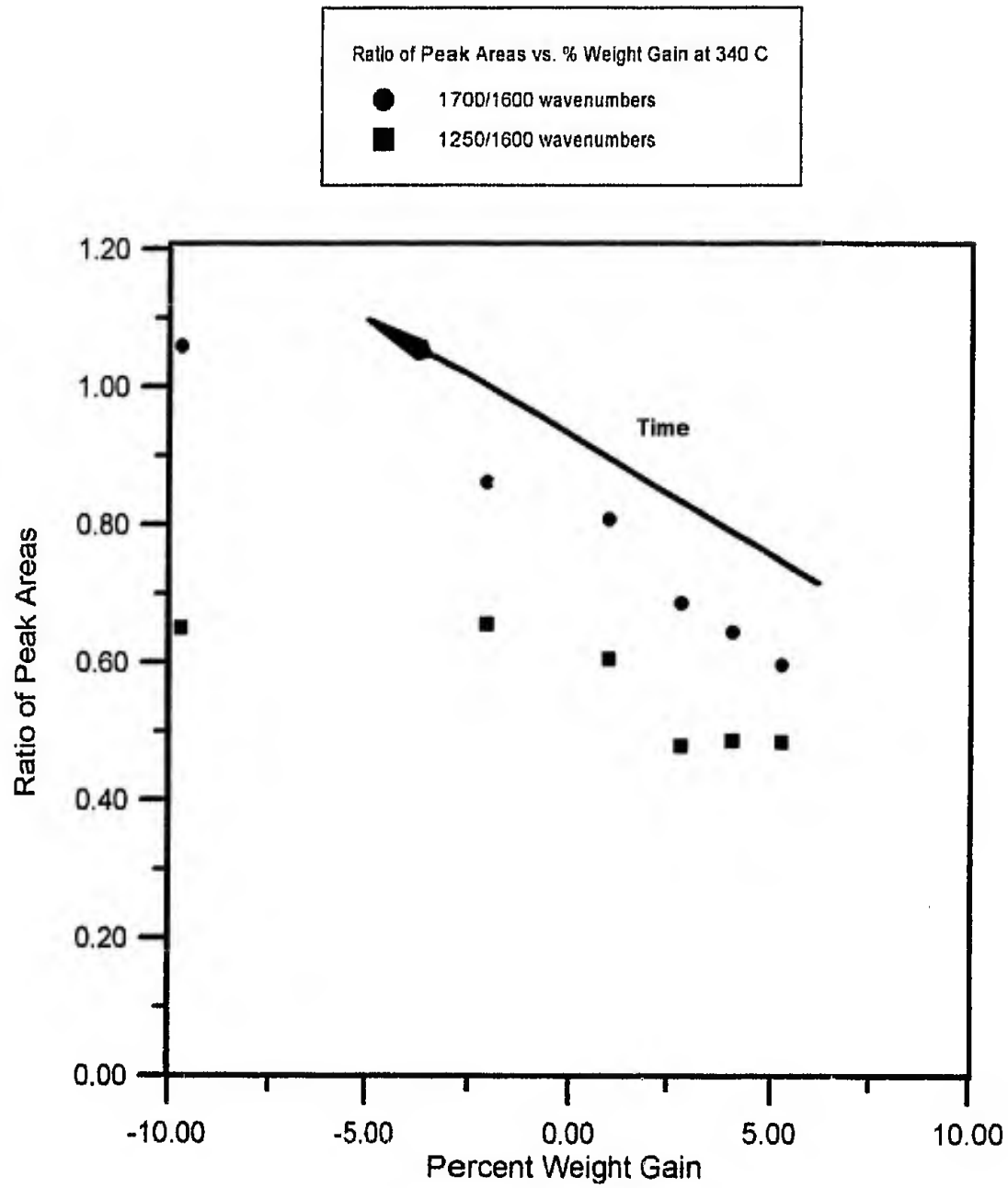

Figure 26. Plot of ratio of peak areas for 1700 and 1250 wavenumbers vs. percent weight gain at 340°C

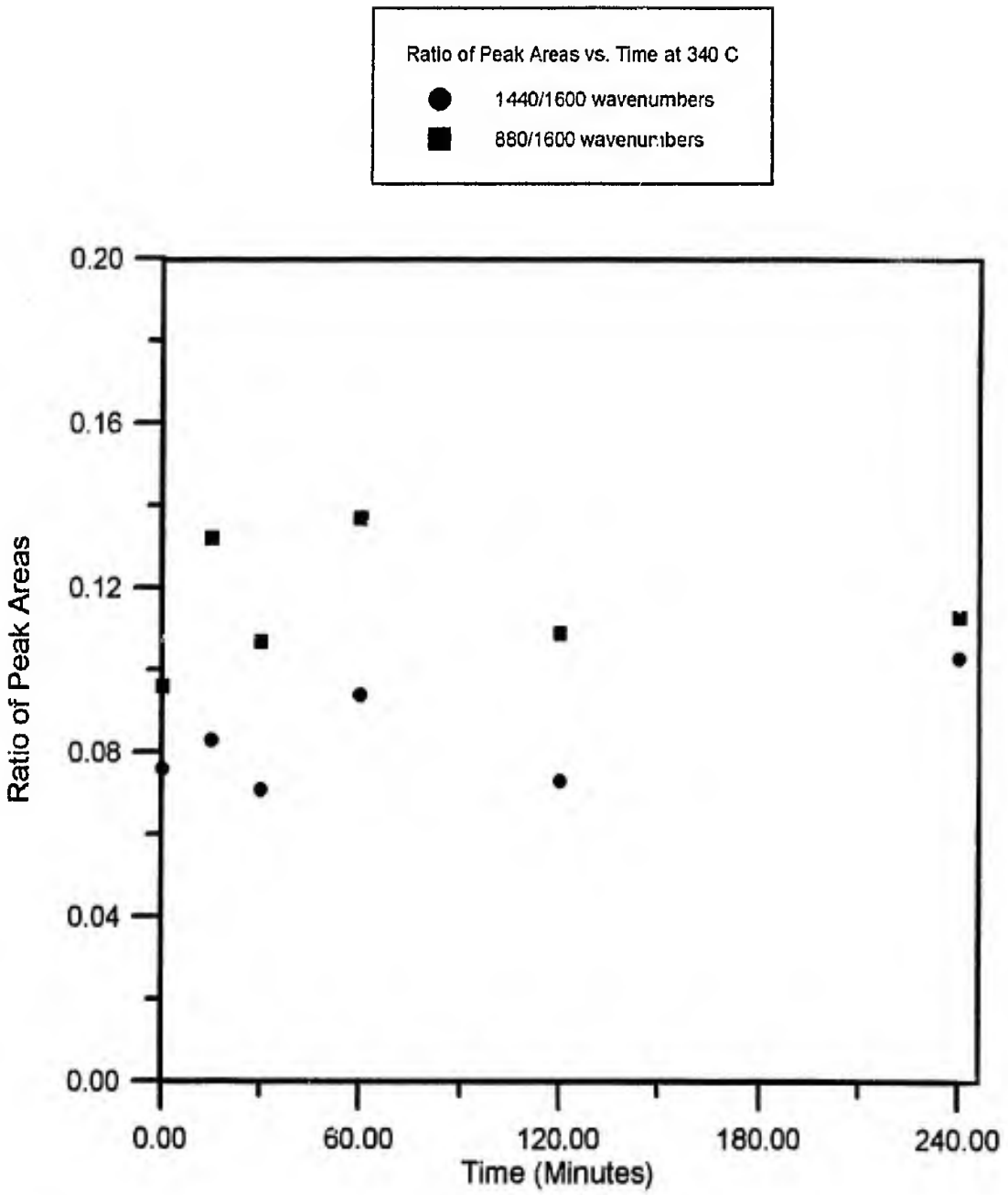

Figure 27. Plot of ratio of peak areas for 1440 and 880 wavenumbers vs. oxidation time at 340°C

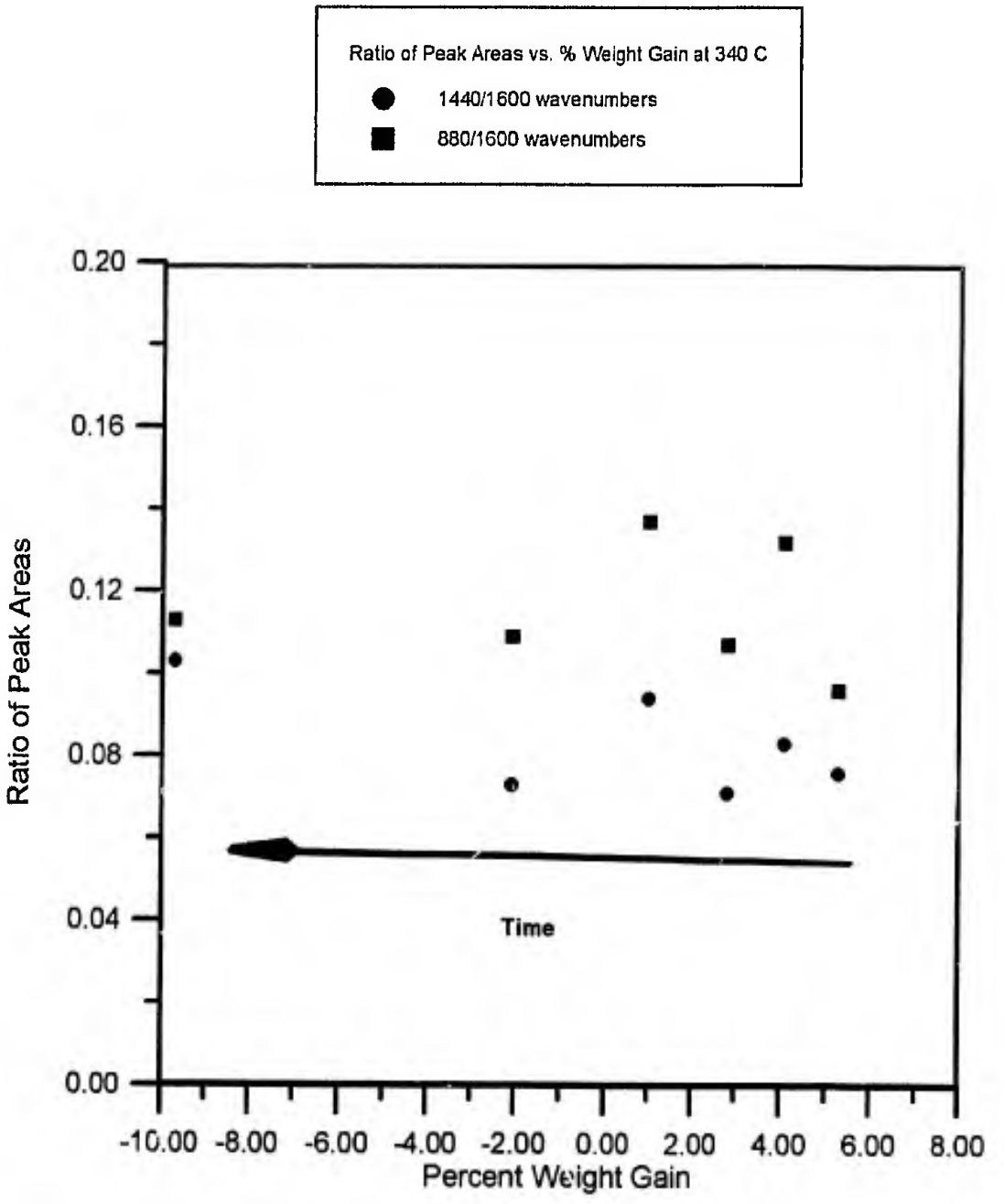

Figure 28. Plot of ratio of peak areas for 1440 and 880 wavenumbers vs. percent weight gain at 340°C

gain and oxygen content. In other words, relative oxygen content is increasing as the pitch loses weight. Figures 27 and 28 show the effect of oxidation at 340°C on the normalized peak area corresponding to methylene hydrogen bending--an indirect measurement of saturated napthenic ring content in the pitch. Both figures indicate that there is no significant loss of napthenic ring structures during the isothermal oxidation profile at 340°C. This indicates that the loss of reactive napthenic rings is completed during the heating ramp to 340°C, the same point in the weight change curve where weight gain is maximized. Subsequently, weight loss does not affect the concentration of napthenic rings in the pitch; the saturated rings were already removed (oxidized) during the weight gain process which was completed during the heating ramp.

It would be beneficial to compare, qualitatively, what occurs during oxidation at the two temperature extremes of 240°C and 340°C. At the relatively low temperature of 240°C, the weight gain process is slow enough that in figures 13 and 15 we witness a monotonic increase in oxygen content along with a similar, steady loss of napthenic ring structures as both oxidation time and weight gain proceed. At the relatively high oxidation temperature of 340°C, oxygen content as indicated by the peak area ratios for 1700 and 1250 wavenumbers, continues to

increase as the pitch loses weight. However, the relative content of napthenic ring structures is not affected. This trend, taken in conjunction with our absorption band analysis, suggests that during initial oxidation, pitch gains weight through the oxidation of napthenic ring structures to form predominately ester and anhydride functionality. Following the oxidation of napthenic rings, the pitch begins to lose weight if the oxidation is allowed to proceed for an extended period of time. The further increase in the normalized peak areas for the 1700 and 1250 wavenumber bands during weight loss can be caused by two major factors. The first is a continued uptake of oxygen as carbonyl functionality or, second, the loss of aromatic carbon. As stated earlier, either of these two factors would result in an increase in the normalized peak areas for the bands at 1700 and 1250 wavnumbers, because they reflect oxygen content relative to aromatic carbon content. Lavin's study [5] indicated a rapid initial weight gain during the oxidation of model pitches based on mixtures of anthracene and dihydroanthracene. This weight gain process involved the uptake of oxygen by the model compounds and the emission of water. Lavin noted that the magnitude and rate of weight gain could be accelerated by increasing the content of dihydroanthracene (which contains methylene hydrogens) in the mixture. At longer time periods and higher

oxidation temperatures, Lavin recorded the production of carbon monoxide and carbon dioxide, along with a concurrent loss of weight. Because the weight gain and weight loss processes seemed to occur separately with the emission of different products, Lavin concluded that they were two distinctly different chemical processes. Weight gain was due to insertion of oxygen in the model compounds with a loss of hydrogen as H_2O. Weight loss was described as a loss of "surface" carbon and oxygen complexes as carbon dioxide and carbon monoxide. Matsumoto and Mochida [7] used X-ray photoelectron spectroscopy to show that oxygen content continued to increase in mesophase pitch during oxidation when weight loss was the predominate process. X-ray photoelectron spectroscopy results indicated that oxygen content in the pitch (based on O_{1s}/ C_{1s} band ratios) was continuing to increase even at 450°C during a ramp of 0.5°C/min, despite the fact that the pitch began to lose weight at 320°C. Furthermore, Matsumoto and Mochida concluded that the content of conjugated carbonyls relative to total oxygen content in the pitch was still increasing at 350°C.

Based on our own results and the studies of Lavin [5] and Matsumoto and Mochida [7], we believe that the continued increase in the normalized peak area bands corresponding to 1700 cm^{-1} and 1250 cm^{-1} to be caused by a combination of

factors. First, oxygen uptake is continuing to occur at higher temperatures and longer time periods, albeit much more slowly because the low energy pathway involving methylene hydrogens is not available. This uptake of oxygen probably results in the formation of more thermally stable, highly conjugated carbonyls. The uptake of oxygen, however, is competing with the loss of carbon and oxygen surface functionality from the pitch, most likely as carbon dioxide and carbon monoxide. The combination of the two factors results in sustained weight loss (as seen in the weight change curves in figure 3) but with a concurrent increase in relative oxygen content as reflected by the increase in normalized peak areas for the 1700 and 1250 wavenumber bands.

4.2 CARBONIZATION

4.2.1 THERMAL GRAVIMETRIC ANALYSIS

The carbonization behavior of pitch as displayed during temperature programmed Thermal Gravimetric Analysis (TGA) did not allow for the development of a kinetic analysis of the carbonization process. Both unoxidized and oxidized pitch samples showed characteristically slow rates of weight loss during carbonization, resulting in derivative curves which were very broad and "noisy" at best. A kinetic analysis of the pitch carbonization process using (for

example) the method of Kissinger [14] requires, for proper utilization, a relatively rapid weight loss process that yields a derivative curve with a definite, identifiable, and reproducible temperature maximum. Furthermore, the actual, qualitative behavior of unoxidized pitch during carbonization was found to be dependent on the heating rate used, over and above the usual temperature dependencies. This factor alone made the determination of an activation energy for the weight loss during carbonization of unoxidized pitch an impossibility. It was also noted that small changes in sample size (weight) had a large effect on the carbonization behavior. The extremely small sample crucible which was used in the TGA experiment resulted in large changes in exposed sample surface area with small changes in sample weight. It is recognized that the behavior of pitch during carbonization is dependent on the ratio of total volume to surface area even in very small samples [3]. These behaviors combined to make us abandon our initial objective of determining the activation energy of pitch carbonization as a function of oxidation history.

Despite these negatives, TGA still yielded some qualitative information on the carbonization behavior of pitch. Figures 29 and 30 show the TGA traces of unoxidized pitch carbonized under N_2 from room temperature to 1000°C at a

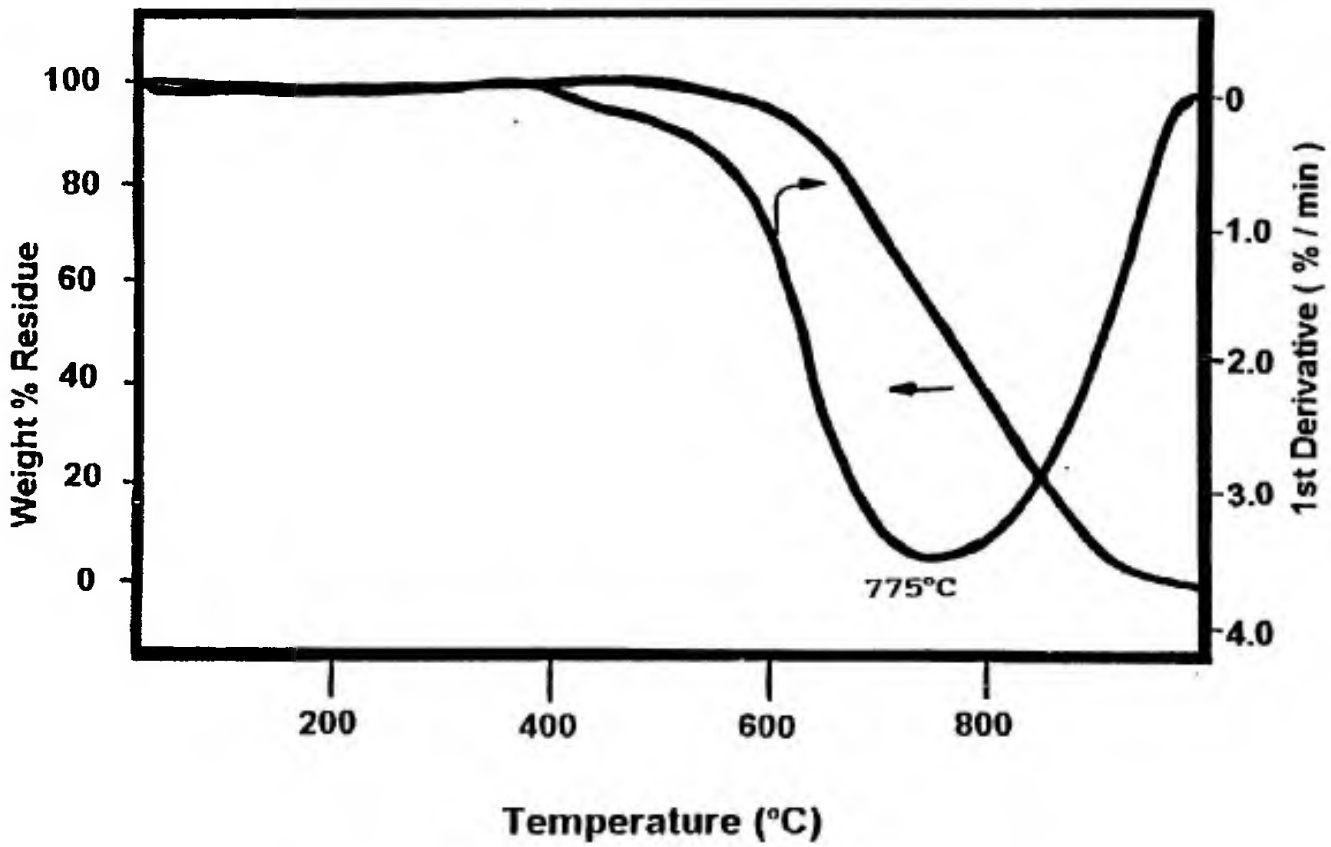

Figure 29. TGA trace and derivative curve for unoxidized pitch heated from room temperature to 1000°C at 10°C per minute; sample size = 5.9 mg

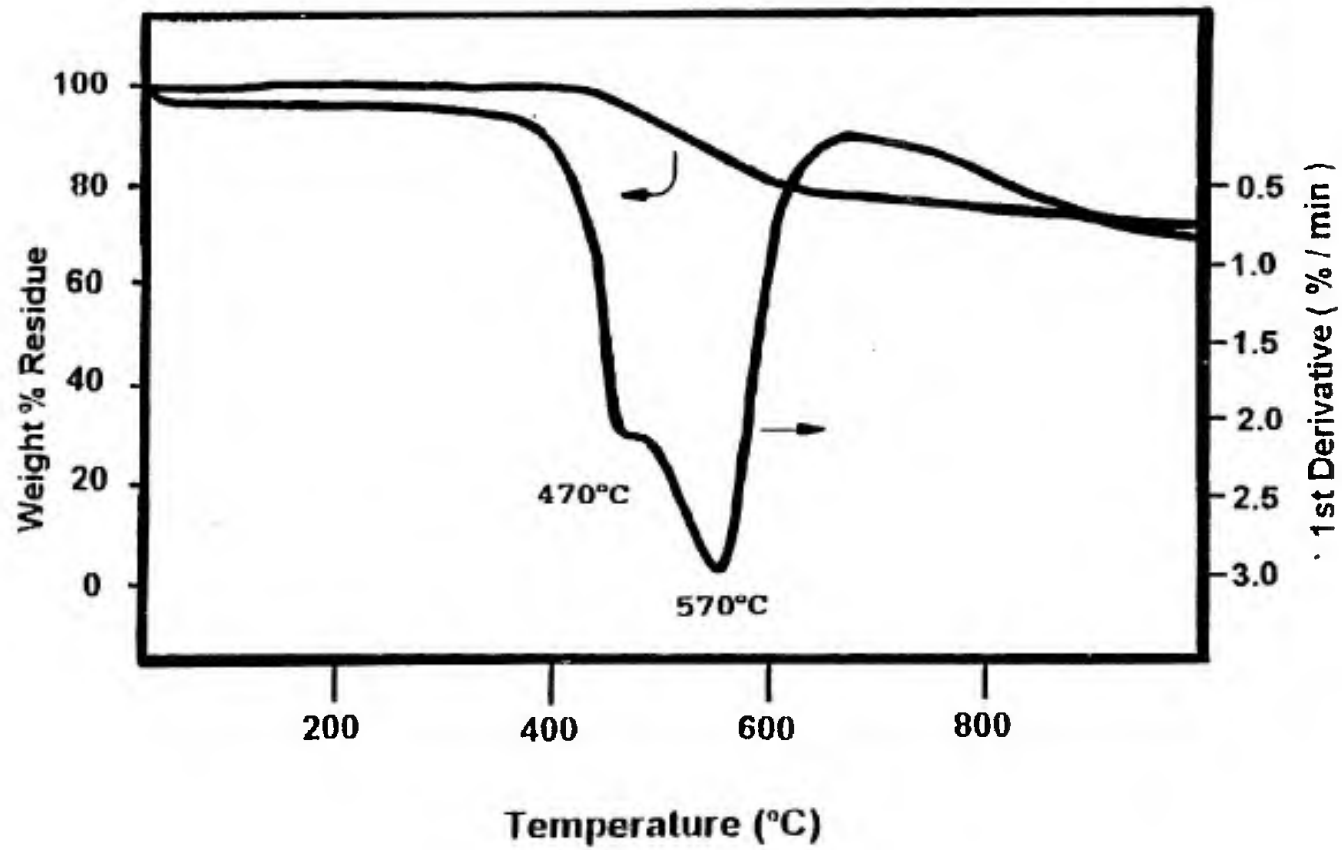

Figure 30. TGA trace and derivative curve for unoxidized pitch heated from room temperature to 1000°C at 20°C per minute; sample size = 7.8 mg

heating rate of 10°C and 20°C per minute, respectively. At a heating rate of 10°C/min, unoxidized pitch begins to lose weight at approximately 600°C, and reaches a maximum rate of weight loss around 775°C. By the time the final temperature of 1000°C is reached, the pitch has completely evaporated. At a heating rate of 20°C/min, unoxidized pitch begins to "bloat" through out-gassing at approximately 450°C, passing through what appeared to be a melt stage in a process which achieved a rate maximum at 570°C. The pitch swelled to approximately 5 to 10 times its original sample volume and routinely overflowed the sample crucible. A qualitative visual analysis of the residue at 1000°C revealed a char with an extensively pock-marked surface, resulting from bubbling or "out-gassing" of volatiles in the pitch during the melting "window". This bloating or melting behavior was reproduced whenever unoxidized pitch was ramped to 1000°C under N_2 at this fast heating rate. Mesophase bloating due to expulsion of pyrolysis gases and/or volatile liquids in unoxidized pitches has been reported previously [20]. Notice (figure30) that the pitch showed a relatively rapid rate of weight loss (3%/min) during the bloating process. Following this weight loss process, the pitch appeared to maintain weight up to 1000°C, in marked contrast to the carbonization behavior at a heating rate of 10°C/min

(figure 29). The TGA apparatus was incapable of providing information on the degradation products, so a detailed explanation for the difference in sample behavior at different heating rates is not possible based on the results of this technique alone. However, at the faster heating rate of 20°C/min, it seems likely that evaporation and loss of some pitch components, with or without prior thermal bond scissions, is responsible for the quantitative retention of mass at 1000°C. At the higher heating rate of 20°C/min, the bloating and associated melting of the pitch might also have facilitated the mobility and chemical rearrangements and fusions of pitch molecules into a more thermally stable, infusible network. It is generally understood that application of a faster heating rate during temperature programmed TGA will tend to emphasize higher temperature processes like melting and fusion, while slower heating rates will favor lower temperature processes.

TGA traces of pitch samples previously subjected to various oxidation time/ temperature profiles at low (240°C) and high (340°C) temperatures are shown in figures 31-34. Oxidized pitches displayed two weight loss processes. In summary, pitches soaked at 240°C or ramped to 340°C under oxygen experienced associated maximum rates of weight loss at approximately 490°C and 790°C. The

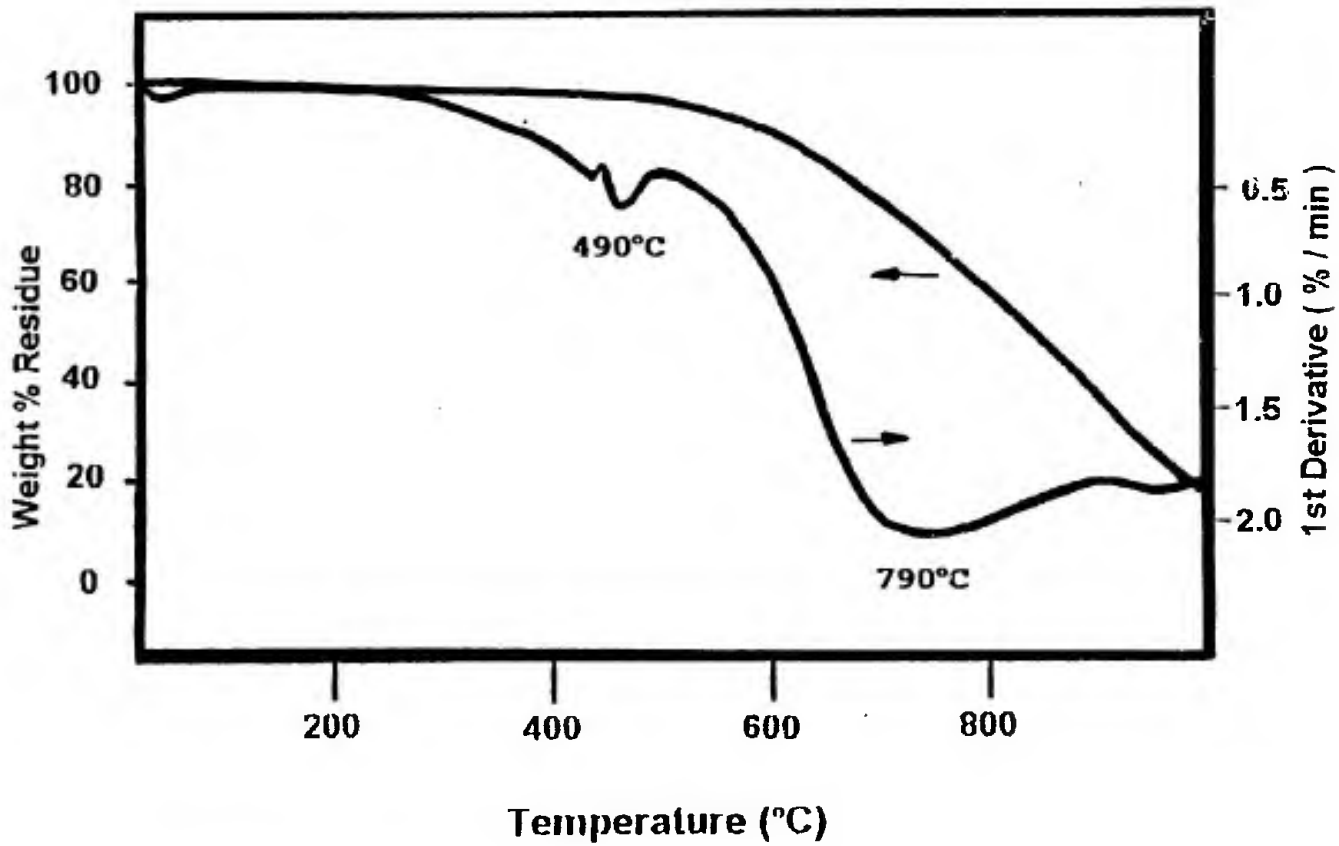

Figure 31. TGA trace and derivative curve for pitch, previously oxidized at 240°C for 15 minutes, heated from room temperature to 1000°C at 10°C per minute; sample size = 6.9 mg

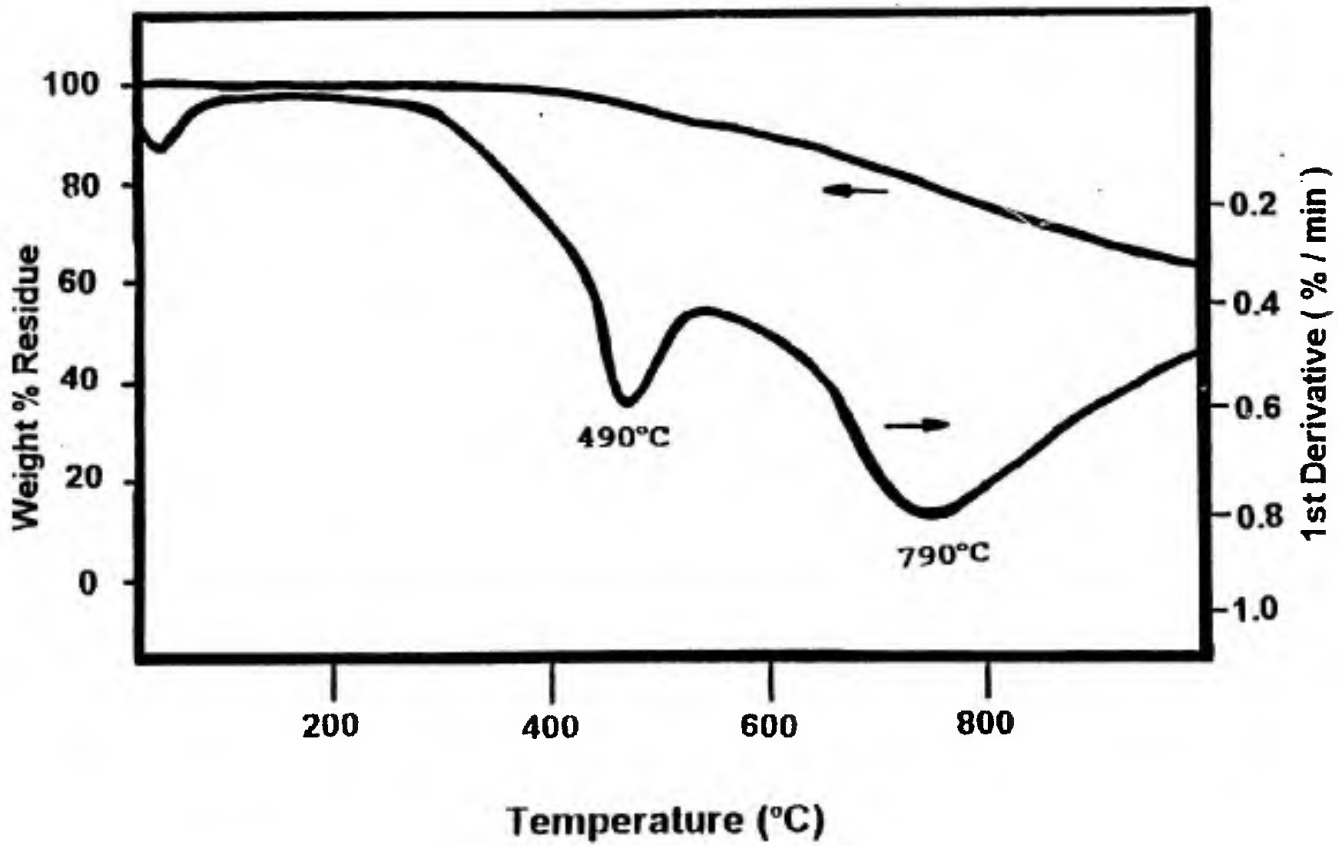

Figure 32. TGA trace and derivative curve for pitch, previously oxidized at 240°C for 60 minutes, heated from room temperature to 1000°C at 10°C per minute; sample size = 6.4 mg

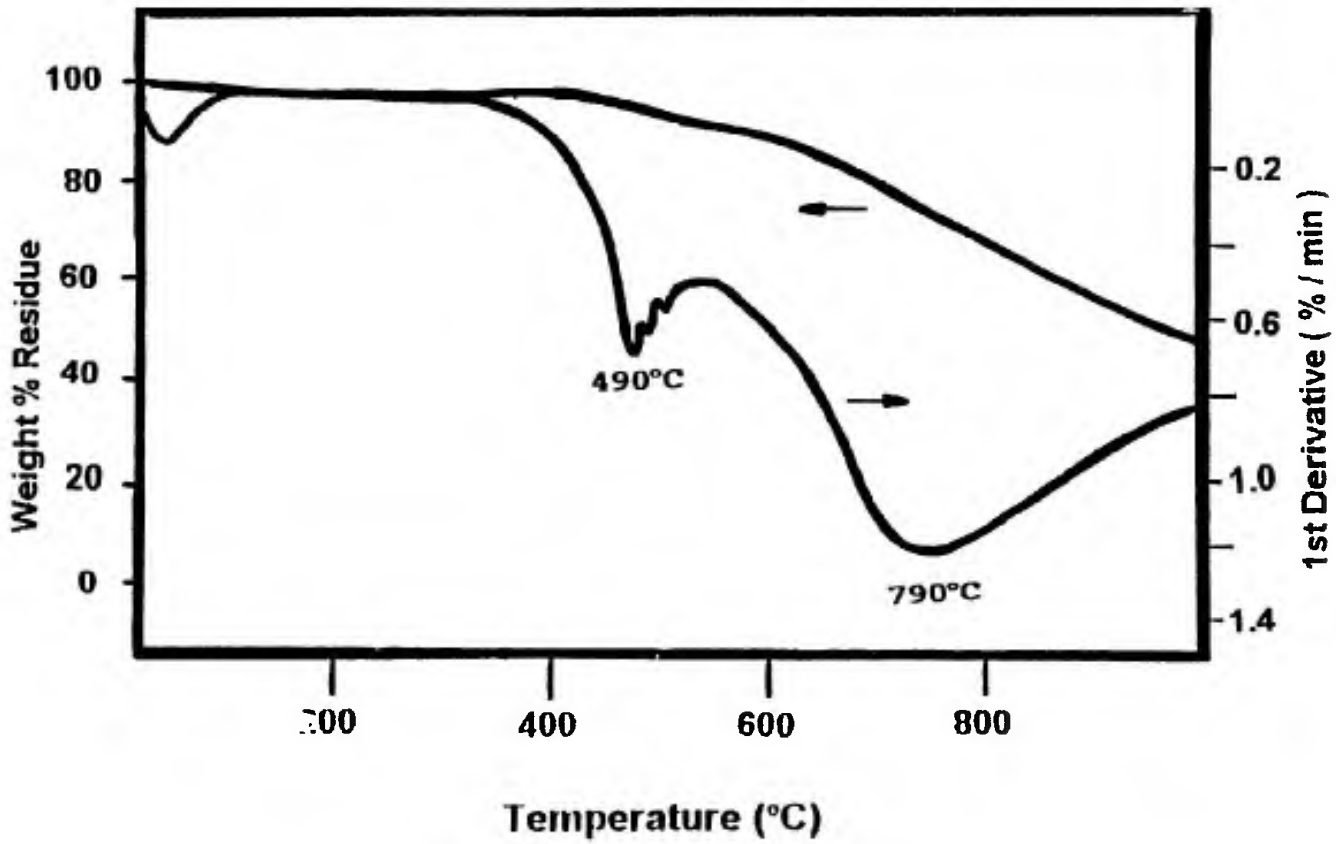

Figure 33. TGA trace and derivative curve for pitch, previously oxidized at 340°C for 0 minutes, heated from room temperature to 1000°C at 10°C per minute; sample size = 8.1 mg

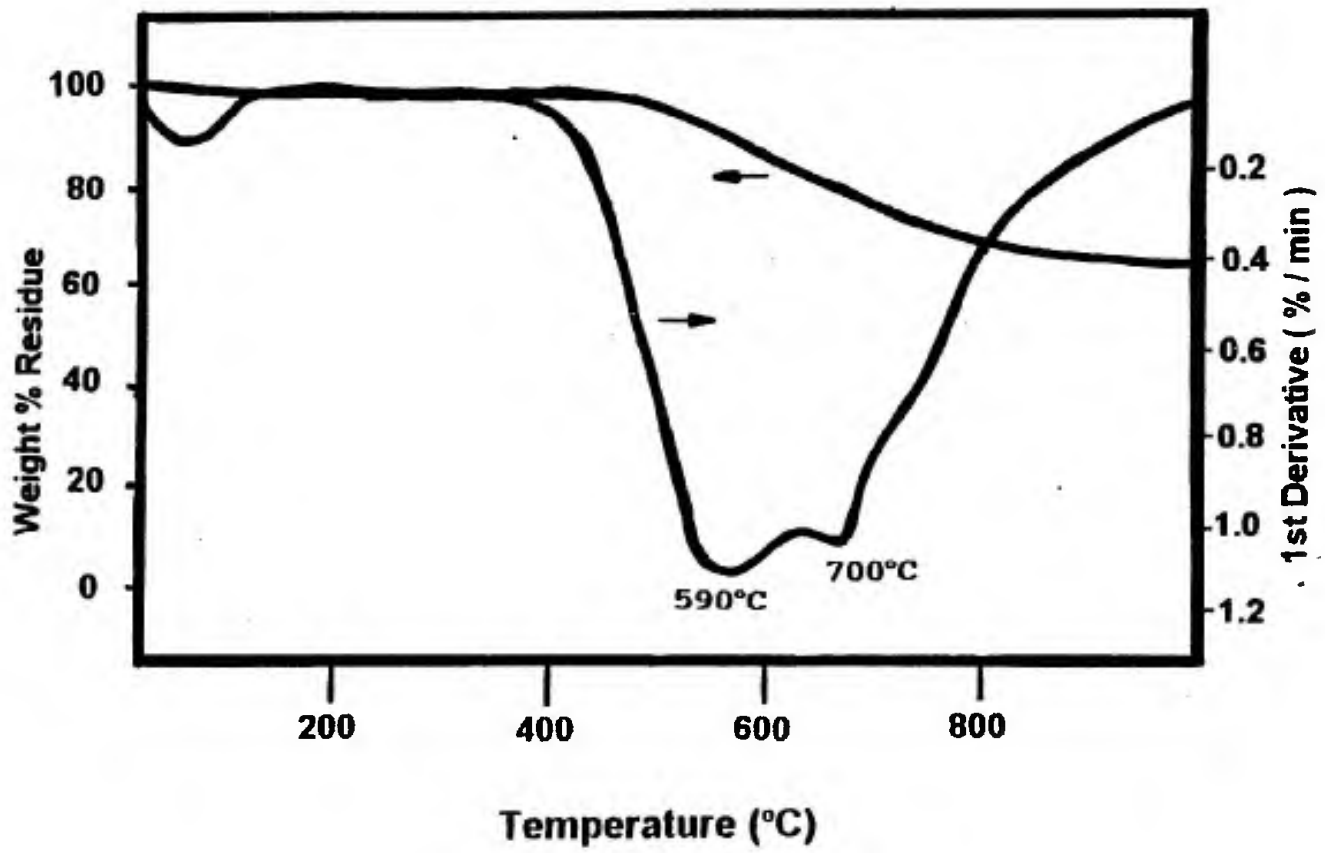

Figure 34. TGA trace and derivative curve for pitch, previously oxidized at 340°C for 240 minutes, heated from room temperature to 1000°C at 10°C per minute; sample size = 11.9 mg

pitch depicted in figure 34, however, had obviously exhausted the 490°C process, to produce a residue which achieved maximum rates of weight loss at 590°C and 700°C. None of the oxidized pitches were subject to the "bloating" behavior displayed by unoxidized pitch. In general, coke yields at 1000°C for oxidized pitches ranged from 50% to 70%. The coke yield was a function of sample size, indicating a diffusion controlled process, with larger beginning sample masses giving greater coke yields.

Figure 31 illustrates the TGA trace of pitch carbonized to 1000°C at a rate of 10°C per minute for a pitch sample which was previously oxidized at 240°C for 15 minutes. This pitch experienced a relatively slow initial rate of weight loss maximizing at about 490°C (0.5%/min) and another, more rapid weight loss process maximizing at around 790°C (2.0%/min). The coke yield at 1000°C for this sample was a relatively low 16% of the initial sample mass.

Figure 32 shows the TGA trace corresponding to the same carbonization profile for a pitch previously oxidized at 240°C for 60 minutes. For this pitch, the two weight loss maxima occurred at approximately 490°C and 790°C, similar to the previous sample. The maximum rates of weight loss were, however, changed to 0.6%/min and 0.8%/min, respectively. In addition, the coke yield at 1000°C

was significantly greater (about 61%) for pitch which had experienced this thermal history.

The minor weight loss process occurring below 200°C in all oxidized pitches is due to the loss of water in the pitch; powdered, oxidized pitch is hygroscopic and pitch samples were not dried prior to carbonization in the TGA apparatus.

The weight loss process maximizing at 490°C is probably due to the loss of some "metastable" intermediate structure formed in the pitch during oxidation. It is of interest to note that this same weight loss process occurs in the TGA trace of pitch previously oxidized at 340°C for zero minutes (figure 33) and is similar in temperature profile to the early weight loss process observed in unoxidized pitch carbonized at 20°C/min. The appearance of this weight loss process (with a temperature maximum at 490°C) indicates that the metastable intermediate resulting from oxidation at 240°C for 60 minutes is also present following oxidation at 340°C for zero minutes (which corresponds to the end of a heating ramp to 340°C).

Figure 34 shows the TGA trace of a pitch previously oxidized at 340°C for 4 hours. This oxidation profile results in two well defined weight loss maxima, one corresponding to a temperature of approximately 590°C and the other at

approximately 700°C. Maximum rates of weight loss were 1.1%/min and 1.0%/min respectively. Apparently, the more severe oxidation profile produces a more highly stabilized intermediate that possesses a higher associated temperature of reaction (590°C compared to 490°C for the other oxidized pitches). This particular pitch had lost about 10% of its total mass during its oxidation profile but still underwent an intermediate temperature weight loss process during carbonization, in similar fashion to pitches which gained weight during their oxidation profiles. This supports our contention that oxidized pitches are retaining introduced oxygen functionality despite weight loss experienced during the oxidation profile.

In summary, TGA results indicate the existence of two weight loss processes associated with the carbonization of previously oxidatively stabilized pitches. One weight loss process shows a rate maximum at approximately 490°C, the other at approximately 790°C. Futhermore, it appears that oxidation at higher temperatures and time periods may shift the early rate maximum to a higher temperature, and the later rate maximum to a lower temperature. This would be consistent with the production of more thermally stable intermediates of oxidation in pitches subjected to more severe oxidation profiles. Further clarification of the

nature of the species resulting from the weight loss circa 490°C in oxidatively stabilized pitches was not possible due to the inherent limitations of the TGA experiment. Table 1 contains a summary of the carbonization data from all TGA experiments.

4.2.2 THERMAL VOLATILIZATION ANALYSIS/SUB-AMBIENT THERMAL VOLATILIZATION ANALYSIS

4.2.2.1 UNOXIDIZED PITCH

The carbonization behavior of unoxidized pitch was successfully characterized through the application of Thermal Volatilization Analysis (TVA) and Sub-Ambient Thermal Volatilization Analysis (SATVA). Figure 35 shows the TVA trace resulting from the carbonization of unoxidized pitch to a temperature of 900°C at a rate of 9°C per minute. TVA indicates two major processes resulting in the emission of volatiles, the first achieving a rate maximum at approximately 490°C, and the second at approximately 770°C. The appearance of a volatile emission peak at 490°C is significant because it is coincident with the weight loss rate maxima seen in the TGA of unoxidized pitch heated at a rate of 20°C/min. Normally, processes that result in the emission of volatiles will occur at lower temperatures under reduced pressure. The same is true for materials degraded in

TABLE 1
CARBONIZATION DATA FROM TGA EXPERIMENTS

OXIDATION HISTORY	% MASS GAINED OR LOST DURING OXIDATION	RATE MAXIMA DURING CARBONIZATION IN TGA EXPERIMENT	% MASS LOST DURING CARBONIZATION	CORRECTED MASS LOST (%) FOR ENTIRE CYCLE[1]
0 min at 240°C	+ 3.18	500°C (0.6 %/min) 790°C (1.80 %/min)	-66.1	-65.0
15 min at 240°C	+ 5.84	490°C (0.5 %/min) 790°C (2.00 %/min)	-84.0	-83.1
60 min at 240°C	+ 7.53	490°C (0.6 %/min) 790°C (0.8 %/min)	-39.0	-34.4
240 min at 240°C	+10.7	490°C (0.65 %/min) 790°C (1.35 %/min)	-46.6	-40.9
480 min at 240°C	+10.1	490°C (0.7 %/min) 700°C (3.00 %/min)	-66.8	-63.4

[1] Oxidative stabilization then carbonization

TABLE 1 (cont.)
CARBONIZATION DATA FROM TGA EXPERIMENTS

OXIDATION HISTORY	% MASS GAINED OR LOST DURING OXIDATION	RATE MAXIMA DURING CARBONIZATION IN TGA EXPERIMENT	% MASS LOST DURING CARBONIZATION	CORRECTED MASS LOST (%) FOR ENTIRE CYCLE [1]
0 min at 290°C	+ 5.22	490°C (0.6 %/min) 750°C (2.70 %/min)	-98.0	-97.9
30 min at 290°C	+ 7.23	500°C (0.7 %/min) 790°C (1.00 %/min)	-39.4	-35.0
60 min at 290°C	+ 7.18	500°C (0.7 %/min)	-29.3	-24.2
240 min at 290°C	+5.82	510°C (0.7 %/min) 760°C (1.25 %/min)	-50.8	-47.9

[1] Oxidative stabilization then carbonization

TABLE 1 (cont.)
CARBONIZATION DATA FROM TGA EXPERIMENTS

OXIDATION HISTORY	% MASS GAINED OR LOST DURING OXIDATION	RATE MAXIMA DURING CARBONIZATION IN TGA EXPERIMENT	% MASS LOST DURING CARBONIZATION	CORRECTED MASS LOST (%) FOR ENTIRE CYCLE [1]
0 min at 340°C	+ 5.26	490°C (0.75 %/min) 750°C (1.30 %/min)	-51.6	-49.1
60 min at 340°C	+ 0.98	700°C (1.90 %/min)	-76.3	-76.1
120 min at 340°C	-2.09	640°C (1.20 %/min) 720°C (1.30 %/min)	-50.1	-51.1
240 min at 340°C	-9.73	590°C (1.10 %/min) 700°C (1.00 %/min)	-36.1	-42.3

[1] Oxidative stabilization then carbonization

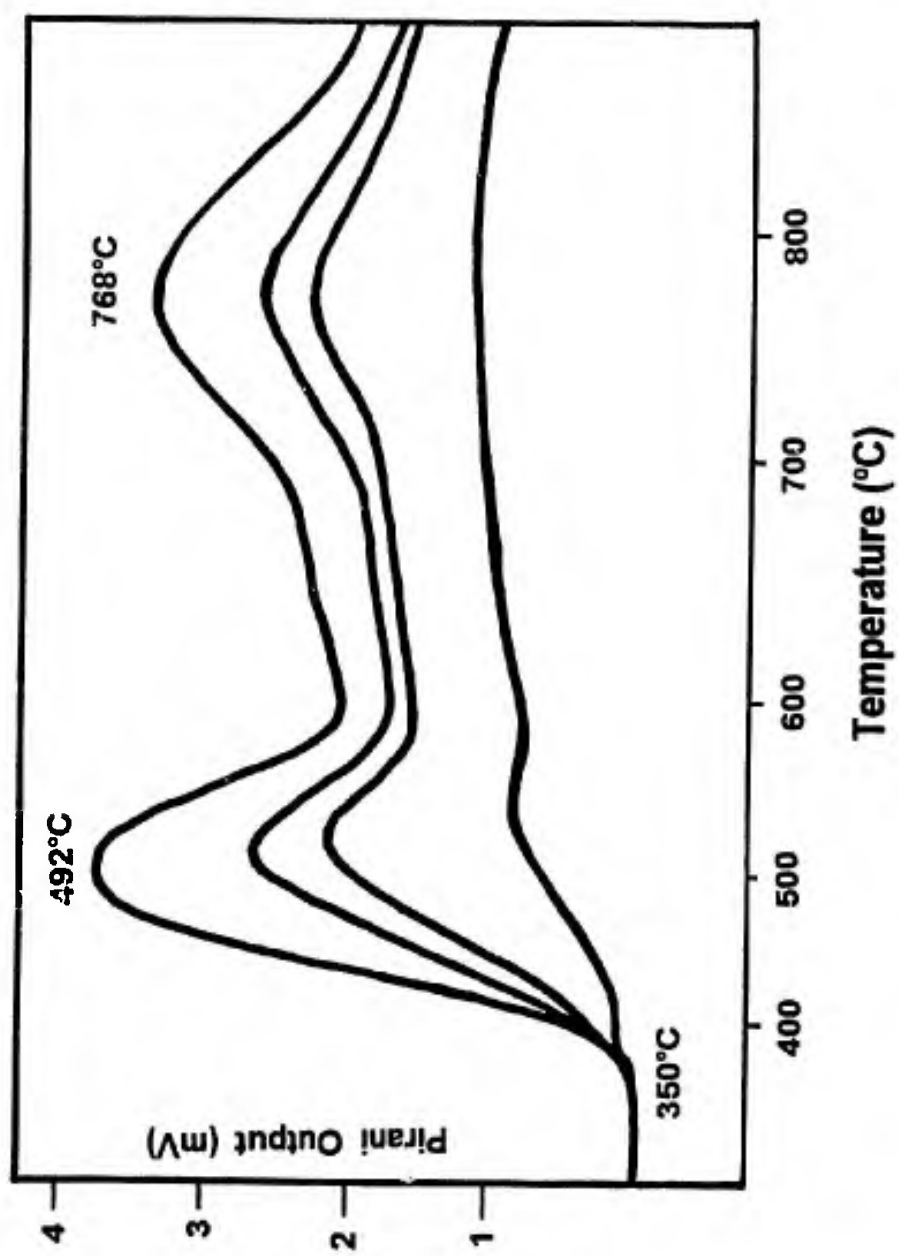

Figure 35. TVA trace for the carbonization of unoxidized pitch to an end temperature of 900°C at a rate of 9°C/min; sample size = 102.3 mg

thinner slices. The sample "thickness" in the TVA experiment is less than that used in the TGA experiment despite the larger sample size. Since our TVA experiments were performed under a vacuum of approximately 10^{-4} Torr, we expect the process maxima appearing at 490°C in the TVA experiment and 570°C in the TGA experiment to be related. Examination of the output corresponding to pirani gauge 4 (bottom trace) in figure 35 indicates that the production of hydrogen gas is occurring throughout the carbonization process, beginning at about 400°C. It was impossible to observe the pitch during carbonization, so it is not known if the pitch "bloated" at approximately 490°C, coincident with the appearance of the first volatile emission peak. Analysis of the coke residue at 900°C revealed that the unoxidized pitch powder had completely melted during carbonization, forming brittle shards of material similar in appearance to molten metal. A second TVA experiment was accomplished to an end temperature of 600°C, following the completion of the first volatile emission process. Analysis of the residue at 600°C indicated that the melting process had indeed occurred. It is likely that melting and fusion of the pitch is concurrent with the first volatile emission peak in the TVA trace.

An SATVA trace of all condensibles collected during the TVA of unoxidized pitch is shown in figure 36. A series of four peaks appears in the SATVA immediately upon initial warm-up of the parrafin wax surrounding the trap, indicating the presence of very low boiling point volatiles. The boiling points of these volatiles, at the corresponding vacuum pressure, are consistent with those for ethane (#1), propane (#2), 4-carbon alkanes (butane, iso-propane #3), and 5-carbon alkanes (#4). Subsequent infrared analysis ruled out the presence of significant quantities of unsaturated hydrocarbons in the product mixture. This assignment was substantiated through application of the relationship [23]

$$\ln P/P_o = - H_v/R [1/T - 1/T_o]$$

with values for the heats of vaporization taken from the literature [24]. The broad peak (#5) appearing beyond 30 minutes in the SATVA is due to water. An SATVA trace for all condensibles produced upon the carbonization to 600°C gave the same results, indicating that the collection of low boiling point alkanes is coincident with the first volatile emission process in the TVA.

An IR spectrum of all condensible gases produced from the carbonization of unoxidized pitch to 900°C is shown in figure 37. There is a very strong absorbance at approximately 2968 cm^{-1}, corresponding to the asymmetric stretching

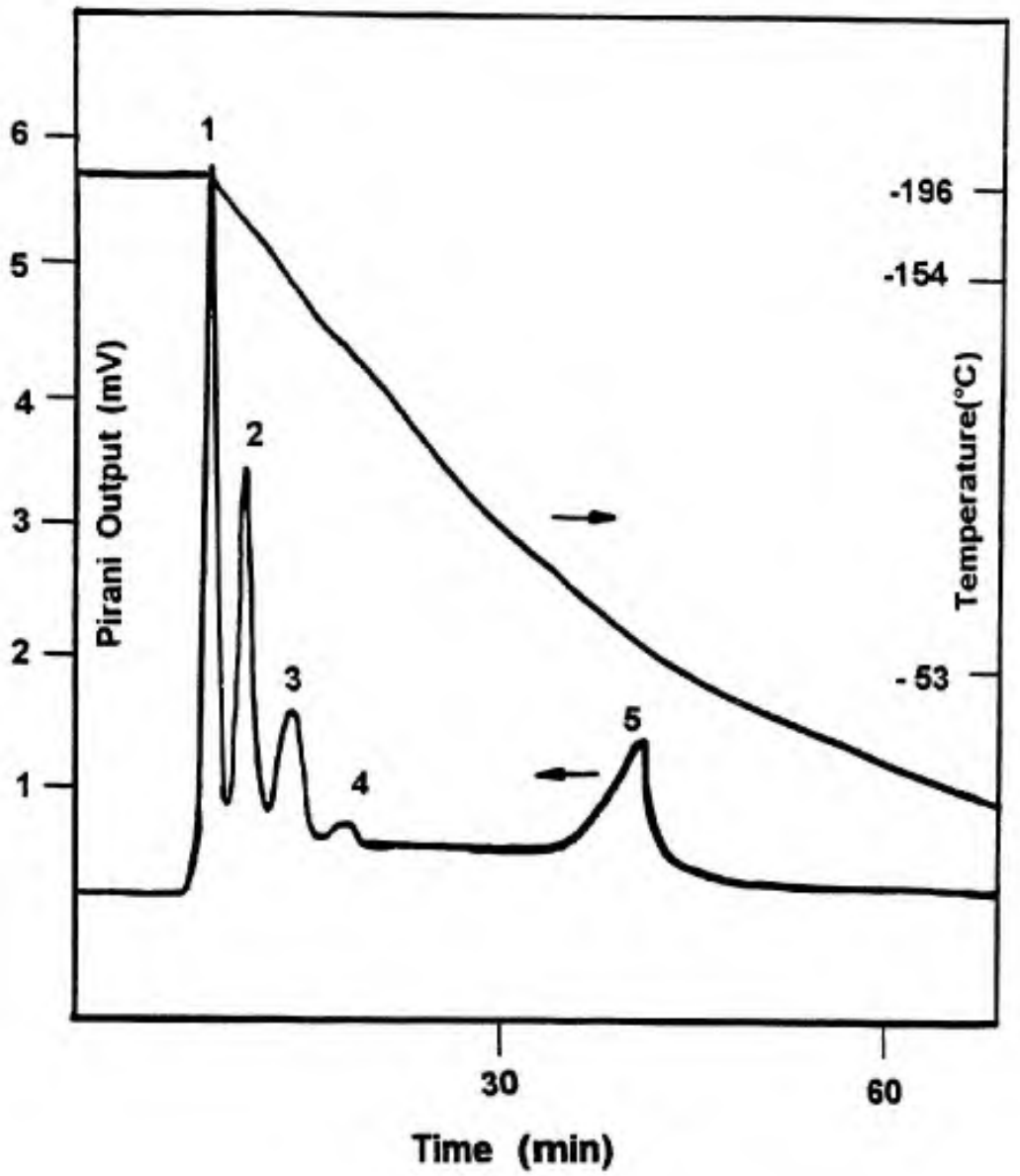

Figure 36. SATVA trace showing all condensible volatiles from carbonization of unoxidized pitch; 1: Ethane, 2: Propane 3: 4-carbon alkanes, 4: 5-carbon alkanes, 5: Water

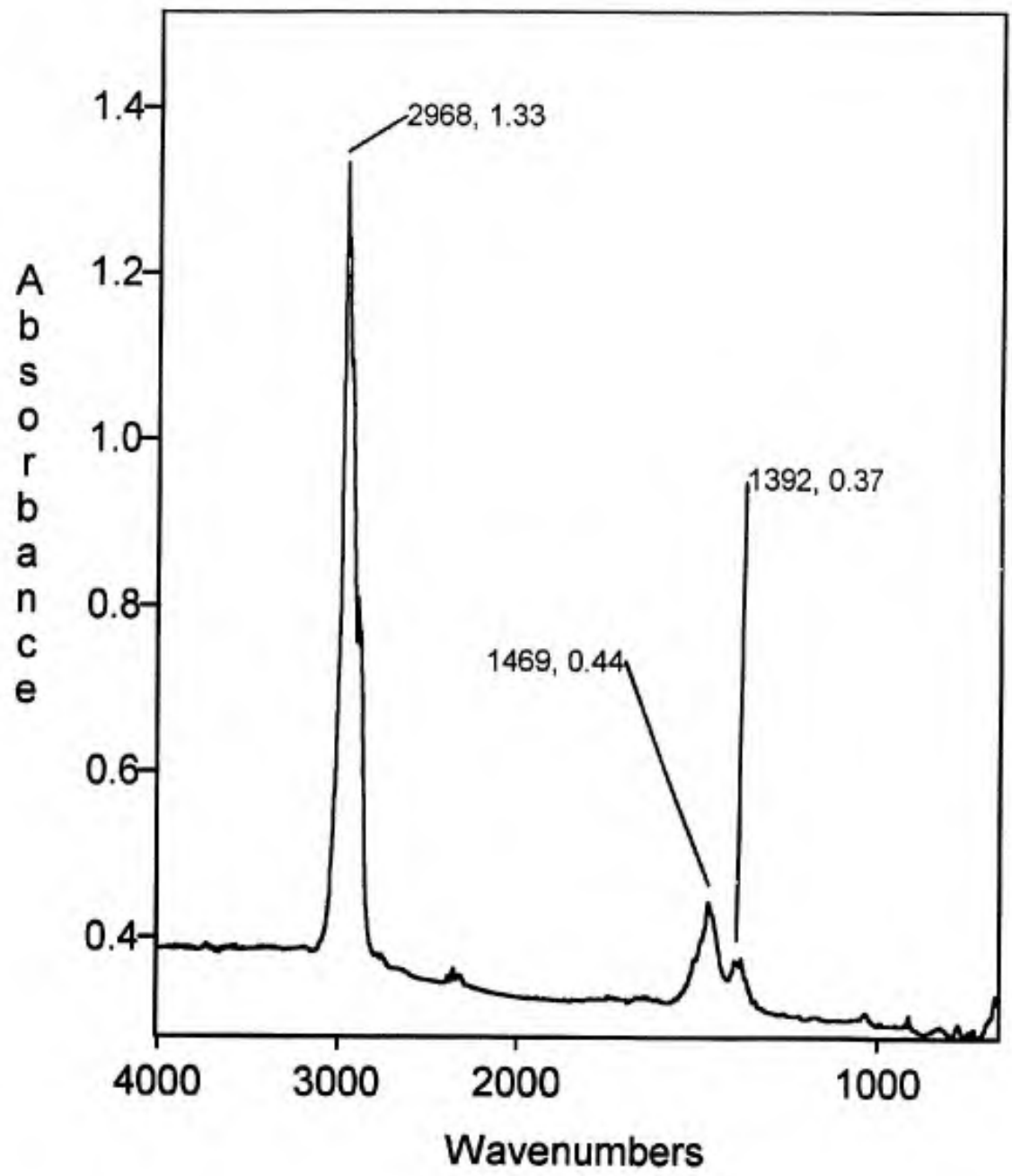

Figure 37. IR spectrum of condensible volatiles from carbonization of unoxidized pitch

mode of methyl hydrogens [21]. Absorbances also appear at approximately 1470 cm^{-1} and 1390 cm^{-1}, corresponding to methyl hydrogen asymmetric and symmetric bending modes, respectively [21]. The spectrum supports the conclusion that unoxidized pitch produces alkane gases at approximately 490°C during carbonization. Notice in figure 37 the absence of a strong C-H out-of-plane bending mode which normally appears between 650 and 1000 cm^{-1} and is characteristic of unsaturated hydrocarbons [21]. This bending mode gives rise to a very strong absorbance at approximately 940 cm^{-1} for ethylene, and 905 cm^{-1} for propylene [25]. Figure 37 also indicates the absence of alkynes in the product mixture because their is neither an sp-hybridized carbon stretching mode between 2100-2260 cm^{-1} nor a C-H stretching mode between 3260-3330 cm^{-1}, both of which are characteristic of alkynes [21].

An IR spectrum of all noncondensible gases (bar hydrogen) produced during the carbonization of unoxidized pitch to an end temperature of 900°C is shown in figure 38. The strong absorbances at approximately 1300 and 3020 cm^{-1} are due to methane [25]. The presence of methane is expected since 2, 3, and 4-carbon alkanes were present also in the condensible volatile product fraction. Whereas ethane, propane, and 4 and 5-carbon alkanes were associated with the first peak

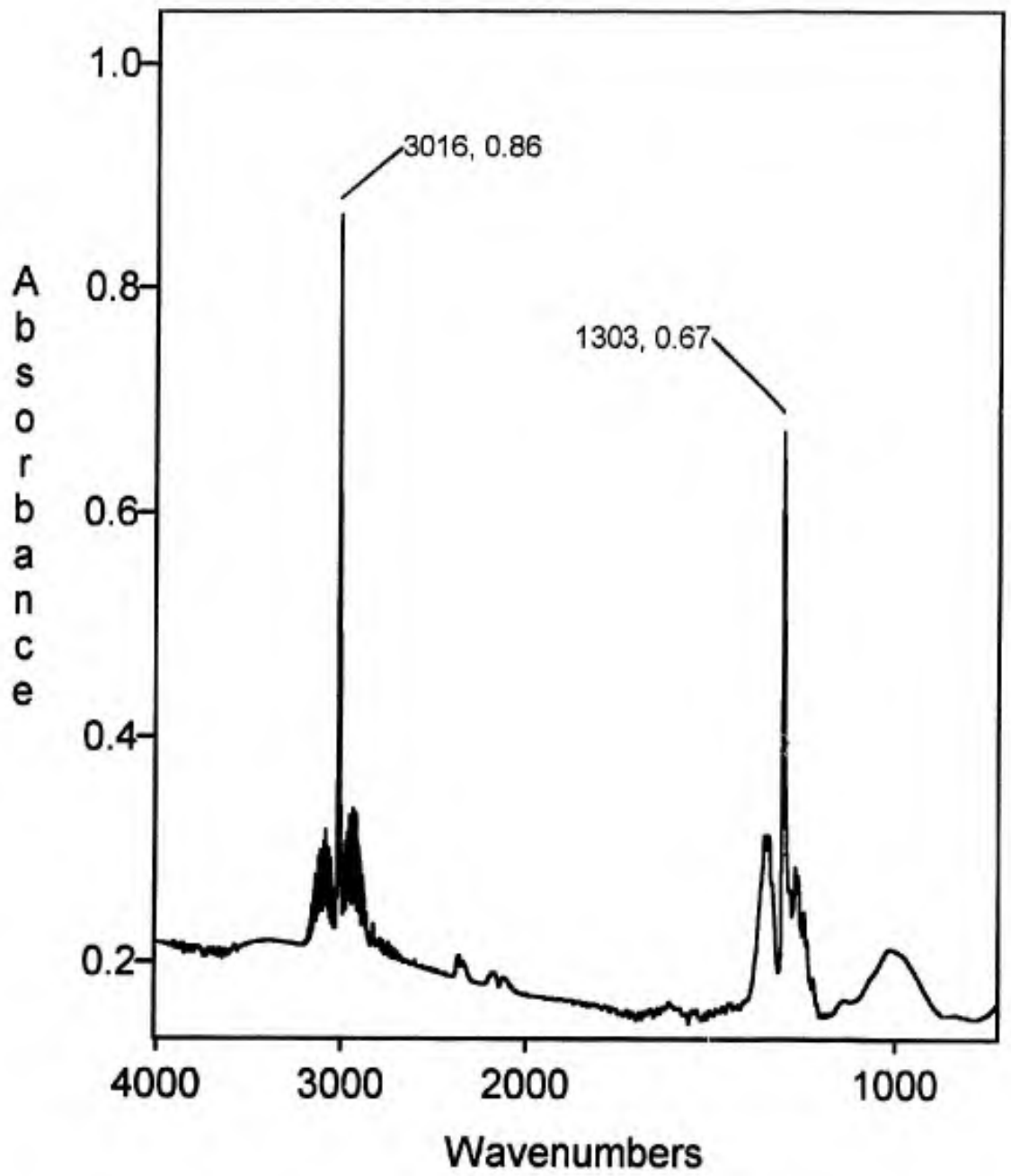

Figure 38. IR spectrum of noncondensible volatiles from carbonization of unoxidized pitch

only in the TVA of unoxidized pitch, methane was present throughout the entire carbonization process. This was verified by allowing all volatiles produced during carbonization up to 600°C to be pumped off to the vacuum line. The volatiles produced between 600°C and 900°C were trapped and subsequent analysis by SATVA and IR verified the production of methane and the non-production of condensible alkanes at these higher temperatures. Therefore, the second process in the TVA experiment observed at approximately 770°C is associated primarily with the emission of hydrogen and methane.

Figure 39 shows the IR spectrum of the oligomeric or "coldring" product fraction collected during unoxidized pitch carbonization. There is a relatively strong absorbance at 2922 and 2850 cm^{-1} corresponding to methylene hydrogen asymmetric and symmetric stretching, respectively [21]. Aromatic structure is also present in the coldring product fraction as indicated by the weak absorbances at 3043 cm^{-1} due to aromatic hydrogen stretching, and at 1600 cm^{-1} due to aromatic carbon stretching [21]. The relative concentration of aromatic and aliphatic carbons in the coldring product fraction is indicated by comparison of the peaks at 1600 and 1460 wavenumbers. Recall that for unoxidized pitch these peaks were of approximate equal intensity (figure 5). In the coldring

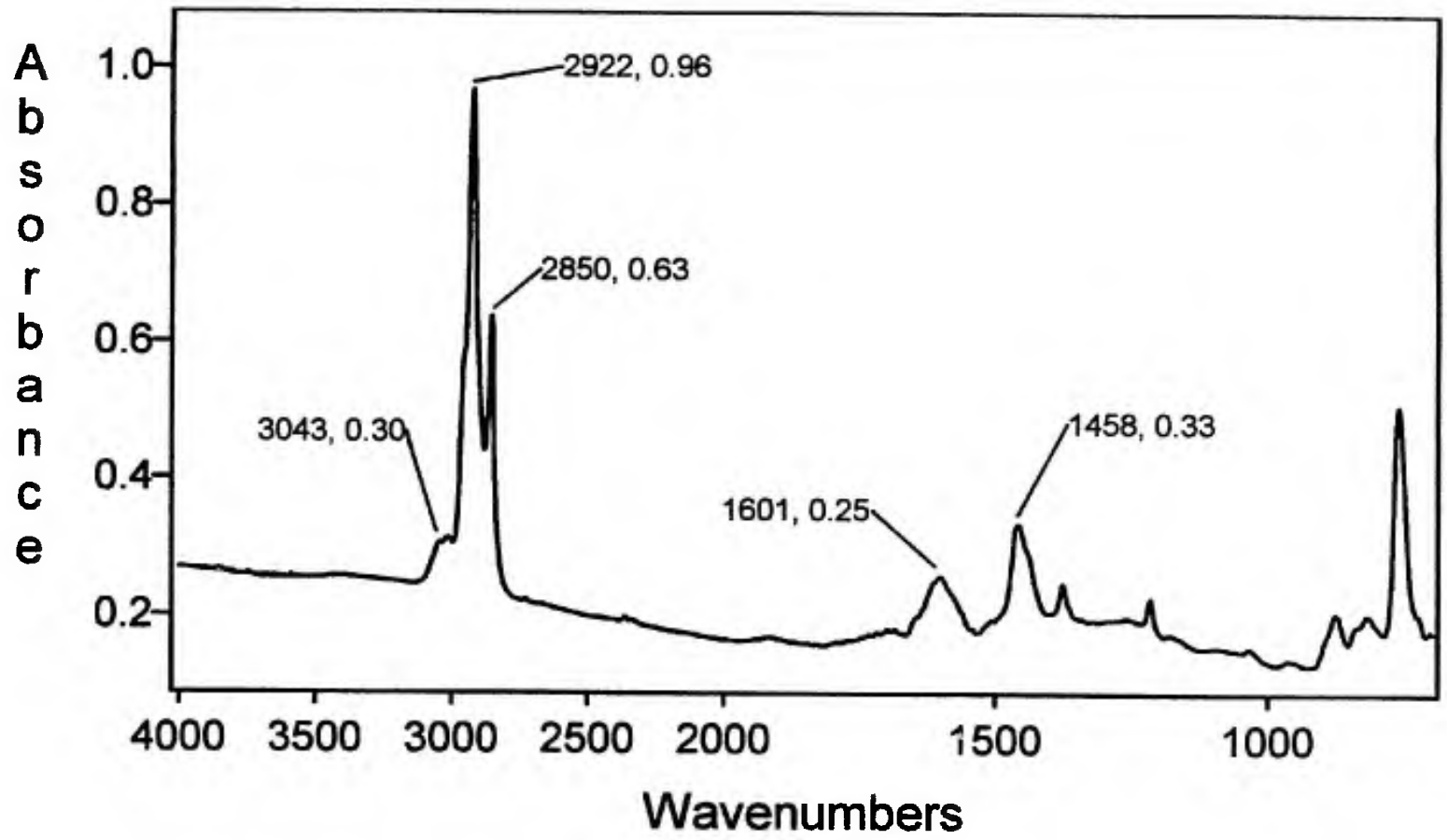

Figure 39. IR spectrum of the coldring product fraction from carbonization of unoxidized pitch

product fraction, the peak at 1460 cm^{-1} corresponding to methylene hydrogen bending is clearly stronger in intensity. The coldring product fraction of unoxidized pitch appears to be richer in aliphatic content than the pre-carbonized, unoxidized pitch itself. The coldring product fraction for unoxidized pitch formed a very significant fraction of the total degradation products--fully 48% by weight. Furthermore, the weight of the coldring product fraction produced up to 600°C was equal to the weight of coldring product fraction produced over the entire carbonization process to 900°C, indicating that the production of oligomers is associated with the first volatile emission process in the TVA experiment.

A comparison of the IR spectra for the coke at 600°C and at 900°C is shown in figure 40. The coke at 600°C shows the triplet of peaks below 900 cm^{-1} corresponding to aromatic hydrogen out-of-plane bending. At 900°C we see only a baseline at a high absorbance value which is due to the scattering of the IR beam by the carbon dispersion (the same is observed with reduced carbon blacks). It appears that the second volatile emission process in the TVA of unoxidized pitch, therefore, involves the loss of aromatic hydrogens. This conclusion is supported by the fact that the coke yield drops only 1% upon carbonization between 600 and 900°C, from a value of 57% to 56%, respectively.

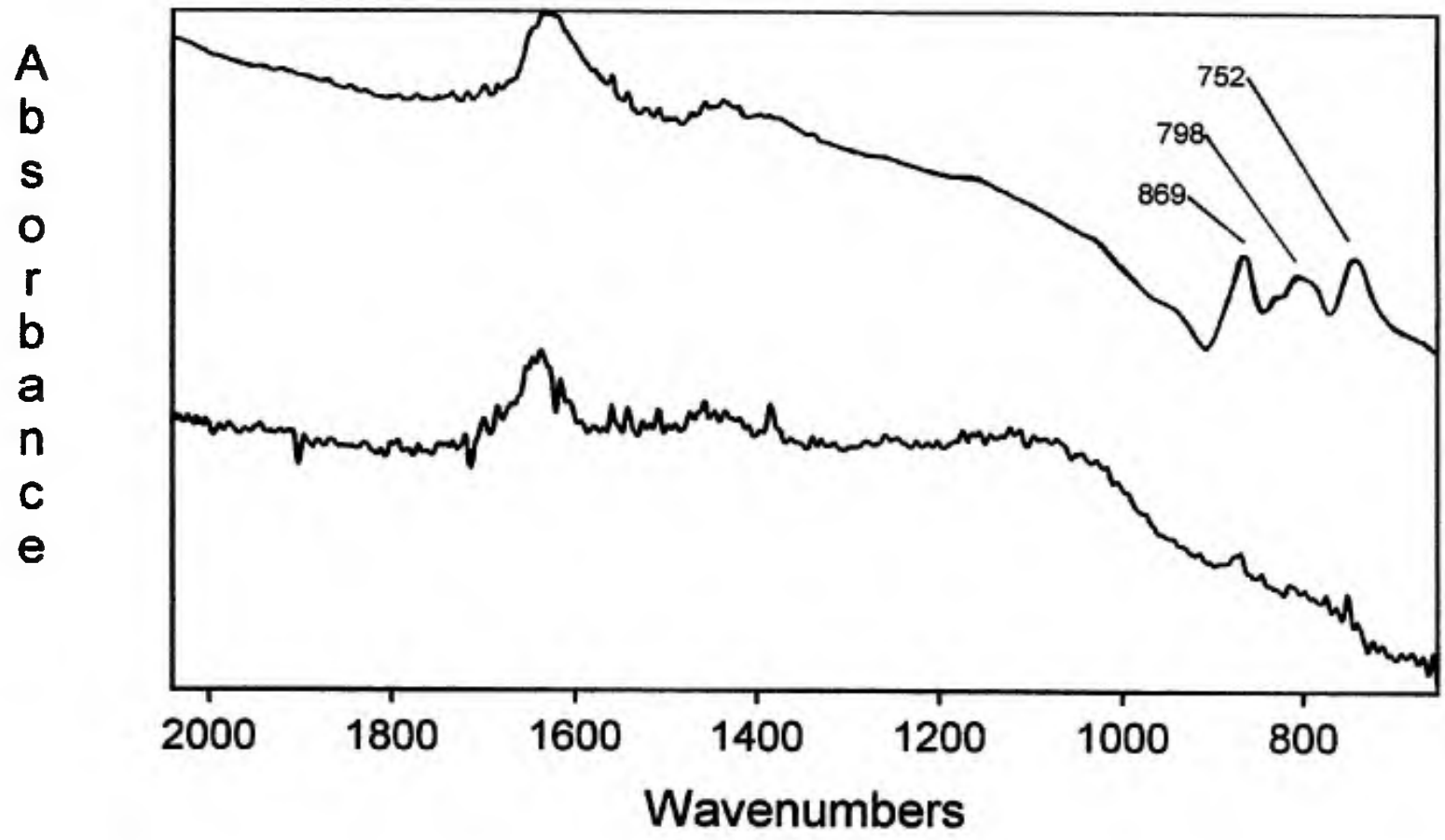

Figure 40. IR spectrum of unoxidized pitch carbonized to an end temperature of 600°C (top) and 900°C (bottom)

Pirani gauge 4 is also indicating the production of hydrogen gas during this period in the carbonization process (figure 35). Thus, the major weight loss process during the carbonization of unoxidized pitch occurs at about 490°C and results in the production of predominately oligomers and some alkane gases. This is in agreement with the TGA experiment as reproduced in figure 30 which shows the major weight loss process occurring between 400 and 600°C. It is probable that this weight loss process involves the thermal scission of relatively weak saturated carbon-carbon bonds, resulting in the production of oligomers and alkane gases and the subsequent "bloating" and melting of the pitch, facilitated by a rapid out-gassing of these materials. The physical appearance of the residue at 900°C at a heating rate of 9°C/min in the TVA experiment was very similar to the residue from the TGA experiment of unoxidized pitch heated at a rate of 20°C/min to an end temperature of 1000°C. Recall that there was no residue collected from the TGA experiment performed at a heating rate of 10°C/min. These results suggest that the production of a residue (coke) during the carbonization of unoxidized pitch might be a function of the efficiency of the removal of degradation products, namely oligomers and alkane gases.

4.2.2.2 FULLY STABILIZED PITCH

In order to compare the carbonization behavior of oxidized pitch to unoxidized pitch, we were required to analyze a pitch sample which was "fully" oxidatively stabilized. We decided to choose a pitch sample that had been oxidized to a point in its weight change curve where weight gain was at a maximum. We felt pitch oxidized at 240°C for 4 hours would be a good choice because we were able to track a steady and reproducible build-up of oxygen content and % weight gain as a function of oxidation time for this particular pitch. The TVA trace for this pitch is shown in figure 41. The curve shape is similar to that for unoxidized pitch in figure 35. There is, once again, a "low" temperature volatile emission process and a "high" temperature volatile emission process. The high temperature process achieves a maximum rate at approximately 750°C--about 20° less than for unoxidized pitch. The biggest differences, however, appear in the low temperature process which shows a shoulder peak at approximately 430°C and a maximum at approximately 525°C.

The SATVA separation for all condensibles collected during the TVA experiment is illustrated in figure 42. There are two peaks corresponding to very low boiling point compounds. The first minor peak (below 1 mV pirani output)

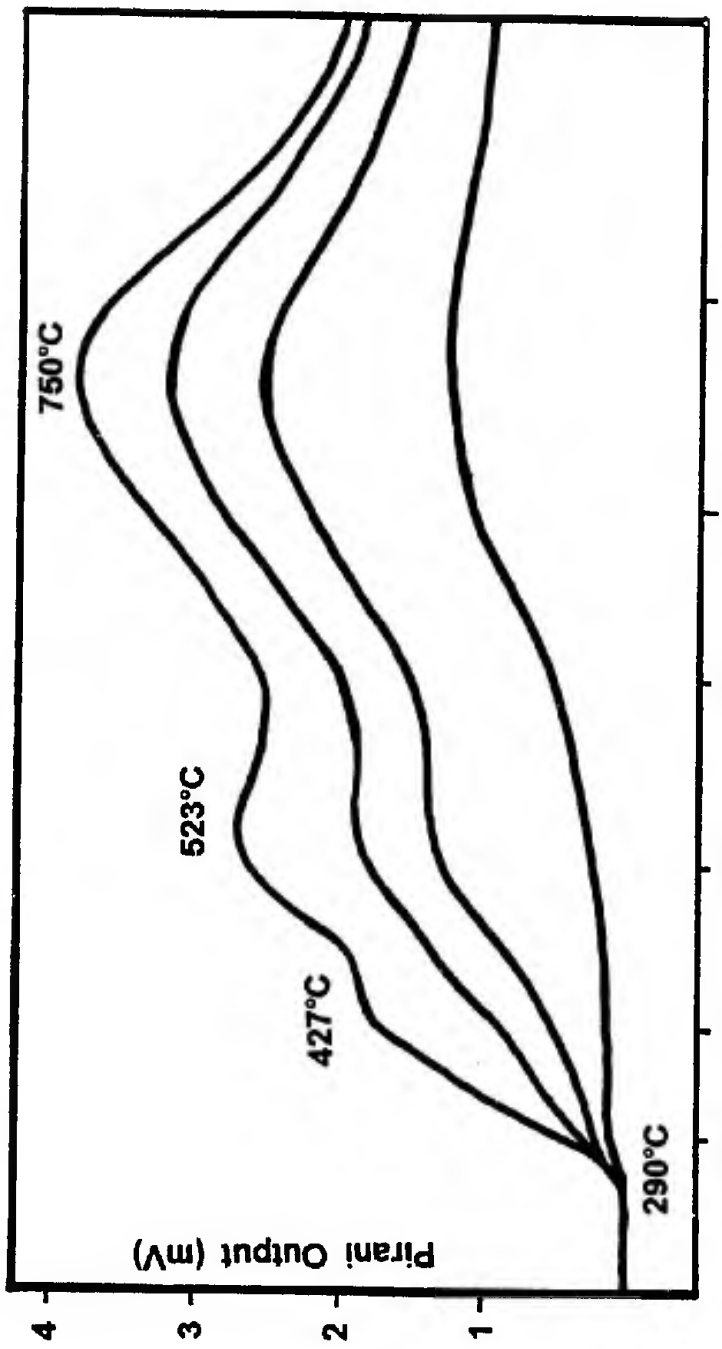

Figure 41. TVA trace for the carbonization of pitch, previously oxidized at 240°C for 240 minutes, to a temperature of 900°C at a rate of 9°C/min; sample size = 104.6 mg

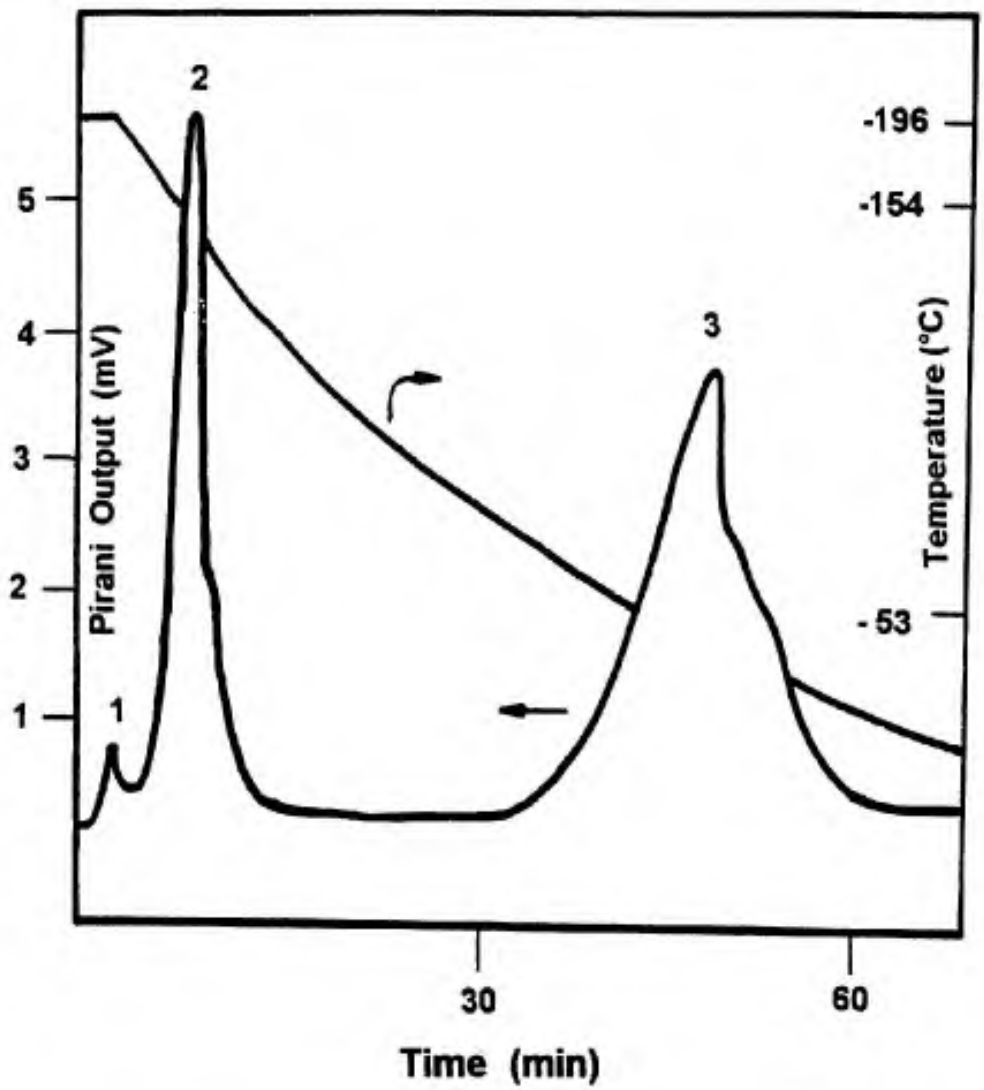

Figure 42. SATVA trace showing all condensible volatiles from carbonization of pitch previously oxidized at 240°C for 240 minutes; 1: Ethane, 2: Carbon dioxide, 3: Water

corresponds to ethane and the second, much larger peak corresponds to carbon dioxide. The presence of carbon dioxide in the condensibles is verified by the IR spectrum in figure 43. The strong doublet at approximately 2350 cm^{-1} is due to carbon dioxide [25]. Notice, also, in the IR spectrum the weak absorbance at 2968 cm^{-1}, indicating the presence of residual alkane gases as suggested by the SATVA trace. It is likely that the carbon dioxide peak in the SATVA trace is overlapping small peaks due to propane and 4-carbon alkanes. Clearly, however, the predominant condensible products of oxidized pitch carbonization are carbon dioxide and water. Water was identified in the IR spectra by the appearance of the very broad O-H stretching band at 3500 cm^{-1} and the O-H bending band at 1640 cm^{-1}. These absorbances were purposely removed from the IR spectra of the condensible volatile fractions for oxidized pitches because they inhibit analysis of modes arising from gases other than water. All IR spectra were collected while the water was still condensed in the cold finger; follow-up spectra were taken after heating the cold finger with a hot air gun to measure water content. The relatively small quantity of alkanes is probably from aliphatic functionality that resisted reaction during the oxidation experiment.

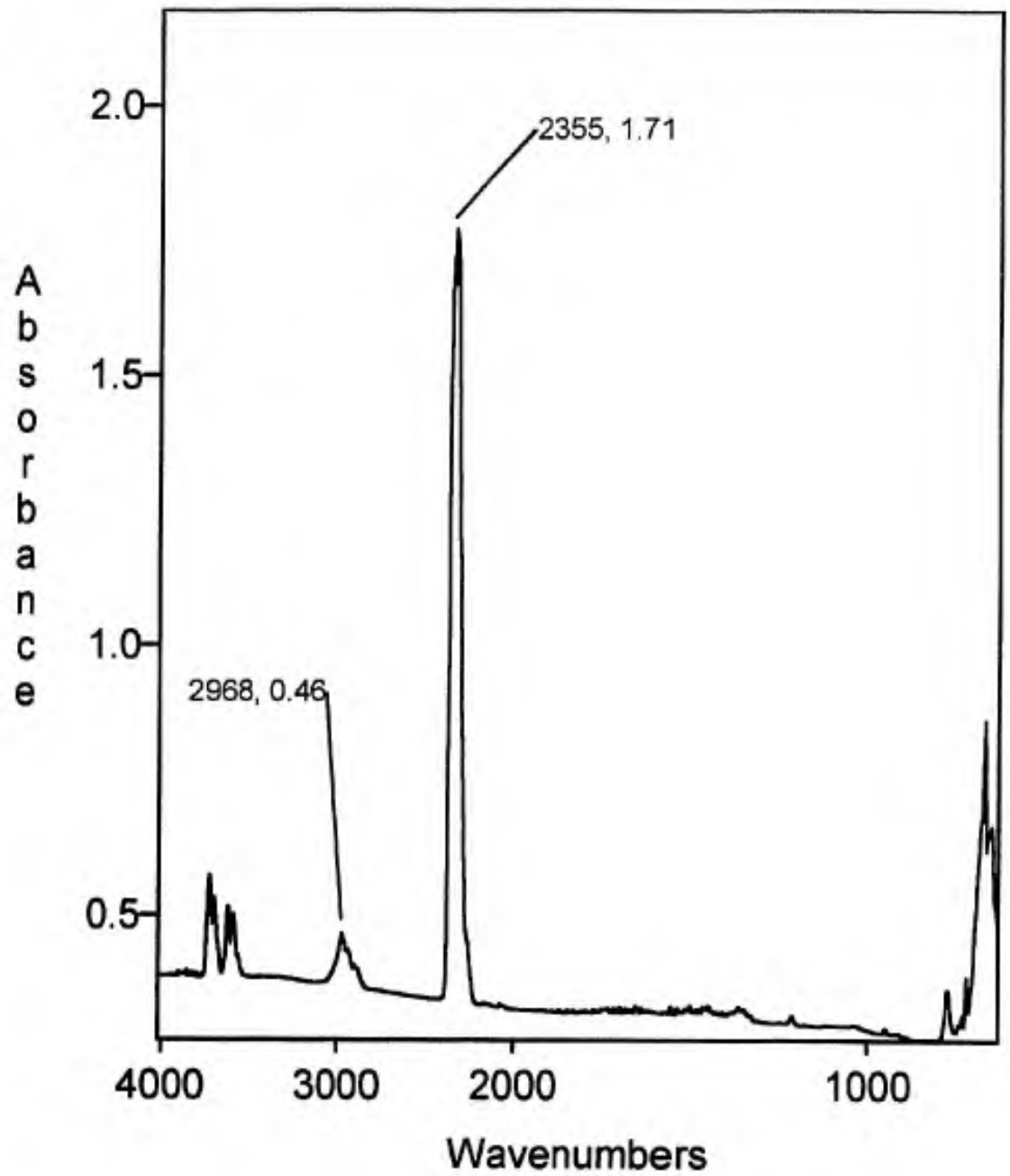

Figure 43. IR spectrum of condensible volatiles from carbonization of pitch previously oxidized at 240°C for 240 minutes

Noncondensible gases resulting from the carbonization of oxidized pitch are shown in the IR spectrum in figure 44. The spectrum indicates, in addition to methane, the production of carbon monoxide, 2170 cm^{-1}, as a result of the carbonization of oxidized residues in the pitch [25].

The coldring product fraction (CRF) for pitch oxidized at 240°C for 4 hours is shown in figure 45. The IR spectrum indicates a significant aliphatic content in the CRF based on the intensity of the methylene hydrogen stretching band at 2920 cm^{-1}. There is a much weaker band due to aromatic hydrogen stretching at about 3030 cm^{-1}. Notice, also, that the relative intensities of the peaks due to aromatic carbon stretching at 1600 cm^{-1} and methylene hydrogen bending at approximately 1460 cm^{-1} indicate a lesser proportion of aromatic material in the CRF of fully oxidized pitch. The appearance of a carbonyl band at approximately 1728 cm^{-1} is a striking feature, however it is not clear if the band is due to ester or ketone functionality. Another significant factor is that the yield of coldring product fraction for this oxidized pitch is only 5% by weight, compared to 48% for unoxidized pitch. Measurements on CRF collected at different points in the TVA experiment showed that the production of oligomers was associated with the low temperature volatile emission process, with the production of CRF complete by

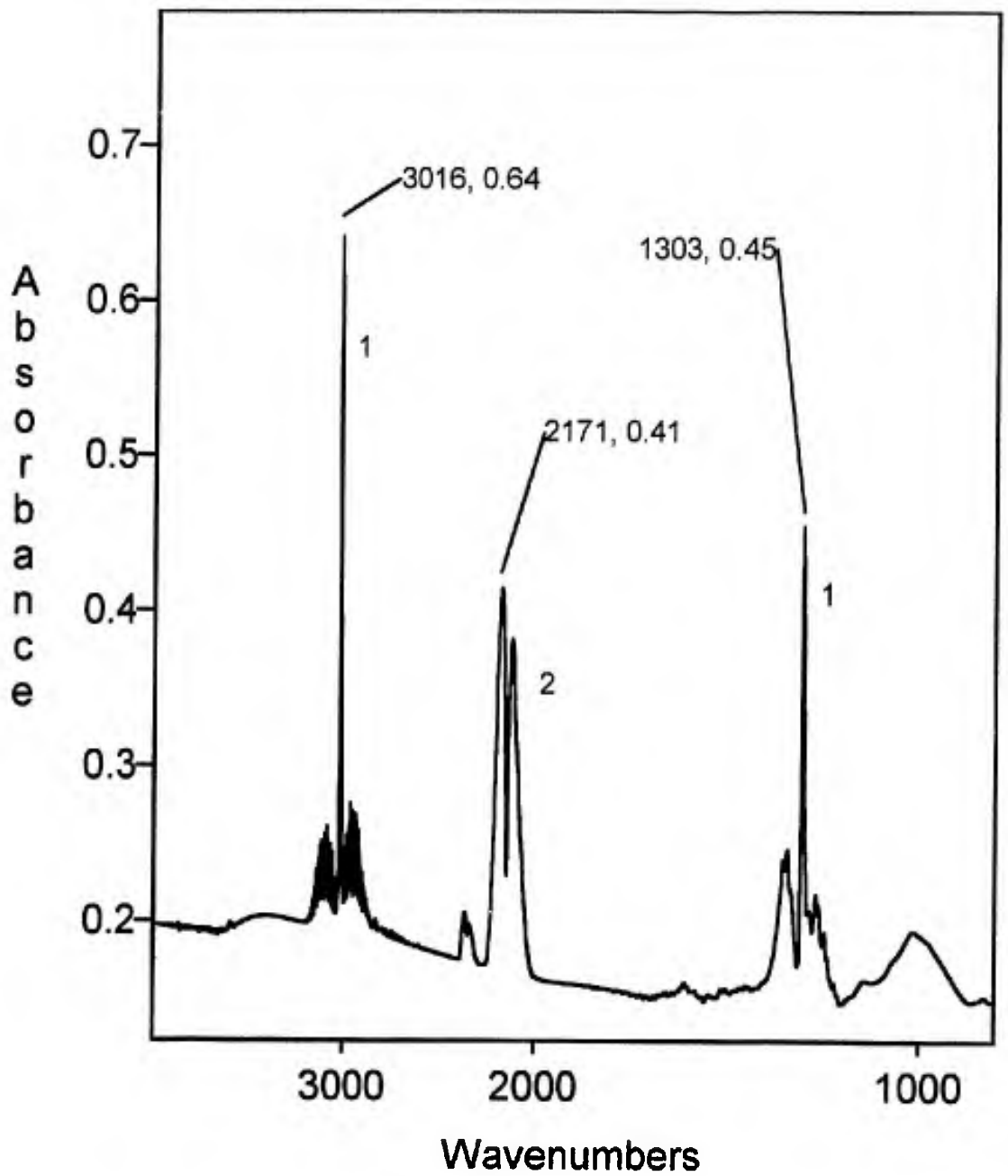

Figure 44. IR spectrum of noncondensible volatiles from carbonization of pitch previously oxidized at 240°C for 240 minutes; 1: Methane, 2: Carbon monoxide

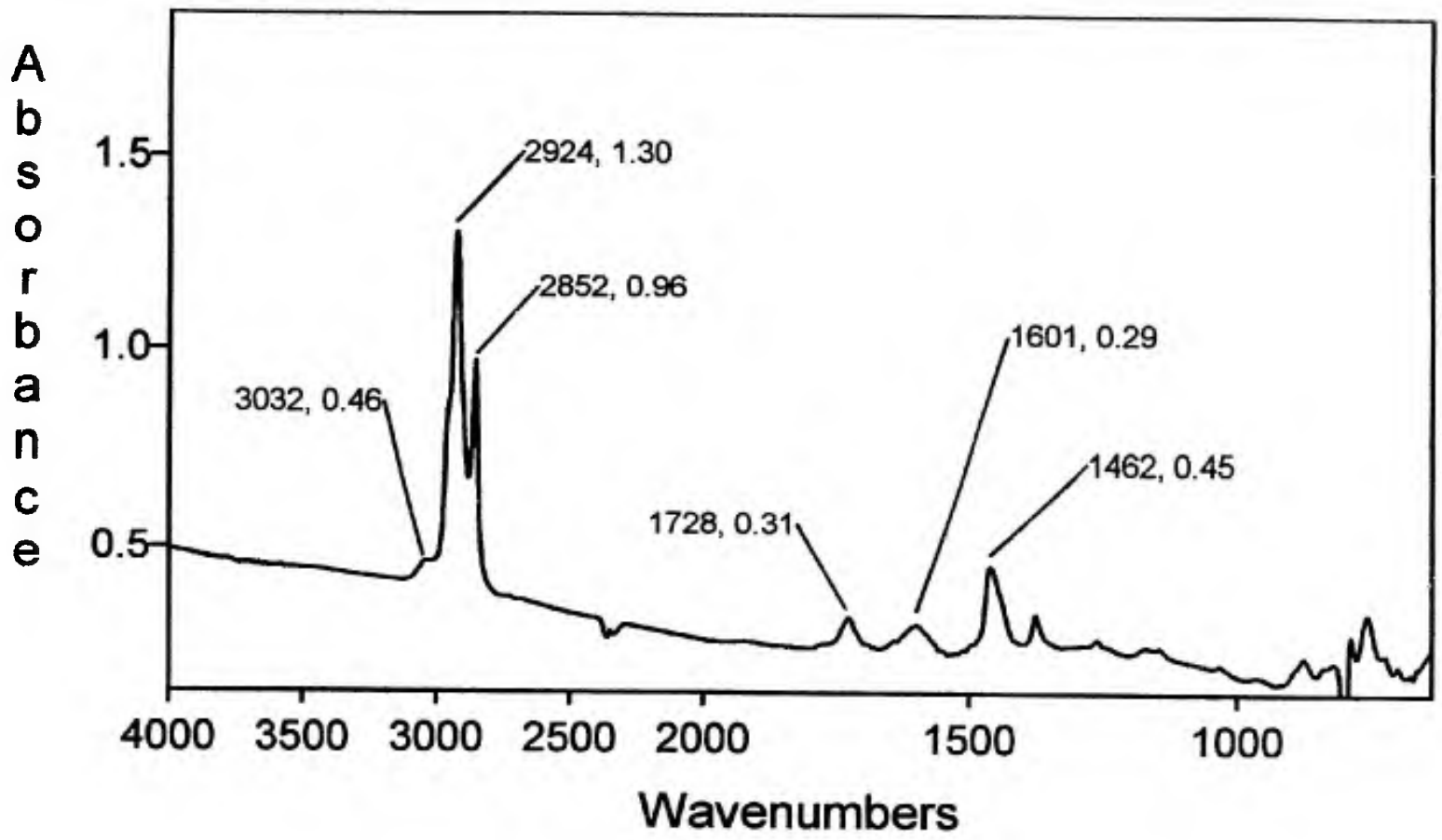

Figure 45. IR spectrum of the coldring product fraction from carbonization of pitch previously oxidized at 240°C for 240 minutes

about 600°C.

A TVA experiment was performed on pitch oxidized at 240°C for 4 hours up to a carbonization temperature of approximately 440°C, corresponding to the completion of the volatile emission process forming the low temperature shoulder peak in the TVA (figure 41). A subsequent SATVA separation of the condensibles indicated the production of only carbon dioxide and water. Therefore, the shoulder peak at 427°C in the carbonization of oxidized pitch corresponds to emission of carbon dioxide and water only. The condensible volatiles associated with the first rate maxima between 440 and 600°C include carbon dioxide, water, and a small quantity of alkanes. The second or high temperature volatile emission process, achieving a maximum at 750°C, creates primarily hydrogen, methane, and some carbon monoxide. These resuits suggest that any remaining aliphatic content in the oxidized pitch is lost in the coldring product fraction, or fragmented to produce light alkane gases during carbonization between 440 and 600°C.

Figure 46 shows a comparison of the IR spectra of oxidized pitch residue after carbonization to 440°C and 600°C. The IR spectra of the residue at 440°C, corresponding to the completion of the "shoulder" peak process in the TVA,

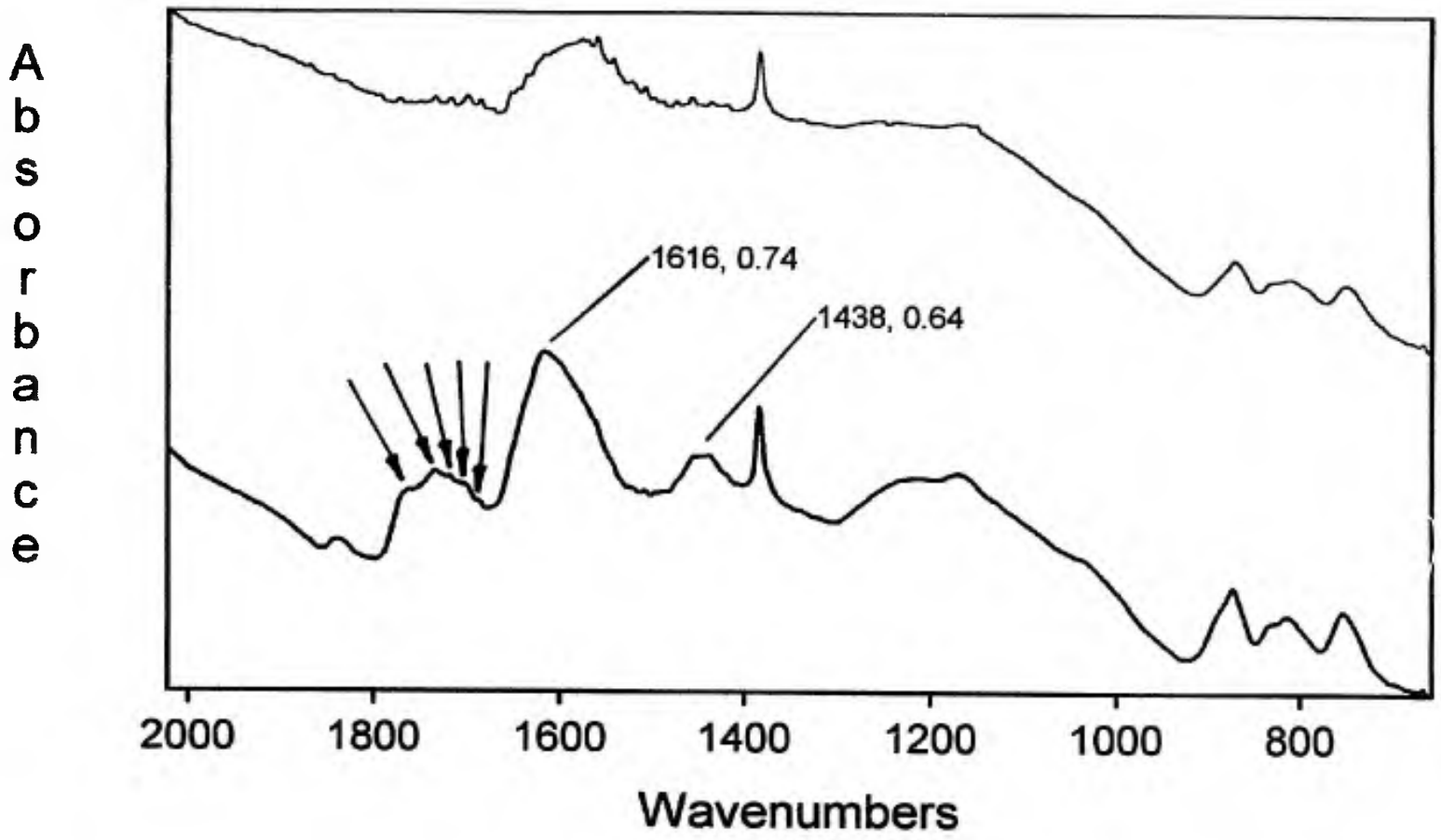

Figure 46. IR spectrum of pitch, previously oxidized at 240°C for 240 minutes, carbonized to 600°C (top) and 440°C (bottom)

shows a band due to methylene hydrogen bending at about 1438 cm^{-1}. This band disappears upon carbonization to 600°C (with the accompanied emission of a small quantity of light alkanes). There is also a distinct band due to carbonyl stretching centered at 1700 cm^{-1} in the IR spectrum for the residue at 440°C. Upon closer examination it can be seen that the band is made-up of the five individual absorbances due to specific carbonyl functionality previously identified in the spectrum of the oxidized, pre-carbonized pitch in figure 10. The band has decreased in intensity relative to the aromatic carbon stretching band at 1600 cm^{-1}. Specifically, the 1700cm^{-1}/1600 cm^{-1} peak area ratio value has decreased to approximately 0.35 from approximately 0.85 as measured for the pre-carbonized, oxidized pitch. This decrease in the intensity of the carbonyl stretching mode is concurrent with the release of carbon dioxide and carbon monoxide gas up to approximately 440°C in the TVA experiment. Furthermore, the carbonyl band has disappeared by carbonization to 600°C, after the further emission of carbon dioxide and carbon monoxide. The disappearance of oxygen functionality in the pitch and the subsequent emission of carbon dioxide/carbon monoxide does not appear to be related to the loss of any specific carbonyl functionality (ester, anhydride, ketone, aldehyde, etc.) because all bands are still represented in the

residue of the oxidized pitch at 440°C in figure 46. It is possible that the loss of oxygen functionality and emission of carbon dioxide proceeds relative to or based on differences in the stability of oxygen functionality as a function of location in the pitch (edge carbons, etc.) rather than as a function of specific carbonyl functionality (ester, anhydride, ketone, aldehyde, etc.).

Pitch previously oxidized at 240°C for 4 hours gave a coke yield of 72% (based on the weight of the oxidized, pre-carbonized pitch) at 900°C, compared to 56% for unoxidized pitch. Furthermore, the oxidized pitch did not fuze or melt upon carbonization, but rather maintained its powdered form.

4.2.2.3 INSUFFICIENTLY STABILIZED PITCH

An insufficiently oxidatively stabilized pitch was selected for TVA and SATVA analysis in order to contrast its carbonization behavior with a fully stabilized pitch. We felt that a pitch which experienced minimal weight gain during its oxidation profile, corresponding to a point near the beginning of its respective weight change curve, would best represent an "insufficiently stabilized" pitch. The pitch selected was previously oxidized at 240°C to the end of its heating ramp (time zero), and its TVA trace is shown in figure 47. The TVA indicates a minor volatile emission process occurring between 270°C and 400°C,

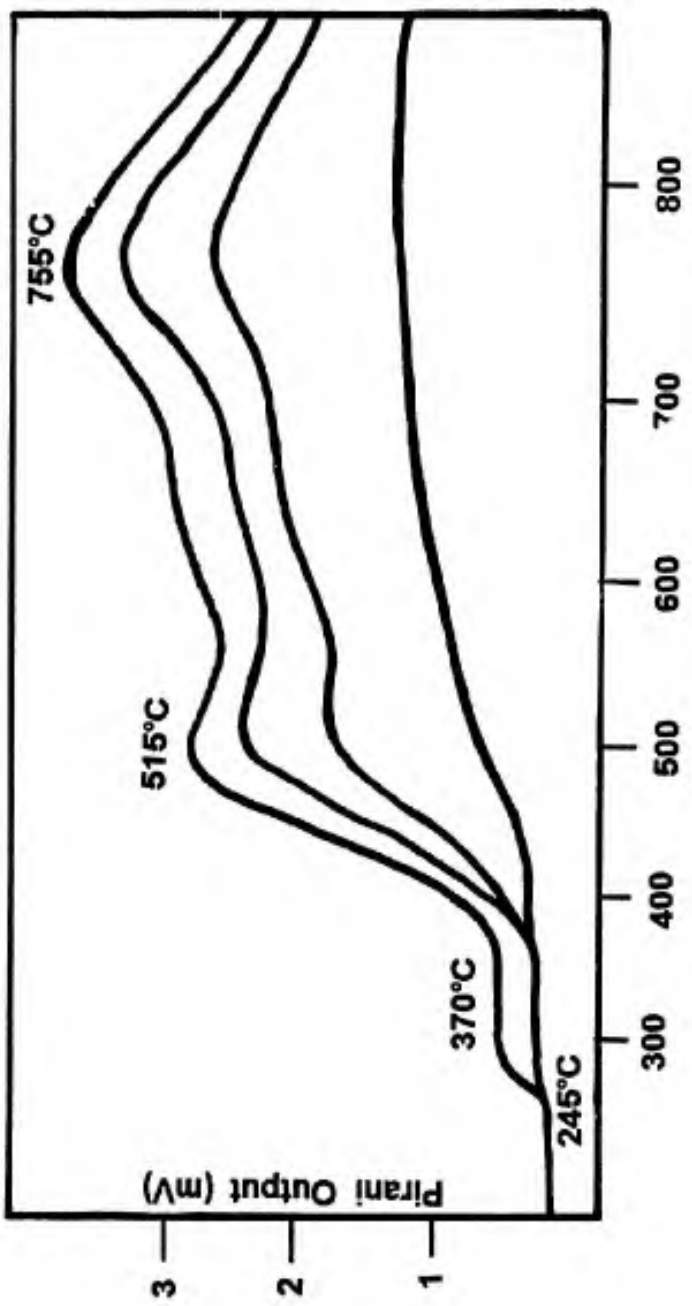

Figure 47. TVA trace for the carbonization of pitch, previously oxidized at 240°C for 0 minutes, to a temperature of 900°C at a rate of 9°C/min; sample size = 100.7 mg

forming a "plateau" in the pirani gauge output. This is in marked contrast to the TVA trace for pitch oxidized at 240°C for 4 hours which shows a steady increase in the rate of volatile emission between 270°C and 400°C. Beyond the "plateau", which is centered at a temperature of 370°C, the TVA trace contains two higher temperature rate maxima at 515°C (compare with 523°C in figure 41) and at 755°C (compare with 750°C in figure 41).

The SATVA trace corresponding to total volatile production during the TVA experiment is shown in figure 48. We observe a series of peaks corresponding to very low boiling point compounds similar to that seen for unoxidized pitch (figure 36). The peaks are assigned to ethane, propane, 4-carbon alkanes, and 5-carbon alkanes--identical to the SATVA for unoxidized pitch with two major differences; the presence of a peak corresponding to carbon dioxide which overlaps the propane peak, and a much larger peak corresponding to water. Not surprisingly, partly stabilized pitch shows a mixture of condensible products characteristic of unoxidized pitch (alkanes), and of fully stabilized pitch (carbon dioxide and water).

An IR spectrum of the condensible volatiles produced upon degradation to 900°C is shown in figure 49. As expected, the IR spectrum contains absorbances

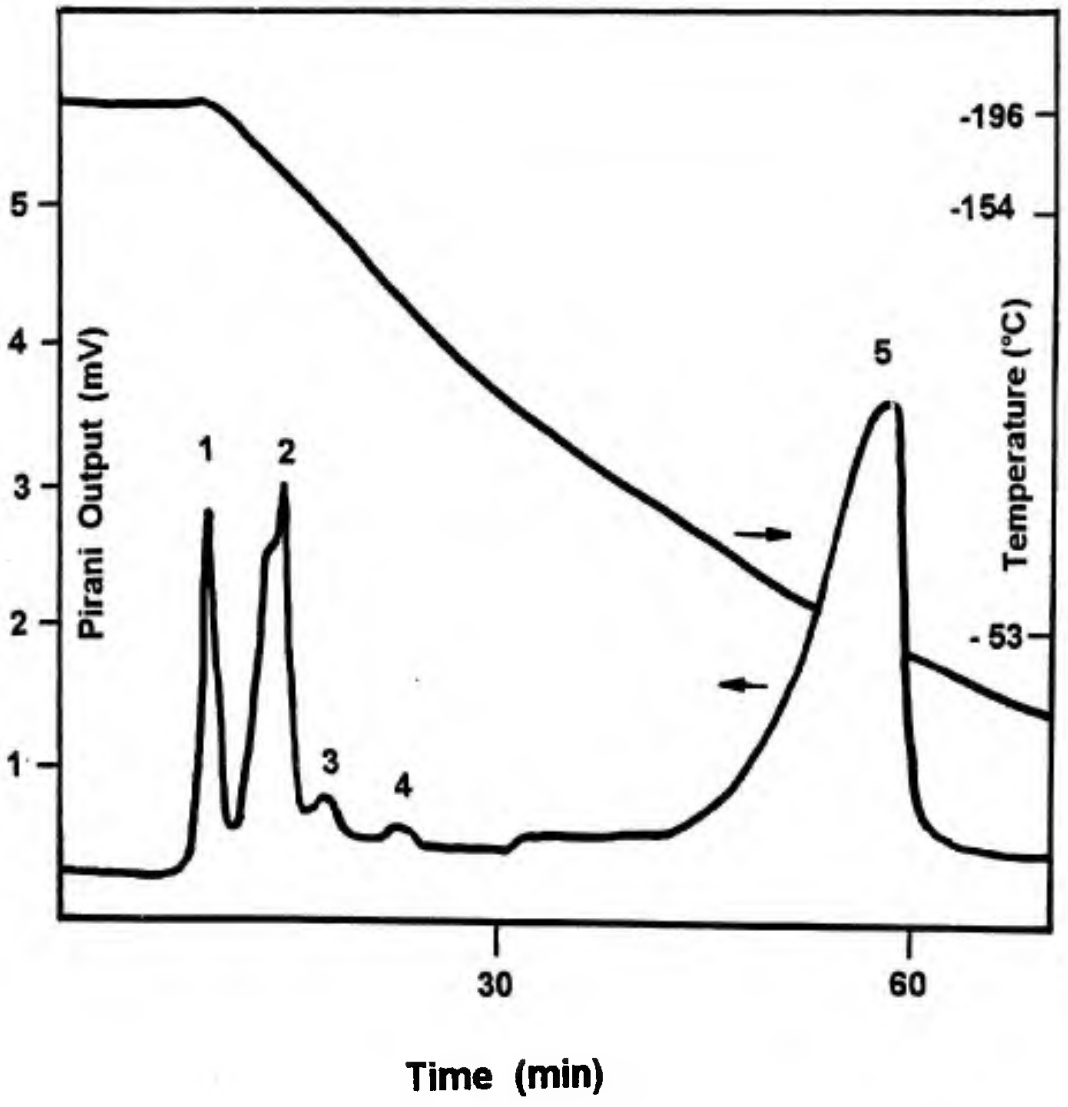

Figure 48. SATVA trace showing all condensible volatiles from carbonization of pitch previously oxidized at 240°C for 0 minutes; 1: Ethane, 2: Propane and carbon dioxide, 3: 4-carbon alkanes, 4: 5-carbon alkanes, 5: Water

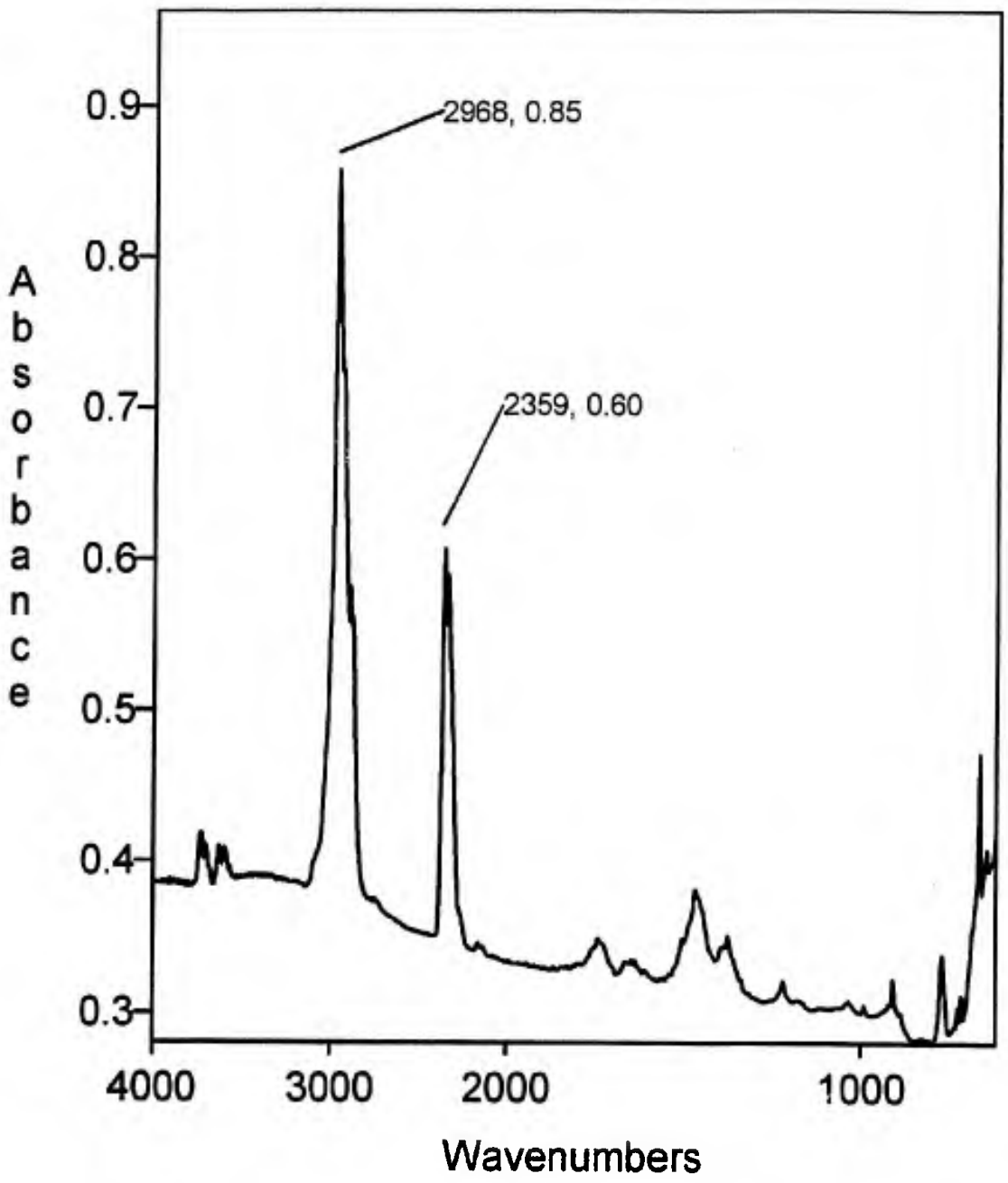

Figure 49. IR spectrum of condensible volatiles from carbonization of pitch previously oxidized at 240°C for 0 minutes

characteristic of alkanes (2968 cm^{-1}) and carbon dioxide (2359 cm^{-1}). An IR spectrum of the noncondensible volatiles resulting from carbonization to 900°C is shown in figure 50. This spectrum indicates the production of mainly methane with small amounts of carbon monoxide (at approximately 2170 cm^{-1}).

A second TVA experiment was performed using this insufficiently stabilized pitch to an end temperature of 400°C, corresponding to the completion of the low temperature "plateau" in the volatile emission curve. The subsequent SATVA trace is shown in figure 51 and indicates only the production of carbon dioxide and water. Another SATVA separation performed on condensibles collected during carbonization to an end temperature of approximately 600°C gave results identical to those shown in figure 48. Therefore, the volatile emission process occurring between approximately 245°C and 400°C is due primarily to the loss of carbonyl functionality as carbon dioxide and water. The volatile emission peak at approximately 515°C in the TVA is due to carbon dioxide, alkanes, and water. Apparently, any remaining unoxidized aliphatic functionality in the pitch is cracked-off during carbonization between 400°C and 600°C, as previously seen for both unoxidized and fully stabilized pitch. The only apparent differences are in the relative quantities of alkanes and carbon dioxide/water produced.

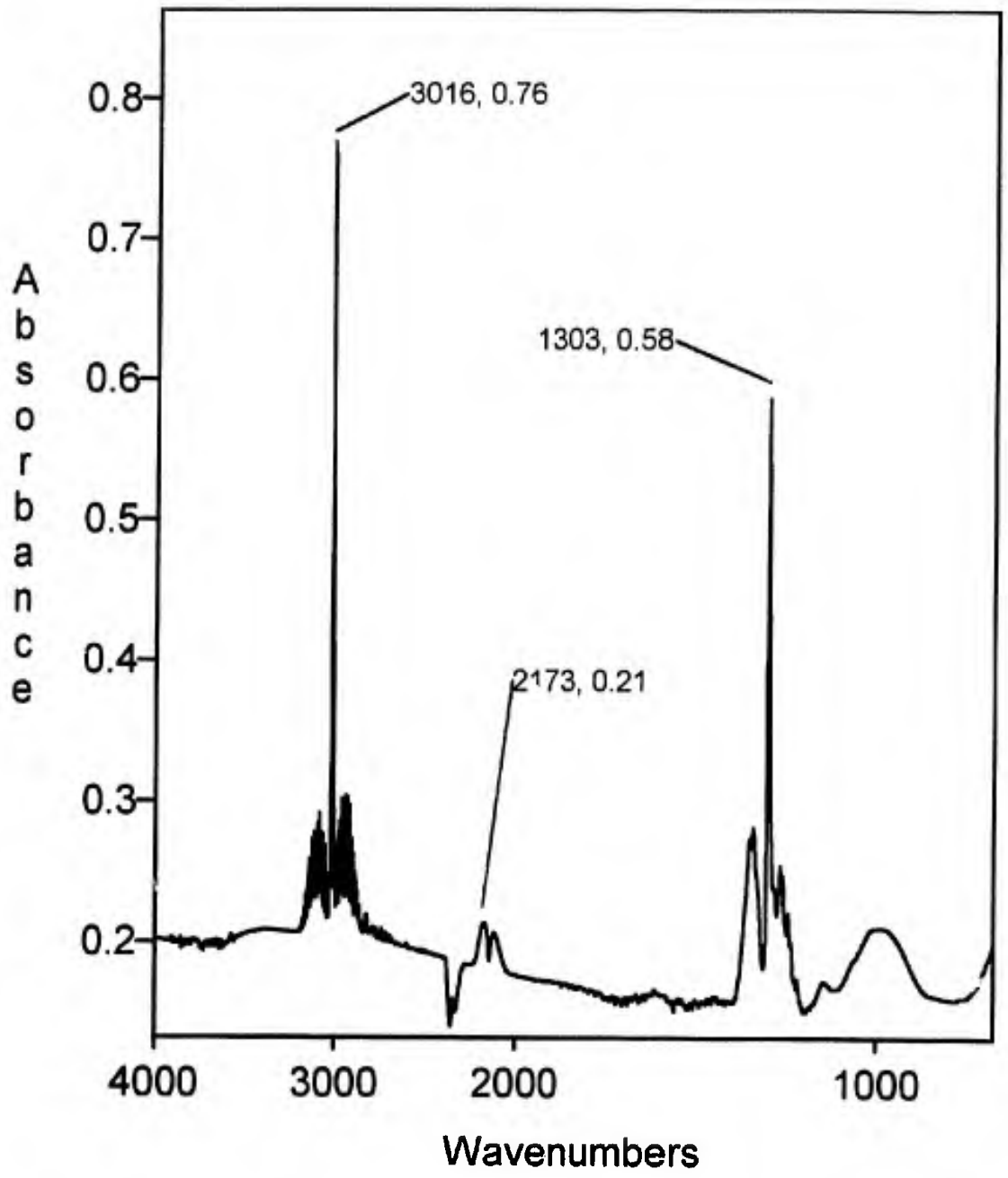

Figure 50. IR spectrum of noncondensible volatiles from carbonization of pitch previously oxidized at 240°C for 0 minutes

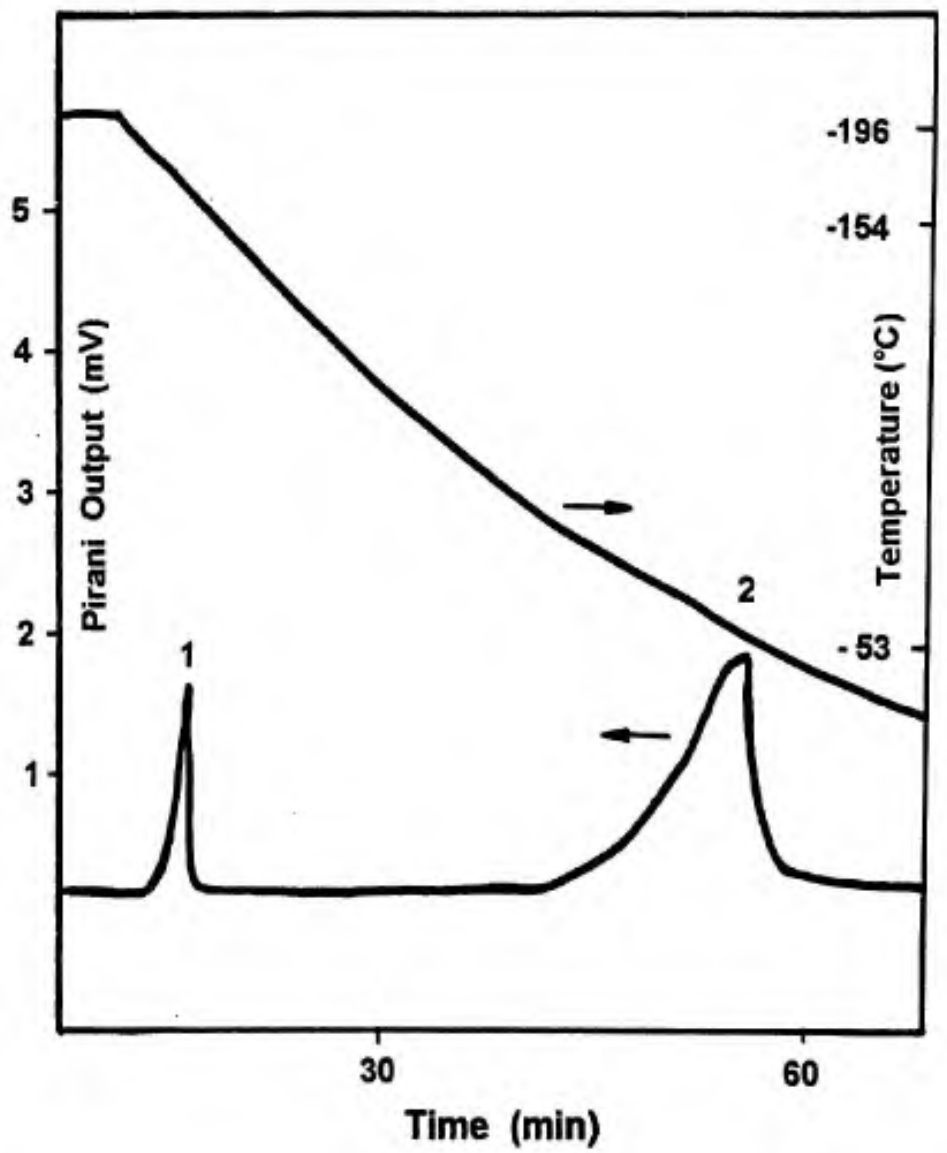

Figure 51. SATVA trace showing condensible volatiles from carbonization of pitch, previously oxidized at 240°C for 0 minutes, to an end temperature of 400°C; 1: Carbon dioxide, 2: Water

The partly stabilized pitch gave a relatively large coldring product fraction--20% by weight, compared to 5% for fully stabilized pitch (compare also with unstabilized pitch with a coldring product fraction of 48%). The IR spectrum of the coldring product fraction is shown in figure 52. Notice that the intensities of peaks due to aromatic carbon stretching (1600 cm^{-1}) and methylene hydrogen bending (1456 cm^{-1}) are similar. This factor, and a more defined aromatic hydrogen stretching absorbance at 3047 cm^{-1}, tend to support the conclusion that the oligomeric fraction of partly stabilized pitch is richer in aromatic content than that from unstabilized pitch. The relatively large aromatic content in the coldring product fraction of partly stabilized pitch is a consequence of the partial removal of aliphatic material through oxidation. The significant decrease in the size of the coldring product fraction (20% as opposed to 48% for unstabilized pitch) is a result of oxidation "fixing" more material into the pre-carbonized lattice and reducing the "solvent" fraction able to be distilled or "cracked" off during carbonization.

It is interesting to note that the coke resulting from the carbonization of partly stabilized pitch to 900°C showed evidence of melting and fusion. Although still in a powdered form similar to the coke for fully stabilized pitch, there was clearly a

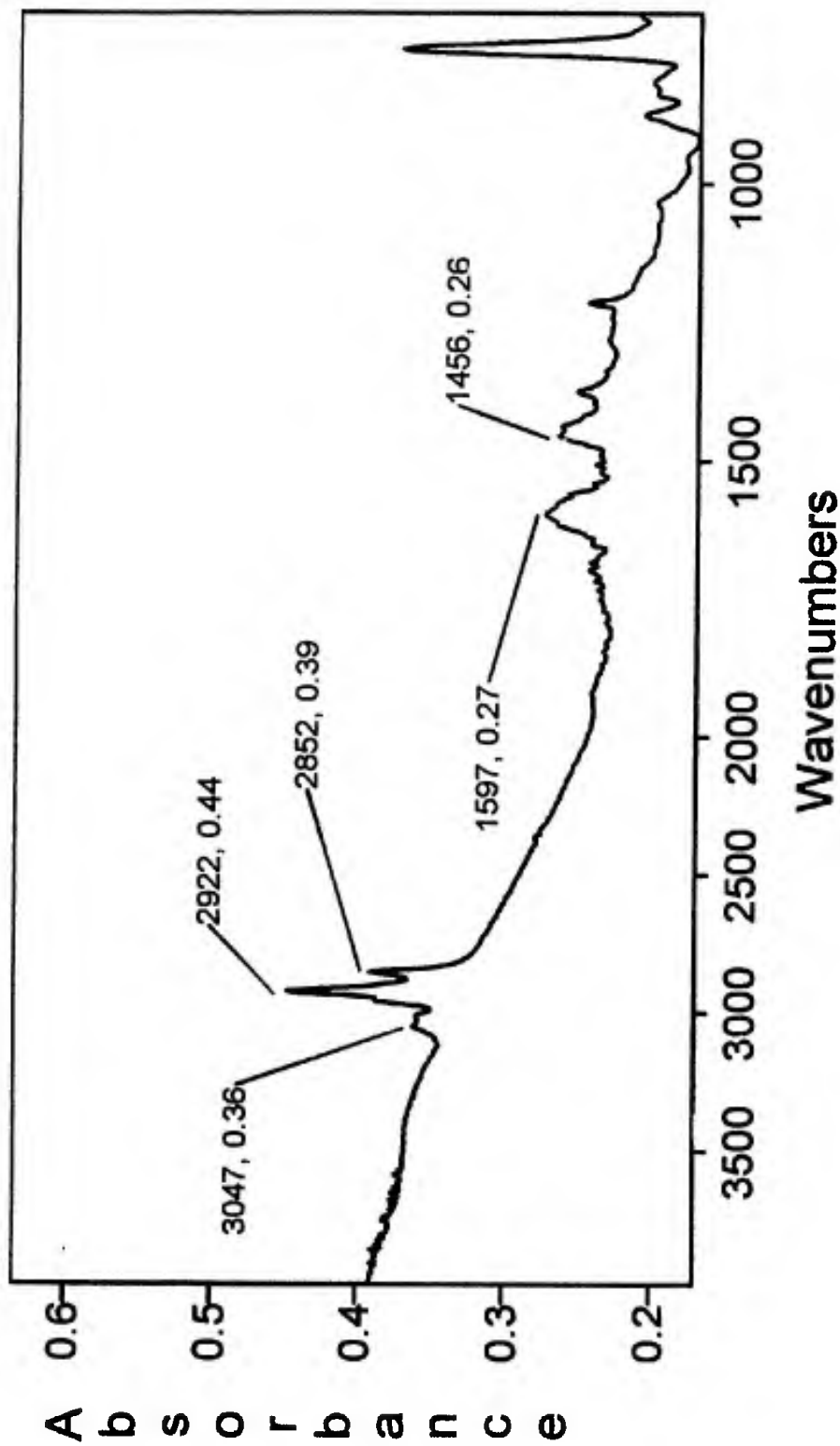

Figure 52. IR spectrum of the coldring product fraction from carbonization of pitch previously oxidized at 240°C for 0 minutes

greater degree of fusion of the pitch particles. A surprising result was that the coke yield was 71% (based on the oxidized, pre-carbonized mass), about the same as for fully stabilized pitch. Whereas fully stabilized pitch gives a small yield of alkane gases and oligomers and a large carbon dioxide/carbon monoxide fraction, partly stabilized pitch gives small quantities of both alkane gases and carbon dioxide but a large oligomeric fraction. In either case, the remaining residue of carbonization (coke) is about 71-72%. We can explain this effect by assuming that the quantity of oxygen required to crosslink the pitch into a fully carbonizable lattice (with a coke yield of 70%) is much less than previously reported. Extra oxidation merely replaces the conversion to light alkanes and heavy oligomer byproducts with the formation of light oxides of carbon during coke formation. The aliphatic content is either oxidized during the oxidative stabilization process and subsequently removed as carbon dioxide and carbon monoxide during carbonization of stabilized pitch, or is "cracked" off as short alkanes and heavier oligomers during carbonization of unstabilized pitch. In either case, the coke yield is steady at 70-73%. The physical appearance of the coke (whether or not the pitch particles show evidence of fusion and melting) is dependent on the nature of product removal from the carbon lattice during carbonization. The emission of

carbon dioxide and carbon monoxide tends to preserve order in the lattice and minimize fusion, while transport and removal of heavy aromatics and oligomers by diffusion through the lattice will result in a loss or disruption of order.

4.2.2.4 PITCH OXIDIZED AT 270°C FOR 15 MINUTES

A mesophase pitch sample previously oxidized at 270°C for 15 minutes was selected for TVA and SATVA analysis because this particular oxidation profile was reported in the literature as the minimum required for sufficient stabilization to prevent fusion of pitch-based fibers during carbonization [10]. The TVA trace for this pitch is shown in figure 53. The trace depicts the familiar low and high temperature volatile emission processes, with maxima at approximately 515°C and 755°C, respectively. Closer examination of the low temperature volatile emission peak reveals the presence of two low temperature shoulders in the curve at approximately 370°C and 440°C. These particular temperatures were observed in previous TVA traces of oxidized pitches as corresponding to rate maxima for the evolution of carbon dioxide. The SATVA separation corresponding to the complete condensible volatile product fraction of carbonization to 900°C is shown in figure 54. It contains a trace peak corresponding to ethane, along with much larger peaks corresponding to carbon dioxide and water. The SATVA separation

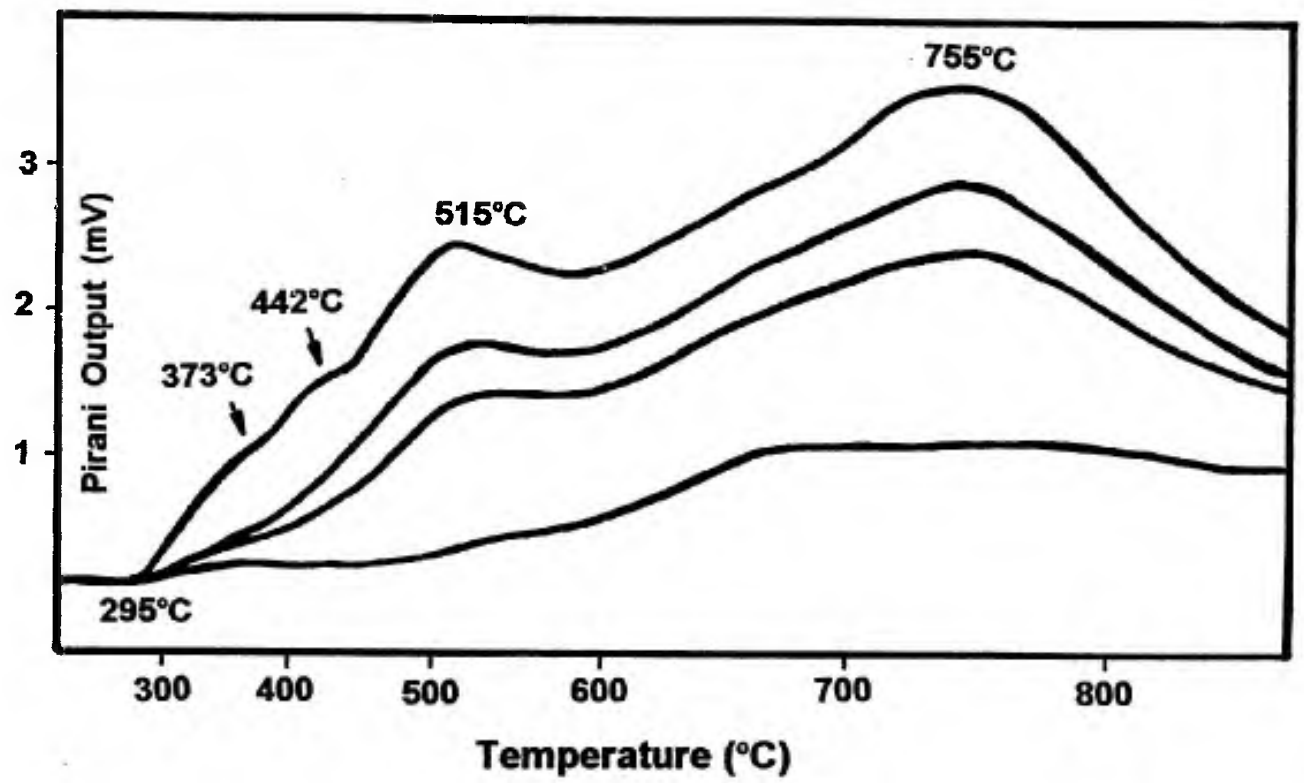

Figure 53. TVA trace for the carbonization of pitch, previously oxidized at 270°C for 15 minutes, to a temperature of 900°C at a rate of 9°C/min; sample size = 99.1 mg

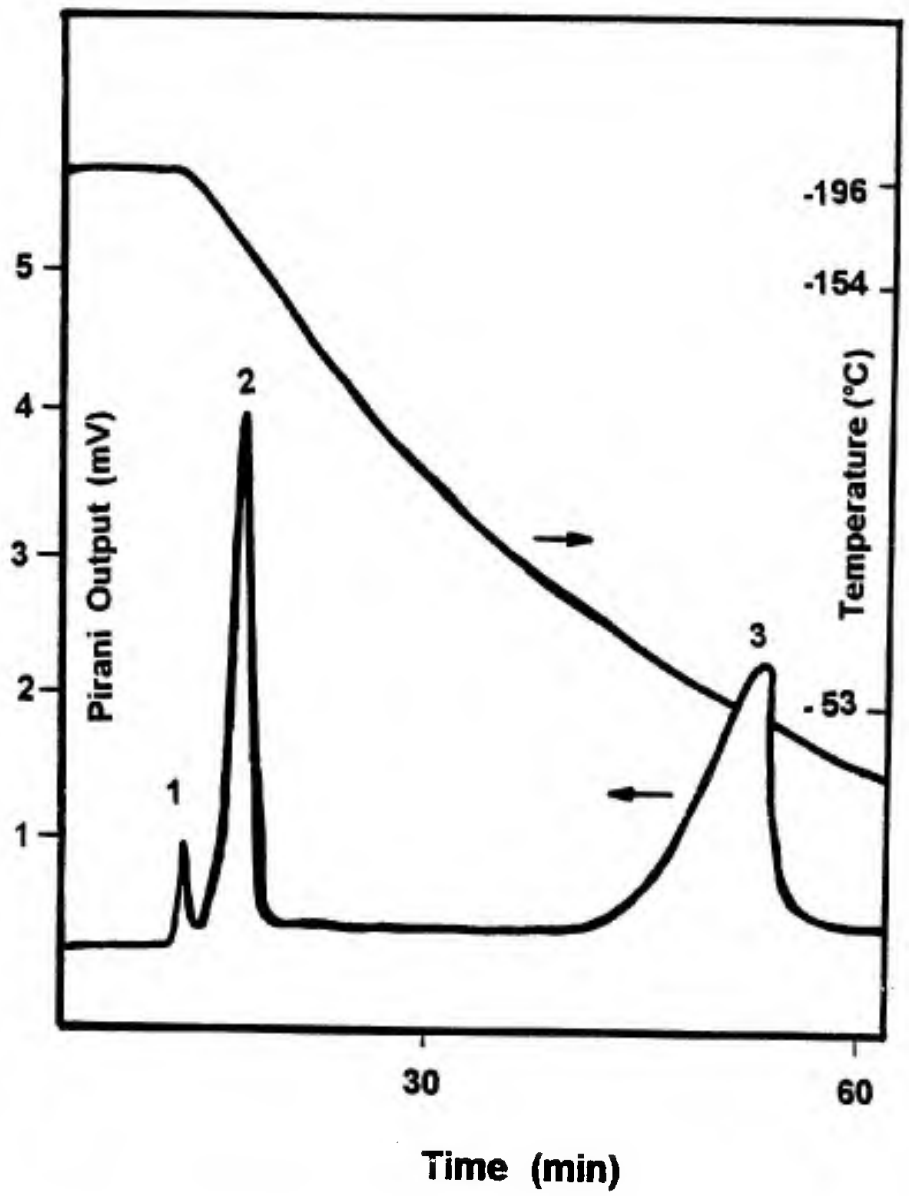

Figure 54. SATVA trace showing all condensible volatiles from carbonization of pitch previously oxidized at 270°C for 15 minutes; 1: Ethane, 2: Carbon dioxide, 3: Water

indicates that pitch oxidized by ramping to 270°C, followed by a 15 minute soak at that temperature, produces carbon dioxide and water as the primary condensible volatile products as opposed to short alkanes. This is verified by the gas phase IR spectrum in figure 55 which indicates the presence of alkanes and carbon dioxide, with carbon dioxide as the major product. The relative quantities of alkane gases and carbon dioxide, as indicated by the IR spectrum, more closely resembles that of products from fully stabilized pitch (figure 43) than from insufficiently stabilized pitch (figure 49).

A TVA experiment performed to an end temperature of 440°C yielded the SATVA separation reproduced in figure 56. Notice that the SATVA trace does not indicate the production of ethane upon carbonization to 440°C, only carbon dioxide and water. The IR spectrum for the condensible products evolved upon carbonization to an end temperature of 440°C is shown in figure 57. The spectrum indicates the presence of a small quantity of light alkanes, but reaffirms carbon dioxide as the primary product. Therefore, the low temperature "shoulders" at 370°C and 440°C in the TVA are due primarily to the production of carbon dioxide and water. The volatile emission peak at 515°C is associated with the production of a relatively small amount of aliphatic content as alkane

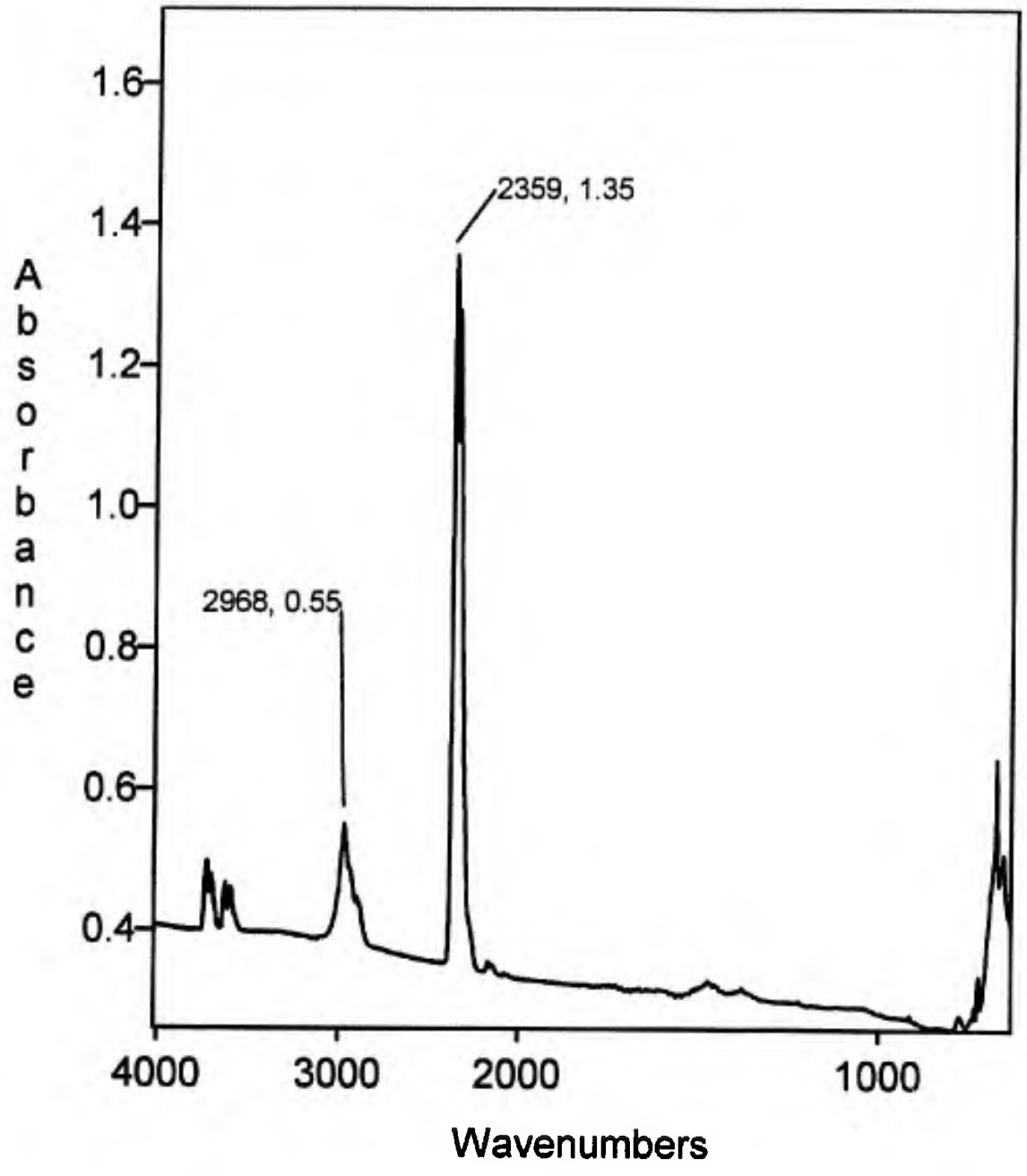

Figure 55. IR spectrum of condensible volatiles from carbonization of pitch previously oxidized at 270°C for 15 minutes

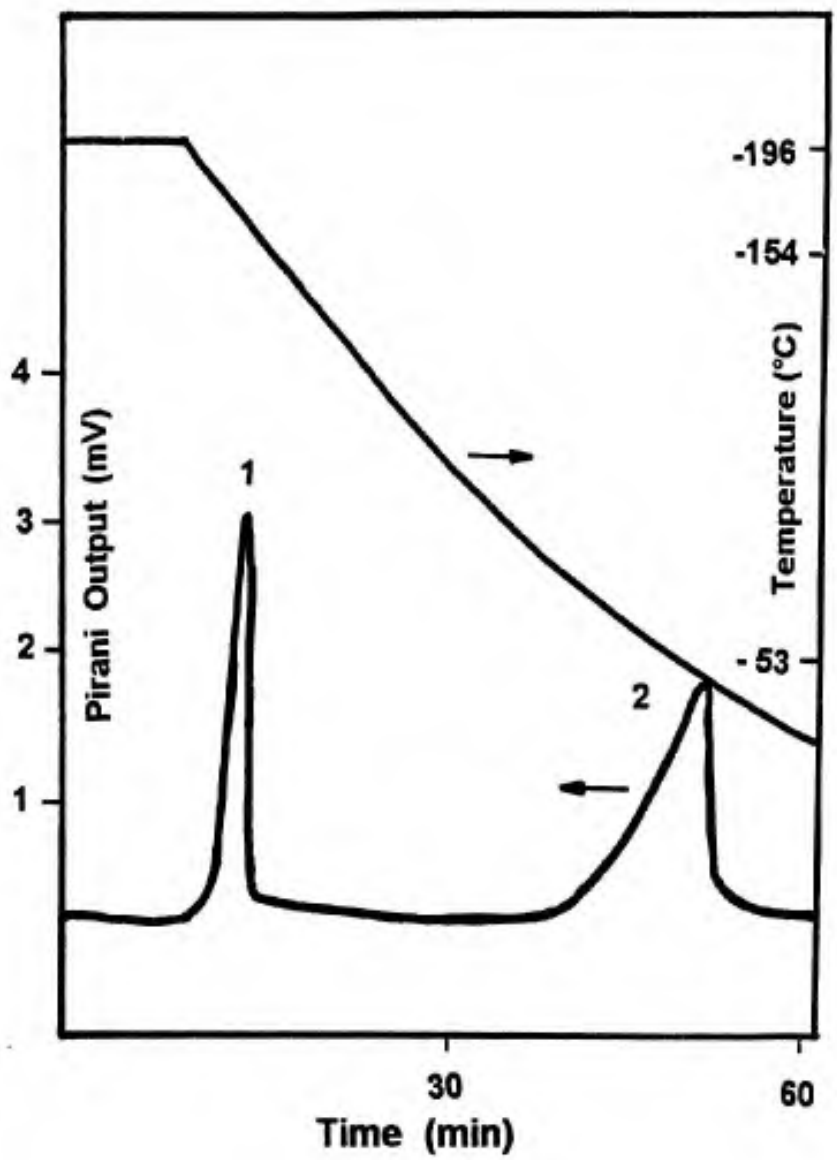

Figure 56. SATVA trace showing condensible volatiles from carbonization of pitch, previously oxidized at 270°C for 15 minutes, to an end temperature of 440°C; 1: Carbon dioxide, 2: Water

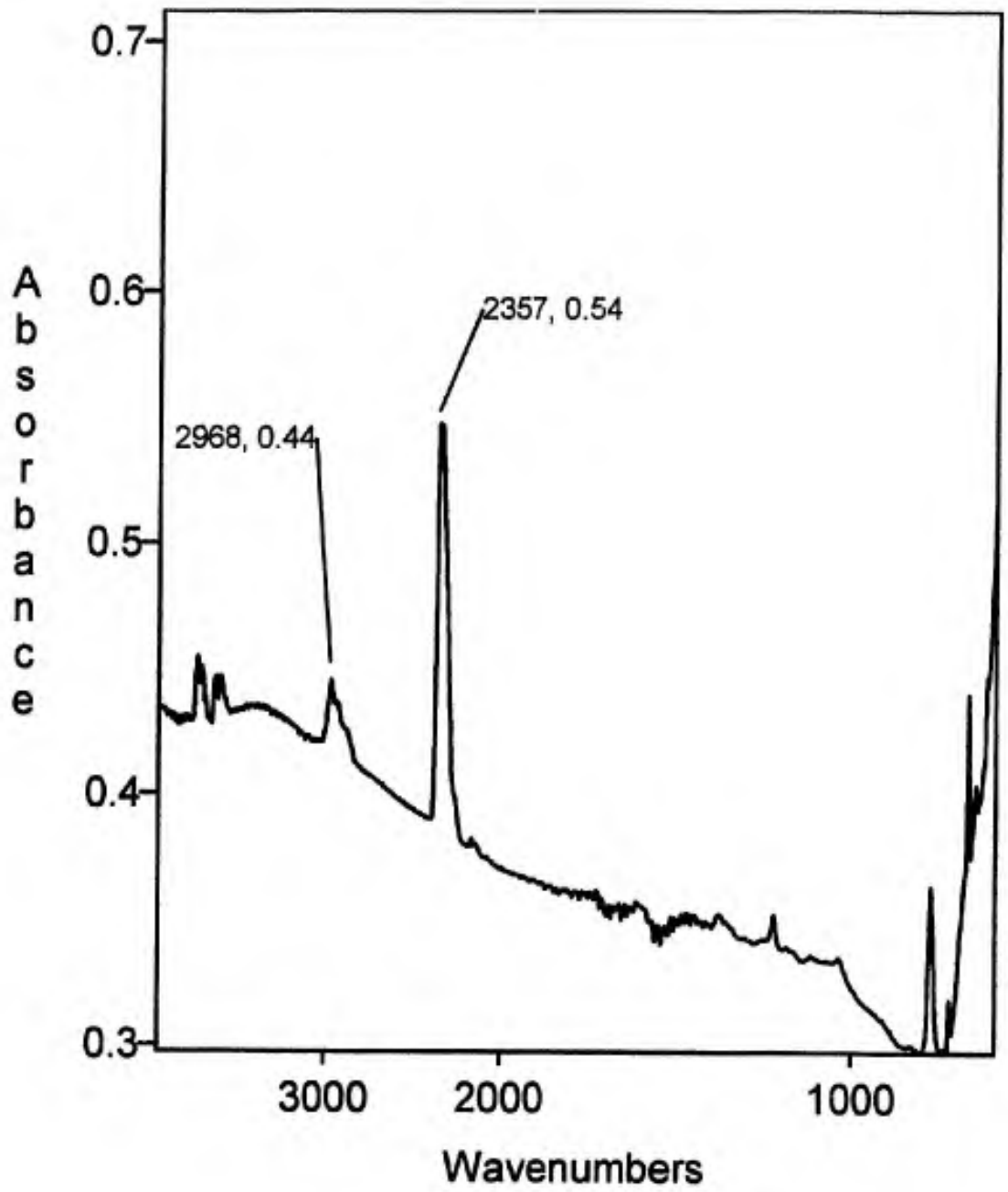

Figure 57. IR spectrum of condensible volatiles from carbonization of pitch, previously oxidized at 270°C for 15 minutes, to an end temperature of 440°C

gases.

The IR spectrum in figure 58 is of the coke resulting from carbonization to an end temperature of 440°C, coincident with the high temperature boundary of the second "shoulder" peak in the TVA experiment (figure53). Notice the relatively strong absorbance at approximately 1440 cm^{-1}, indicating that aliphatic carbon content is still present in the pitch after carbonization to 440°C. This peak is significantly weaker in the IR spectrum for the coke at 600°C, as shown in figure 59, once again indicating that aliphatic content is removed from the pitch as short alkanes at higher temperatures between 440°C and 600°C. The IR spectrum of coke carbonized to 440°C (figure 58) also shows the presence of carbonyl functionality as indicated by the absorbance band centered at 1700 cm^{-1}. Notice that this band contains peaks of approximate equal intensity at 1699 cm^{-1} due to aromatic ketone functionality, and at 1734 cm^{-1} due to ester functionality, indicating that both types of structure are still present in the pitch at 440°C during carbonization. The carbonyl band disappears upon further carbonization to 600°C as shown in figure 59. The volatile emission peak at 515°C in the TVA is therefore due to the emission of both alkanes and carbon dioxide. Analysis of the noncondensible volatile product fraction indicated the production of both

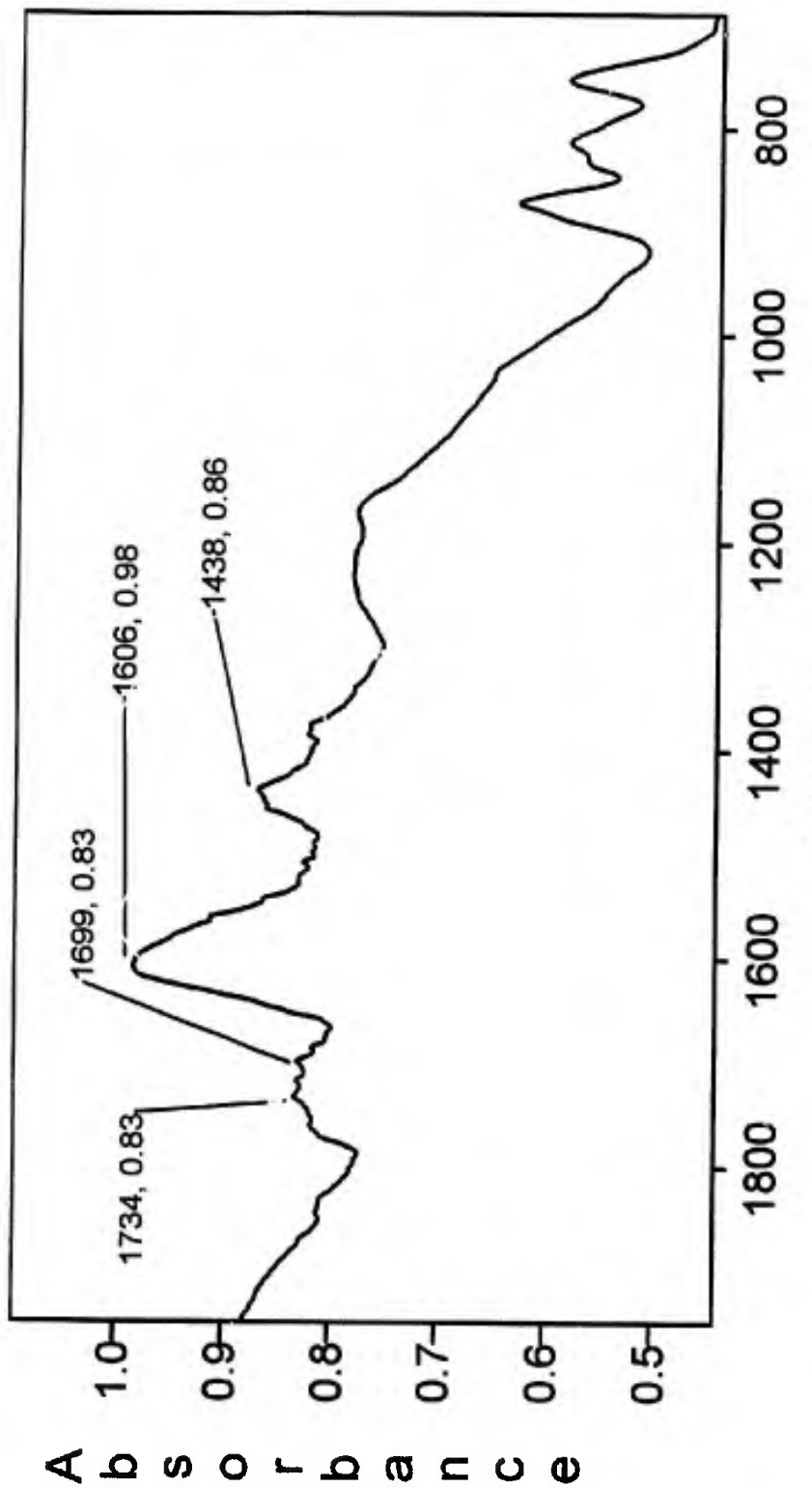

Figure 58. IR spectrum of pitch, previously oxidized at 270°C for 15 minutes, carbonized to 440°C

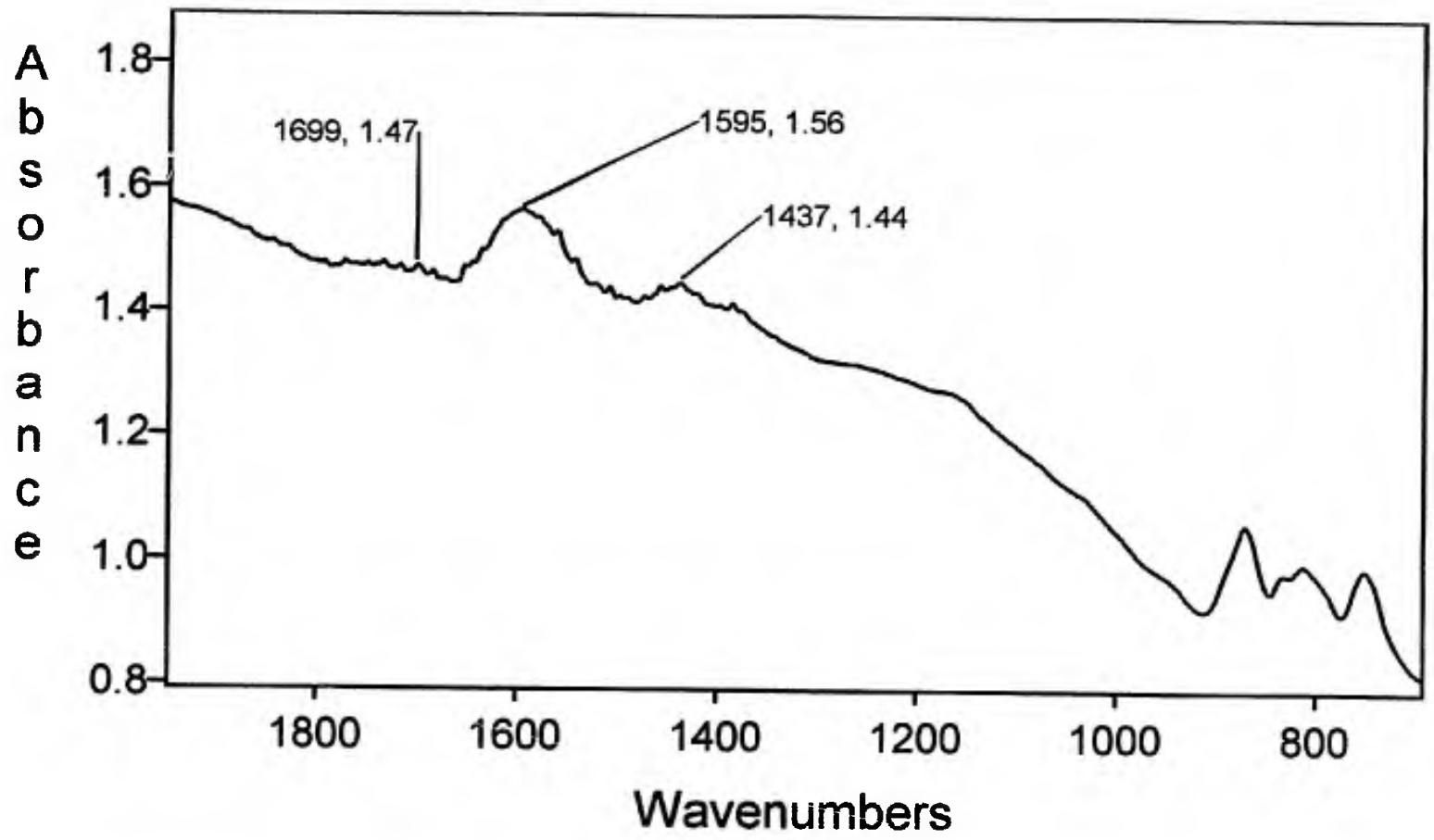

Figure 59. IR spectrum of pitch, previously oxidized at 270°C for 15 minutes, carbonized to 600°C

methane and carbon monoxide. Carbon monoxide production was associated with the lower temperature volatile emission maxima and "shoulders" (similar to carbon dioxide), as well as the higher temperature volatile emission maxima. Methane evolution was associated with both the low and high temperature volatile emission maxima as well.

Comparing the intensities of the three peaks due to aromatic hydrogen bending centered at 800 cm^{-1} in figures 58 and 59 indicates that aromatic hydrogen content is not significantly reduced during carbonization from 440°C to 600°C. This is supported through examination of the output of pirani gauge 4 in the TVA experiment (figure 53) which indicates a negligible production of hydrogen gas up to about 600°C and a quantitative production of hydrogen at higher temperatures.

The coldring product fraction resulting from the carbonization of pitch previously oxidized at 270°C for 15 minutes was approximately 10% of the total product yield by weight. This yield was closer to that for fully stabilized pitch (5%) than for insufficiently (or partly) stabilized pitch (20%). The aromatic content of the coldring product fraction, as indicated in figure 60 by comparing the relative intensities of the IR bands at 1600 cm^{-1} and 1460 cm^{-1}, is also similar

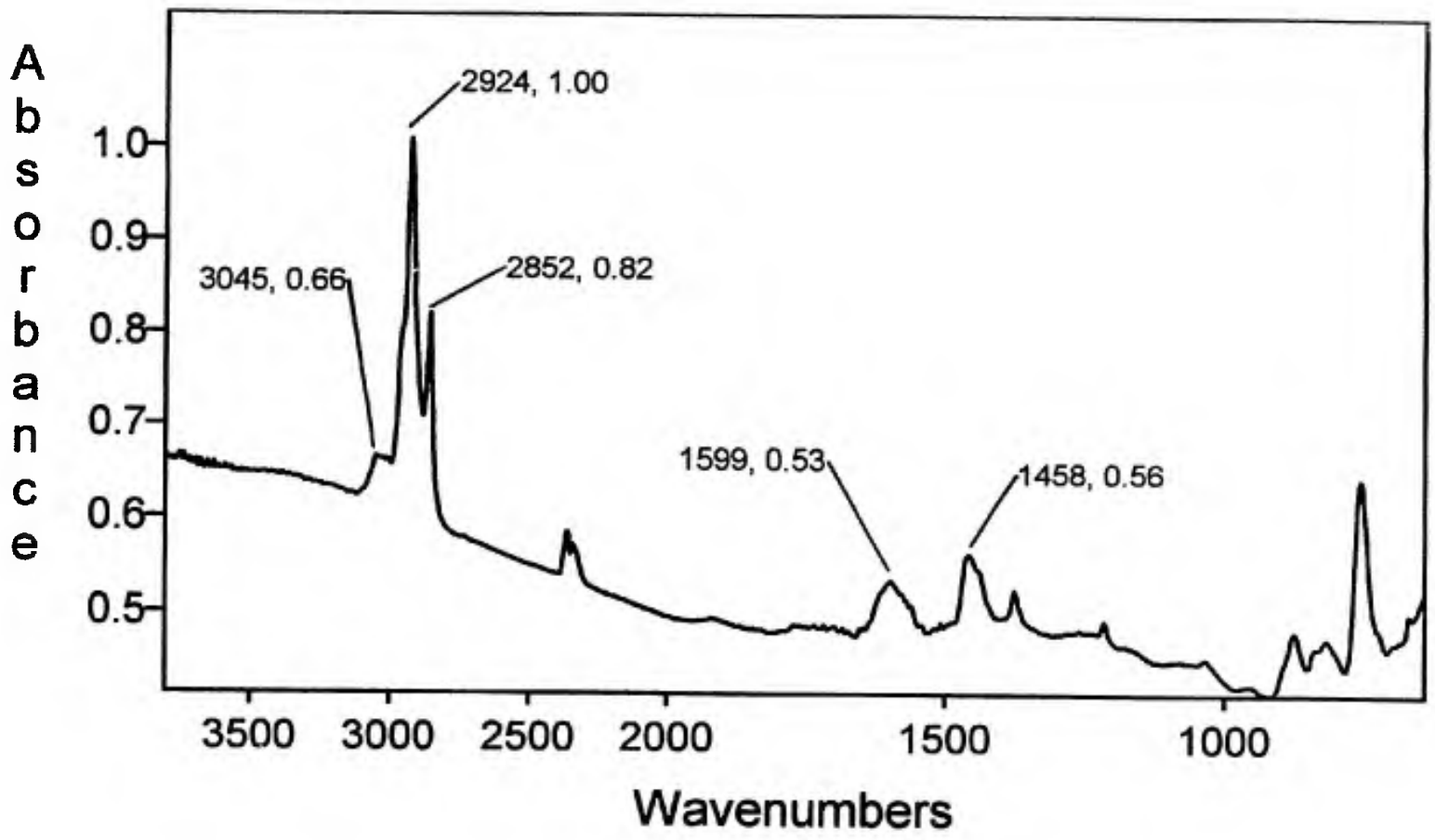

Figure 60. IR spectrum of the coldring product fraction from carbonization of pitch previously oxidized at 270°C for 15 minutes

to that from fully stabilized pitch. These results indicate that stabilization for 15 minutes at 270°C is sufficient to oxidize most of the aliphatic content in the pitch, thereby decreasing the yield of light alkanes from cracking of napthenic rings and the cracking-off (or evaporation) of coldring fraction products from the pitch. In a series of experiments designed to more thoroughly characterize the production of oligomers during carbonization, individual 50 mg samples of pitch previously oxidized at 270°C for 15 minutes were carbonized to end temperatures of 370°C, 440°C, 600°C, and 900°C. The coldring product fractions were collected and weighed. These experiments proved that the percent yield (by weight) of coldring product fraction had reached approximately 10% at 440°C, with no further increase to end temperatures of 600°C or 900°C. Only a trace of coldring product fraction was detected upon carbonization to 370°C. The production of oligomers was, therefore, associated with reactions which proceed during carbonization between 370°C and 440°C for this pitch, coincident with the emission of carbon dioxide/carbon monoxide, and just prior to the emission of both carbon dioxide/ carbon monoxide and alkanes during the higher temperature process which peaks at 515°C.

A qualitative analysis of the coke at 900°C (yield = 73%) indicated a minimal degree of fusion of the pitch particles, similar to that observed in pitch oxidized at 240°C for 4 hours. Overall, the TVA and SATVA results indicated that oxidation at 270°C for 15 minutes is a satisfactory oxidation profile for preventing fusion of the pitch particles and for eliminating the production of a large oligomeric fraction. Furthermore, the emission of carbon dioxide and water as the primary condensible volatile products is similar to that observed on carbonization of fully stabilized pitch.

4.2.2.5 EXCESSIVELY STABILIZED PITCH

We have investigated the carbonization behavior of "fully" stabilized pitch and "insufficiently" or partly stabilized pitch, basing our selections on the location of the sample in its respective weight change curve. Thus, we have looked at a pitch sample at its maximum weight gain point (240°C at 4 hours) and at the beginning of its weight change curve (240°C at zero minutes). We have also examined a sample stabilized between these two extremes (270°C at 15 minutes). The final major area of the weight change curve that remains to be investigated is that corresponding to significant weight loss. For this we chose a pitch previously oxidized at 340°C for 4 hours which lost 10% of its total mass during oxidation.

The TVA trace for pitch previously oxidized at 340°C for 4 hours is shown in figure 61. There is a striking difference in the appearance of the low temperature volatile emission rate maximum at 540°C compared to that observed in pitches with less extreme stabilization histories. The low temperature process is both more pronounced and with a broader temperature profile than that of the high temperature process which maximizes at 760°C. In addition, there is a lack of "shoulder" peaks below 500°C on the low temperature volatile emission curve, indicating a lack of unstable oxidation intermediates, presumably due to their removal during stabilization. The relatively large magnitude of the low temperature process indicates that a rather large quantity of volatile products are associated with this process, including--presumably, carbon dioxide, as this stabilization regime produces a peak area ratio value of 1.06 corresponding to the integrated intensity of the carbonyl band centered at 1700 cm^{-1} to the aromatic stretch at 1600 cm^{-1}. This ratio was the largest observed for any pitch sample studied by us.

The SATVA separation of the total condensible volatile products of carbonization of excessively oxidized pitch is shown in figure 62. The very intense peak corresponding to carbon dioxide reinforces our conclusion that this pitch has

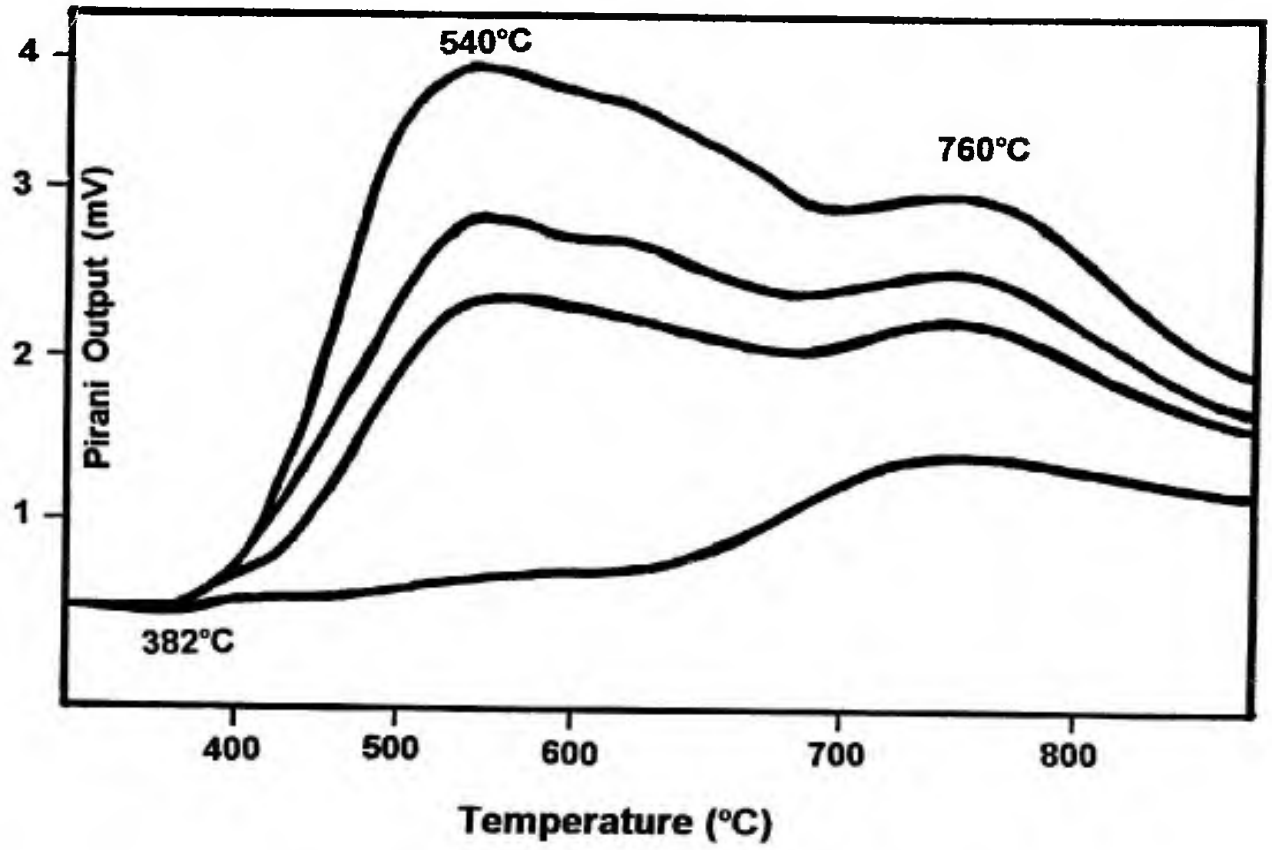

Figure 61. TVA trace for the carbonization of pitch, previously oxidized at 340°C for 240 minutes, to a temperature of 900°C at a rate of 9°C/min; sample size = 101.2 mg

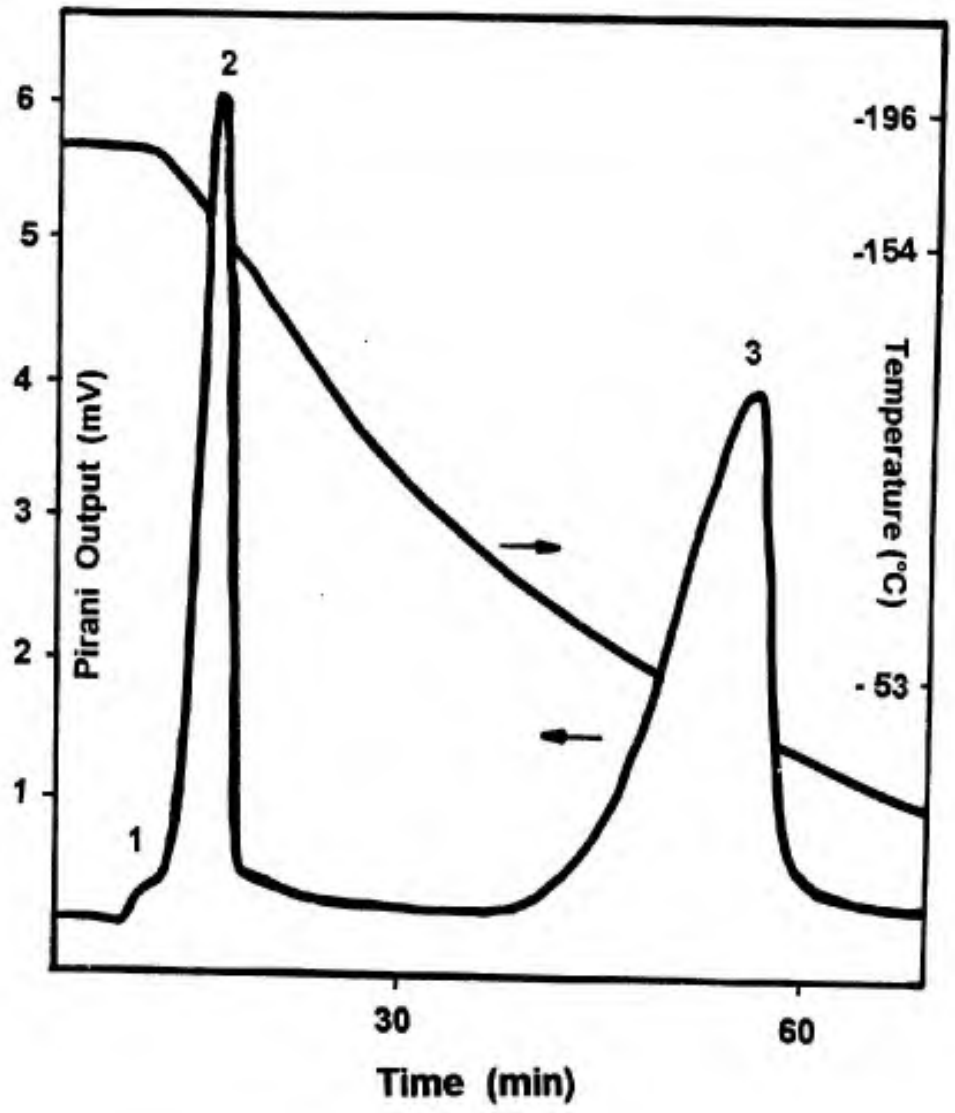

Figure 62. SATVA trace showing all condensible volatiles from carbonization of pitch previously oxidized at 340°C for 240 minutes; 1: Ethane, 2: Carbon dioxide, 3: Water

achieved a very large oxygen content during oxidation despite losing 10% of its total mass. Furthermore, there is no indication of the presence of alkane gases except for a very slight response from the pirani gauge where we would expect to see ethane gas. The IR spectrum of the total condensible volatile product fraction of carbonization to 900°C is shown in figure 63. We observe a very strong peak due to carbon dioxide at approximately 2352 cm^{-1} and a very weak absorbance at approximately 2968 cm^{-1} corresponding to alkanes. Clearly, at this point in the oxidation profile we are experiencing a further build-up of oxygen functionality in the pitch even as the overall mass is being reduced through sample ablation.

The IR spectrum corresponding to all of the noncondensible volatiles produced during carbonization is shown in figure 64. Here we observe a very strong peak due to carbon monoxide at 2171 cm^{-1}, approximately equal in intensity to the peak arising from methane at 3016 cm^{-1} (all other pitch samples studied showed a methane peak which was consistently stronger in intensity than the carbon monoxide peak). These results suggest that despite weight loss during oxidation, the pitch is gaining an even greater oxygen content at the expense of saturated (aliphatic) carbon functionality.

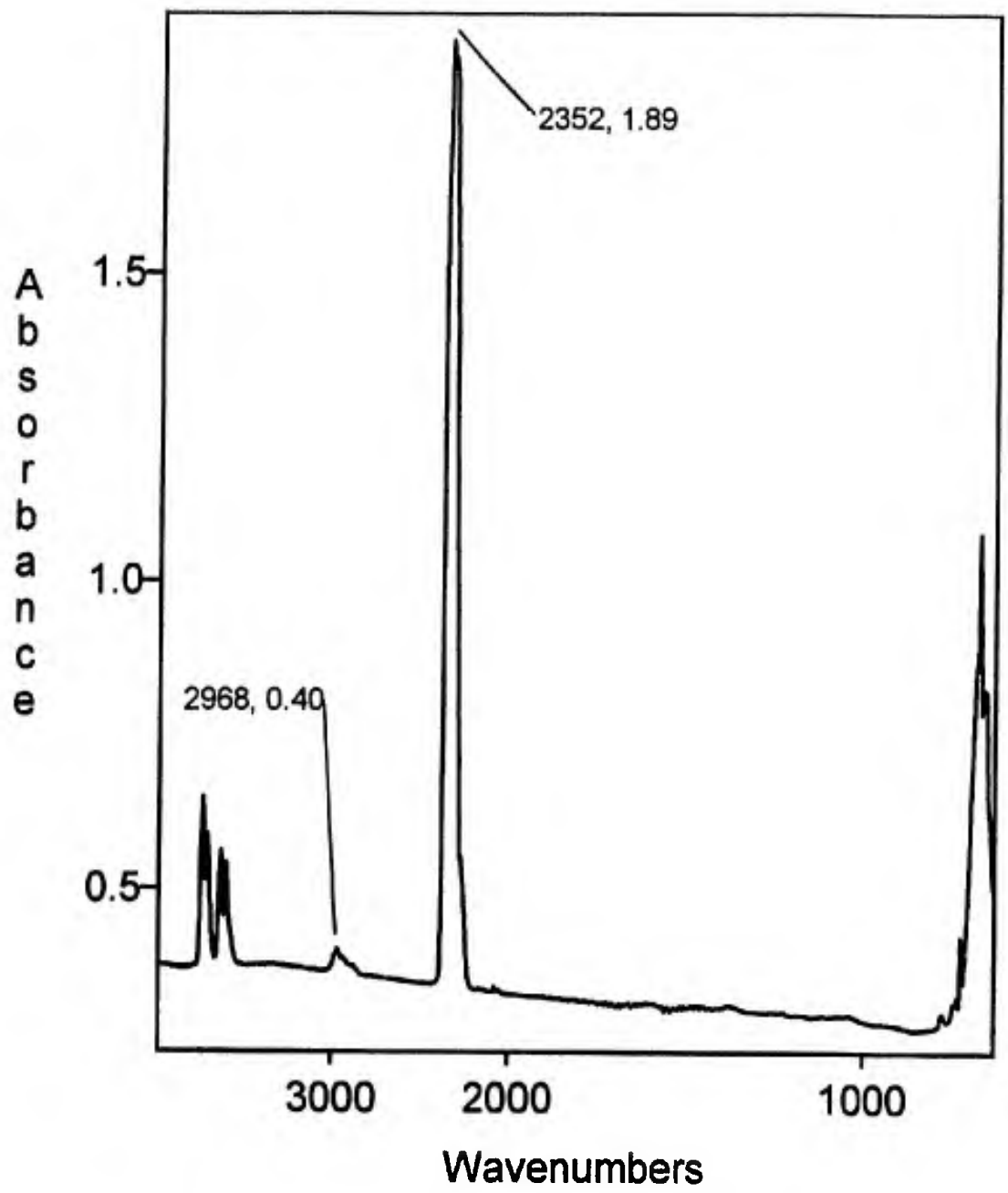

Figure 63. IR spectrum of condensible volatiles from carbonization of pitch previously oxidized at 340°C for 240 minutes

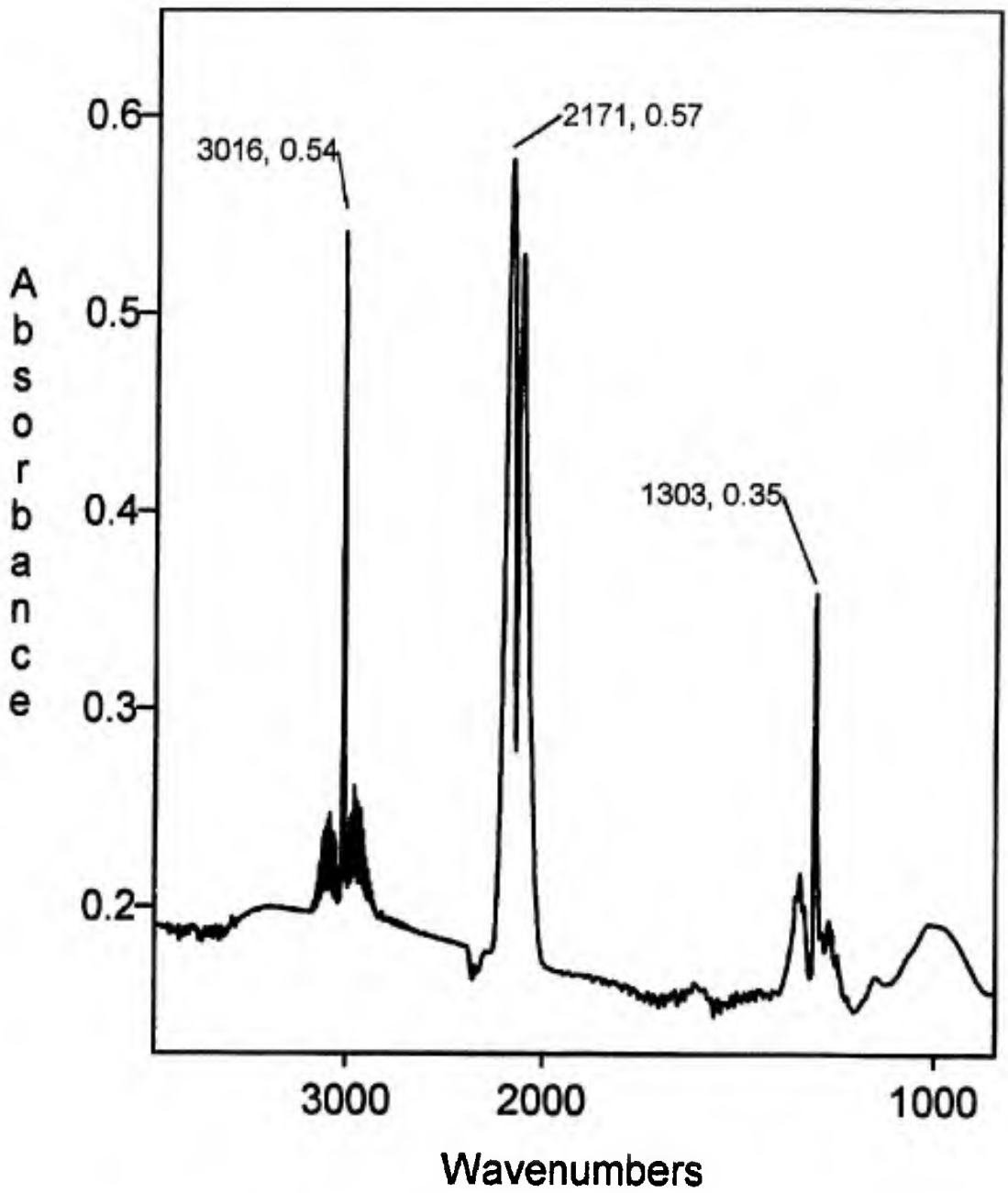

Figure 64. IR spectrum of noncondensible volatiles from carbonization of pitch previously oxidized at 340°C for 240 minutes

The yield of coldring or oligomeric products from this pitch, only 3.7% by weight, suggests that over-oxidation has resulted in further crosslinking of molecules and a more quantitative removal of aliphatic functionality from this pitch. Figure 65 depicts the IR spectrum of the coldring product fraction from this pitch. Notice the very weak absorbance at 1600 cm^{-1} due to aromatic carbon stretching. Compared to the peak at 1460 cm^{-1} due to methylene hydrogen bending and the peaks at 2920 cm^{-1} and 2850 cm^{-1} due to methylene hydrogen asymmetric and symmetric stretching, respectively, it indicates a very small aromatic content in the coldring product fraction. This suggests that further crosslinking of aromatic ring systems by oxygen is taking place and that these reactions reduce "cracking" during carbonization. Furthermore, even with this high proportional content of aliphatic material in the coldring product fraction, the relatively small mass of the oligomeric fraction itself suggests a minimal amount of aliphatic content remaining in the pitch following oxidation able to be "cracked" during carbonization. The presence of an, albeit, very weak absorbance at 1734 cm^{-1} indicates the presence of ester functionality in this coldring product fraction.

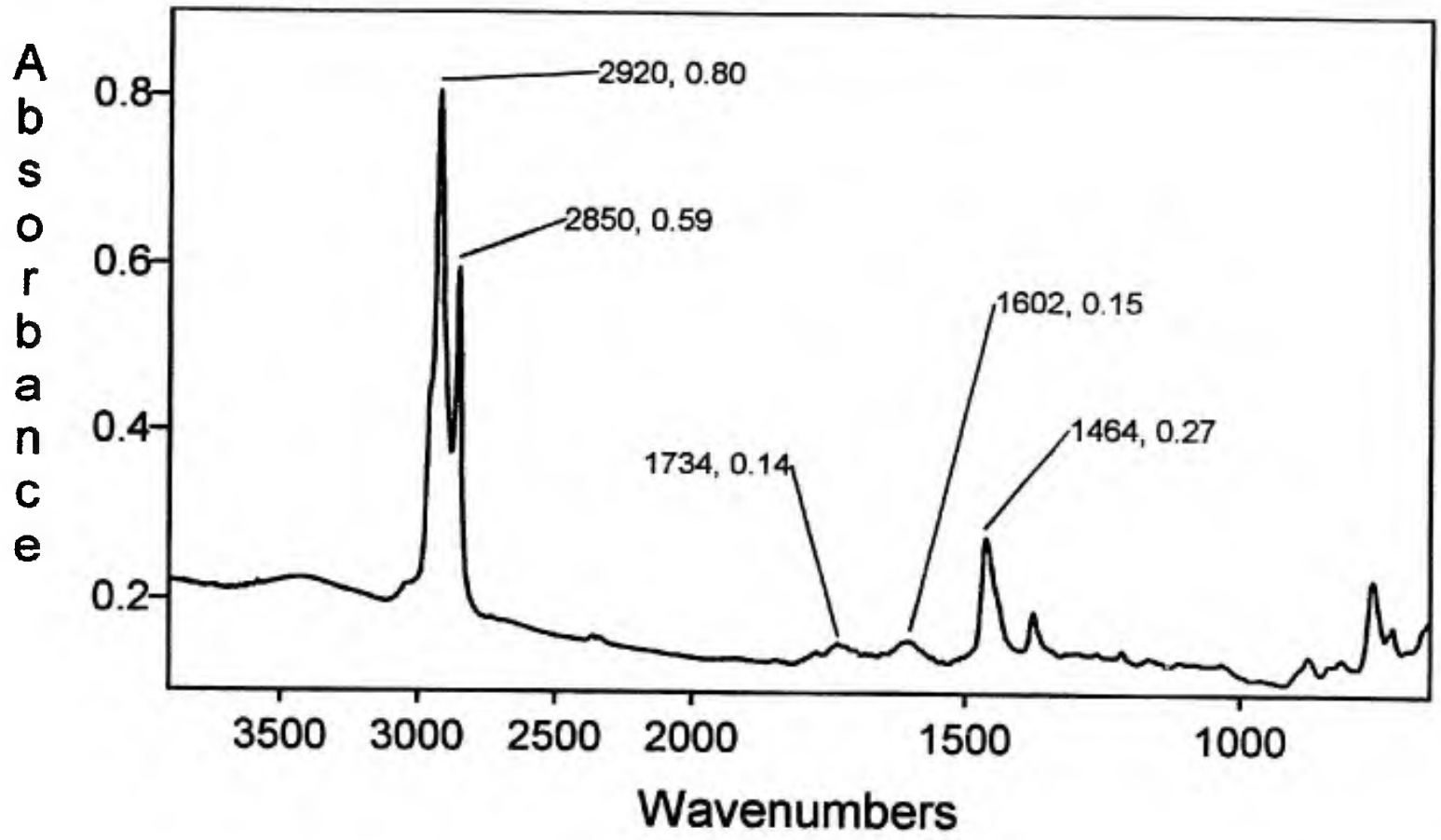

Figure 65. IR spectrum of the coldring product fraction from carbonization of pitch previously oxidized at 340°C for 240 minutes

Figure 66 shows the IR spectrum of the coke from this pitch resulting from carbonization to an end temperature of approximately 600°C. At this relatively high temperature we can still observe a band centered at 1700 cm^{-1} due to carbonyl functionality. Notice that the band is comprised of several individual absorbances, including those at 1734 cm^{-1} due to ester functionality and a relatively strong band at 1699 cm^{-1} ascribed to aromatic ketone. Prior to carbonization, the bands at 1734 and 1772 wavenumbers, corresponding to ester and anhydride functionality, respectively, were much stronger in intensity than the ketone band at 1699 cm^{-1}. This suggests that ester and anhydride functionality may undergo decarboxylation below 600°C to release carbon dioxide and produce ketone functionality which is itself removed at higher temperatures during carbonization. This conclusion was supported by a subsequent TVA experiment designed to collect volatiles emmitted between 600°C and 900°C during carbonization. Results showed a small quantity of carbon dioxide and water in the condensibles, with a noncondensible fraction of methane and carbon monoxide. It is possible that ketone functionality is removed with the subsequent emission of carbon monoxide during later stages of the carbonization process (above 600°C).

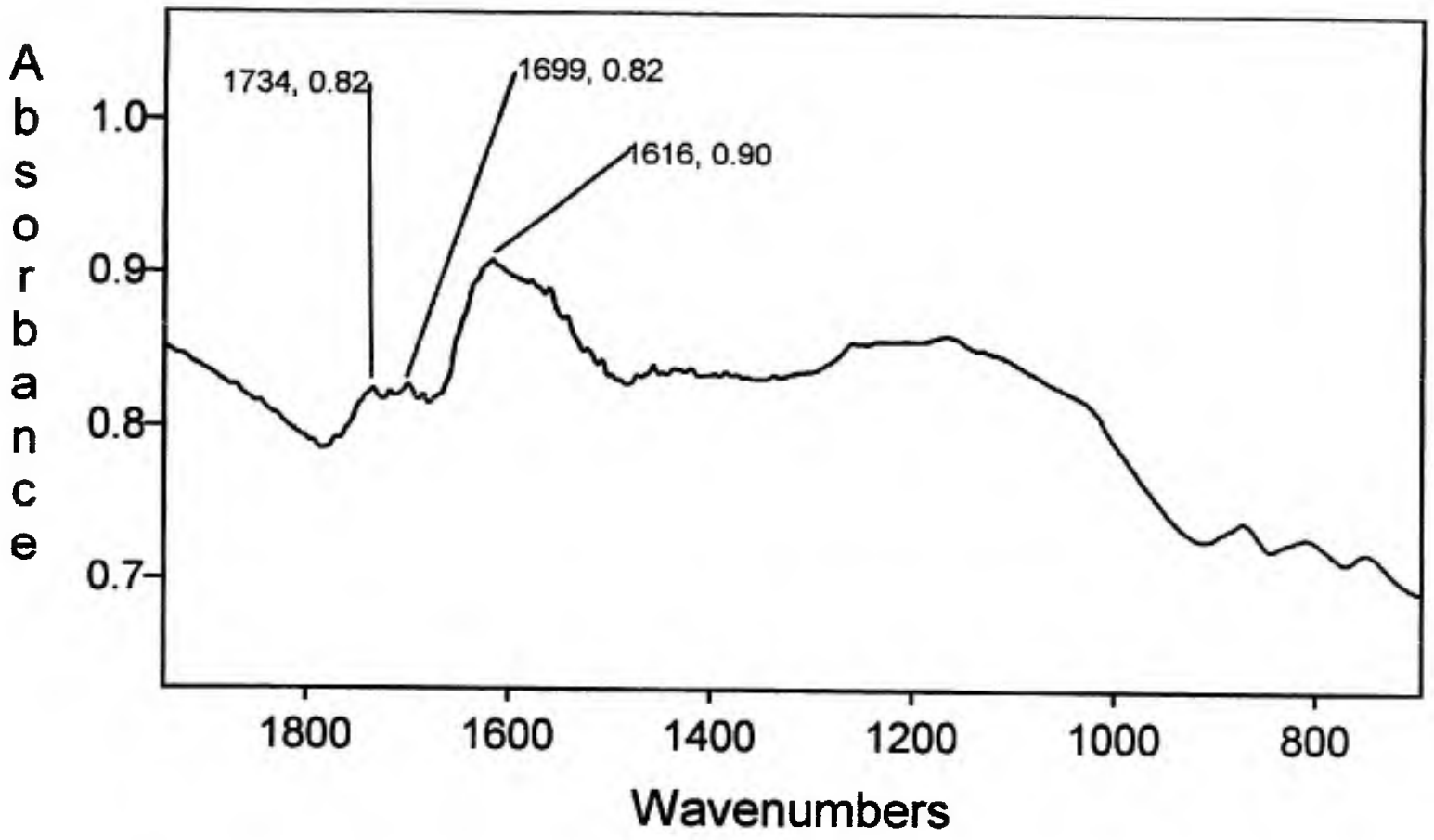

Figure 66. IR spectrum of pitch, previously oxidized at 340°C for 240 minutes, carbonized to 600°C

A qualitative analysis of the coke at 900°C revealed the smallest degree of fusion of the pitch particles in any sample studied. This suggests that fusion or melting of pitch is probably related to the "cracking" of napthenic rings to produce oligomers and short alkanes. The cracking process and the bloating associated with the transport of heavy products from the pitch possibly allows for the subsequent large-scale reorientation of pitch molecules which is observed as melting or fusion. The coke yield for this overoxidized pitch was only 63%, based on the weight of an oxidized, pre-carbonized sample. Recall that the yield was consistently between 70% and 73% for the other oxidized pitches studied, all of which were taken from the weight gain portion of the weight change curve. Apparently, oxidation to a point where sustained weight loss occurs results in the loss of carbon from the sample which is reflected in the decreased coke yield upon carbonization. This supports the theory that oxidation at higher temperatures and longer time periods results in the accelerated loss of carbon and oxygen surface complexes as carbon dioxide and carbon monoxide, while the concentration of oxygen remaining in the pitch continues to increase relative to carbon. This is reflected during carbonization in the product spectrum, where we observe a large carbon dioxide and carbon monoxide fraction, a small oligomeric fraction,

and a decreased coke yield.

4.2.3 SEMI-QUANTITATIVE ANALYSIS OF MESOPHASE PITCH CARBONIZATION

Table 2 contains the results of TVA experiments performed on several additional mesophase pitch samples. All of the samples studied beyond those already described displayed behaviors during carbonization which were understandable given the previous discussion. As expected, behavior during carbonization was a function of oxidation history and could be predicted based on the sample's location on the oxidation profile.

Table 2 lists all pitches examined according to oxidation history and mass (all sample masses fell within a few percent of 100 mg). The normalized peak area corresponding to the 1700 cm^{-1} band is included to give an indication of the sample's relative oxygen content prior to carbonization. Notice in table 2 that the coke yield at 900°C for all samples is within a few percentage points of 70%, except for that from unoxidized pitch. The four samples which give coke yields below 70% (180 minutes at 290°C, 60 minutes at 340°C, 120 minutes at 340°C, and 240 minutes at 340°C) were all taken from later points on the weight change curve where weight loss was occurring (i.e., beyond the point of maximum weight

TABLE 2
CARBONIZATION DATA FROM TVA EXPERIMENTS

OXIDATION HISTORY (min / °C)	SAMPLE [1] MASS (mg)	RATIO [1] 1700/1600 cm^{-1}	900°C [2] COKE YIELD (%)	COLDRING [2] FRACTION (%)
Unoxidized	102.3	0.000	56.3	48.4
0 / 240	100.7	0.244	70.7	19.9
240 / 240	104.6	0.821	71.8	4.88
15 / 270	99.1	0.480	73.1	10.2
120 / 270	99.8	0.635	70.8	7.76

[1] Corresponds to an oxidized, pre-carbonized specimen

[2] Weight percent yield based on mass of oxidized, pre-carbonized specimen

TABLE 2 (cont.)
CARBONIZATION DATA FROM TVA EXPERIMENTS

OXIDATION HISTORY (min / °C)	SAMPLE [1] MASS (mg)	RATIO [1] 1700/1600 cm^{-1}	900°C [2] COKE YIELD (%)	COLDRING [2] FRACTION (%)
30 / 290	100.3	0.669	71.8	8.61
180 / 290	100.3	0.661	68.8	5.24
0 / 340	101.9	0.597	71.4	12.4
60 / 340	101.7	0.808	69.9	5.00
120 / 340	101.2	0.862	67.1	3.37
240 / 340	101.2	1.060	63.3	3.66

[1] Corresponds to an oxidized, pre-carbonized specimen

[2] Weight percent yield based on mass of oxidized, pre-carbonized specimen

gain). Furthermore, the coke yield was lowest (63.3%) for the pitch sample which had lost the most weight (10%) during oxidation. A convincing trend is shown in table 2 for the four samples oxidized at 340°C. Notice that all 4 samples were about 101 mg prior to carbonization and that oxygen content (as indicated by the normalized peak area at 1700 cm^{-1}) increased steadily as oxidation time increased from 0 to 60 to 120 to 240 minutes. Even so, the coke yield at 900°C drops steadily from 71.4% for the pitch oxidized for zero minutes at 340°C to 63.3% for that oxidized for 240 minutes at 340°C. These results support our conclusion that weight loss during oxidation results in a loss of carbon from the pitch even while oxygen content continues to increase. The loss of carbon content during oxidation is reflected in the decreased coke yield.

The remaining pitch samples gave coke yields between 70.7% and 73.1% and were all taken from the area in their respective weight change curves where weight gain was either maximized or still increasing.

The data in table 2 suggests also that the yield of coldring product fraction is a function of oxidation history, and, specifically, the location of a sample on its respective weight change curve. In general, samples which were taken from the weight loss portion of the curve gave the smallest coldring product fractions.

Therefore, barring unoxidized pitch, samples which give the smallest coke yields (less than 70%) also give the smallest coldring product fractions (less than 6%). Furthermore, the size of the coldring product fraction is generally seen to be inversely proportional to oxygen content based on the 1700/1600 wavenumber band area ratio. Samples which are either unoxidized or insufficiently oxidized have the smallest ratio values and give the largest coldring product fractions, while samples with higher ratio values give smaller coldring product fractions. This result supports our conclusion that oxidation removes aliphatic, napthenic content from the pitch, thereby decreasing the production of oligomers during carbonization from thermal "cracking"of those rings.

The data in table 2 are summarized graphically in figure 67. The curve resulting from the plot of % coke yield vs. normalized peak area for the 1700 cm^{-1} absorbance band illustrates that the coke yield is not a strong function of the oxygen content in the pitch over a wide range of pre-oxidation profiles. Coke yield remains relatively constant at about 70% except for pitches which lost significant weight during oxidation. The coldring product fraction, however, is clearly a stronger function of oxygen content, and decreases significantly with higher oxygen content in the pitch. The curves in figure 67 support our previously

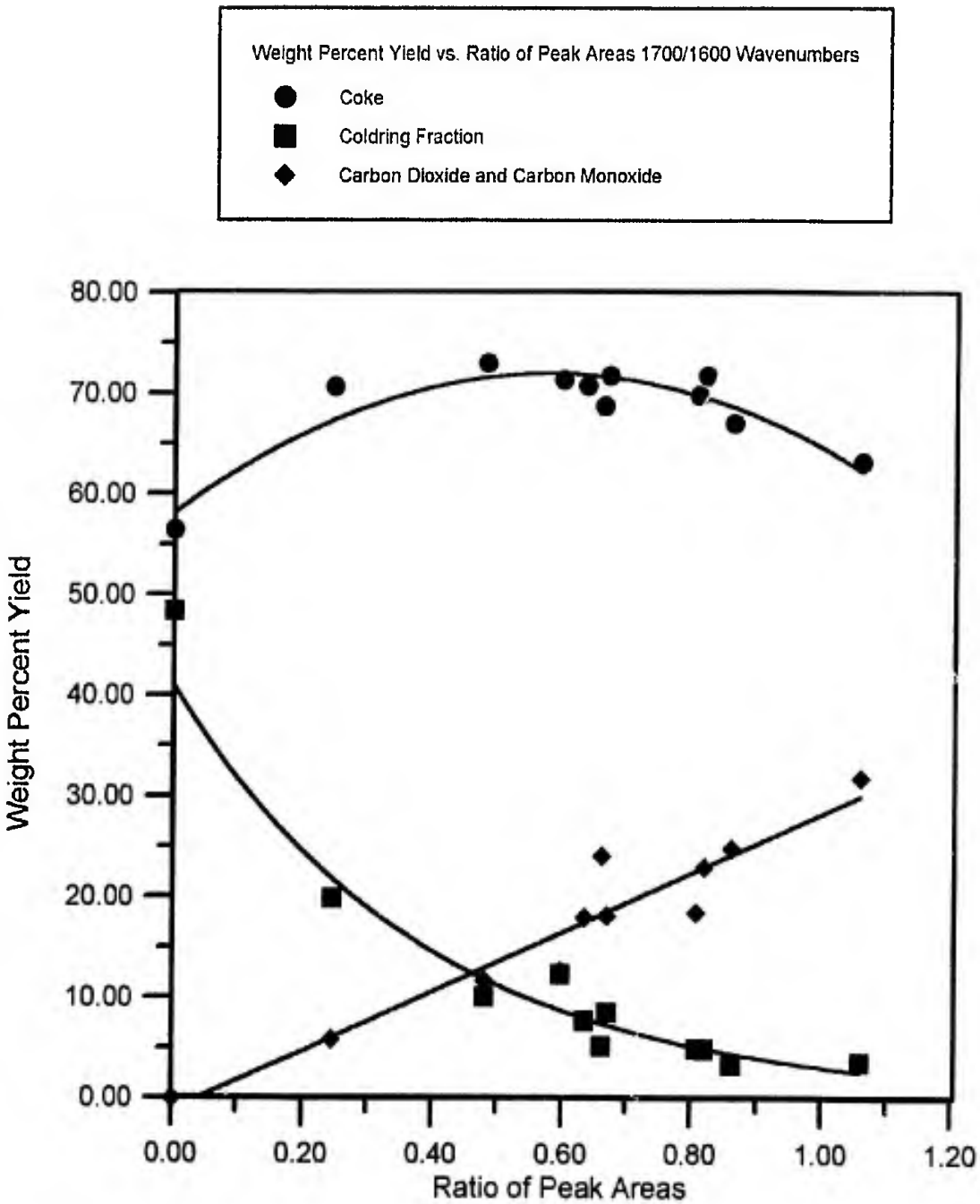

Figure 67. Plot of weight percent yield of coke, coldring fraction, and carbon dioxide/carbon monoxide vs. ratio of peak areas 1700/1600 wavenumbers for carbonization of mesophase pitch to 900°C

arrived at conclusion that changing the oxidation profile within wide limits does not markedly effect the coke yield, but does affect the relative yield of oligomers and volatiles, primarily exchanging carbon dioxide and carbon monoxide for light alkanes and oligomers. This is because the aliphatic content in the pitch does not lend itself to the final coke yield, but is either oxidized during the oxidation profile or "cracked" off to form oligomers during carbonization. The result (as shown in figure 67) is a relatively steady coke yield and a steadily decreasing coldring product fraction as a function of oxygen content.

Table 3 summarizes the data from the SATVA experiments. It is immediately apparent that carbon dioxide, carbon monoxide, and methane yields, as well as alkane absorbances, are functions of the oxygen content in the pitch. The weight percent yield of carbon monoxide, carbon dioxide, and methane were determined by manipulating known pressures and volumes of pure gasses on a vacuum line and distilling them into a gas IR cell for subsequent quantitative FT-IR analysis. The calibration curves for carbon monoxide, carbon dioxide, and methane are illustrated in figures 68, 69, and 70, respectively. Carbon dioxide and carbon monoxide yields increase with the oxygen content in the pitch (as measured by the normalized peak area for the 1700 wavenumber band in the pre-carbonized pitch).

TABLE 3
CARBONIZATION DATA FROM SATVA EXPERIMENTS

OXIDATION HISTORY (min / °C)	RATIO [1] 1700/1600 cm^{-1}	CO_2 [2] YIELD (%)	CO [2] YIELD (%)	CH_4 [2] YIELD (%)	ALKANE [3] ABSORBANCE
Unoxidized	0.00	0.00	0.00	3.50	0.96
0 / 240	0.244	2.98	2.99	3.05	0.48
240 / 240	0.821	11.9	11.1	2.20	0.08
15 / 270	0.480	6.19	5.51	2.45	0.17
120 / 270	0.635	8.85	9.15	2.24	0.10

[1] Corresponds to an oxidized, pre-carbonized specimen

[2] Weight percent yield based on mass of oxidized, pre-carbonized specimen

[3] Normalized to 100 mg specimen of oxidized, pre-carbonized pitch

TABLE 3 (cont.)
CARBONIZATION DATA FROM SATVA EXPERIMENTS

OXIDATION HISTORY (min / °C)	RATIO [1] 1700/1400 cm^{-1}	CO_2 [2] YIELD (%)	CO [2] YIELD (%)	CH_4 [2] YIELD (%)	ALKANE [3] ABSORBANCE
30 / 290	0.669	7.89	10.3	2.62	0.15
180 / 290	0.661	10.1	14.0	2.17	0.06
0 / 340	0.597	6.46	6.26	2.26	0.19
60 / 340	0.808	9.12	9.38	2.01	0.08
120 / 340	0.862	10.9	13.9	1.71	0.06
240 / 340	1.060	13.6	18.3	1.65	0.04

[1] Corresponds to an oxidized, pre-carbonized specimen
[2] Weight percent yield based on mass of oxidized, pre-carbonized specimen
[3] Normalized to 100 mg specimen of oxidized, pre-carbonized pitch

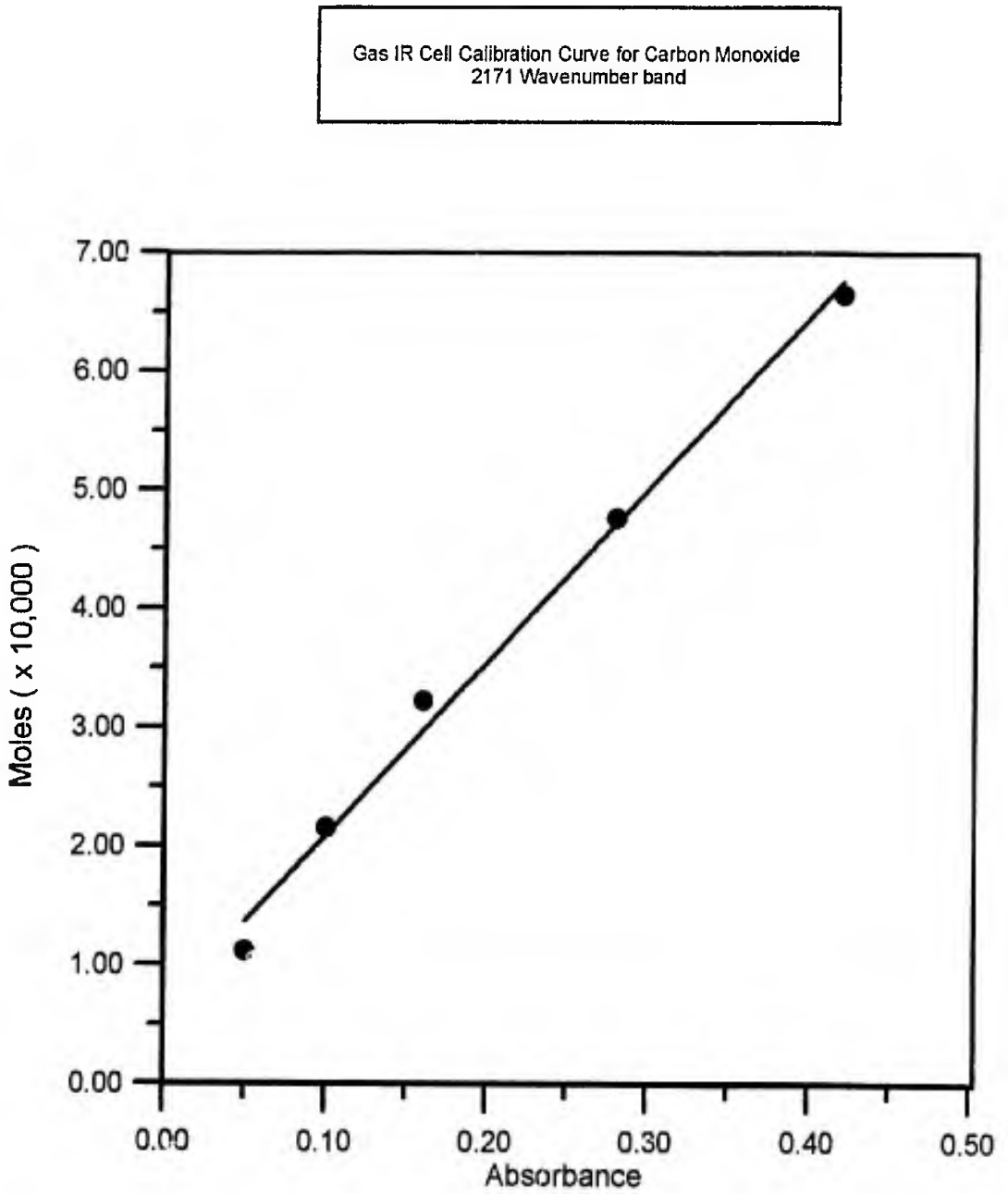

Figure 68. Calibration curve for the quantitative analysis of carbon monoxide; R = 0.996

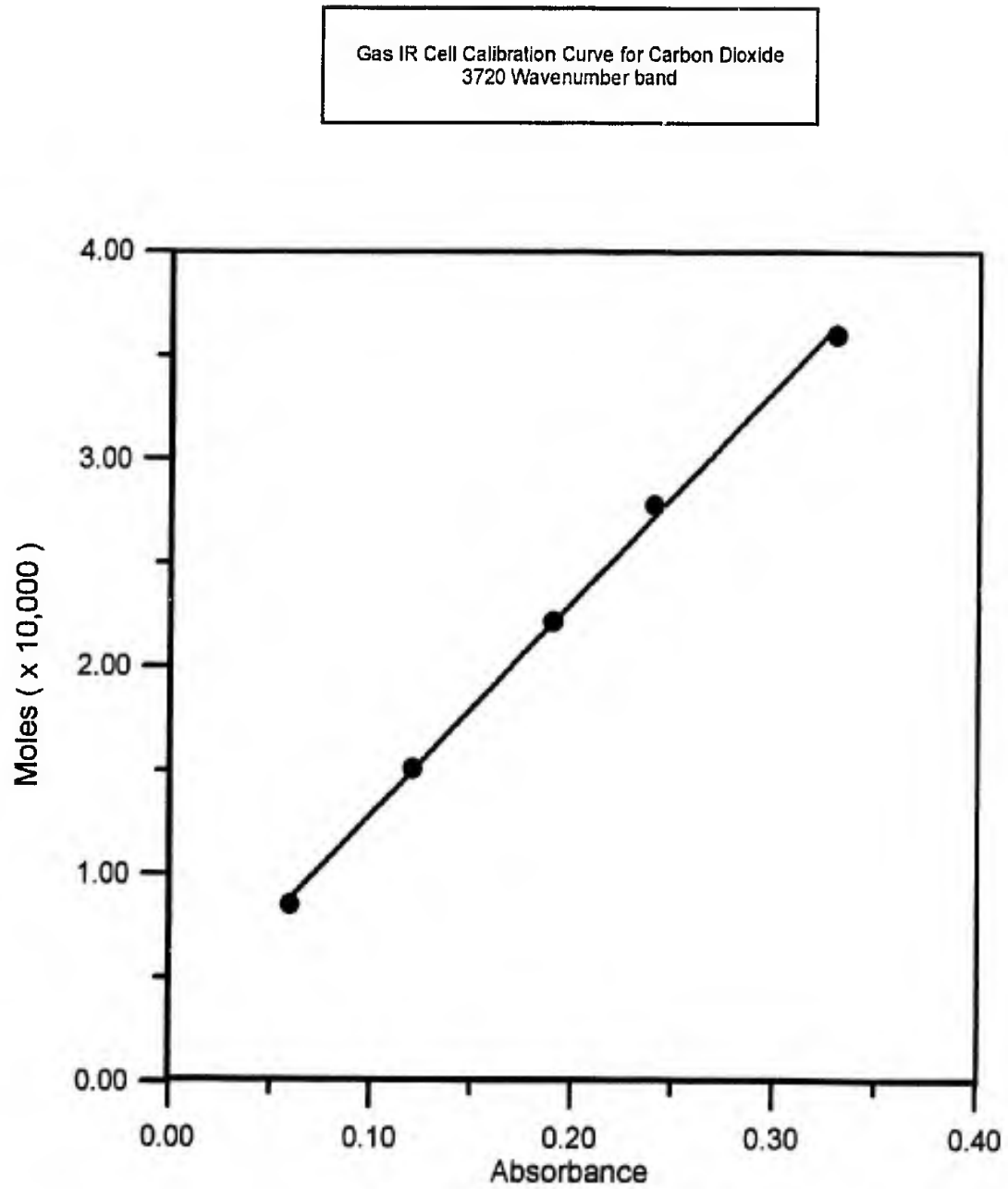

Figure 69. Calibration curve for the quantitative analysis of carbon dioxide; R = 0.999

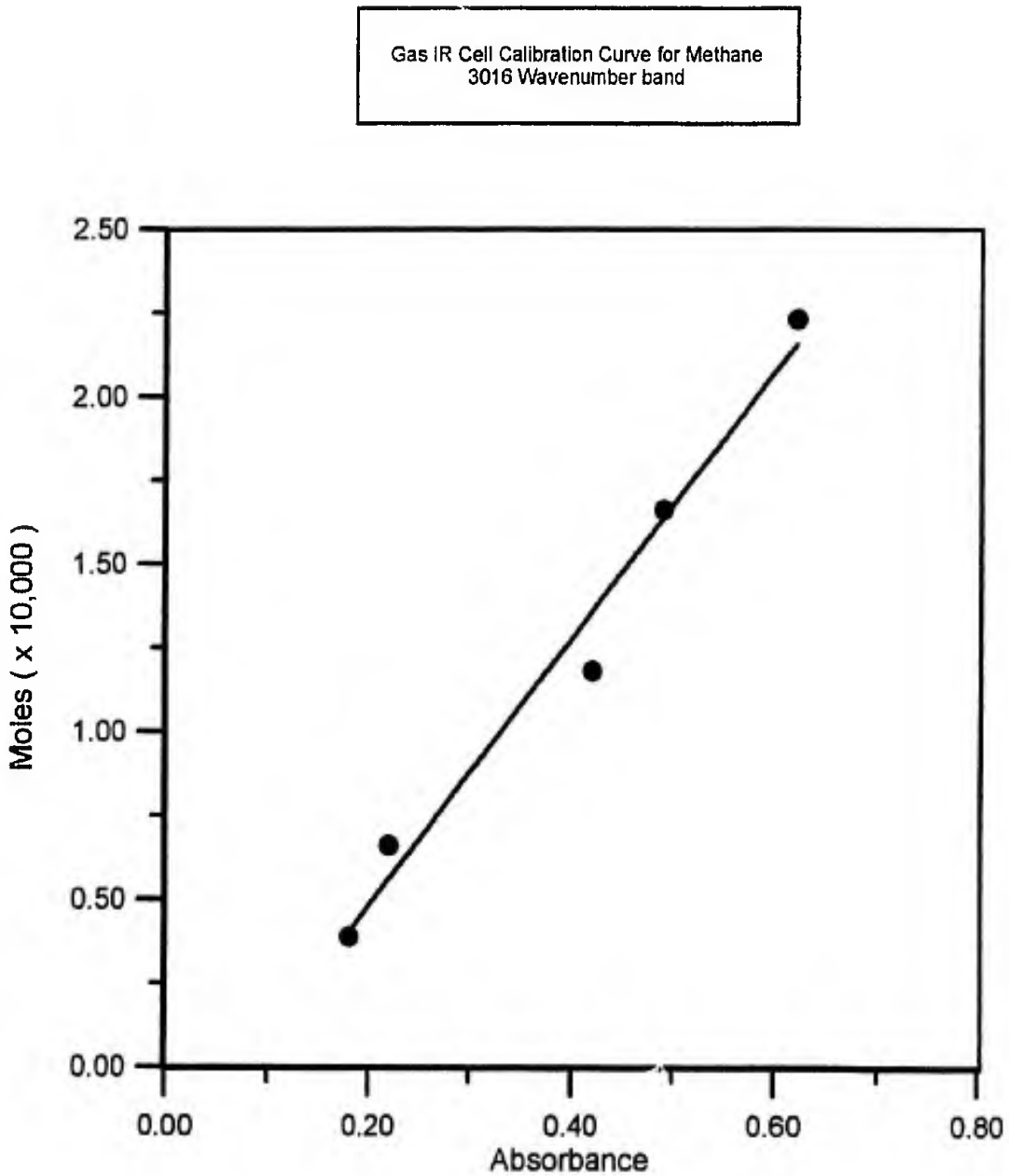

Figure 70. Calibration curve for the quantitative analysis of methane; R = 0.989

This is illustrated graphically in figure 67 where the combined yield of carbon dioxide and carbon monoxide is plotted against the ratio of peak areas corresponding to the 1700/1600 wavenumber bands in the oxidized pitch prior to carbonization. The yield of light alkanes decreases with increasing oxygen content in the pre-carbonized pitch. This relationship seems to hold irrespective of the specific nature of the oxidation profile. Generally speaking, samples which gave large relative yields of carbon dioxide and carbon monoxide gave also small yields of alkanes and vice-versa. This is illustrated by comparing the curve in figure 67 for carbon dioxide/carbon monoxide yield to the curve in figure 71 for methane yield, and the curve in figure 72 for alkane absorbance. The alkane absorbance, measured at 2968 cm^{-1}, is a semi-quantitative measure of the yield of 2, 3, 4, and 5-carbon alkanes. Because it represents a mixture of gasses, we were unable to calibrate the gas IR cells for a mass-based determination of the yield.

The three curves in figure 67 help also to explain our reasoning as to why the coke yield at 900°C rapidly reaches approximately 70% and then remains constant over a wide range of pre-oxidation histories. The aliphatic content of the pre-oxidized pitch makes-up a constant weight fraction of the pitch. During oxidation it is rapidly oxidized to carbonyl functionality. During subsequent

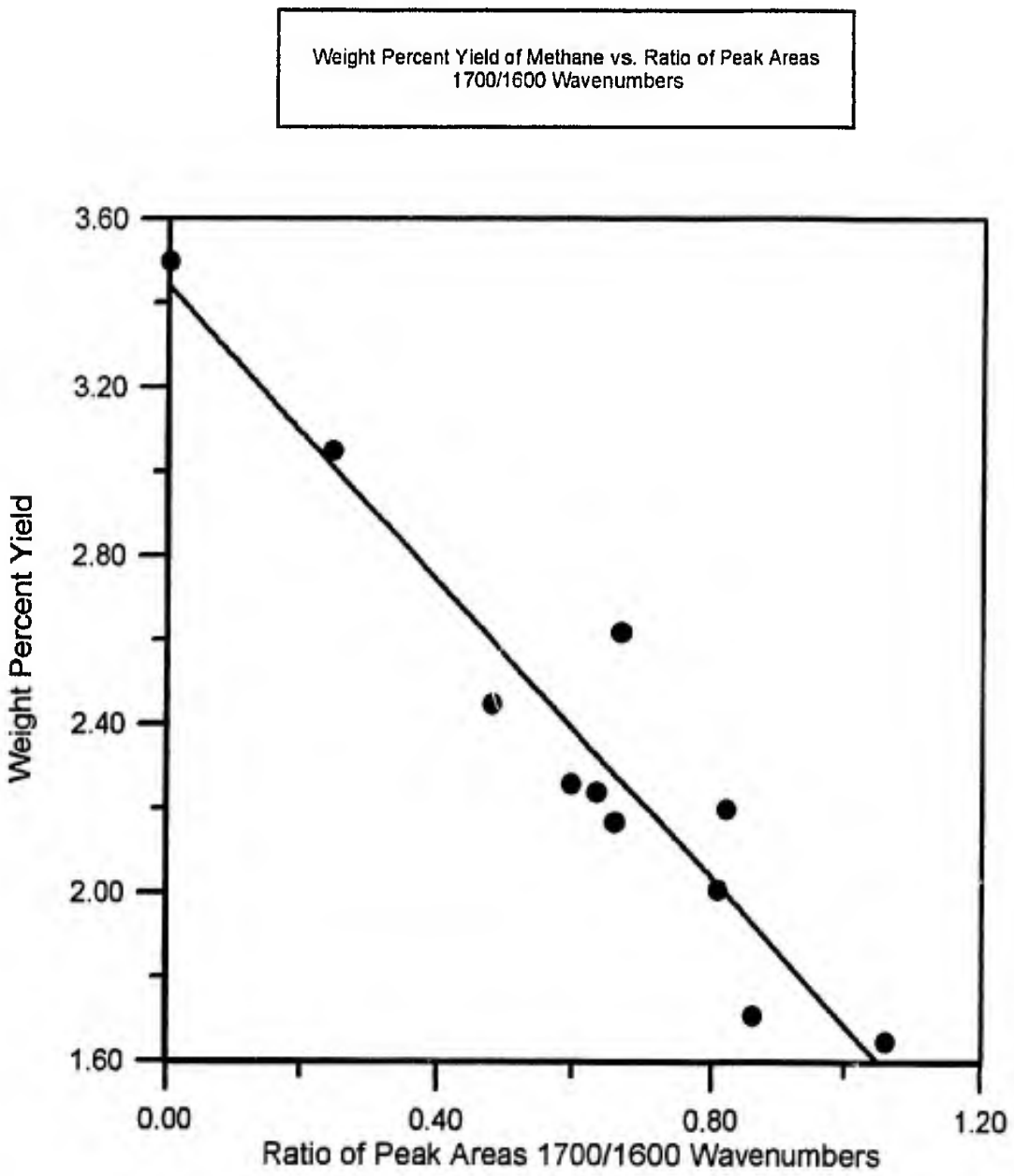

Figure 71. Plot of weight percent yield of methane vs. ratio of peak areas 1700/1600 wavenumbers for carbonization of mesophase pitch to 900°C

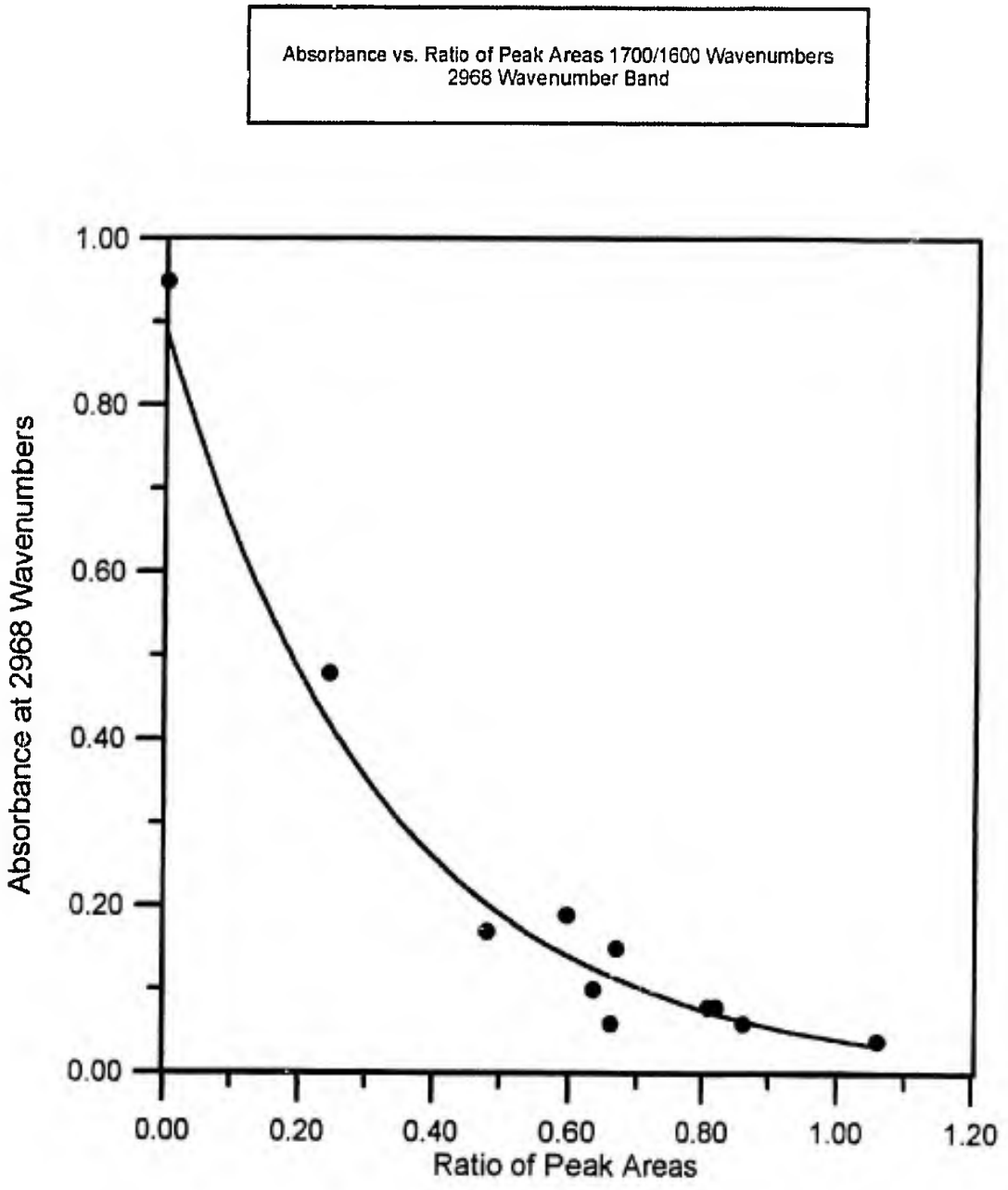

Figure 72. Plot of alkane absorbance vs. ratio of peak areas 1700/1600 wavenumbers for carbonization of mesophase pitch to 900°C

carbonization, unoxidized aliphatic content is thermally "cracked", forming oligomers, while oxidized aliphatic content is removed as carbon dioxide and carbon monoxide. Although the resultant product mixture shows a competition between oligomers and carbon dioxide/carbon monoxide, the resulting coke yield remains steady at about 70%-73%. This is shown clearly in figure 67 where samples yielding a small coldring product fraction gave large carbon dioxide and carbon monoxide yields on carbonization, while samples producing large coldring product fractions gave small yields of carbon dioxide and carbon monoxide. Furthermore, the yield of alkanes appears to be directly proportional to the yield of coldring product fraction, suggesting that the "cracking" process which produces oligomers produces also the light alkanes.

The results contained in tables 2 and 3 suggest that ultimate coke yield at 900°C over a wide range of oxidation histories is primarily a function of the aliphatic/aromatic ratio in the pre-oxidized pitch. Differences in oxidation profiles affect primarily the relative composition of the product fractions from carbonization, with a competition between oligomers/alkanes and carbon dioxide/carbon monoxide/water as the primary products. The coke yield becomes a function of sample history only for unoxidized pitch and for pitches which lose significant

weight during oxidation, generally 10% or more. Pitches which lose weight during oxidation give a decreased coke yield as a result of the decrease in the relative carbon content in the sample.

To summarize, it would appear that only a very light oxidation history is sufficient to "crosslink" or "fix" the carbonizable fraction into the pitch. It must be noted that a "most desired" oxidation profile incorporates significantly more oxygen into the pitch than is required to reach the plateau yield of carbon (about 70%). Ancillary considerations, such as the avoidance of internal voids and surface fusion of the fibers on carbonization, must be met by a more severe oxidation profile (but still within the weight gain-plateau region). These physical considerations must be best met through a proper balance of the oligomer and light alkane/CO, CO_2, H_2O product ratio. It is possible that an "ideal" oxidation history may be best expressed in terms of this product ratio, irrespective of the time/temperature profile of oxidation prior to carbonization.

4.3 PROPOSED MECHANISMS

4.3.1 OXIDATIVE STABILIZATION

Any proposed mechanisms for the oxidative stabilization of pitch must support the experimental evidence reported in this study. Such factors would

include, from our own experiments, rapid initial weight gain, loss of methylene hydrogens, and an introduction of oxygen as carbonyl (first as aldehyde/ketone/ acid/ functionality and then ester and anhydride functionality). A satisfactory mechanism for oxidative stabilization must also include a process or processes to account for weight loss which we know becomes dominant at longer oxidation time periods and/or higher oxidation temperatures. In addition to supporting our own experimental results, we feel that any proposed mechanisms should support the experimental evidence gathered by Lavin in his study of model pitch compound oxidations [5], namely the production of H_2O during weight gain, and the production of carbon dioxide and carbon monoxide during weight loss. We feel Lavin's results are especially relevant because he studied the oxidation behavior of model pitch compounds based on anthracene and dihydroanthracene, which contain chemical structures very similar to those in our synthetic mesophase pitch (figure 1). Furthermore, he performed his oxidation experiments at temperatures similar to ours, specifically, 240°C, 270°C, and 300°C.

Figure 73 illustrates a proposed mechanism for the initial stages of oxidation, resulting in weight gain by uptake of oxygen as ketone functionality, and the loss of methylene hydrogens. The mechanism also satisfies the requirement for the

Radical Initiation:

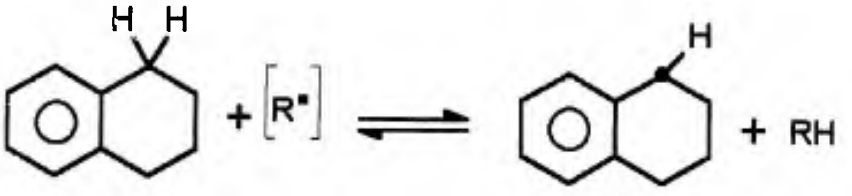

Attack by Oxygen:

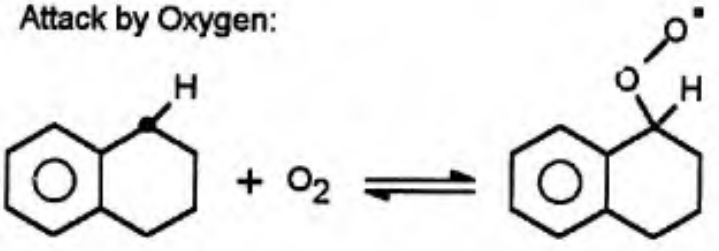

Hydrogen abstraction and propagation:

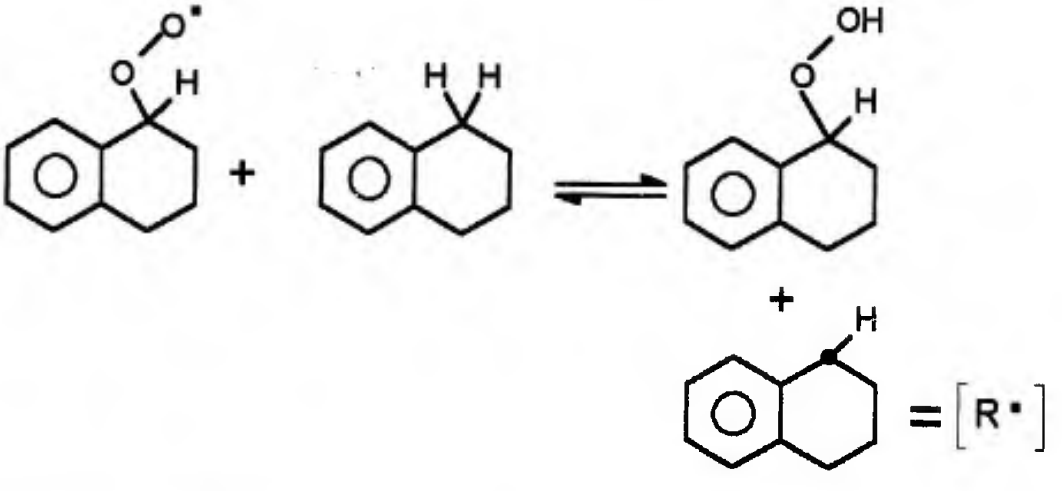

Concerted peroxide decomposition with production of water:

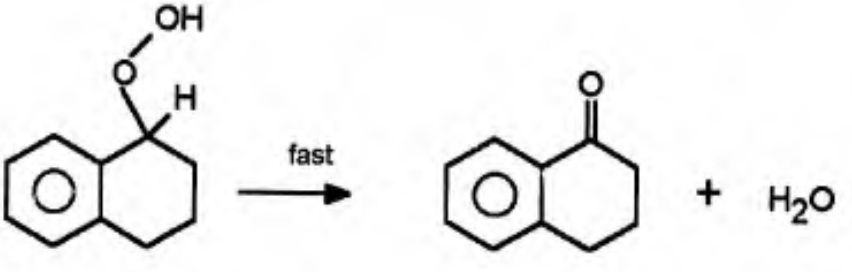

Figure 73. Mechanism for initial weight gain through ketone formation during oxidation via a hydroperoxide intermediate

production of water, which results from the decomposition of the peroxide intermediate. We use the compound 1,2,3,4-tetrahydronapthalene as a model compound in our mechanisms to simplify the illustrations. It represents the primary oxidizable chemical structures present in our synthetic mesophase pitch molecules (figure 1) as it contains both aromatic and aliphatic carbons, as well as aromatic and methylene hydrogens. The mechanism sketched in figure 73 shows the resultant addition of one oxygen atom with the loss of two methylene hydrogens and the production of one molecule of water, giving a net weight gain of 10.6%. Of course, it is possible for the saturated napthenic ring on the tetrahydronapthalene molecule to add more than one oxygen atom, with further loss of methylene hydrogens and emission of water. We are showing for simplicity the addition of one oxygen atom and the loss of two hydrogens in a model system containing one saturated and one aromatic ring. The fact that the theoretical % weight gain (10.6%) is close to the experimental maximum % weight gain (10.7%) achieved, for example, upon oxidation at 240°C for 240 minutes, suggests that this stoichiometric relationship might be accurate. The literature [10] reports approximately 5 napthenic carbons per structural unit for this pitch, with an average molecular weight of about 600 per structural unit. Assuming all 5

napthenic carbons are oxidized to ketone with the loss of two methylene hydrogens, the net weight gain would be 11.7%.

A second mechanism, illustrated in figure 74, gives the same rapid initial weight gain, addition of oxygen as carbonyl, and loss of methylene hydrogens with the production of water using an alcohol oxidation mechanism [26]. This mechanism requires more steps to form the α-hydroperoxy alcohol intermediate, but results in a more efficient chain reaction (through the production of more radicals [R°] per cycle).

The proposed mechanisms in figures 73 and 74 account only for the rapid weight gain, formation of ketones, loss of methylene hydrogens, and production of water. We must also account for the production of carboxylic acids, aldehydes, esters, and anhydrides, as well as for the weight loss process observed at longer times and for the subsequent production of carbon dioxide and carbon monoxide. We must also describe the formation of oxygenated crosslinkages between pitch molecules which are essential for the production of a high coke yield and reduced fusion and production of oligomers during carbonization.

There are numerous mechanistic routes available to explain these phenomena, but all must begin with thermally induced homolytic bond cleavage in order to

Nonconcerted peroxide decomposition (after peroxide formation as shown in figure 73):

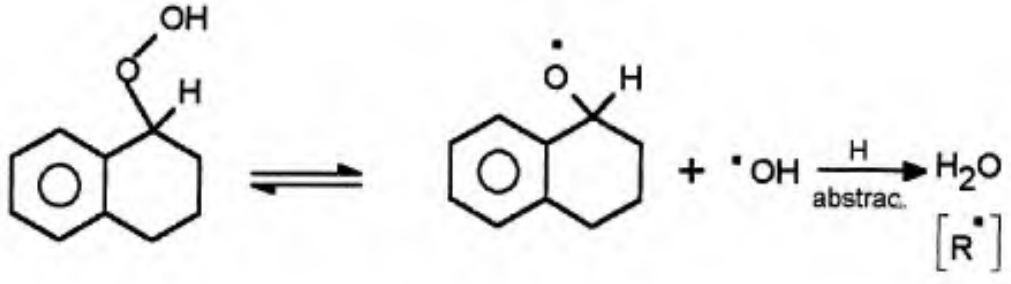

Hydrogen abstraction and propagation (alcohol formation):

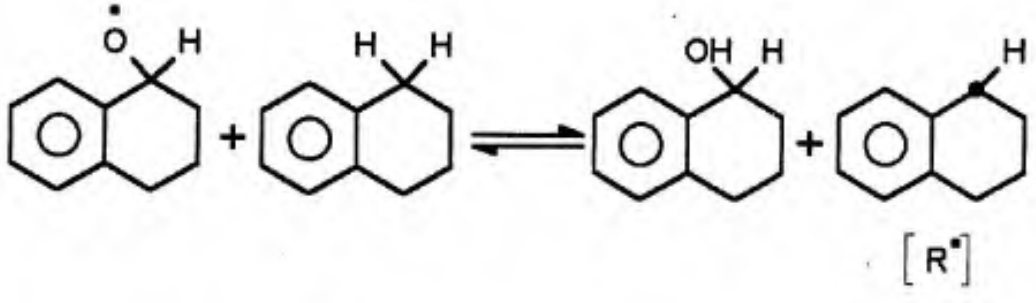

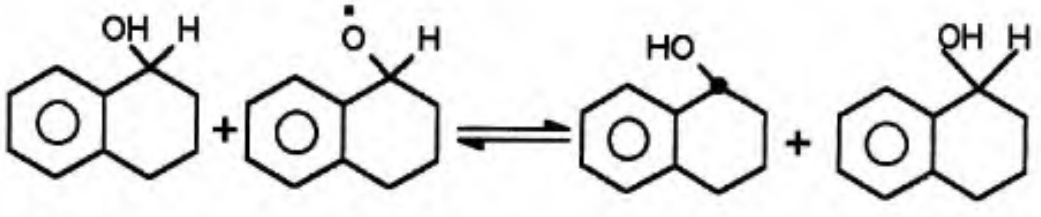

Attack of oxygen:

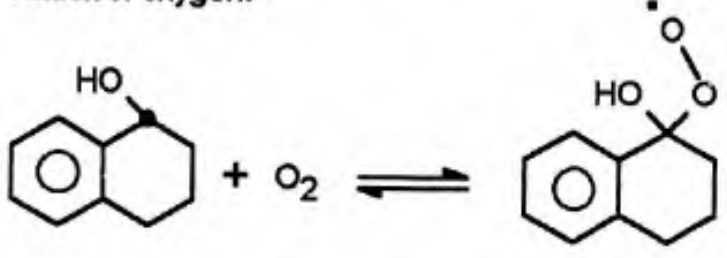

Figure 74. Mechanism for initial weight gain during oxidation through ketone formation via an alpha-hydroxy hydroperoxide intermediate

Alcohol oxidation:

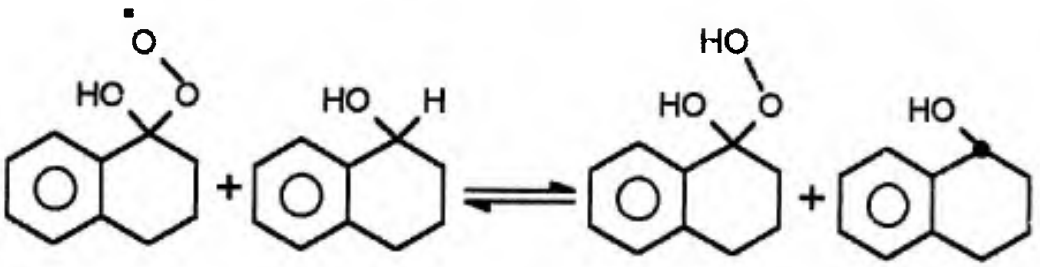

Concerted alpha-hydroxy hydroperoxide decomposition with production of hydrogen peroxide:

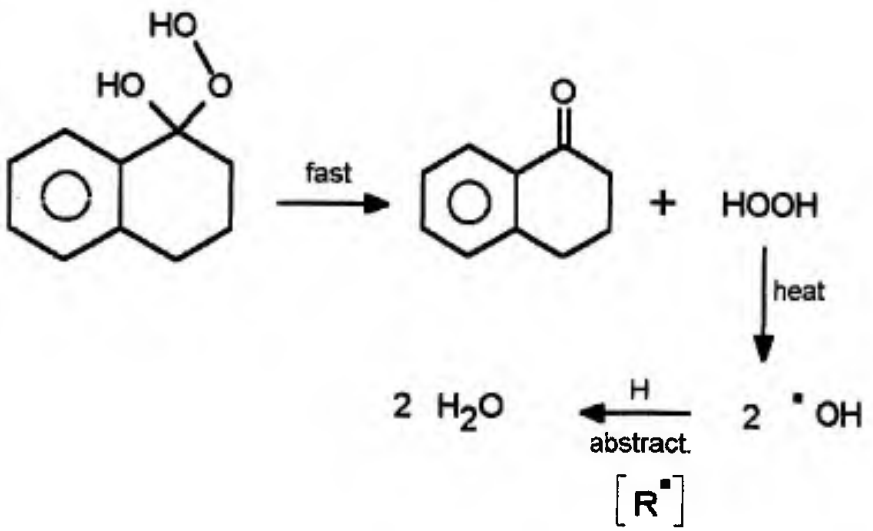

Figure 74 (cont). Mechanism for initial weight gain during oxidation through ketone formation via an alpha-hydroxy hydroperoxide intermediate

Source: Jay K. Kochi, Volume 2, Chapter 12 in "Free Radicals", Jay Kochi (Ed.), Wiley & Sons, New York, (1973).

allow for the insertion of oxygen between carbon atoms. Figure 75 shows a mechanism involving the formation and decomposition of a tetroxide intermediate to yield aldehyde and carboxylic acid intermediates of oxidation [26, 27]. Recall from our experimental results that aldehyde and carboxylic acid functionality predominate during the shallow oxidation profile of a heating ramp to 240°C. More simple and direct routes for the formation of aldehydes and carboxylic acids are shown in figures 76 and 77, respectively. These mechanisms involve the simple abstraction of hydrogen by radical intermediates and would probably prevail early in the oxidation process when relatively large amounts of methylene hydrogens are still present and able to engage in chain transfer reactions.

After thermal bond scissions have occurred and aldehydes and carboxylic acids have been formed, there exist several paths for the creation of esters and anhydrides. We will show only a few of these mechanistic pathways, some of which result in the loss of carbon atoms as carbon dioxide or carbon monoxide. We want to avoid proposing mechanisms like the Baeyer-Villiger reaction or the simple condensation of two carboxylic acids, which involve the transfer of protons and/or electron pairs and the formation of numerous charged transition states. These types of mechanisms are more favorable for solvent-based reaction systems.

Thermal bond scission:

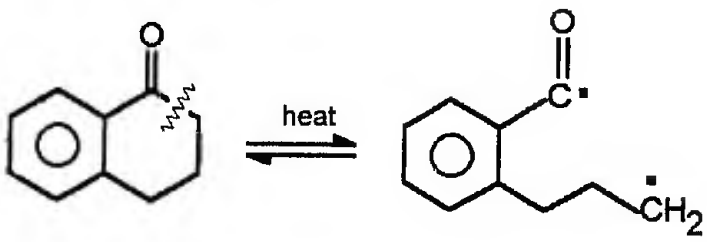

Attack by oxygen:

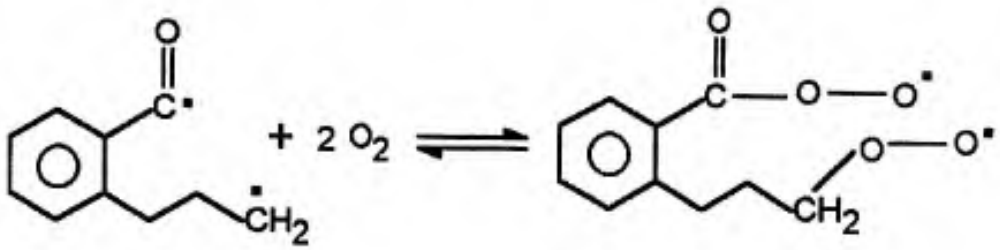

Formation and decomposition of cyclic tetroxide intermediate:

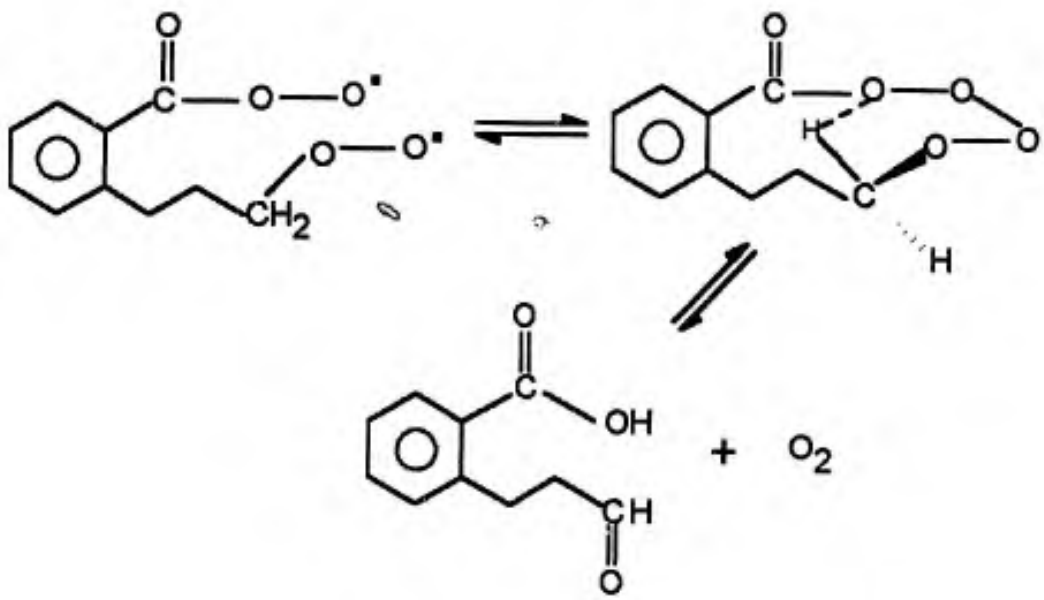

Figure 75. Formation of aldehyde and carboxylic acid after alpha-Keto bond scission from a tetroxide intermediate [26]

Thermal bond scission:

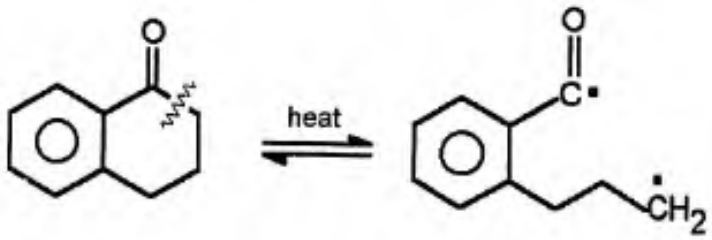

Hydrogen abstraction to form aldehyde:

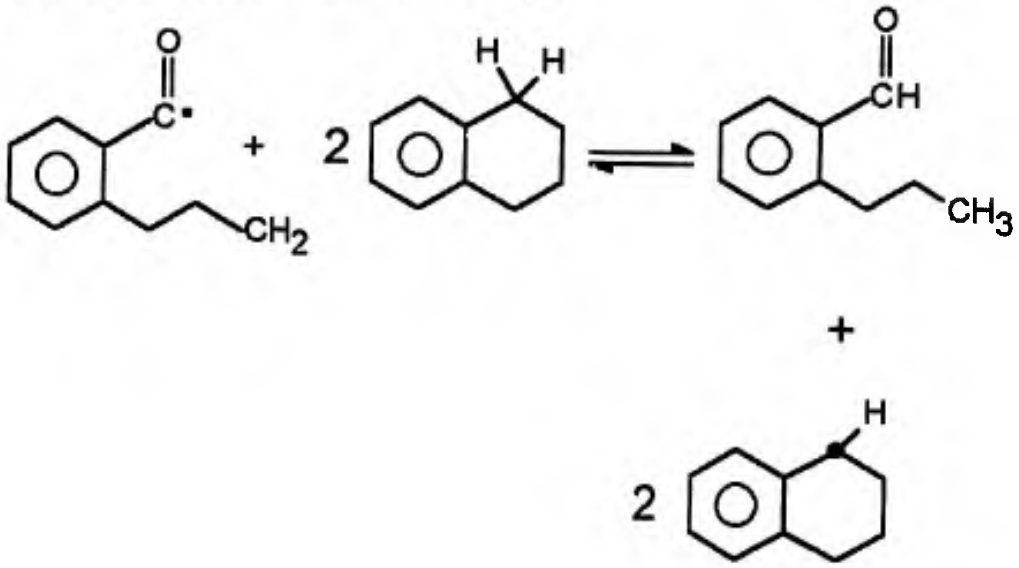

Figure 76. Alpha-Keto bond scission followed by hydrogen abstraction enroute to aldehyde functionality

Attack of oxygen to form peroxy acid:

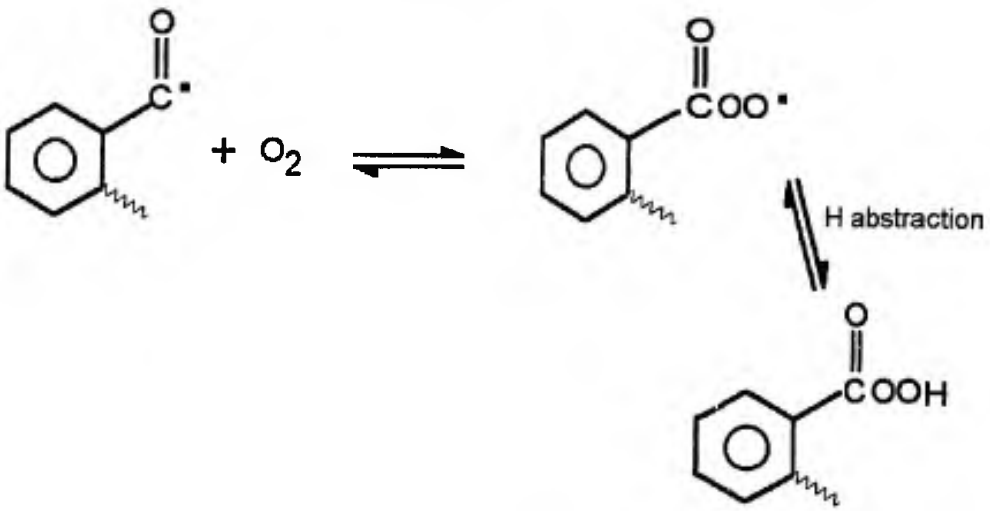

Decomposition of peroxy acid, formation of carboxylic acid:

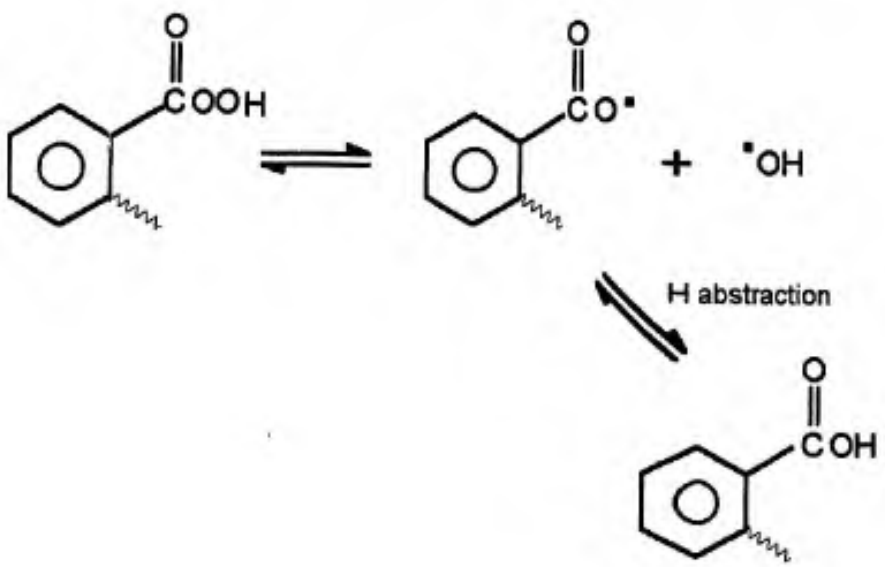

Figure 77. Alpha-Keto bond scission followed by peroxy acid formation enroute to carboxylic acid functionality

We will instead promote those reactions that involve single electron transfer and radical intermediates, and which we feel are more feasible in our reaction medium.

The first such mechanism (figure 78) involves the decomposition of a peroxy acid followed by the formation of a diacyl peroxide. The diacyl peroxide then undergoes direct displacement by a second radical aldehyde intermediate to yield an anhydride [28]. The mechanism in figure 78 involves the formation of an intramolecular diacyl peroxide. The diacyl peroxide may be formed intermolecularly as well, but in either case the direct displacement by the second radical results in an oxygen crosslink between two separate pitch molecules. If the direct displacement is the result of an alkyl or phenyl radical, as shown in figure 79, the result is an ester crosslinkage. Figure 79 shows the formation of an intermolecular diacyl peroxide. Notice that the diacyl peroxide does not have to be initiated by the decomposition of peroxy acid, but can be formed by the attack of oxygen to link two acyl radicals. We have included in figures 78 and 79 the mechanistic pathways for the formation of carbon dioxide, reactions which we feel become more favorable at higher oxidation temperatures. The end result is removal of carbon from the pitch with subsequent weight loss.

Formation of peroxy acid:

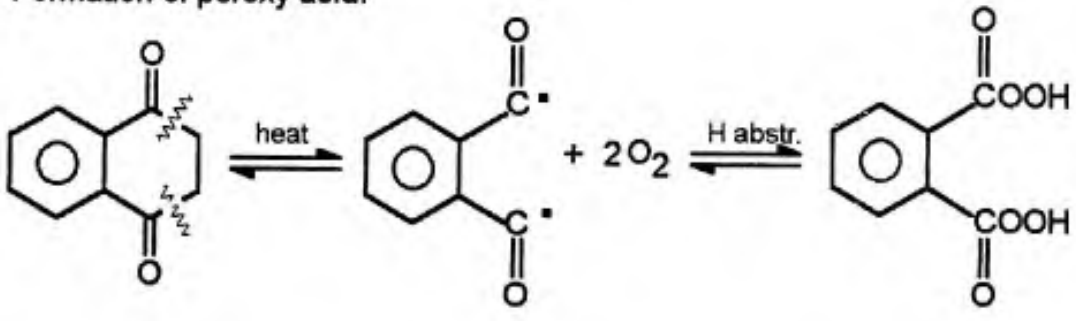

Peroxy acid decomposition:

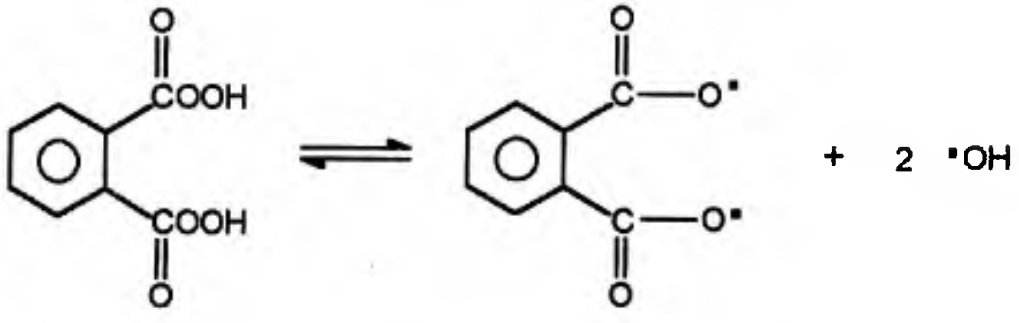

Formation of intramolecular diacyl peroxide:

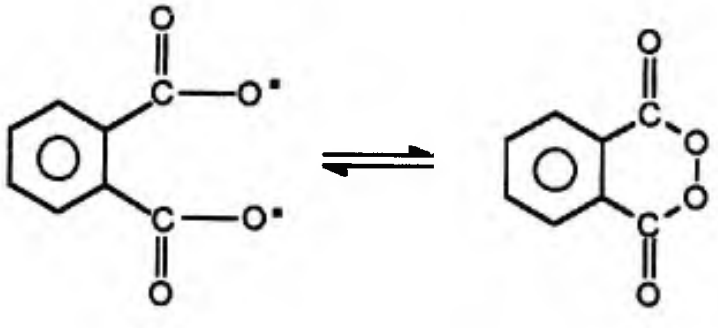

Figure 78. Formation and direct displacement of intramolecular diacyl peroxide

Direct displacement by second radical:

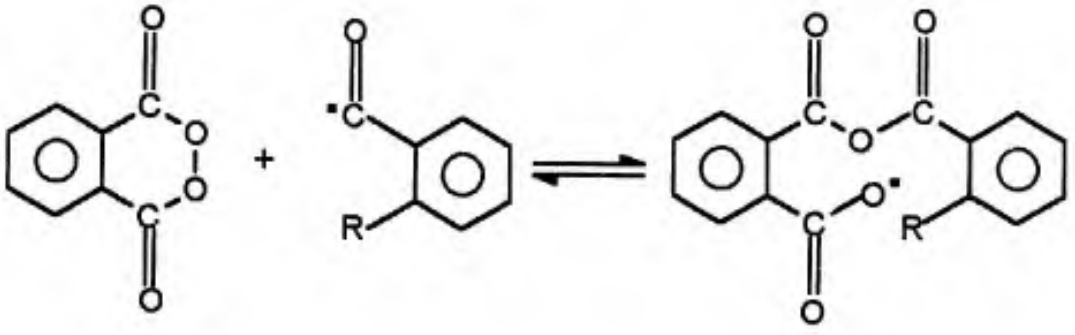

Carbon dioxide formation:

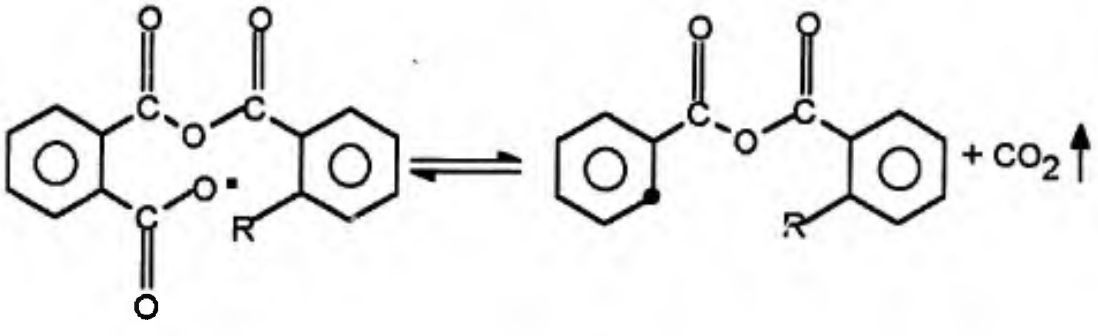

Figure 78 (cont). Formation and direct displacement of intramolecular diacyl peroxide

Source: Jay K. Kochi, Volume 1, Chapter 3 in "Free Radicals", Jay Kochi (Ed.), Wiley & Sons, New York, (1973).

Intermolecular diacyl peroxide formation:

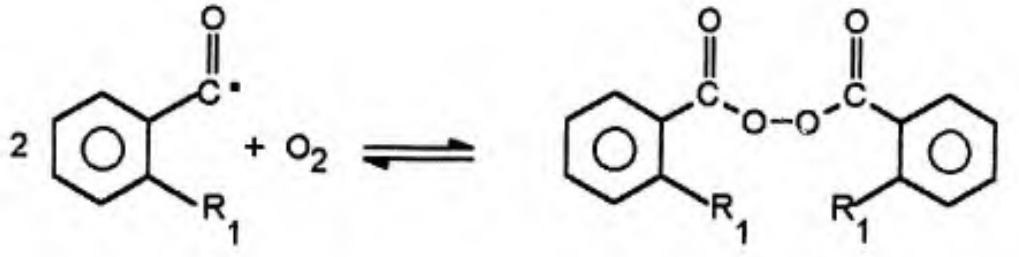

Direct displacement by second radical (loss of carbon dioxide):

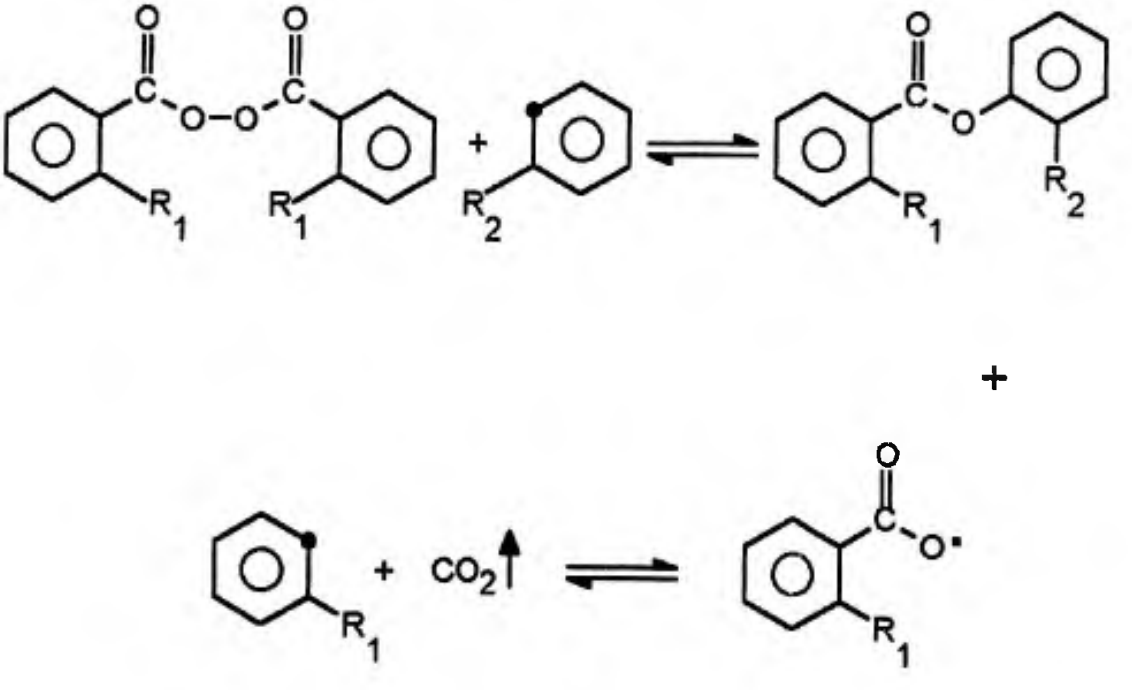

Figure 79. Formation and direct displacement of intermolecular diacyl peroxide

Source: Jay K. Kochi, Volume 1, Chapter 3 in "Free Radicals", Jay Kochi (Ed.), Wiley & Sons, New York, (1973).

Figure 80 illustrates an alternative mechanism for ester formation from diacyl peroxides by way of "carboxyl inversion" [28, 29]. This mechanism was proposed to explain the decomposition of diacyl peroxides to yield carbon dioxide and the ester functionality without a radical intermediate. We believe this mechanism to be more feasible than others illustrated in figures 78 and 79 (the direct displacement mechanism requires a second radical to migrate to the diacyl peroxide). As shown in figure 80, the carboxyl inversion can occur between carbon-oxygen surface complexes without migration of radical species. The carboxyl inversion satisfies also the requirement of carbon dioxide emission.

4.3.2 CARBONIZATION

4.3.2.1 CARBONIZATION OF UNOXIDIZED PITCH

Mechanisms for the carbonization of mesophase pitch will depend on whether or not the pitch has been previously subjected to an oxidation regime. We know from our experimental results that carbonization products are a function of oxidation history with unoxidized pitch and oxidized pitch samples producing different products during the carbonization process.

The major carbonization products from unoxidized pitch are oligomers (the coldring product fraction), short alkanes, and hydrogen. The coldring product

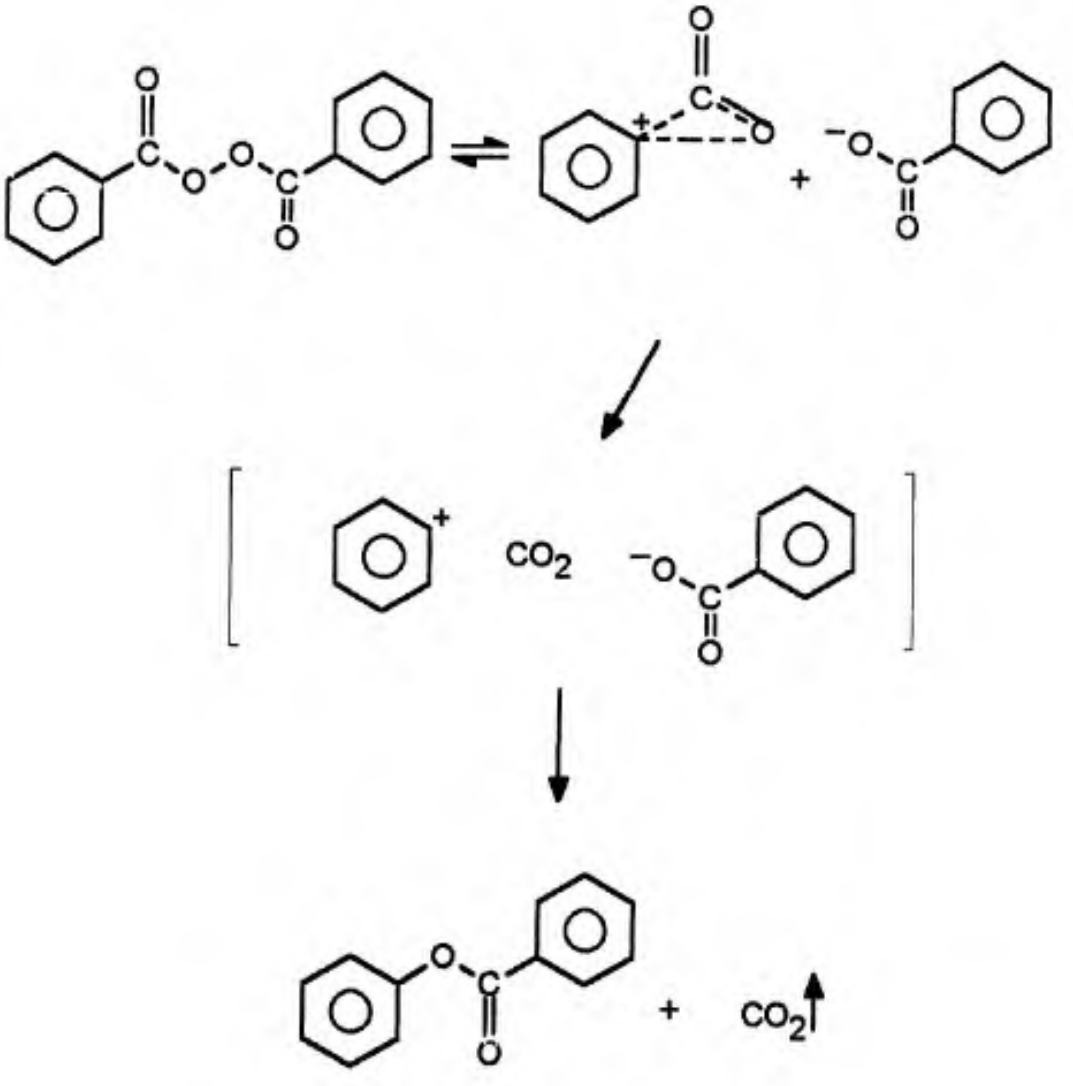

Figure 80. Carboxyl inversion in diacyl peroxide

Source: Jay K. Kochi, Volume 1, Chapter 3 in "Free Radicals", Jay Kochi (Ed.), Wiley & Sons, New York (1973).

fraction is soluble in chloroform and IR spectra indicate a relatively high aliphatic content. This would suggest that the oligomers are relatively small, aliphatic-rich molecules as opposed to highly condensed aromatic ring systems. The production of oligomers and alkanes are associated with the volatile emission process that reaches a maximum at approximately 490°, as indicated by TVA experiments. In this temperature region we would expect thermally induced homolytic bond cleavage to be energetically accesible, and to provide the major route toward the production of oligomers and short alkanes. Figure 81 illustrates possible mechanisms for the carbonization of unoxidized pitch circa 500°C to produce oligomers. FT-IR spectra of coldring product fractions indicate absorbances due to both methylene (CH_2) and methyl (CH_3) hydrogen bending modes. Therefore, oligomers are likely produced from the "cracking" open of napthenic rings in addition to formation as products of the "cracking" off of entire napthenic ring systems. Both routes are shown in figure 81.

The production of short alkanes during carbonization of unoxidized pitch is shown in figure 82. The "cracking" of any aliphatic side chains in the pitch (figure 1) is a likely route to alkanes, as is the "cracking" open of napthenic rings with subsequent bond scissions (and in both instances, followed by hydrogen

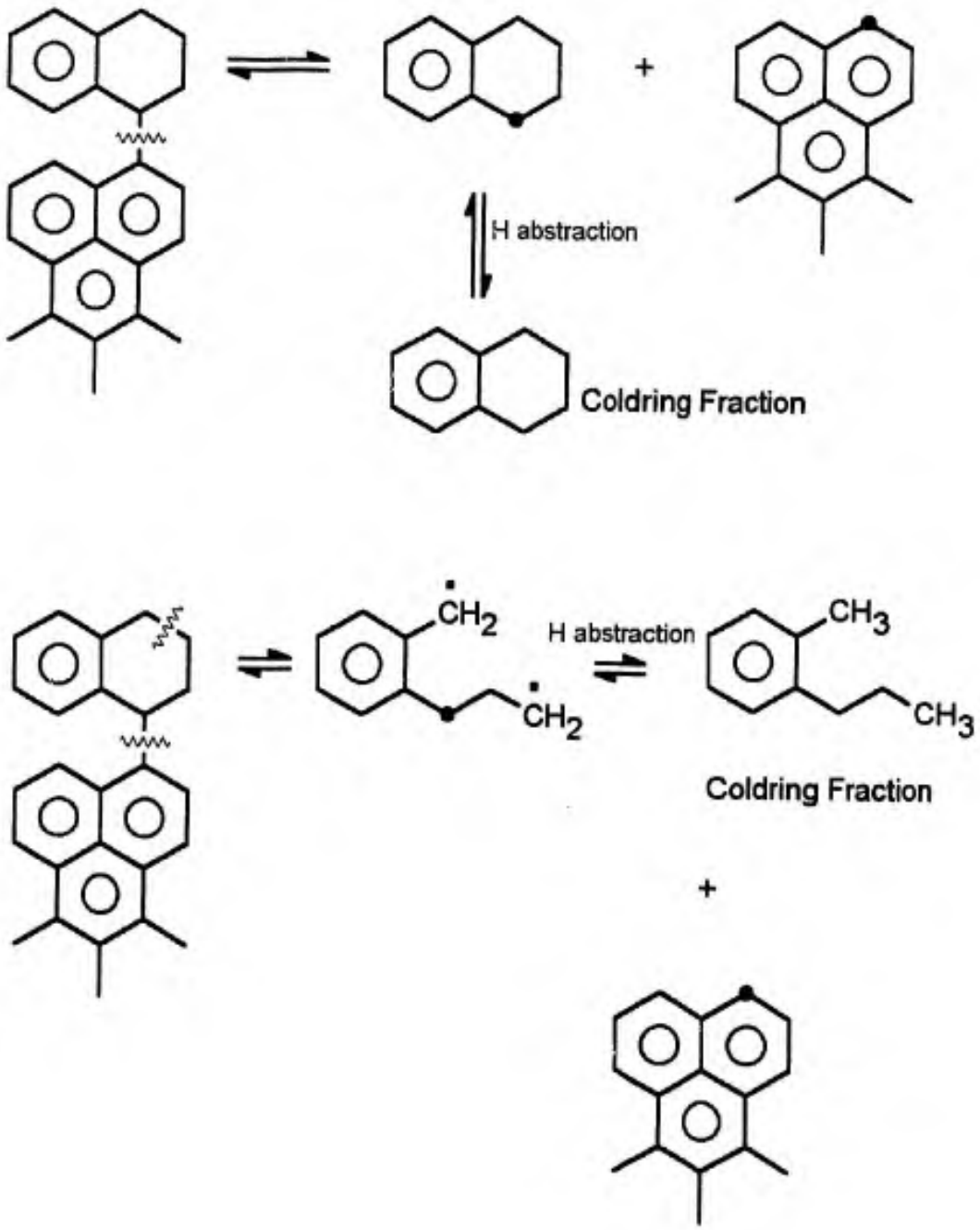

Figure 81. Production of oligomers during carbonization of representative structures in unoxidized mesophase pitch

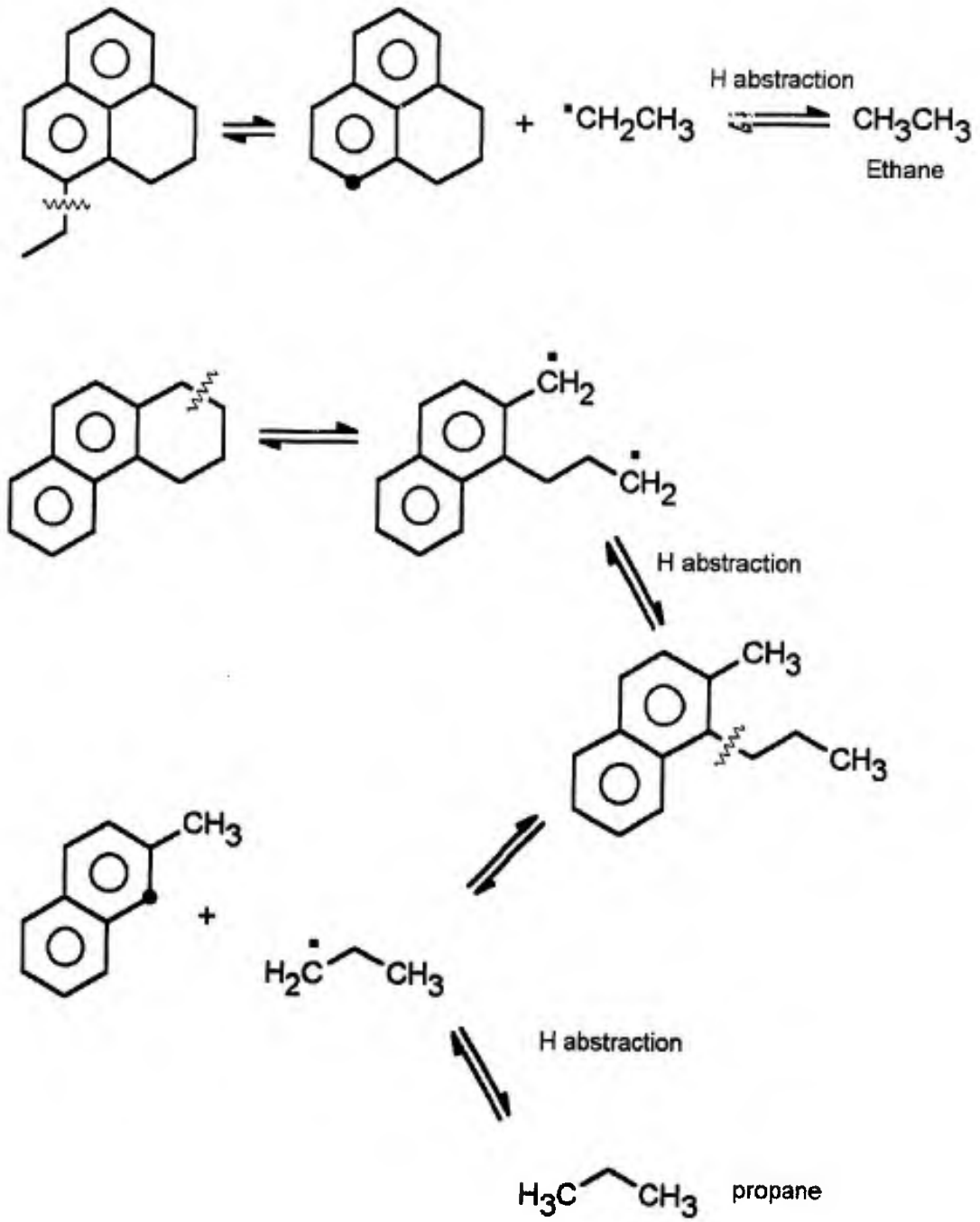

Figure 82. Production of short alkanes during carbonization of representative structures in unoxidized mesophase pitch

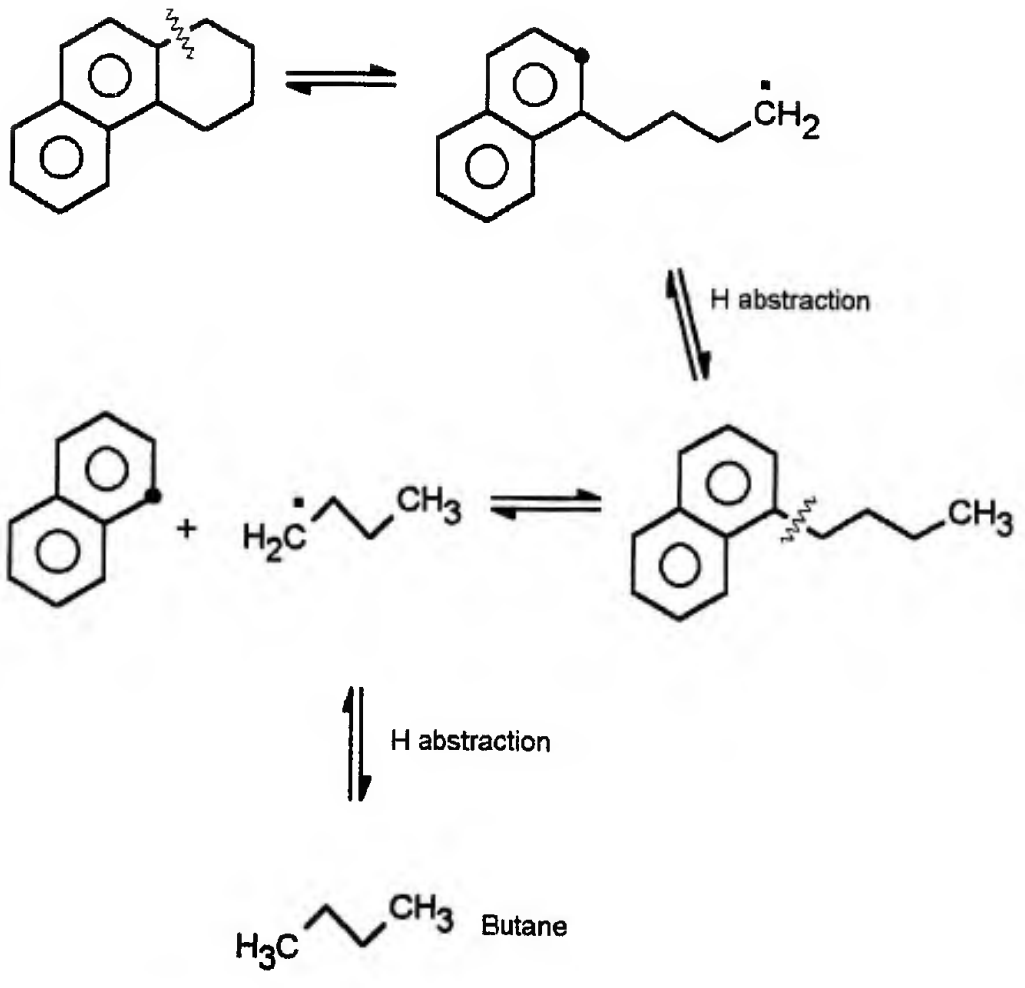

Figure 82 (cont). Production of short alkanes during carbonization of representative structures in unoxidized mesophase pitch

abstraction). Both routes are illustrated in figure 82. It is important to note that the mechanisms shown in figures 81 and 82 are similar and can easily occur in parallel as is suggested by the results of TVA experiments which indicate that the production of oligomers and short alkanes is concurrent.

Aromatic radical systems produced as a result of thermal bond scissions (figures 81 and 82) may combine or fuze together with the loss of hydrogen to give more condensed aromatic ring systems. This process is illustrated in figure 83. The condensation of aromatic radicals would most likely be preceeded by large-scale molecular rearrangements to facilitate radical combinations, resulting in the extensive melting or fusion of the pitch molecules as seen in carbonized pitches that have not been previously oxidized. Notice that fusion of aromatic radicals by this mechanism requires the concurrent production of hydrogen gas. This is in agreement with TVA results which show hydrogen gas as a product around 500°C, along with oligomers and light alkanes.

The mechanism for aromatic radical condensations (figure 83) is also valid for the volatile emission process occurring at about 770°C during carbonization, which TVA results show to involve primarily the emission of hydrogen. The aromatic radicals formed at this high temperature are primarily due to the loss of

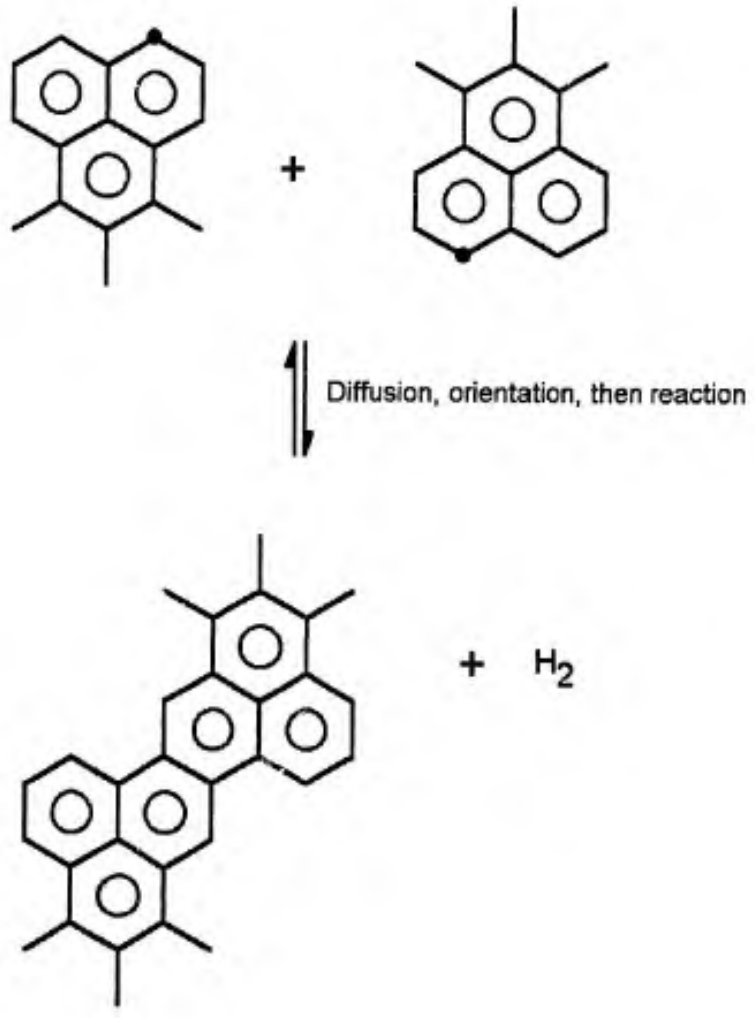

Figure 83. Condensations or fusion of aromatic radicals in representative mesophase pitch structures to yield larger aromatic systems

aromatic hydrogen, as indicated by IR spectra of coke residues at 600°C. The radicals formed by this process can then combine as shown in figure 83, resulting in the further loss of aromatic hydrogen as hydrogen gas.

4.3.2.2 CARBONIZATION OF OXIDIZED PITCH

The carbonization of oxidized pitch produced as byproducts primarily carbon dioxide, carbon monoxide, water, and hydrogen gas, along with smaller quantities of methane and light alkanes. In comparison with unoxidized pitches, coldring product fractions were considerably smaller for pitches which had been previously oxidized (see table 2). However, as with the unoxidized pitch, the oligomeric or coldring product fractions were relatively rich in aliphatic content. For this reason, we believe that oligomers produced during the carbonization of oxidized pitch are the result of the same types of thermal bond scission or "cracking" processes in unoxidized pitch as were illustrated in figure 81. The relatively small proportion of the sample mass which constitutes the coldring product fractions indicates that only a minimal aliphatic content is present in the pitch following oxidation. Furthermore, the production of short alkanes is proportional to the size of the coldring product fraction for samples of oxidized pitch (tables 2 and 3); further proof that the "cracking" process which produces oligomers is also the

most likely source of short alkanes.

Figure 84 illustrates a possible mechanism for the condensation of two aromatic ring systems previously connected by an ester linkage. A simple, thermally induced decarboxylation would produce carbon dioxide along with two aromatic radicals. These aromatic radicals would be advantageously positioned to recombine without prior rearrangement or migration, as was necessary for similar structures in unoxidized pitch. This could explain the lack of melting or fusion experienced during the carbonization of previously oxidized pitch.

Figure 85 sketches a possible mechanism for the decomposition of an anhydride functionality to produce two aromatic radicals along with carbon dioxide and carbon monoxide. Because of the nature of the anhydride functionality, the two aromatic radicals are again in a favorable position to recombine without prior rearrangement, and would yield a more highly condensed, fuzed aromatic ring system after emission of hydrogen gas. This is again in agreement with the results of TVA experiments which show that hydrogen gas is a product of reaction between approximately 400°C and 600°C, along with carbon dioxide and carbon monoxide.

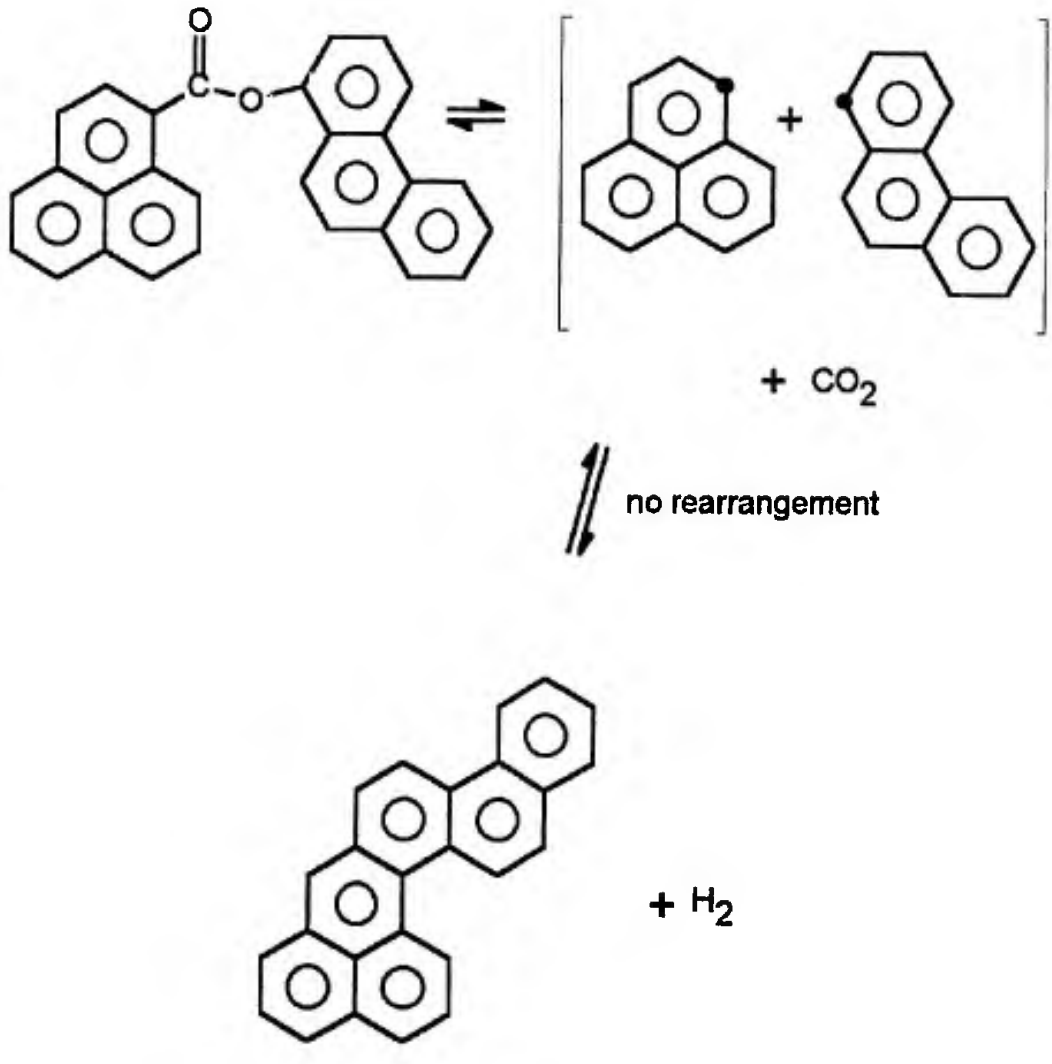

Figure 84. Decomposition of a sample ester crosslink during carbonization of oxidized mesophase pitch

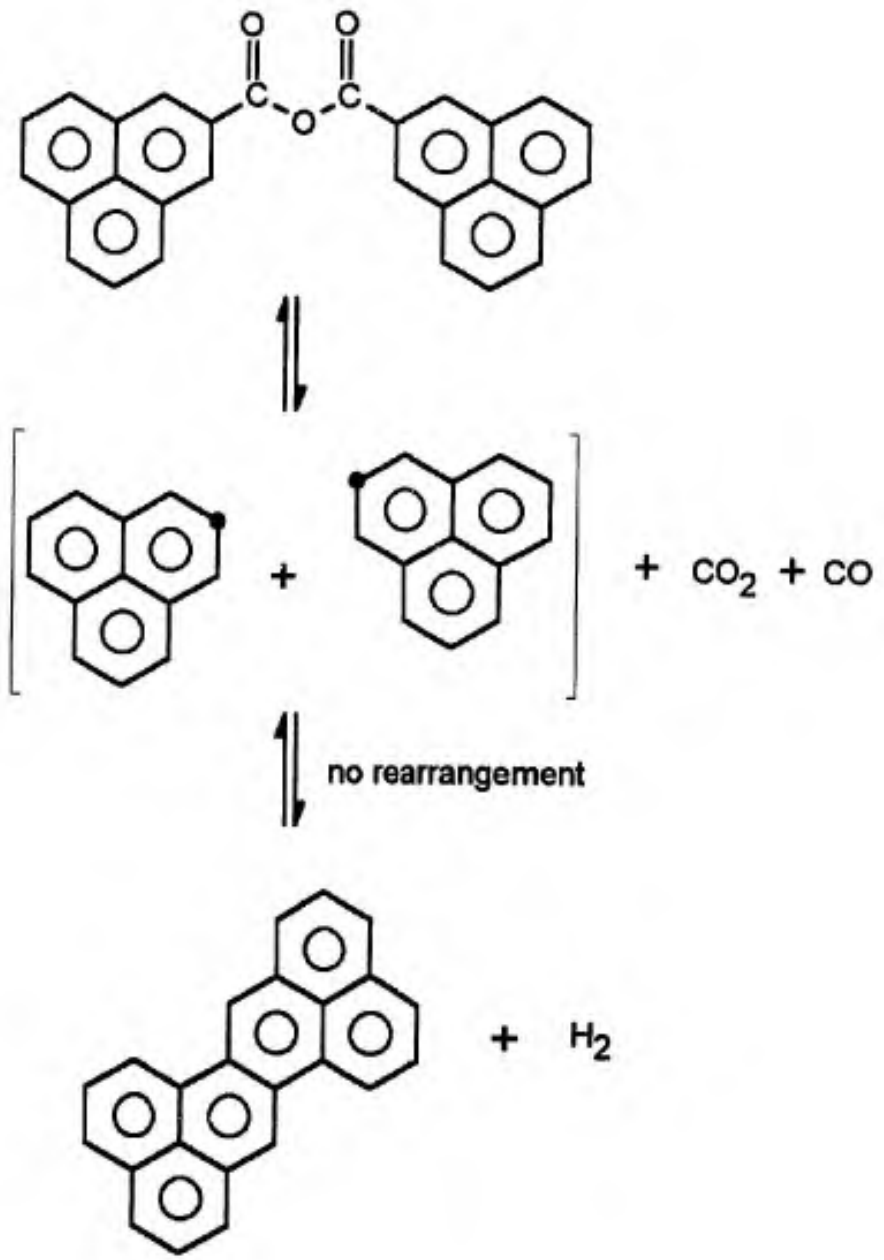

Figure 85. Decomposition of a sample anhydride crosslink during carbonization of oxidized mesophase pitch

Figure 86 illustrates some possible mechanistic pathways for the degradation of ketone, carboxylic acid, and aldehyde functionalities during carbonization. Of the three functionalities, only a ketone can form a crosslink between two aromatic ring systems without prior diffusion and rearrangement of the combining radicals. The decomposition of a carboxylic acid group results in the production of an aromatic radical which must undergo "migration" prior to combination with a second radical. Aldehyde likely decomposes to produce carbon monoxide with rapid recombination of the resultant aldehydic hydrogen and aromatic radicals. The production of water as a major product fraction in the carbonization of oxidized pitch suggests that relatively large concentrations of carboxylic acid groups are present in oxidized pitch. It is probable, also, that the production of water during the carbonization of oxidized pitch is a result of oxygen liberated during the degradation of oxygenated intermediates in the pitch. The oxygen produced by these degradation routes can then react with aromatic hydrogens in the pitch, removing them in the form of H_2O as opposed to H_2--a process that would be much more energetically favorable.

The second major volatile emission process during the carbonization of oxidized pitch occurs between 700°C and 800°C, as indicated by TVA results.

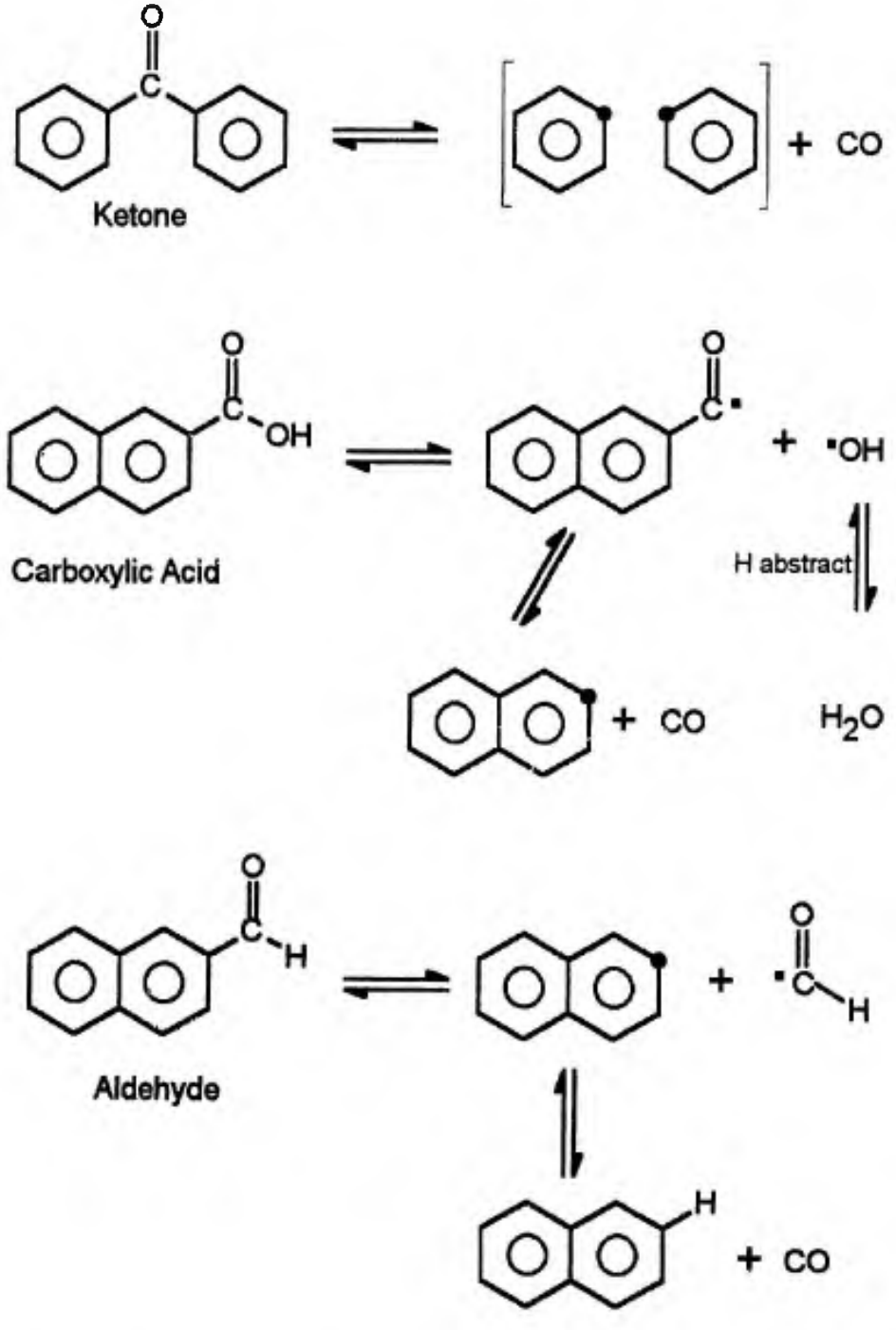

Figure 86. Decomposition of a representative ketone, carboxylic acid, and aldehyde functional group during carbonization of oxidized mesophase pitch

This process is associated primarily with the emission of hydrogen gas, along with smaller quantities of methane and carbon monoxide. We believe the primary process involved here to be the loss of aromatic hydrogen to produce hydrogen gas and aromatic radicals which lead to further ring fusions. These aromatic radicals then combine to form a more highly developed aromatic system as shown in figure 83 for representative structures in unoxidized pitch. We believe the loss of aromatic hydrogen and subsequent aromatic condensations in this high temperature region to be similar for oxidized and unoxidized pitches.

There are thusly two major differences in the carbonization pathways in unoxidized and in oxidized pitch. The first resides in the relative size of the oligomeric or coldring product fraction. Unoxidized pitches possess a relatively higher aliphatic content and therefore sustain more "cracking" processes that produce oligomers and short alkane products. Oxidized pitches have been shown to lose most of their aliphatic content during the oxidation profile and, consequently, cannot sustain the same degree of thermal "cracking". This results in the production of a smaller coldring product fraction and in a smaller yield of short alkanes. Secondly, unoxidized pitch forms aromatic radicals during "cracking" processes that are not favorably positioned for subsequent recombination without

prior rearrangement or migration. This may result in fusion or melting during carbonization. Oxidized pitch, on the other hand, contains ester and anhydride functionality which decompose during carbonization to produce carbon monoxide and carbon dioxide, along with aromatic radicals that are favorably positioned for subsequent recombination without prior rearrangement or migration.

5. CONCLUSIONS

This study was successful in characterizing the chemical processes involved in the oxidative stabilization and carbonization of a synthetic mesophase pitch.

Oxidative stabilization involves both weight gain and weight loss processes with weight gain being the dominant chemical process during lower temperature and shorter time periods of oxidation. The weight gain reaction involves an uptake of oxygen by the pitch as carbonyl functionality with the concurrent loss of methylene hydrogens. The weight loss process becomes the primary reaction pathway at longer time periods of oxidation and/or at higher oxidation temperatures. This process results in a further increase in the oxygen content of the pitch, most likely as highly conjugated carbonyl functionality, with the concurrent loss of carbon content as (most likely) carbon dioxide and carbon monoxide. The weight gain reaction has a lower over-all activation energy than the weight loss reaction, and both reactions occur at an accelerated rate as the oxidation temperature is increased. At oxidation temperatures above 320°C, the weight gain reaction is completed during the heating ramp to the final oxidation temperature.

TGA experiments were successful in defining the overall weight loss process occurring during carbonization but were not successful in gaining a kinetic-based interpretation of the carbonization process. TVA and SATVA experiments were successful in characterizing the full product spectrum resulting from the carbonization of unoxidized and oxidized (stabilized) pitches to an end temperature of 900°C. The relative yields of the defined product fractions (short alkanes, light oxides of carbon, water, oligomers, and coke) were directly related to the sample's oxidation history prior to carbonization. Unoxidized or insufficiently oxidized pitches gave large yields of oligomers and short alkanes, and little or no oxides of carbon (carbon monoxide and carbon dioxide). Sufficiently oxidatively stabilized pitches gave very small oligomeric product fractions and large quantities of CO and CO_2. Excessively stabilized pitches which lost significant weight during their oxidation profiles gave the smallest yields of oligomers and the largest yields of CO and CO_2. Coke yield during carbonization under a high vacuum (70-73%) was determined to be independent of oxidation history, except for pitches which lost weight during oxidation. For these pitches, coke yield decreased in proportion to the weight loss sustained during oxidation. Unoxidized or insufficiently oxidized pitches showed fusion or melting of the pitch particles

during carbonization. Sufficiently oxidized pitches maintained their powdered form during carbonization with little or no fusion of the individual pitch particles.

In summary, this study suggests that a proper oxidative stabilization profile might be better expressed in terms of the relative size of the resultant product fractions from carbonization rather than in terms of the time or temperature profile of oxidation itself.

LIST OF REFERENCES

[1] Harry Marsh, Chapter 1 in "Introduction to Carbon Science", Harry Marsh (Ed.), Butterworths, London (1989).

[2] Harry Marsh, Chapter 2 in "Introduction to Carbon Science", Hary Marsh (Ed.), Butterworths, London (1989).

[3] Harry Marsh, Chapter 3 in "Introduction to Carbon Science", Harry Marsh (Ed.), Butterworths, London (1989).

[4] Dr. William T. K. Stevenson's Research Proposal to USAF, 1993.

[5] J. Gerard Lavin, Carbon, 30 (3), 351 (1992).

[6] Isao Mochida, Hiroshi Toshima, Yozo Korai, and Tadayuki Matsumoto, Journal of Materials Science, 25, 76 (1990).

[7] Tadayuki Matsumoto and Isao Mochida, Carbon, 30, 1041 (1992).

[8] Isao Mochida, Hiroshi Toshima, Yozo Korai, and Tadayuki Matsumoto, Journal of Materials Science, 24, 2191 (1989).

[9] Seong Ho Yoon, Seh-Min Oh, and Yang-Duk Park, Journal of Materials Science, 27, 5199 (1992).

[10] Isao Mochida, Kiyoyuki Shimizu, Yozo Korai, Hiroyuki Otsuka, Yukio Sakai, and Susumu Fujiyama, Carbon, 28 (2/3), 311 (1990).

[11] Yozo Korai, Munehiro Nakamura, Isao Mochida, Yukio Sakai, and Susumu Fujiyama, Carbon, 29 (4/5), 561 (1991).

[12] Ryuji Fujiura, Takashi Kojima, Koichi Kanno, Isao Mochida, and Yozo Korai, Carbon, 31 (1), 97 (1993).

[13] Joseph H. Flynn and Leo A. Wall, Polymer Letters, 4, 323 (1966).

[14] Homer E. Kissinger, Analytical Chemistry, 29, 1702 (1957).

[15] I.C. McNeill, Chapter 2 in "Developments in Polymer Degradation I", N. Grassie (Ed.), Applied Science Publishers, London (1977).

[16] I.C. McNeill, L. Ackerman, S.N. Gupta, M. Zulfiqar, and S. Zulfiqar, Journal of Polymer Science, Polymer Chem Ed., 15, 2381 (1977).

[17] I.C. McNeill, Polymer Engineering and Science, 20 (10), 668 (1980).

[18] Personal communications to the author from Dr. Joseph Hager, Major (USAF-Retired), Non-metallic Materials Laboratory, Wright-Patterson Air Force Base, Ohio.

[19] I.C. McNeill, European Polymer Journal, 3, 409 (1967).

[20] J.L. White and P.M. Sheaffer, Carbon, 27(5), 697 (1989).

[21] Robert M. Silverstein, G. Clayton Bassler, and Terence C. Morrill, Chapter 3 in "Spectrometric Identification of Organic Compounds", John Wiley & Sons, New York, (1981).

[22] Charles Q. Yang and John R. Simms, Carbon, 31(3), 451 (1993).

[23] Gilbert W. Castellan, Chapter 12 in "Physical Chemistry", 3rd Edition, Benjamin/Cummings Publishing Company, Menlo Park, California, (1983).

[24] "The CRC Handbook of Chemistry and Physics", 65th Edition, Robert C. Weast (Ed.), CRC Press, Inc., Boca Raton, Florida (1985).

[25] Raymond H. Pierson, Aaron N. Fletcher, and E. St. Clair Gantz, Analytical Chemistry, 28 (8), 1218 (1956).

[26] Jay K. Kochi, Volume 2, Chapter 12 in "Free Radicals", Jay K. Kochi (Ed.), John Wiley & Sons, New York, (1973).

[27] G. A. Russell, Journal of the American Chemical Society, 79, 3871 (1957).

[28] Jay K. Kochi, Volume 1, Chapter 3 in "Free Radicals", Jay K. Kochi (Ed.), John Wiley & Sons, New York, (1973).

[29] C. Walling, H. P. Waits, J. Milovanovic, and C. Pappiannou, Journal of the American Chemical Society, 92, 4927 (1970).